

(12)

DNA 5803F

AD A118456

# MASS FIRE MODEL CONCEPT

J. C. Sanderlin

J. A. Ball

G. A. Johanson

Mission Research Corporation

P.O. Drawer 719

Santa Barbara, California 93102

31 May 1981

Final Report for Period 8 September 1980—31 May 1981

CONTRACT No. DNA 001-80-C-0351

APPROVED FOR PUBLIC RELEASE;  
DISTRIBUTION UNLIMITED.

DTIC FILE COPY

THIS WORK SPONSORED BY THE DEFENSE NUCLEAR AGENCY  
UNDER RDT&E RMSS CODE B345080462 G54CAXYX97001 H2590D.

Prepared for

Director

DEFENSE NUCLEAR AGENCY

Washington, D. C. 20305

DTIC  
ELECTE  
AUG 23 1982  
S B D

82 08 02 043

Destroy this report when it is no longer  
needed. Do not return to sender.

PLEASE NOTIFY THE DEFENSE NUCLEAR AGENCY,  
ATTN: STTI, WASHINGTON, D.C. 20305, IF  
YOUR ADDRESS IS INCORRECT, IF YOU WISH TO  
BE DELETED FROM THE DISTRIBUTION LIST, OR  
IF THE ADDRESSEE IS NO LONGER EMPLOYED BY  
YOUR ORGANIZATION.



UNCLASSIFIED

SECURITY CLASSIFICATION OF THIS PAGE (When Data Entered)

REPORT DOCUMENTATION PAGE		READ INSTRUCTIONS BEFORE COMPLETING FORM
1. REPORT NUMBER DNA 5803F	2. GOVT ACCESSION NO. AD A118456	3. RECIPIENT'S CATALOG NUMBER
4. TITLE (and Subtitle)  MASS FIRE MODEL CONCEPT		5. TYPE OF REPORT & PERIOD COVERED Final Report for Period 8 Sep 80 - 31 May 81
		6. PERFORMING ORG. REPORT NUMBER MRC-R-636
7. AUTHOR(s) J. C. Sanderlin                      G.A. Johanson J. A. Ball		8. CONTRACT OR GRANT NUMBER(s)  DNA 001-80-C-0351
9. PERFORMING ORGANIZATION NAME AND ADDRESS Mission Research Corporation P.O. Drawer 719 Santa Barbara, California 93102		10. PROGRAM ELEMENT, PROJECT, TASK AREA & WORK UNIT NUMBERS  Subtask G54CAXYX970-01
11. CONTROLLING OFFICE NAME AND ADDRESS Director Defense Nuclear Agency Washington, D.C. 20305		12. REPORT DATE 31 May 1981
		13. NUMBER OF PAGES 330
14. MONITORING AGENCY NAME & ADDRESS (if different from Controlling Office)		15. SECURITY CLASS (of this report)  UNCLASSIFIED
		15a. DECLASSIFICATION/DOWNGRADING SCHEDULE N/A Since UNCLASSIFIED
16. DISTRIBUTION STATEMENT (of this Report)  Approved for public release; distribution unlimited.		
17. DISTRIBUTION STATEMENT (of the abstract entered in Block 20, if different from Report)		
18. SUPPLEMENTARY NOTES  This work was sponsored by the Defense Nuclear Agency under RDT&E RMSS Code B345080462 G54CAXYX97001 H2590D		
19. KEY WORDS (Continue on reverse side if necessary and identify by block number) Mass Fire                                      Rothermel Fire Model Fire Storm Simulation Models Fire Behavior Models		
20. ABSTRACT (Continue on reverse side if necessary and identify by block number)  Review of the literature pertaining to mass fire onset and development indicates there exist no models that describe the onset and development of mass fires. The state-of-the-art is such that a low confidence level, parametric model can be developed. The theoretical basis, and a preliminary implementation, are described for a low confidence level, parametric model of mass fire onset and development in an urban environment.		

DD FORM 1 JAN 73 1473

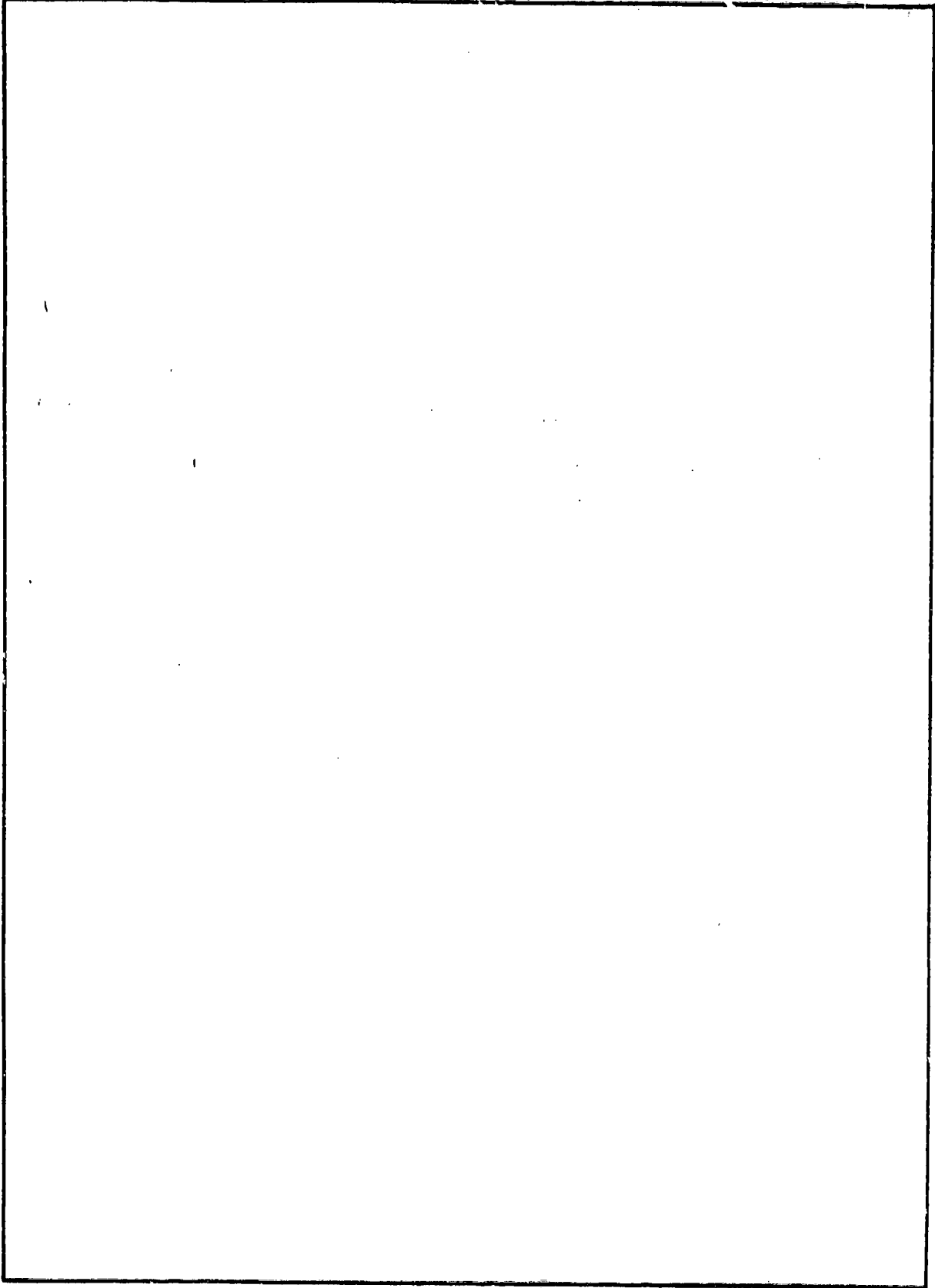
EDITION OF 1 NOV 65 IS OBSOLETE

UNCLASSIFIED

SECURITY CLASSIFICATION OF THIS PAGE (When Data Entered)

UNCLASSIFIED

SECURITY CLASSIFICATION OF THIS PAGE(When Data Entered)



UNCLASSIFIED

SECURITY CLASSIFICATION OF THIS PAGE(When Data Entered)



## TABLE OF CONTENTS

<u>Section</u>	<u>Page</u>
LIST OF ILLUSTRATIONS	4
LIST OF TABLES	12
1 INTRODUCTION	13
1.1 BACKGROUND	13
1.2 CONCLUSIONS AND RECOMMENDATIONS	15
1.2.1 Hydrodynamic Modeling	15
1.2.2 Branding and Contagion	16
1.2.3 Simulation Grid and Subgrid Characteristics	16
1.3 SUMMARY	18
2 MASS FIRE MODELING (STATE-OF-THE-ART)	20
2.1 SUMMARY	20
2.2 BACKGROUND	20
2.3 INITIAL CONDITIONS	21
2.4 SPREAD MODELS	22
2.5 FIRESTORM MODELS	23
2.6 WILDLAND FIRES	24
3 ANALYSIS OF ROTHERMEL RATE OF SPREAD EQUATION	25
3.1 SUMMARY AND CONCLUSIONS	25
3.2 THEORETICAL BASIS	27
3.2.1 Effective Heating Number	29
3.2.2 Propagating Flux	29
3.2.3 Reaction Intensity	29
3.2.4 The Effects of Wind and Slope	30
3.3 EMPIRICAL DEFINITIONS	31

## TABLE OF CONTENTS (continued)

<u>Section</u>	<u>Page</u>
3.4 GENERALIZATION OF THE ROTHERMEL RATE OF SPREAD (RROS) EQUATION	31
3.5 PROPAGATION MODEL EMBODYING THE RROS EQUATION	41
3.5.1 Fire Front Propagation Algorithm (FFPA)	41
3.5.2 Local Directional Spread Rate Algorithm (LDSR )	45
3.6 ANALYSIS OF THE RROS EQUATION	50
4 URBAN MASS FIRE BEHAVIOR MODEL CONCEPT	54
4.1 INTRODUCTION	54
4.2 MODEL ALTERNATIVES	57
4.2.1 Detailed Hydrodynamic Calculation	57
4.2.2 Low-Resolution (Lumped-Parameter) Hydrodynamic Calculation	58
4.2.3 Parameterized Multiple Plumes	59
4.3 ATMOSPHERIC MOTION	60
4.3.1 Single Fire Plumes	64
4.3.2 Multiple Fire Plumes and Area Fires	70
4.4 PROPAGATION BY BRANDING	73
4.4.1 Brand Transport	73
4.4.2 Fire Parameters and Brand Production	76
4.4.3 Branding Discussion	78
4.5 CONTIGUOUS FIRE SPREAD (CONTAGION)	79
4.5.1 Summary of Contagion Concepts	80
4.6 CONCEPT SUMMARY	83
5 DESCRIPTION OF DEMONSTRATION URBAN FIRE SIMULATION	85
5.1 DEMONSTRATION SIMULATION STRUCTURE AND OPERATION	85
5.2 DYNAMIC DATA BASE DESCRIPTION	88
5.3 IGNITE MODULE	92
5.4 BURNING CELL UPDATE (BCUPDT) MODULE	104
5.5 ADJACENT CELL UPDATE (ACUPDT) MODULE	116

## TABLE OF CONTENTS (continued)

<u>Section</u>	<u>Page</u>
5.6 FIRE UPDATE (FUPDT) MODULE	135
5.6.1 Fire Geometry (FGEOM) Subroutine	140
5.6.2 Fire Physical Data (FPHYSD) Subroutine	148
5.7 BRANDING (BRANDG) MODULE	151
5.8 OUTPUT MODULES (WVMAP, CSMAP, QMAP)	160
6 EXAMPLE MODEL RESULTS	161
6.1 LARGE AREA FIRE WITH NO AMBIENT WIND	162
6.2 LARGE AREA FIRE WITH 10 M/SEC AMBIENT WIND	178
6.3 LINE FIRE WITH NO AMBIENT WIND	193
6.4 LINE FIRE WITH 10 M/SEC AMBIENT WIND	205
6.5 RING FIRE WITH NO AMBIENT WIND	223
6.6 THREE SMALL FIRES WITH NO AMBIENT WIND	238
6.7 SMALL AREA FIRE WITH AMBIENT WIND	253
REFERENCES	324



Accession For	
NTIS GRA&I	<input checked="checked" type="checkbox"/>
DTIC TAB	<input type="checkbox"/>
Unannounced	<input type="checkbox"/>
Justification	
By	
Distribution/	
Availability Codes	
Dist	Avail and/or Special
A	

## LIST OF ILLUSTRATIONS

<u>Figure</u>		<u>Page</u>
3-1	The set of points defining the perimeter at $T_0$ .	44
3-2	The outward direction at each point.	44
3-3	Preliminary perimeter at $T_1$ .	44
3-4	Final perimeter at $T_1$ .	44
3-5	Graphical representation of RROS model output components.	47
4-1	Small area fire.	61
4-2	Separated small area fires.	63
4-3	Large area fire (spontaneous break-up into separate flame columns). "Countryman Descriptive Model."	63
4-4	Plume geometry and sinks.	65
4-5	Non-dimensional velocity functions of single vertical plane.	68
4-6	Contagion across streets.	81
5-1	Block diagram of demonstration urban fire model.	86
5-2	Logic flow of IGNITE module.	93
5-3	Logic flow of burning cell initialization module.	95
5-4	Logic flow of wind velocity subroutine.	101
5-5	Functional form of cell heat production rate.	106
5-6	Logic flow of burning cell update module.	107
5-7	Adjacent cell update module.	117
5-8	Logic flow of fire update module.	136
5-9	Logic flow of fire geometry subroutine.	141
5-10	Example of fire-subfire partitioning.	146
5-11	Logic flow of fire physical data subroutine.	149
5-12	Logic flow for branding module.	152
5-13	Logic flow for typical MAP module.	159

## LIST OF ILLUSTRATIONS (continued)

<u>Figure</u>		<u>Page</u>
6-1	Cell state map for area fire.	164
6-1(a)	Cell state map for area fire.	165
6-1(b)	Cell state map for area fire.	166
6-1(c)	Cell state map for area fire.	167
6-1(d)	Cell state map for area fire.	168
6-1(e)	Cell state map for area fire.	169
6-1(f)	Cell state map for area fire.	170
6-1(g)	Cell state map for area fire.	171
6-1(h)	Heat production rate contour for area fire.	172
6-1(i)	Heat production rate contour for area fire.	173
6-1(j)	Cell heat production rate map for area fire.	174
6-1(k)	Cell heat production rate map for area fire.	175
6-1(l)	Cell heat production rate map for area fire.	176
6-1(m)	Wind velocity map for area fire.	177
6-2	Cell state map for area fire with 10 m/s ambient wind.	179
6-2(a)	Cell state map for area fire with .10 m/s ambient wind.	180
6-2(b)	Cell state map for area fire with .10 m/s ambient wind.	181
6-2(c)	Cell state map for area fire with .10 m/s ambient wind.	182
6-2(d)	Cell state map for area fire with .10 m/s ambient wind.	183
6-2(e)	Cell state map for area fire with .10 m/s ambient wind.	184
6-2(f)	Cell state map for area fire with .10 m/s ambient wind.	185
6-2(g)	Cell state map for area fire with .10 m/s ambient wind.	186
6-2(h)	Heat production rate contour for area fire with .10 m/s ambient wind.	187
6-2(i)	Heat production rate contour for area fire with .10 m/s ambient wind.	188
6-2(j)	Cell heat production rate map for area fire with .10 m/s ambient wind.	189
6-2(k)	Cell heat production rate for area fire with .10 m/s ambient wind.	190

## LIST OF ILLUSTRATIONS (continued)

<u>Figure</u>		<u>Page</u>
6-2(l)	Wind velocity map for area fire with .10 m/s ambient wind.	191
6-2(m)	Wind velocity map for area fire with 10 m/s ambient wind.	192
6-3	Cell state map for line fire.	194
6-3(a)	Cell state map for line fire.	195
6-3(b)	Cell state map for line fire.	196
6-3(c)	Cell state map for line fire.	197
6-3(d)	Cell state map for line fire.	198
6-3(e)	Cell state map for line fire.	199
6-3(f)	Cell state map for line fire.	200
6-3(g)	Cell state map for line fire.	201
6-3(h)	Heat production rate contour for line fire.	202
6-3(i)	Heat production rate contour for line fire.	203
6-3(j)	Cell heat production rate map for line fire.	204
6-3(k)	Cell heat production rate map for line fire.	205
6-3(l)	Wind velocity map for line fire.	206
6-3(m)	Wind velocity map for line fire.	207
6-4	Cell state map for line fire with .10 m/s ambient wind.	209
6-4(a)	Cell state map for line fire with .10 m/s ambient wind.	210
6-4(b)	Cell state map for line fire with .10 m/s ambient wind.	211
6-4(c)	Cell state map for line fire with .10 m/s ambient wind.	212
6-4(d)	Cell state map for line fire with .10 m/s ambient wind.	213
6-4(e)	Cell state map for line fire with .10 m/s ambient wind.	214
6-4(f)	Cell state map for line fire with .10 m/s ambient wind.	215
6-4(g)	Cell state map for line fire with .10 m/s ambient wind.	216
6-4(h)	Heat production rate contour map for line fire with .10 m/s ambient wind.	217
6-4(i)	Heat production rate contour map for line fire with .10 m/s ambient wind.	218

## LIST OF ILLUSTRATIONS (continued)

<u>Figure</u>	<u>Page</u>
6-4(j) Cell heat production rate map for line fire with .10 m/s ambient wind.	219
6-4(k) Cell heat production rate map for line fire with .10 m/s ambient wind.	220
6-4(l) Wind velocity for line fire with .10 m/s ambient wind.	221
6-4(m) Wind velocity for line fire with .10 m/s ambient wind.	222
6-5 Cell state map for ring fire.	224
6-5(a) Cell state map for ring fire.	225
6-5(b) Cell state map for ring fire.	226
6-5(c) Cell state map for ring fire.	227
6-5(d) Cell state map for ring fire.	228
6-5(e) Cell state map for ring fire.	229
6-5(f) Cell state map for ring fire.	230
6-5(g) Cell state map for ring fire.	231
6-5(h) Heat production rate contour map for ring fire.	232
6-5(i) Heat production rate contour map for ring fire.	233
6-5(j) Cell heat production rate map for ring fire.	234
6-5(k) Cell heat production rate map for ring fire.	235
6-5(l) Wind velocity map for ring fire.	236
6-5(m) Wind velocity map for ring fire.	237
6-6 Cell state map for three clump fires.	239
6-6(a) Cell state map for three clump fires.	240
6-6(b) Cell state map for three clump fires.	241
6-6(c) Cell state map for three clump fires.	242
6-6(d) Cell state map for three clump fires.	243
6-6(e) Cell state map for three clump fires.	244
6-6(f) Cell state map for three clump fires.	245
6-6(g) Cell state map for three clump fires.	246
6-6(h) Heat production rate contour for three clump fires.	247

## LIST OF ILLUSTRATIONS (continued)

<u>Figure</u>	<u>Page</u>
6-6(i) Heat production rate contour for three clump fires.	248
6-6(j) Cell heat production rate map for three clump fires.	249
6-6(k) Cell heat production rate map for three clump fires.	250
6-6(l) Wind velocity map for three clump fires.	251
6-6(m) Wind velocity map for three clump fires.	252
6-7 Cell state map for small area fire with ambient wind = 10 m/s.	254
6-7(a) Cell state map for small area fire with ambient wind = 10 m/s.	255
6-7(b) Cell state map for small area fire with ambient wind = 10 m/s.	256
6-7(c) Cell state map for small area fire with ambient wind = 10 m/s.	257
6-7(d) Cell state map for small area fire with ambient wind = 10 m/s.	258
6-7(e) Cell state map for small area fire with ambient wind = 10 m/s.	259
6-7(f) Cell state map for small area fire with ambient wind = 10 m/s.	260
6-7(g) Cell state map for small area fire with ambient wind = 10 m/s.	261
6-7(h) Heat production rate contour for small area fire with ambient wind = 10 m/s.	262
6-7(i) Heat production rate contour for small area fire with ambient wind = 10 m/s.	263
6-7(j) Cell heat production rate map for small area fire with ambient wind = 10 m/s.	264
6-7(k) Cell heat production rate map for small area fire with ambient wind = 10 m/s.	265
6-7(l) Wind velocity map for small area fire with ambient wind = 10 m/s.	266
6-7(m) Wind velocity map for small area fire with ambient wind = 10 m/s.	267
6-8 Cell state map for small area fire, ambient wind = 20 m/s.	268



# LIST OF ILLUSTRATIONS (continued)

<u>Figure</u>		<u>Page</u>
6-8(a)	Cell state map for small area fire, ambient wind = 20 m/s.	269
6-8(b)	Cell state map for small area fire, ambient wind = 20 m/s.	270
6-8(c)	Cell state map for small area fire, ambient wind = 20 m/s.	271
6-8(d)	Cell state map for small area fire, ambient wind = 20 m/s.	272
6-8(e)	Cell state map for small area fire, ambient wind = 20 m/s.	273
6-8(f)	Cell state map for small area fire, ambient wind = 20 m/s.	274
6-8(g)	Cell state map for small area fire, ambient wind = 20 m/s.	275
6-8(h)	Heat production rate contour for small area fire, ambient wind = 20 m/s.	276
6-8(i)	Heat production rate contour for small area fire, ambient wind = 20 m/s.	277
6-8(j)	Cell production rate map for small area fire, ambient wind = 20 m/s.	278
6-8(k)	Cell production rate map for small area fire, ambient wind = 20 m/s.	279
6-8(l)	Wind velocity map for small area fire, ambient wind = 20 m/s.	280
6-8(m)	Wind velocity map for small area fire, ambient wind = 20 m/s.	281
6-9	Cell state map for small area fire, ambient wind = 30 m/s.	282
6-9(a)	Cell state map for small area fire, ambient wind = 30 m/s.	283
6-9(b)	Cell state map for small area fire, ambient wind = 30 m/s.	284
6-9(c)	Cell state map for small area fire, ambient wind = 30 m/s.	285
6-9(d)	Cell state map for small area fire, ambient wind = 30 m/s.	286
6-9(e)	Cell state map for small area fire, ambient wind = 30 m/s.	287
6-9(f)	Cell state map for small area fire, ambient wind = 30 m/s.	288
6-9(g)	Cell state map for small area fire, ambient wind = 30 m/s.	289
6-9(h)	Heat production rate contour for small area fire, ambient wind = 30 m/s.	290
6-9(i)	Heat production rate contour for small area fire, ambient wind = 30 m/s.	291

# LIST OF ILLUSTRATIONS (continued)

<u>Figure</u>		<u>Page</u>
6-9(j)	Cell heat production rate map for small area fire, ambient wind = 30 m/s.	292
6-9(k)	Cell heat production rate map for small area fire, ambient wind = 30 m/s.	293
6-9(l)	Wind velocity map for small area fire, ambient wind = 30 m/s.	294
6-9(m)	Wind velocity map for small area fire, ambient wind = 30 m/s.	295
6-10	Cell state map for small area fire, ambient wind = 40 m/s.	296
6-10(a)	Cell state map for small area fire, ambient wind = 40 m/s.	297
6-10(b)	Cell state map for small area fire, ambient wind = 40 m/s.	298
6-10(c)	Cell state map for small area fire, ambient wind = 40 m/s.	299
6-10(d)	Cell state map for small area fire, ambient wind = 40 m/s.	300
6-10(e)	Cell state map for small area fire, ambient wind = 40 m/s.	301
6-10(f)	Cell state map for small area fire, ambient wind = 40 m/s.	302
6-10(g)	Cell state map for small area fire, ambient wind = 40 m/s.	303
6-10(h)	Heat production rate for small area fire, ambient wind = 40 m/s.	304
6-10(i)	Heat production rate for small area fire, ambient wind = 40 m/s.	305
6-10(j)	Heat production rate for small area fire, ambient wind = 40 m/s.	306
6-10(k)	Cell heat production rate map for small area fire, ambient wind = 40 m/s.	307
6-10(l)	Wind velocity map for small area fire, ambient wind = 40 m/s.	308

# LIST OF ILLUSTRATIONS (concluded)

<u>Figure</u>	<u>Page</u>
6-10(m) Wind velocity map for small area fire, ambient wind = 40 m/s.	309
6-11 Cell state map for small area fire, ambient wind = 50 m/s.	310
6-11(a) Cell state map for small area fire, ambient wind = 50 m/s.	311
6-11(b) Cell state map for small area fire, ambient wind = 50 m/s.	312
6-11(c) Cell state map for small area fire, ambient wind = 50 m/s.	313
6-11(d) Cell state map for small area fire, ambient wind = 50 m/s.	314
6-11(e) Cell state map for small area fire, ambient wind = 50 m/s.	315
6-11(f) Cell state map for small area fire, ambient wind = 50 m/s.	316
6-11(g) Cell state map for small area fire, ambient wind = 50 m/s.	317
6-11(h) Heat production rate contour map for small area fire, ambient wind = 50 m/s.	318
6-11(i) Heat production rate contour map for small area fire, ambient wind = 50 m/s.	319
6-11(j) Cell heat production rate map for small area fire, ambient wind = 50 m/s.	320
6-11(k) Cell heat production rate map for small area fire, ambient wind = 50 m/s.	321
6-11(l) Wind velocity map for small area fire, ambient wind = 50 m/s.	322
6-11(m) Wind velocity map for small area fire, ambient wind = 50 m/s.	323

## LIST OF TABLES

<u>Table</u>		<u>Page</u>
3-1	Defining equations for RROS equation	32
3-2	RROS equation input parameters	34
3-3	RROS equation input parameters within the i-th fuel category and j-th fuel size class of each fuel cell	36
3-4	RROS equation variables summary	52

## SECTION 1

### INTRODUCTION

This section presents information that is introductory to the following sections. However, it goes beyond a simple introduction by incorporating a summary of this report together with conclusions drawn from the work performed, and recommendations regarding future related work.

#### 1.1 BACKGROUND

The purpose of developing a model of urban mass fires is to predict the spread, development, and ultimate effects of uncontrolled urban fires. The model predictions need to be in sufficient detail and accuracy to provide decision makers with information regarding the mitigation and/or encouragement of selected mass fire effects. As always, the ideal is precise and accurate predictions. However, the detail and precision that can be useful to decision makers may be far less than that required by fire phenomenology researchers.

For these reasons, and in the interest of providing decision makers with a (minimally useful) model as early as possible, we have defined a mass fire model concept and developed a demonstration implementation of the concept. It is anticipated that the phenomenology models employed may be criticized as being premature, imprecise, and/or insufficiently substantiated by empirical data. We agree, beforehand, with these allegations. The evolutionary concept of simulation development demands that the physical models be continuously subject to improvement.

This work is concerned with simulating fires initiated in urban areas by nuclear detonations. Such fires are characterized by a large number of more or less simultaneous ignitions distributed over an area perhaps hundreds of square kilometers in extent. The only fire behavior experience, which approaches these circumstances, is limited to the mass fires of World War II. These mass fires resulted from conventional incendiary bombing of German and Japanese cities and from the nuclear detonations over Hiroshima and Nagasaki. In addition, some large wildland fires, burning in heavy fuels and rapidly propagating by branding far ahead of the main fire front, may have produced sufficient densities of discrete ignitions to have approximated mass fire conditions.

Observer reports and ex post facto reconstructions of these events establish some qualitative and semiquantitative features of mass fires, which a valid model must replicate, but which alone cannot furnish a sufficient basis for developing a model of mass fire behavior. A model of urban mass fire behavior, thus, cannot be totally based upon the results of full scale empirical observations. The data are either inadequate or nonexistent, and are likely to remain so. Enough documented fire behavior experience does exist, however, to provide critical checks upon the results of any mass fire behavior model. For example, a useful fire behavior model should replicate the development of the Hamburg fire storm, as well as the failure of fire storms to develop in Berlin.

In the development of a computerized simulation of physical phenomena, it is important to address the computational basis of the simulation as well as its physical basis. Complete knowledge of the relevant physical processes will not assure development of a useful simulation, unless suitably timely, detailed, accurate, and economical computations are possible.

The work described in this report addresses both of these aspects of the problem by describing a concept for a computerized simulation of mass fire behavior, which incorporates physically based fire phenomenology models.

## **1.2 CONCLUSIONS AND RECOMMENDATIONS**

The most important results of this work are the model concept and the demonstration model. The demonstration model is an implementation of the model concept in simplified form. The demonstration model shows the feasibility of developing a computerized simulation of mass fires based on the concept described in Section 4. Additionally, the demonstration model has potential for both short-term and long-term utility.

In the short term, it is recommended that the physical realism of the fire phenomenology models be improved, that the simulation be calibrated and that parametric results be generated. In the construction of the demonstration model, it was not possible to address the fire phenomenology models in the required detail. Consequently, a great deal of improvement in overall model realism can be accomplished with a modest investment to improve the phenomenology models.

### **1.2.1 Hydrodynamic Modeling**

The total atmospheric perturbation, and the part of it describing street level winds, is essential not only to describe mass fire conditions but also to model the spread and development of an urban mass fire. The coarse resolution global atmospheric hydrodynamics of a large area fire is a useful, but limited, approach. Both experimental and theoretical evidence indicates that the actual distribution of separated fires, and the spontaneous breakup of area fires into separate columns exercise major influence upon fire-induced winds. Not necessarily to the

exclusion of other approaches, our model concept opts for a hydrocalculation based upon parameterized multiple plume properties, which can incorporate the requisite resolution. The feasibility, in principle, of this approach is shown by the demonstration model, but further investigation and theoretical study is required to develop these ideas into reliable computational procedures.

### **1.2.2 Branding and Contagion**

Limits of spatial resolution, uncertainties of fuel properties, and insufficient understanding of phenomenology are difficulties that models of spread mechanisms in urban fires must confront, even when hydrodynamic flow fields are specified. Our demonstration model includes the two propagation mechanisms of branding and contagion (flaming contact). Radiative ignition is omitted, but could be included as well. Some aspects of these spread mechanisms are amenable to simple physical estimation. An important goal is to improve the estimates and extend the areas in which estimates can be made beyond the level presently employed in the demonstration model. Where possible, physical estimates inspire confidence not otherwise obtainable. In view of the difficulties mentioned above, there are definite limits upon these physical refinements and the degree to which they could be used to model propagation mechanisms. Recognition of these limits and their implications for modeling procedures is an important research effort in model development.

### **1.2.3 Simulation Grid and Subgrid Characteristics**

From consideration of the tradeoffs between the desire for detail and accuracy, and the need for computational economy and storage efficiency, it was decided that the demonstration model would employ a spatial grid of city block sized elements (i.e., cells). Over these cells, uniform values of variables and effects would be assumed. For



example, a cell would be characterized by a fuel type, the wind velocity would be constant over a cell, and combustion would be (spatially) uniform over a cell. City block sized grid cells are physically appropriate in that each cell is, thus, surrounded by a line fuel break (i.e., street) of specifiable width. In this grid configuration, the fire, in order to spread, must be able to propagate over the streets. In the process of developing and debugging the demonstration simulation, it became clear that the city block sized resolution was insufficient to describe effects to a city block sized level of detail. For example, ignition of a non-burning cell by a burning cell depends on how and where the fuel is burning within the ignited cell. Indeed, it was necessary to incorporate some subgrid detail in the demonstration model. The grid structure employed and the nature and detail of the subgrid calculations can significantly impact the computational economy and storage efficiency of any mass fire model. For these reasons, it is recommended that a more detailed study be made of the simulation grid structure and the nature and detail of the subgrid calculations to be employed. This study should recognize that these two subjects are not independent and that they both relate to the problem of fuel specification.

The simulation can be calibrated against historical data on large fires and should be able to replicate at least gross details of known situations. A model, calibrated to even this degree, is of potential use to decision makers. Parametric studies of historical fires in which selected parameters are varied to produce fire effects as a function of the varied parameter will provide additional, sensitivity information for use by decision makers.

In the long term, the structure of the demonstration model will provide the vehicle for an evolving mass fire simulation. An intimate understanding of the need for, and the nature of evolving simulations is explicit in the design of the demonstration model structure. It readily

allows for modification of existing, or incorporation of new, computation processes and data types.

### 1.3 SUMMARY

Section 2 presents a succinct description of the state-of-the-art in urban mass fire modeling. An exhaustive review of the literature was not attempted; however, the important sources are discussed and referenced. It was found that, although work is in progress on the constituent parts of a mass fire behavior model, no satisfactory model exists.

Section 3 describes the USDA Forest Service-developed Rothermel model that has been used to predict the behavior of fires in lower level (grass, brush, etc.) wildland fuels. The Rothermel model is described in considerable detail in order to clearly point out why it is considered inappropriate for describing fires in an urban environment.

Section 4 presents the physical basis for a computerized simulation of the initialization and spread of uncontrolled urban fires, including the onset and development of mass fires. Such a simulation must incorporate physically based models of all the pertinent phenomena. These models must parametrically define cause-effect relationships for all of the important variables and variable interactions involved in the effects to be simulated. The required physically-based phenomenology models are described and discussed in detail. Particular emphasis is placed on the development of useful (as opposed to ideal) phenomenological models for timely incorporation in a mass fire simulation.

Section 5 presents the computational basis for a computerized simulation of urban mass fires. A demonstration version of the simulation is described in terms of the overall simulation structure, the mathematical and logic structure of each major model, and data entry, management, and output.

Section 6 presents sample results for eleven example cases. These cases involve different initial ignition densities and patterns, together with different initial ambient wind conditions. These results show the initiation and development of uncontrolled urban fires in terms of fire geometry, heat production rates, and wind velocities.

## SECTION 2

### MASS FIRE MODELING (STATE-OF-THE-ART)

#### 2.1 SUMMARY

There presently exists no satisfactory model by which the development of nuclear-induced urban fires may be described. Research into the constituent mechanisms required as components of such a model is in progress, but model development need not wait for this research to be completed. Modeling is possible at any state of knowledge, and, with proper structuring, can be done in an open-ended fashion to incorporate new knowledge when it develops.

Significant advances of understanding have been acquired since the existing models were devised. The need to incorporate fire spread and mass fire phenomena as related parts of a unified simulation is the major requirement, which can be met at this time. The potentially lengthy and costly effort to determine fuel properties and inventories can be guided by the degree to which any practical model can make use of them.

#### 2.2 BACKGROUND

The initiation, development, and effects of mass fires resulting from nuclear attack on urban areas has been a problem of concern since the advent of nuclear weapons. Investigations motivated by this problem have amassed a volume of material, dealing with its various aspects, which is summarized in the review of Martin (Reference 1), supplemented by the recent report of Small and Brode (Reference 2). Both of these documents

contain extensive bibliographies. Since 1978, the Defense Civil Preparedness Agency, now part of the Federal Emergency Management Agency, has sponsored an integrated research program aimed at achieving a reliable method for predicting the incendiary outcome of nuclear attack. A periodic report and assessment of this program has been published yearly (References 3 and 4). The following discussion here does not attempt to repeat these general surveys, but focuses specifically upon certain modeling problems.

### 2.3 INITIAL CONDITIONS

Much of the previous and presently ongoing research is devoted to establishing the initial fire conditions resulting from nuclear attack. The effect of the thermal pulse, as modified by distance and atmospheric conditions, in producing ignition of various inflammable materials exposed to it; the potential of these ignitions to spread and result in full building involvement; and the effect of blast to (1) alter substantially the fuel properties and distribution; (2) to extinguish or enhance primary ignitions; and (3) to produce secondary ignitions by breakage of gas and power lines are all important aspects of the initiation problem (Reference 4). These very important processes, which others are investigating, are not our direct concern here. Given the initial conditions (of both ignitions and fuel), we are interested in modeling the fire development.

Though not our immediate concern, the faithful incorporation of these very detailed mechanisms to initialize a model is an outstanding problem. Given uncertainties of structural behavior and the impossibility of resolving small detail in a city-wide simulation, some judicious modeling choices are required, even assuming adequate understanding of basic mechanisms.

## 2.4 SPREAD MODELS

Existing fire spread models are reviewed by Weisbecker and Lee (Reference 5) and Alger and Martin (Reference 3). Many models of fire spread within compartments and buildings have been built, but attempts at spread models on a city-wide scale are limited to three models. These are the SSI (Scientific Services, Inc.), the URS (URS Research Company), and the IITRI (Illinois Institute of Technology Research Institute) models and their modifications. Relying upon the conclusions of the papers cited above, it appears that all of these models (which were developed in the late 1960's) may suffer serious defects.

All of these models stress fuel distributions, which are incorporated at a level of detail ranging from high detail (actual building and content surveys) in the SSI model to use-factor classification of areas in the URS and IITRI models. Fuel representation does not account for blast damage, which is viewed as a serious restriction. The basic spread mechanism of all these models is radiative contagion, with some simplified spread by firebrands in the IITRI and URS models. The failure to adequately model fire parameters, upon which these processes depend, is considered a shortcoming. In practice these models spread the fire in a stochastic manner, based upon fuel type. A final, and perhaps decisive, criticism of these pioneering models is their lack of any interactive features of mass fire phenomena, fire-induced winds, their effect upon spread, and plume coalescence.

Consistent with the Project Flambeau results, we do not agree with the emphasis upon radiation as a primary spread mechanism, but believe that both branding and flame contact are of equal, if not greater, importance. Mass fire phenomena are essential to determine spread. Without minimizing the true role of fuel properties, it may be that this problem aspect has been overemphasized in the past. Resolution limitations will, in any model, limit the detail of fuel descriptions.

In any case, the accumulation of understanding permits substantial improvement upon these early spread models.

## 2.5 FIRESTORM MODELS

The presence of strong, hurricane-force winds directed radially inward toward the large urban fires of WWII has prompted diverse attempts to understand and model this phenomenon, called a "firestorm."

An analysis of historical experience (Reference 6) established some preliminary conditions thought necessary for firestorm phenomena. By employing historical analysis in conjunction with modeling, Lommanssen, et al (Reference 7) developed buildup and existence criteria for firestorms. Firestorm criteria were also developed (Reference 8) on the basis of WWII experience and empirical data on flame merging.

The need for experimental data motivated two programs to test the behavior of large fires: the Flambeau program (References 9 and 10), and the Euroka fire in Australia (Reference 11), a fire of 260 meter radius. The data from these fires, though none were as large as an urban mass fire, fills an important gap between historical mass fires and laboratory fires. We have found the insights reported by Countryman from the Flambeau program especially valuable.

Aside from fire plume modeling, done by several investigators, the theoretical work of Nielsen (Reference 12) and Nielsen and Tao (Reference 13) specifically models the global hydrodynamics of a large urban fire. Recently, a new approach to atmospheric disturbances and physical parameters of large area fires has been initiated (Reference 2). Some detailed, two-dimensional analytic models of fire plumes in the atmosphere have been published (References 14 through 17).

We believe the hydrodynamic properties of urban mass fires to be of central importance. The extent to which global (low-resolution) hydrodynamics is sufficient needs further examination. The firestorm phenomenon, however, is only one aspect of the problem. The hydrodynamic modeling must be broadly enough structured to encompass any developmental behavior which occurs. A good part of the problem is to understand what can happen.

## 2.6 WILDLAND FIRES

Our task excludes wildland fires, but any discussion of the state-of-the-art for modeling large fires must take cognizance of the Rothermel Model (Reference 18), which occupies a unique status as the only well-verified spread model in existence. This model, its limitations, and possible applicability to the urban fire problem, are examined in detail in Section 3.



### SECTION 3

#### ANALYSIS OF ROTHERMEL RATE OF SPREAD EQUATION

##### 3.1 SUMMARY AND CONCLUSIONS

The Rothermel rate of spread (RROS) equation (Reference 18) for estimating localized rate of fire spread in a homogeneous fuel bed is described in terms of a qualitative theoretical basis and a quantitative empirical definition. Generalizations of the basic rate of spread equation are described that allow estimation of fire spread rates over an area of interest in heterogeneous, natural understory fuels. It is shown that local scalar spread rate is necessary but insufficient to allow fire growth estimates to be made. A fire front propagation algorithm and a local directional spread rate algorithm are described, together with local scalar spread rate, that provide a computational procedure for estimating the growth of wildland fires. Difficulties associated with input data acquisition and data management resulting from the fuel characteristics required by the rate of spread equation are discussed and their resolution is described.

The Rothermel rate of spread equation is demonstrably suitable (Reference 19) for estimating the growth of free burning fires in lower story, natural fuels. From the analyses described here, and in the referenced report, it is concluded that the Rothermel equation is of limited utility in estimating the growth of urban fires for the following reasons:

1. The quantitative coefficients of the RROS equation are valid only for understory natural fuels (i.e., grass, brush, etc.). They were experimentally determined from

laboratory fires in continuous fuel beds where the fuel was simulated by uniform, homogeneous constructs of uniform fuel particles and the environment was simulated by a wind tunnel.

2. The fire front propagation and local directional spread rate algorithms, required for wildland fire growth estimates were developed specifically for understory natural fuels and are not applicable to estimating the growth of fires in an urban fire environment.
3. It is explicit in the quantitative coefficients of the RROS equation that wildland fires in natural understory fuels are largely propagated by the combustion of loosely packed fine fuels at the periphery of the fire; loosely packed fine fuels do not occur in significant quantities in urban fuel beds.
4. The RROS equation describes a free burning fire in which venting effects are quantitatively controlled by fuel packing. In an urban fire venting effects are generally controlled by the building structure within which the fire is burning.
5. Wind effects in the RROS equation are open loop; it has wind-fire coupling, but no fire-wind coupling.
6. The effects of branding are not addressed by the RROS equation.
7. It is not economically nor physically practicable to experimentally quantify the detailed interparticle heat exchange mechanisms for all urban fuels of interest in analogy with the experiments that were performed for natural fuels.
8. There is no mechanism in the RROS for allowing fire propagation across a break in the fuel bed, analogous to a street in the urban environment.

The RROS can be used to describe fire growth in significant areas of natural fuels within the urban environments of interest. Even for this purpose, however, modifications will be necessary to account for trees and the energy release rate of unconsumed fuels burning within the fire perimeter. These conclusions regarding the inapplicability of the RROS equation to the growth of urban fires contribute nothing positive toward the solution of this problem. However, Section 4 of this report presents a methodology for describing the growth of fires in urban environments of interest.

### 3.2 THEORETICAL BASIS

The theoretical basis of the RROS is largely due to Fons (Reference 20), Tarifa and Torralbo (Reference 21), and Frandsen (Reference 22). Fons was the first to describe fire spread by a mathematical model. The Fons model embodied a contagion concept in which fire spread in a fuel bed is considered to consist of successive ignitions occurring at a rate controlled primarily by the ignition times and distances between successive fuel particles. Tarifa and Torralbo confirmed Fons' ideas by showing that heating of the fuel ahead of a progressing flame front is the first and most essential process of the flame propagation mechanism. Frandsen applied the principle of energy conservation to a unit volume of fuel ahead of an advancing flame front in a homogeneous fuel bed to obtain the following expression for the quasi-steady rate of fire spread:

$$R = \frac{I_{xig} + \int_{-\infty}^0 (\partial I_z / \partial z)_{z_c} dx}{\rho_{be} Q_{ig}} \quad (3-1)$$

where

$R$  = quasi-steady rate of spread (ft/min)

$I_{xig}$  = horizontal heat flux absorbed by a unit volume of fuel at the time of ignition (Btu/ft<sup>2</sup>-min)

$\rho_{be}$  = effective bulk density (the amount of fuel per unit volume of the fuel bed raised to ignition temperature ahead of the advancing fire) (lb/ft<sup>3</sup>)

$(\partial I_z / \partial z)_{z_c}$  = the gradient of the vertical intensity evaluated in a plane at a constant depth,  $z_c$ , of the fuel bed (Btu/ft-min)

$Q_{ig}$  = heat of ignition of unit volume of fuel (Btu/lb).

Equation 3-1 is a theoretically rigorous description of the rate of spread of a line fire through a homogeneous fuel bed of uniform depth in terms of a ratio of the heat flux received by, to the heat required for ignition of, a unit volume of fuel ahead of the advancing flame front. Equation 3-1 contains heat flux terms for which the mechanisms of heat transfer are not known, and consequently, it cannot be solved analytically. Definition of an approximate form of Equation 3-1 that can be solved analytically resulted from examination of each term and determination of analytical and empirical methods for evaluating the unknown mechanisms of heat transfer (Reference 18).

The form of Equation 3-1 was simplified by the definition of the following set of terms.

### 3.2.1 Effective Heating Number

The amount of fuel involved in the ignition process is specified in the denominator of Equation 3-1 as the effective bulk density  $\rho_{be}$ . The effective heating number  $\epsilon$  is defined as the dimensionless ratio of the effective bulk density to the actual bulk density. Hence,

$$\epsilon = \rho_{be} / \rho_b \quad (3-2)$$

### 3.2.2 Propagating Flux

The numerator of 3-1 is defined to be the propagating flux  $I_p$  where

$$I_p = I_{xig} + \int_{-\infty}^0 (\partial I_z / \partial z)_{z_c} dx \quad (3-3)$$

The propagating flux consists of two terms, the horizontal flux and the cumulative gradient of the vertical flux up to the fire front. The vertical flux is most significant for wind driven and upslope fires, for which there is an effective flame tilt and an increased heat transfer to the unignited fuel by radiation, convection, and conduction. It is assumed that the vertical flux is small for no slope, no wind fires; and the heat flux for these conditions is defined as

$$(I_p)_0 = I_{xig} \quad (3-4)$$

### 3.2.3 Reaction Intensity

The energy release rate of the fire front produced by burning gases resulting from pyrolysis of the fuel bed ahead of the fire front is defined as the reaction intensity  $I_r$  where

$$I_r = -h(dw/dt) \quad (3-5)$$

and

$dw/dt$  = mass loss rate per unit area in the fire front, (lb/ft<sup>2</sup>-min)

$h$  = heat content of fuel (Btu/lb).

The reaction intensity is the source of the no wind propagating flux,  $(I_p)_0$ , and it is assumed that the no wind propagating flux and the reaction intensity  $I_r$  can be evaluated independently and then correlated. Thus, the coefficient relating  $(I_p)_0$  and  $I_r$  is

$$\xi = \frac{(I_p)_0}{I_r} \quad (3-6)$$

Knowledge of this correlation will allow  $(I_p)_0$  to be determined from  $I_r$ , which can be determined from parameters that describe the fuel bed complex.

#### 3.2.4 The Effects of Wind and Slope

The effects of wind and slope are defined as changes in the propagating heat flux, that alter the heat received by potential fuels due to convection and radiation. Based on the assumptions that the contribution of the vertical intensity ( $\partial I/\partial z$ ) to  $(I_p)_0$  is small and that the effects of wind and slope on the propagating flux are independent, the total propagating flux is defined to be of the form

$$I_p = (I_p)_0 \cdot (1 + \phi_w + \phi_s) \quad (3-7)$$

where

$\phi_w$  = a dimensionless coefficient dependent on wind speed,

$\phi_s$  = a dimensionless coefficient dependent on slope.

### 3.3 EMPIRICAL DEFINITIONS

Substitution of Equations 3-2 through 3-7 into Equation 3-1 yields the Rothermel rate of spread (RROS) equation in the form

$$R = I_r \epsilon \frac{(1 + \phi_w + \phi_s)}{\rho_b \epsilon Q_{fg}} \quad (\text{ft/min}) \quad (3-8)$$

Each term of Equation 3-7 was analyzed and transformed into a format appropriate for experimental quantification. This resulted in a set of experimentally determined relationships by which rate of spread estimates can be obtained from 3-8 in terms of parameters describing the fuel bed, terrain slope, and wind speed (Reference 18). These experimentally determined relationships (Reference 7) are given in Table 3-1.

The use of Equations 3-8 through 3-26 to provide estimation of fire spread rate requires specification of the parameters shown in Table 3-2.

### 3.4 GENERALIZATION OF THE ROTHERMEL RATE OF SPREAD (RROS) EQUATION

The RROS equation given by Equations 3-8 through 3-26 provides local rate of spread in a homogeneous fuel bed. Use of the RROS equation in describing a propagating fire front necessitates generalization to include spread rates for heterogeneous fuels distributed over an area.

Table 3-1. Defining equations for RROS equation.

Equation	Description	Equation Number
$I_r = r' w_n h n_M n_s$	Reaction intensity (Btu/ft <sup>2</sup> -min)	(3-9)
where:		
$r' = r'_{\max} (\beta/\beta_{op})^A \exp[A(1-\beta/\beta_{op})]$	Optimum reaction velocity (min <sup>-1</sup> )	(3-10)
$r'_{\max} = \sigma^{1.5} (495 + .0594\sigma^{1.5})^{-1}$	Maximum reaction velocity (min <sup>-1</sup> )	(3-11)
$\beta_{op} = 3.348\sigma^{-.8189}$	Optimum packing ratio	(3-12)
$A = 1/(4.774\sigma^{.1} - 7.27)$		(3-13)
$\eta_M = 1 - 2.59 \frac{M_f}{M_x} + 5.11 \left(\frac{M_f}{M_x}\right)^2 - 3.52 \left(\frac{M_f}{M_x}\right)^3$	Moisture dampening coefficient	(3-14)
$\eta_s = 0.174 e_S^{-.19}$	Mineral damping coefficient	(3-15)
$\xi = (192 + 0.2595\sigma)^{-1} \times \exp[0.792 + 0.681\sigma^{.5}](\beta + 0.1)]$	Propagating flux ratio	(3-16)
$\phi_w = CU^B \left(\frac{\beta}{\beta_{op}}\right)^{-E}$	Wind coefficient	(3-17)
$C = 7.47 \exp(-0.133\sigma^{.55})$		(3-18)
$B = 0.02526\sigma^{.54}$		(3-19)
$E = 0.715 \exp(-3.59 \times 10^{-4}\sigma)$		(3-20)



Table 3-1. Defining equations for RROS equations (concluded).

$W_n = \frac{w_o}{1 + S_T}$	Net fuel loading (lb/ft <sup>2</sup> )	(3-21)
$\phi_s = 5.275 \beta^{-.3} (\tan \phi)^2$	Slope factor	(3-22)
$\rho_b = w_o / \delta$	Ovendry bulk density (lb/ft <sup>3</sup> )	(3-23)
$\epsilon = \exp(-138/\sigma)$	Effective heating number	(3-24)
$Q_{ig} = 250 + 1,116 M_f$	Heat of pre- ignition (Btu/lb)	(3-25)
$\beta = \frac{\rho_b}{\rho_p}$	Packing ratio	(3-26)

Table 3-2. PROS equation input parameters.

Parameter	Description
$w_o$	oven dry fuel loading (lb/ft <sup>2</sup> )
$h$	fuel particle low heat content (Btu/lb)
$\rho_p$	ovendry particle density (lb/ft <sup>3</sup> )
$M_f$	fuel particle moisture content ( $\frac{\text{lb moisture}}{\text{lb ovendry wood}}$ )
$S_T$	fuel particle total mineral content ( $\frac{\text{lb minerals}}{\text{lb ovendry wood}}$ )
$S_e$	fuel particle effective material content ( $\frac{\text{lb silica-free minerals}}{\text{ovendry wood}}$ )
$U$	wind velocity at midflame height (ft/min)
$\tan \phi$	slope, vertical rise/horizontal distance
$M_x$	moisture content of extinction.

A generalization of the RROS equation to include heterogeneous fuels is described in Reference 18 (pp. 28-33). This generalization allows definition of an arbitrary number of uniformly distributed fuel categories and size classes. For natural, understory fuels, two categories (live and dead) and four to five size classes are used. Since neither all size classes nor all categories are equally effective in fire front propagation, a weighting procedure is described in Reference 18 for combining the descriptions of understory fuel size classes and categories into a single spread rate.

A generalization to allow computation of spread rates over an area is accomplished by defining a computational mesh over the area of interest and specifying all of the parameters required for the RROS equation in each cell of the mesh. The specification of mean parameter values for the i-th fuel category and j-th fuel size class requires estimation of each input parameter shown in Table 3-3 for each cell of the computational mesh.

Two weighting parameters based on the surface area of the fuel within each category and size class are defined by

$$f_{ij} = \frac{\bar{A}_{ij}}{\bar{A}_i} \quad \text{Ratio of surface area of the j-th size class to total surface of the i-th category per unit fuel cell} \quad (3-27)$$

and

$$f_i = \frac{\bar{A}_i}{\bar{A}_T} \quad \text{Ratio of surface area of the i-th category to total surface area per unit fuel cell.} \quad (3-28)$$

Table 3-3. RROS equation input parameters within the i-th fuel category and j-th fuel size class of each fuel cell.

Parameter	Description
$(\bar{w}_o)_{ij}$	= ovendry loading (lb/ft <sup>2</sup> )
$(\bar{\sigma})_{ij}$	= surface-area-to-volume ratio (ft <sup>2</sup> /ft <sup>3</sup> )
$(\bar{S}_T)_{ij}$	= mineral content (lb minerals/lb wood)
$(\bar{S}_e)_{ij}$	= effective mineral content $\left(\frac{\text{lb minerals} - \text{lb silica}}{\text{lb wood}}\right)$
$(\bar{h})_{ij}$	= low heat value (Btu/lb)
$(\bar{M}_F)_{ij}$	= moisture content (lb moisture/lb wood)
$(\bar{\rho}_p)_{ij}$	= ovendry particle density (lb/ft <sup>3</sup> )
Mean value within the i-th category:	
$(M_X)_i$	= moisture content of extinction (lb moisture/ovendry wood)
Mean fuel array properties:	
$\bar{\delta}$	= depth of fuel (ft)
$\tan \phi$	= slope (ft vertical rise/ft horizontal)
U	= wind velocity at midflame height (ft/min)
m	= total number of categories
n	= number of size classes within the i-th category.

where

$$\bar{A} = \frac{(\bar{\sigma})_{ij} (\bar{w}_o)_{ij}}{(\rho_p)_{ij}}$$

Mean total surface area of fuel of i-th category and j-th size class per unit fuel cell (3-29)

$$\bar{A}_i = \sum_{j=1}^{j=n} \bar{A}_{ij}$$

Mean total surface area of fuel of i-th category per unit fuel cell. (3-30)

$$\bar{A}_T = \sum_{i=1}^{i=m} \bar{A}_i$$

Mean total surface area of fuel per unit cell. (3-31)

In terms of the above weighting factors and the parameters defined in Table 3-3, the reaction intensity is given by

$$I_R = r' \sum_{i=1}^{i=m} f(\tilde{w}_n)_i \tilde{h}_i(\tilde{n}_d)_i (\tilde{n}_M)_i \quad , \quad (3-32)$$

where the characteristic parameters weighted by surface area are as follows:

$$(\tilde{w}_n)_i = \sum_{j=1}^{j=n} f_{ij} (\bar{w}_n)_{ij}$$

Net loading of i-th category (3-33)

$$(\bar{w}_n)_{ij} = \frac{(\bar{w}_o)}{1 + (\bar{S}_T)_{ij}}$$

Net loading of j-th class (3-34)

$$\bar{h}_i = \sum_{j=1}^{j=n} f_{ij} \bar{h}_{ij} \quad \text{Low heat content value of } i\text{-th category} \quad (3-35)$$

$$(\bar{\eta}_s)_i = 0.174(\bar{S}_e)_i^{-.19} \quad \text{Mineral damping coefficient of } i\text{-th category} \quad (3-36)$$

$$(\bar{S}_e)_i = \sum_{j=1}^{j=n} f_{ij} (\bar{S}_e)_{ij} \quad \text{Characteristic effective mineral coefficient of } i\text{-th category} \quad (3-37)$$

$$(\bar{\eta}_M)_i = 1 - 2.59(\bar{r}_M)_i + 5.11(\bar{r}_M)_i^2 - 3.52(\bar{r}_M)_i^3 \quad (3-38)$$

Moisture damping co-efficient of i-th category

$$(\bar{r}_M)_i = \frac{(\bar{M}_f)_i}{(\bar{M}_{ext})_i} \quad \text{Moisture ratio of } i\text{-th category.} \quad (3-39)$$

$$(\bar{M}_f)_i = \sum_{j=1}^{j=n} f_{ij} (\bar{M}_f)_{ij} \quad \text{Moisture content of } i\text{-th category.} \quad (3-40)$$

The potential reaction velocity ( $r'$ ) is an experimentally determined function of the fuel bed packing ratio ( $\beta$ ) and fuel particle size as characterized by fuel particle surface-to-volume ratio ( $\sigma$ ). Thus,

$$r' = r'_{\max} (\bar{\beta}/\bar{\beta}_{op})^A \exp[A(1 - \bar{\beta}/\bar{\beta}_{op})] \quad (3-41)$$

where

$$r'_{\max} = (\bar{\sigma})^{1.5} / (495 + 0.0594 (\sigma)^{1.5}) \quad (3-42)$$

$$\bar{\rho}_{\text{op}} = 3.348 (\bar{\sigma})^{0.8189} \quad (3-43)$$

$$A = (4.774 (\bar{\sigma})^{0.1} - 7.27)^{-1} \quad (3-44)$$

and where

$$\bar{\sigma} = \sum_{i=1}^{i=m} f_i \bar{\sigma}_i \quad \text{Characteristic surface-area-to-volume ratio of the fuel complex.} \quad (3-45)$$

$$\bar{\sigma}_i = \sum_{j=1}^{j=n} f_{ij} \bar{\sigma}_{ij} \quad \text{Characteristic surface area-to-volume of } i\text{-th fuel ratio category.} \quad (3-46)$$

$$\bar{\rho} = \frac{1}{\bar{\sigma}} \sum_{i=1}^{i=m} \sum_{j=1}^{j=n} \frac{(\bar{w}_o)_{ij}}{(\rho_p)_{ij}} \quad \text{Mean packing ratio} \quad (3-47)$$

$$\bar{\rho}_b = \frac{1}{\bar{\sigma}} \sum_{i=1}^{i=m} \sum_{j=1}^{j=n} (\bar{w}_o)_{ij} \quad (3-48)$$

This completes the calculations for the reaction intensity ( $I_r$ ) term of the RROS Equation 3-8 for nonhomogeneous fuels. The remaining terms are treated similarly. The no-wind propagating flux ratio is given by

$$\xi = (192 + 0.2595 \bar{\sigma})^{-1} \exp[(0.792 + 0.681 \bar{\sigma}^{.5})(\bar{\beta} + 0.1)] \quad (3-49)$$

The denominator of Equation (8), which contains the heat sink terms, is given by

$$\rho_b \epsilon Q_{ig} = \bar{\rho}_b \sum_{i=1}^{i=m} f_i \sum_{j=1}^{j=n} f_{ij} \left[ \exp\left(\frac{-138}{\bar{\sigma}_{ij}}\right) \right] (\bar{Q}_{ig})_{ij} \quad (3-50)$$

where

$$(\bar{Q}_{ig})_{ij} = 250 + 1,116 (\bar{M}_f)_{ij} \quad \text{The heat of pre-ignition (3-51)} \\ \text{for j-th size class within} \\ \text{the i-th category.}$$

The wind and slope multiplication factors are given by

$$\phi_w = CU^B (\bar{\beta}/\bar{\beta}_{op})^{-E} \quad (3-52)$$

$$\phi_s = 5.275 (\bar{\beta})^{-0.3} (\tan \phi)^2 \quad (3-53)$$

where,

U = mean windspeed at midflame height (ft/min)

$$C = 7.47 \exp(-.133 \bar{\sigma}^{.55}) \quad (3-54)$$

$$B = 0.02526 \bar{\sigma}^{.54} \quad (3-55)$$

$$E = 0.715 \exp(-3.59 \times 10^{-4} \bar{\sigma}) \quad (3-56)$$



### 3.5 PROPAGATION MODEL EMBODYING THE RROS EQUATION

The generalized RROS equation provides estimates of local rate of fire spread in heterogeneous fuels over an area of interest. This is, however, insufficient to allow estimates of fire growth, which require in addition a fire front propagation algorithm and a local directional spread rate algorithm.

#### 3.5.1 Fire Front Propagation Algorithm (FFPA)

The FFPA described here was developed specifically for fires in understory wildland fuels (Reference 19) and is probably not applicable to urban fuels. It is described, however, as an example of the types of considerations involved in applying the RROS equation to fire growth estimates.

It is assumed that all propagation interactions occur at the perimeter of a wildland fire at the interface between the flame front and unignited fuel. FFPA has these characteristics:

1. The algorithm must accept required data and provide results of variable, user specified resolution.
2. Perimeter resolution must be variable from fire-to-fire, perimeter-to-perimeter, and point-to-point within a perimeter.
3. A perimeter should not cross an earlier perimeter or itself. That is, a fire is assumed to always grow toward unburned fuel.
4. The algorithm should be able to simulate fires burning through nonhomogeneous, discontinuous wildland fuels in uneven terrain.
5. The shape of the fire should be a priori, indeterminate, and dependent upon local fuel, topographical and meteorological conditions

over the region within which the fire is situated.

6. It should be possible to initiate the model from an arbitrary perimeter definition (a point, geometric shape, set of points, etc.).

In the FFPA, each perimeter is described by a set of points connected by straight-line segments. The basic function of the propagation model is to estimate the location and shape of the next perimeter by an outward propagation of the points that define segments of the current perimeter. The use of variable (i.e., segment length) resolution over each perimeter permits detailed description of the perimeter where desired while allowing a significant reduction in the total number of calculations and the amount of data required to describe the perimeter.

The user specifies a minimum ( $\delta s$ ) and a maximum ( $\Delta s$ ) allowable spacing between any two adjacent points within a perimeter. An internal algorithm defines the spacing between each successive pair of points such that

1. The spacing falls within the specified limits,
2. The spacing is a function of the maximum of the propagation rates at the two points, and
3. The greatest density of points occurs where the fire front propagation rates are highest.

Thus, the spacing  $ds_{ij}$  between two adjacent points  $p_i$  and  $p_j$  is given by

$$ds_{ij} = f(\max[R_i, R_j]) \quad (3-57)$$

and

$$\delta s \leq ds_{ij} \leq \Delta s \quad , \quad (3-58)$$

where

$R_i$  = propagation rate at point  $p_i$ ,

$R_j$  = propagation rate at point  $p_j$ .

Let a perimeter at time  $T_0$  be completely defined by the set of 10 points shown in Figure 3-1. By completely defined, we mean that no further operations are required upon the specified set of points to complete the description of the perimeter. Since the function of the propagation model is to estimate the next perimeter in terms of the set of points that define the current perimeter, it does not matter how the perimeter at  $T_0$  was obtained. It could have been calculated from an earlier perimeter, it could have been estimated, or it could have been obtained as input from measured data. Given the perimeter at  $T_0$ , we will very briefly describe the sequence of operations required to estimate the next perimeter.

The outward direction at each point of the perimeter is defined as the bisector of the angle formed by the two line segments intersecting at each point, as shown in Figure 3-2. The directional spread rate is calculated at each point; the propagation direction is determined at each point (the outward direction is used in this example); and each point is propagated in the specified direction, at the specified rate over a specified interval to the next perimeter at  $T_1$  as shown in Figure 3-3.

The newly defined set of points that describe the perimeter at  $T_1$  are tested to determine if Equations 3-1 and 3-2 are satisfied for each candidate perimeter segment, and

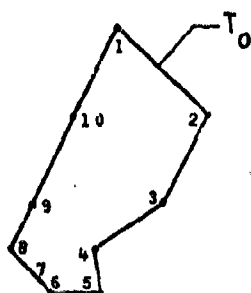


Figure 3-1. The set of points defining the perimeter at  $T_0$ .

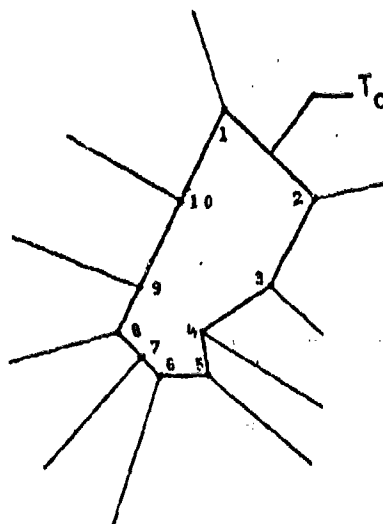


Figure 3-2. The outward direction at each point.

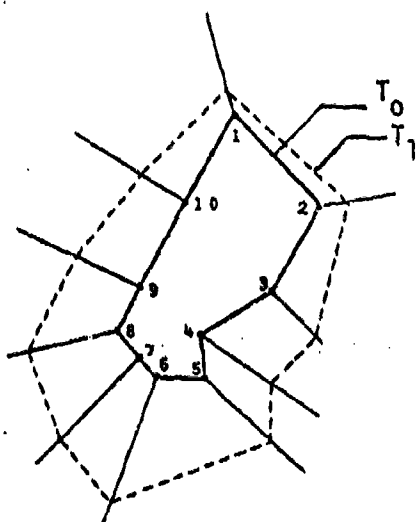


Figure 3-3. Preliminary perimeter at  $T_1$ .

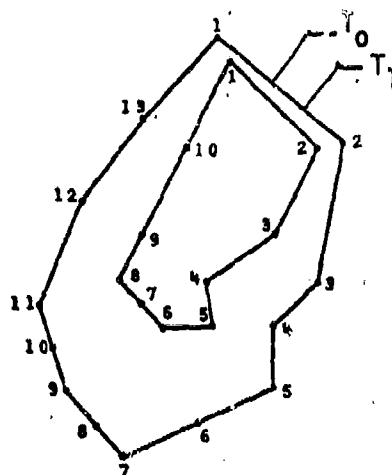


Figure 3-4. Final perimeter at  $T_1$ .

1. a new point is added at the center of each segment that is too long,
2. a point is deleted from each segment that is too short, and
3. the process is repeated until all segments satisfy the above together with Equations 3-1 and 3-2.

For this example a point was added to each of segments (5,6), (7,8), and (8,9), as shown in Figure 3-4.

The collection of points is then tested to determine if the perimeter contains any loops (i.e., crosses itself). If such a condition is detected, the points contained within each minor loop are deleted. The remaining points are enumerated, and the current perimeter is by definition completely described by this set of points, as shown in Figure 3-4, and the entire sequence of operations is repeated to obtain the next perimeter.

### 3.5.2 Local Directional Spread Rate Algorithm (LDSRA)

Local spread rate estimates are based on the RROS Equation 3-8, which is rewritten for convenience in the form (Reference 5)

$$R(q_1, q_2, \dots, q_N, u, \phi) = R_0(q_1) [1.0 + \phi_w(u, q_1) + \phi_s(\phi, \beta)] \quad (3-59)$$

where

$R(q_1, q_2, \dots, q_N, u, \phi)$  = spread rate in direction of local wind velocity,

$q_N$  = fuel parameters,

$u$  = local wind speed

$\phi$  = angle of local slope measured from the local horizontal,

$R_0(q_i)$  = no wind, no slope spread rate,

$\phi_w(u, q_i)$  = wind function

$q_i$  = fuel particle area-to-volume ratio,

$\phi_s(\phi, \beta)$  = slope function,

$\beta$  = fuel packing ratio.

There is no explicit directional dependence in the RROS equation. However, development of the RROS equation was heavily dependent upon empirical data obtained from wind tunnel simulations of wildland fires. The empirically deduced effects of wind ( $\phi_w$ ) and slope ( $\phi_s$ ) are, thus, defined to be for the down-wind and up-slope directions, respectively.

The RROS Equation 3-59 predicts that, in the absence of wind and slope, a point fire will spread circularly at the rate  $R_0$ . The qualitative basis for a local directional spread rate is the assumption that, in the presence of wind and/or slope, a point fire will spread elliptically as a function of  $R_0$ ,  $\vec{\phi}_w = \phi_w \hat{a}_w$ , and  $\vec{\phi}_s = \phi_s \hat{a}_s$  where  $\hat{a}_w$  and  $\hat{a}_s$  are unit vectors in the directions of down-wind and up-slope, respectively.

The components obtained from the RROS model are shown in Figure 3-5 in a two-dimensional reference frame with origin at the point of interest. It is assumed that the data upon which  $R_0$ ,  $\vec{\phi}_w$  and  $\vec{\phi}_s$  are based apply at least to the point of interest. The reference frame used consists of earth-tangent-plane coordinates E (east) and N (north), so that the angles  $\alpha_s$  and  $\alpha_w$  are azimuthal angles. The unit vector  $\hat{a}_w$  is in the direction toward which the wind is blowing (opposite to common, meteorological convention). The unit vector  $\hat{a}_s$  is the negative horizontal

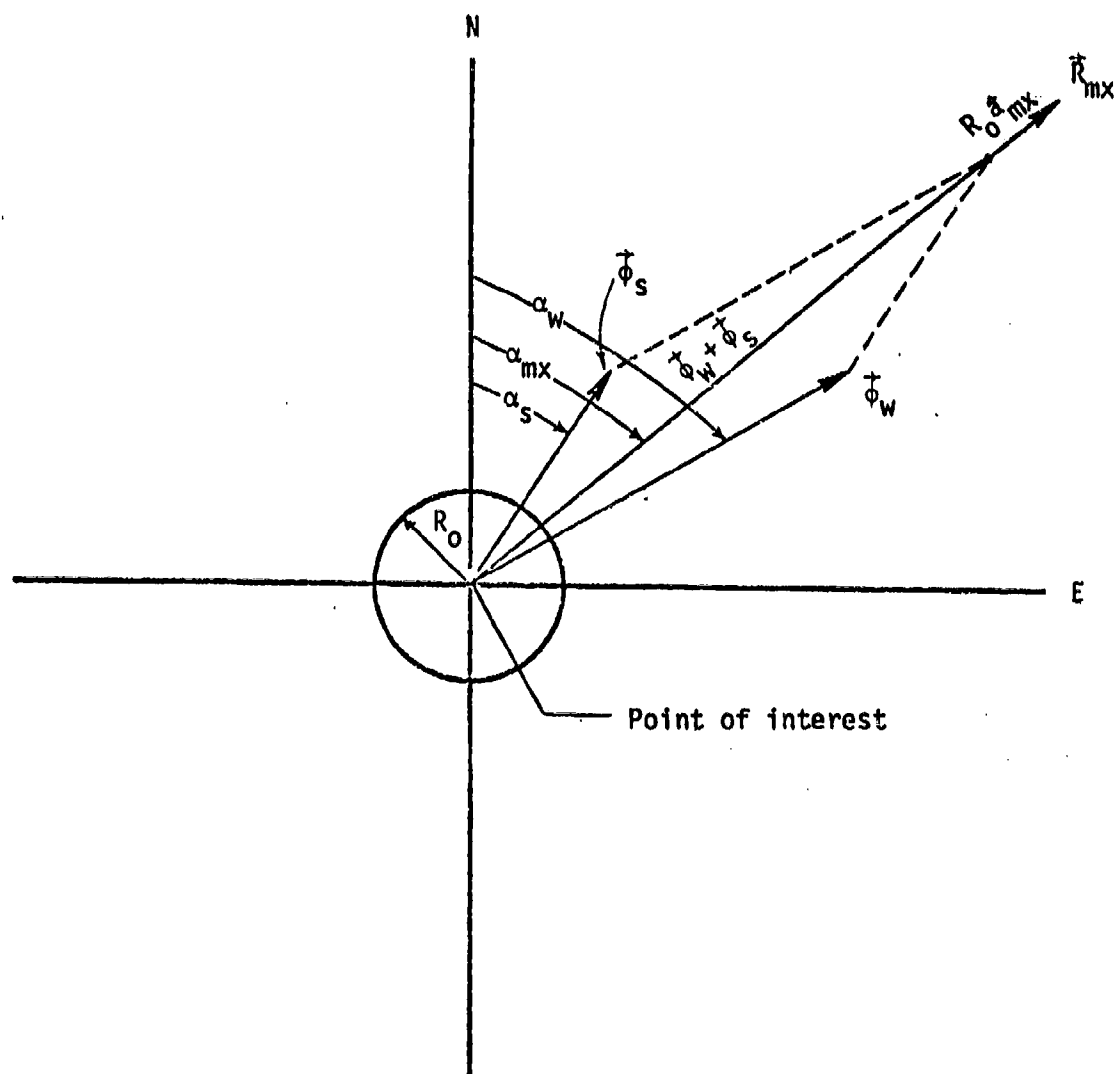


Figure 3-5. Graphical representation of RROS model output components.

projection of the local surface normal, and thus points in the up-slope direction.

An ellipse can be completely defined in terms of the location of one focus, the line of apsides, the apoapsis distance, and the semi-latus rectum. Define the point of interest as the location of the occupied focus. Define the line of apsides along a unit vector  $\hat{a}_{mx}$  where

$$\hat{a}_{mx} = (\hat{\phi}_W + \hat{\phi}_S) / |\hat{\phi}_W + \hat{\phi}_S|. \quad (3-60)$$

Define the semi-latus rectum  $R_N$  by

$$R_N = R_O + |\hat{\phi}_W \times \hat{a}_{mx}| + |\hat{\phi}_S \times \hat{a}_{mx}| \quad (3-61)$$

Define the apoapsis distance  $R_{mx}$  as shown in Figure 3-5 by

$$R_{mx} = R_O + (\hat{\phi}_W \cdot \hat{a}_{mx}) + (\hat{\phi}_S \cdot \hat{a}_{mx}) \quad (3-62)$$

where,

$\hat{a}_{mx}$  = a unit vector in the direction of maximum spread area,

$R_{mx}$  = the magnitude of maximum spread rate,

$R_N$  = spread rate in the direction normal to maximum spread rate.

The azimuthal angle  $\alpha_{mx}$  of  $R_{mx}$  as shown in Figure 3-5 is given by

$$\alpha_{mx} = \arctan [(\phi_W \sin \alpha_W + \phi_S \sin \alpha_S) / (\phi_W \cos \alpha_W + \phi_S \cos \alpha_S)]. \quad (3-63)$$



The eccentricity of the ellipse is by definition

$$e = 1 - R_N/R_{mx} \quad (3-64)$$

and the directional spread rate in the azimuthal direction ( $\theta$ ) is then given by

$$R(\theta) = R_{mx} (1-e)/(1 + e \cos \theta) \quad (3-65)$$

where  $\theta = \pi + \alpha - \alpha_{mx}$

An important characteristic of Equation 3-65 is that it preserves the magnitude of spread rate in the direction implied by Equation 3-59.

It was determined from comparing computational results with actual wildland fire growth data that the LDSRA defined by Equation 3-65 predicts local elliptical spread rate patterns exhibiting excessive eccentricity. This was considered to be a result of the dependence of Equation 3-59 upon experimental data from simulated fires in laminar wind fields. Laminar wind flow is rare in nature, particularly near the ground in rough terrain and vegetation. The effect of local turbulence is considered to decrease the eccentricity of the local directional spread rate pattern as a function of local wind speed. The eccentricity of the local spread rate ellipse was, thus, modified in accordance with wildland fire growth data. The resulting LDSRA is given by

$$R(\alpha) = R_{mx} (1 - e')/(1 + e' \cos \alpha) \quad (3-66)$$

where

$$e' = ef(u) \quad (3-67)$$

and

$$f(u) = 1.0 - 0.02u, \quad 0 \leq u < 10 \text{ (mph)} \quad (3-68)$$

$$f(u) = 0.8 - 0.0054(u - 10), \quad 10 \leq u \leq 80 \text{ (mph)} \quad (3-69)$$

### 3.6 ANALYSIS OF THE RROS EQUATION

Formulation of a computational procedure embodying the RROS equation for estimating the growth of wildland fires revealed problems related to input data, computation, and data management requirements. These problems derive from the use of a grid structure over the potential burn area and the detailed fuel descriptions specified for the RROS equation.

The required cell size and expected fire size define the amount of data to be entered, the computational detail required, and the amounts of data to be accessed and stored. Cell size is determined by the most limiting of the rate of change of terrain slope, wind velocity, fuel diversity and desired firefront resolution. Consideration of these parameters indicated a minimum practical cell size of about one acre for wildland fires. The historical data on wildland fires of interest implied that a potential burn area of about  $10^4$  cells would not be unreasonable. Reference to Table 3-3 for two fuel categories and six size classes shows that 98 fuel parameters plus five additional parameters are required as input data for each cell. For  $10^4$  cells this is a very large amount of data and is comprised largely of detailed fuel characteristics. For this reason, the RROS equation was analyzed to determine the sensitivity of spread rate estimates to each of the input data elements.

An initial analysis (Reference 23) examined the sensitivity of RROS equation results to independent changes in each variable over the range of values that each variable might exhibit. This analysis partitioned the RROS equation variables into two sets, strong and weak variables. Each strong variable resulted in a maximum rate of change of estimated rate of spread with respect to the value of the subject variable that was greater than ten percent. Weak variables were below this threshold.

The strong variables were identified to be  $u$ ,  $\sigma$ ,  $\delta$ ,  $M_f$ , and  $M_x$  and the weak variables were  $W_0$ ,  $h$ ,  $\rho_p$ ,  $S_T$ ,  $S_E$ , and  $\tan \phi$  (see Table 3-2 for variable definitions). A subsequent analysis examined the effects upon RROS equation results of all independent variables, all physically realizable couplings between strong variables, all weak variables combined and all strong variables combined. The results of this analysis are shown in Table 3-4. Examination of the standard deviation of the distribution of percentage change in estimated spread rate for each tested variable set reveals that

1. There are three strong variables ( $u$ ,  $\sigma$ , and  $M_f$ )
2. The weak variables  $W_0$ ,  $h$ ,  $\rho_p$ ,  $S_T$ ,  $S_E$ , and  $\tan \phi$  can be treated as constants
3. The two intermediate variables  $\delta$  and  $M_x$  can be accommodated with two levels of quantization.

As a result of these analyses, it was possible to reduce the number of data elements required per cell from approximately 100 to 6. All of the fuel characteristics were determined in terms of the fuel type within a cell and its age. The remaining four data elements consisted of the wind velocity components and the slope components. This reduction in the

Table 3-4. RROS equation variables summary.

CASE	MEAN (R/ $\bar{R}$ )	MODE ( $\bar{R}/R$ )	STD. DEV. $\sigma_{R/\bar{R}}$	80% CONF. LIMITS	
				R/ $\bar{R}$ (10)	R/ $\bar{R}$ (20)
<u>WEAK VARIABLES</u>					
$W_o$	1.00	1.00	0.01	0.99	1.01
$h$	1.00	1.02	0.07	0.89	1.09
$\rho_p$	1.00	1.00	0.007	0.99	1.01
$S_T$	1.00	0.99	0.02	0.97	1.03
$S_e$	1.01	0.99	0.07	0.93	1.08
$\tan \phi$	1.00	1.01	0.05	0.94	1.06
<u>STRONG VARIABLES</u>					
$u$	1.18	0.74	0.68	0.30	2.01
$\sigma$	1.06	1.12	0.42	0.49	1.56
$\delta$	1.00	1.03	0.15	0.78	1.18
$M_f$	1.07	0.93	0.40	0.63	1.52
$M_x$	0.99	1.00	0.14	0.88	1.07
<u>COUPLED STRONG VARIABLES</u>					
$u, \sigma$	1.22	0.38	0.91	0.26	2.45
$u, \delta$	0.96	1.11	0.56	0.23	1.76
$\sigma, \delta$	1.06	0.96	0.45	0.46	1.69
$u, \sigma, \delta$	1.24	0.32	0.97	0.19	2.52
$M_f, M_x$	1.10	0.94	0.43	0.67	1.66
<u>COUPLED STRONG, WEAK AND ALL VARIABLES</u>					
All Weak	1.03	1.01	0.11	0.85	1.14
All Strong	1.34	0.34	1.28	0.12	2.89
All Variables	1.29	0.62	1.13	0.16	2.99

amount of data to be processed, coupled with the use of the segmented perimeter propagation model described in Section 4, allowed efficient simulation of large wildland fires.

## SECTION 4

### URBAN MASS FIRE BEHAVIOR MODEL CONCEPT

#### 4.1 INTRODUCTION

No conventional state-of-the-art exists, in either a theoretical or empirical sense, which suffices to immediately construct an urban mass fire behavior model. Previous investigations provide a foundation, but in themselves are insufficient for the purpose. Consequently, a model concept must have a high judgemental content based upon assessment of the most important physical processes and factors together with extrapolation from better understood situations. The present, or reasonably short-range, possibility for computing or estimating the major physical processes is a necessity. Simulation of a complex interactive situation is, however, something more than straightforward computation. The organizational structure, which chooses and sequences the separate aspects and their interactions, can equal the physical calculations in importance. The unique model structure described in Section 5 is an essential part of our model concept. The present section concentrates on physical aspects of the model.

Our concept aims at a model description of the behavior and propagation of a mass urban fire in order to assess its ultimate effect and to explore the requisite conditions in which various modes of development (propagating line fire, firestorm, etc.) occur. This emphasis upon fire development elevates propagation mechanisms to primary importance.

We consider mass fire propagation mechanisms, in order of spread potential, to be

1. Firebrand transport (transport of burning material)  
~ 0-5 km
2. Contiguous spread or pilot ignition (flame and hot gas contact, convection) ~ 0-50 m
3. Flame radiation ~ 0-10 m
4. Heat conduction ~ cm.

Heat conduction influences pyrolysis rate (burning rate) of already ignited material, but is otherwise negligible. Flame radiation provides an essential feedback of heat to burning material, but propagation by this mechanism is rather short range. It becomes important only when view factors approach a solid angle of  $4\pi$ , as in closed compartments or dense fuel beds. Fire spread between closely spaced buildings may occur by flame radiation, although, in this case, it may be obscured by convective mechanisms. Only in the absence of other propagation mechanisms does flame radiation become significant. The important feature of the remaining major propagation mechanisms, branding and convection, is their dependence upon the details of the gaseous hydrodynamics.

Hydrodynamic motions of ambient atmosphere (wind and updrafts), flame columns, and fire plumes are determined by the background meteorology as well as the state of the fire, which includes the spatial distribution and intensity of burning, both current and past. In turn, the burning state and its changes are determined by hydrodynamic (wind and convection) effects upon burning rate and propagation. Despite the fact that any fire involves hydrodynamics, small scale burning in the open apparently does not require explicit consideration of the mutual, two-way interaction between fire and wind. The small scale fire is affected by

the wind, but the perturbation of wind by the fire is negligible. The success of the Rothermel Spread Model (Reference 18) description of fire propagation demonstrates the validity of neglecting the reverse effect of open fires upon wind, at least for brush fires, which, in this sense, are small scale. On the other hand, models of compartment fires in still intact buildings require a hydrodynamic description of the interaction between air flow (ventilation) and burning rate. In the case of open fires, as the number, intensity, and areal distribution of burning regions grow, the atmospheric perturbation increases to the point where fire development becomes substantially influenced by the fire itself. Our concept of an urban mass fire model emphasizes this reciprocal interactive effect, which we expect to assume significance in conflagrations on the scale to be considered. The potential presence of a high-velocity fire-induced wind as a damage mechanism is also of interest in itself.

In addition to the fire-hydrodynamic reciprocal interaction, mass fire behavior, of course, depends upon the effective (after blast) initial ignitions (spatial and temporal distribution) and other factors, all of which can be considered fuel parameters. Fuel loadings of burnable material and its effective heat content, rates of combustion, fuel distribution (building heights and spacing, streets, and open areas as firebreaks, vegetation, etc.) are all essentially fuel descriptors. These parameters, perhaps drastically modified by air blast, clearly underlie the behavior of nuclear-induced urban mass fires, and define the modeled situation. Recall that the major research effort in producing the Rothermel model was quantification of the effects of fuel parameters, which are central to it. In the urban model context one requires fuel parameters in sufficient detail to define the situation, but propagation (branding, pilot ignitions) and burning characteristics, insofar as they are fuel dependent, must be handled partly parametrically since detailed information is lacking. We advocate reasonable functional behavior and idealized physical models to estimate these effects. Any model of urban



fire development, whether it includes reciprocal fire-wind interaction or not would, at the present level of knowledge, suffer equally from these fuel-related uncertainties.

Once the reciprocal fire-hydrodynamic (fire-wind, for short) interaction is selected as the central aspect of urban mass-fire behavior, we must consider methods for its calculation and exploitation. Our concept is essentially the choice of an approach to this problem.

## **4.2 MODEL ALTERNATIVES**

Mass fire development, considered as an interactive fire-wind problem, demands a three-dimensional description of the flow of hot gases and ambient air. Although heat sources are localized on or near the surface, brand transport depends upon velocities aloft, and winds near the surface--important for pilot ignitions--are only a special part of the unified total flow. Later we will examine some evidence from the Flambeau tests which indicates the need for three-dimensional resolution even in the near-surface region of heat production and active flaming.

### **4.2.1 Detailed Hydrodynamic Calculation**

A detailed 3-d hydrodynamic calculation, based upon fundamental equations of motion, could in principle be used to determine the flow field. A major practical problem with this approach is the need for high spatial resolution, sufficient to resolve irregularities and discontinuities in zones of burning and convection, which are certainly present at ignition and immediately after, and which may persist for extended periods. Such calculations of detailed 3-d flow fields would be expensive and lengthy to perform, even if sufficient memory capacity for the computer calculations were available.

A physical problem with this approach arises in the need to compute the effects of turbulence, which, in this case, is largely produced by buoyancy of hot gases. It is not clear whether there is an expeditious method for calculating the behavior of buoyant, turbulent flows directly from fundamental principles. Second-order closure schemes of turbulence modeling are far too demanding to be practical in a model which, in addition, performs many other types of calculation and which must be repetitively run to assess the effects of varying conditions. At this level of detail, turbulent exchange approximations based upon mixing length hypotheses do not alleviate the computational burden significantly and of themselves introduce large uncertainties.

Numerical computation of detailed flow fields at high resolution is perhaps a last resort, and other avenues should be explored first.

#### 4.2.2 Low-Resolution (Lumped-Parameter) Hydrodynamic Calculations

At the other extreme, we might consider only a global, comparatively low resolution description of the flow field. Previous approaches to the mass fire problem have calculated the axially symmetric flow field resulting from a single large area circular fire (with assumed smoothed and uniform heat production rates per unit surface area). By invoking either mixing length assumptions or turbulent entrainment assumptions, the calculations have produced reasonable solutions for the single large fire plume in the asymptotic region at large altitudes above the source. These calculations, however, typically yield unrealistic behavior in the region near the ground. One effect (Reference 12) is rapid convergence of the rising hot gases to the center of the burning area to form a narrow plume, which then expands normally in its subsequent rise. This exaggerated behavior is not necessarily inherent in the model type, being, we believe, a consequence of oversimple assumptions. The single plume formed at high altitudes by coalescence of hot turbulent gases from many separate heat

sources may be adequately represented by this type calculation. The coalescence process itself and the detail of wind fields at lower elevations resulting from discrete burning zones requires something in addition, or perhaps a different approach. Though potentially useful for determining large scale atmospheric perturbations and overall flow fields, these low resolution hydrodynamic models fall short of providing the crucial small scale structure needed to model fire development.

#### **4.2.3 Parameterized Multiple Plumes**

In the face of the limited understanding of mass fire phenomena and the recognized inadequacy of previous approaches to the problem, we have evolved a concept for modeling fire development, which does not attempt a first principles calculation of the hydrodynamics. Instead, the flow fields are deduced as a superposition of velocities resulting from the actual distribution of segmented burning zones and their attendant entraining plumes. This approach requires that the major features of individual burning zones and fire plumes be parameterized in terms of comparatively few variables: heat production rate per unit area, areal extent, and wind description being the principal variables. Heavy reliance is placed upon similarity solutions together with laboratory and field experiments, supplemented by physical arguments and scaled to mass fire conditions. In situations where this procedure is considered inadequate, parameterized functional relations, which summarize results of off-line hydrocode calculations of single plumes, could be employed. Essentially each burning zone (or subdivision) is represented by sources and sinks of mass distributed in three dimensions. From this distribution, atmospheric flow external to plumes and flames can be calculated. The external flow reacts back upon the plumes to establish the location of the source-sink distribution in a self-consistent manner. Once established, the wind field determines burning rates and propagation to advance the fire development.

The approach is not without difficulties and leads to several problem areas, which require investigation. However, it exploits experimental measurements and qualitative insights obtained in previous research, avoids the inherent difficulty of turbulence calculations, and can achieve detail and resolution without excessive computation.

By keying the description to a simple demonstration model, the following sections illustrate the model concept and clarify the procedure to implement it. Problem areas are discussed as they are encountered.

#### 4.3 ATMOSPHERIC MOTION

First, we briefly sketch our conception of the relevant phenomenology of fires burning in the open as derived from previous research and observations. From the standpoint of urban mass fires, all detailed tests have been small fires. Leaving aside, for the moment, the effects of atmospheric stratification and scale height, these small fires are governed by the same physical parameters as larger ones. The effect of larger distance scales is quantitative, not qualitative, and we presume relations between nondimensioned groups of variables may be used in large scale as well as small scale fires.

Figures 4-1(a) and 4-1(b) picture the features of a small area laboratory fire. Vertically, the fire consists of a flame zone, a zone of intermittent flaming, and a buoyant plume, which quickly assumes the asymptotic behavior of a weakly buoyant plume, since mixing with cool ambient air is rapid. At small burning rates  $\dot{Q}$  (J/s), the flame column shows convergence, but at higher burning rates the flame column diverges almost immediately as it rises. This distinct behavior must depend upon both  $\dot{Q}$  and the fire area  $A$ ; but as long as the area is small enough, the burning takes place in a simple flame column. The work of McCaffrey

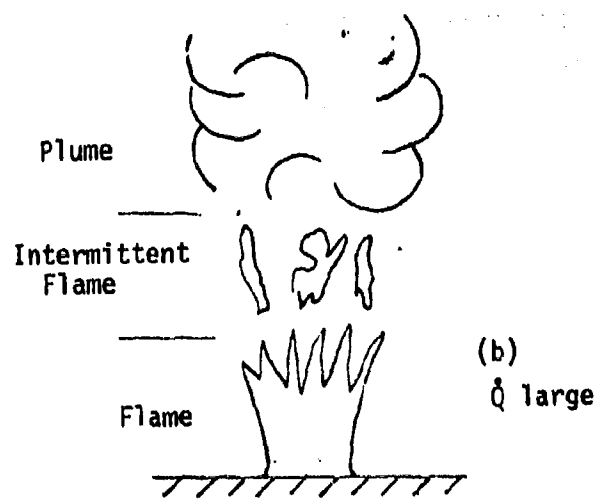
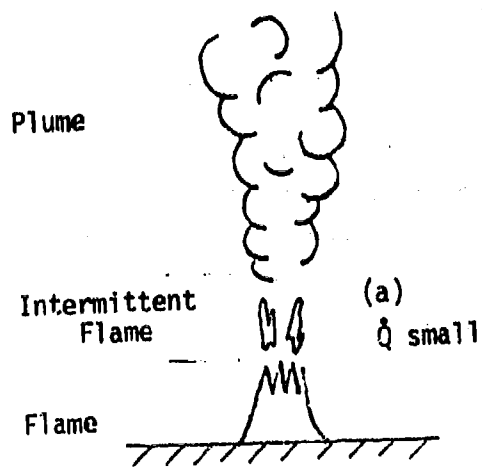


Figure 4-1(a) and (b). Small area fire.

(Reference 24) and Cox and Chitty (Reference 25) has provided reliable parameterizations of these single fires, but the area effect awaits investigation.

When several small area fires are burning in proximity, one expects the situation shown in Figure 4-2. Each separate fire and its plume entrains air. The effective "sinks" of all plumes produce an air velocity, which tips the plumes inward and brings them together at a coalescence height, after which the buoyant gases form a single plume. We encounter here a fire-induced wind, strongest at the location of the peripheral fires, which may influence their spread.

If all the small area fires coalesce, or if a large area is burning without gaps, the situation approaches that illustrated in Figure 4-3. In this case, according to the observation of Countryman (Reference 9) in the Flambeau tests, a single flame column does not persist. Instead, the fire spontaneously divides into separate flame columns and plumes, which maintain their identity through a short transition zone before combining into a simple plume. Although detailed analysis of the reason for this behavior is lacking, it clearly is a manifestation of the dynamic instability of a single flame column in certain conditions. It may be related to the Raleigh-Taylor buoyancy instability, or to the requirement of an air supply for burning, which may favor the large surface/volume ratio of multiple flame columns. Here again, the fire character must depend not only upon the total  $\dot{Q}$  but also upon the fire area,  $A$ . This behavior has a strong effect upon fire-induced winds, since a large amount of entrainment must occur in the transition and flame zones below the base of the combined plume. Wind estimates depend upon resolution of these features.

The configuration of Figure 4-3 is similar to that of Figure 4-2, but the separate columns have different origins. In the one case, they are imposed by physical separation of the fires, and in the other are

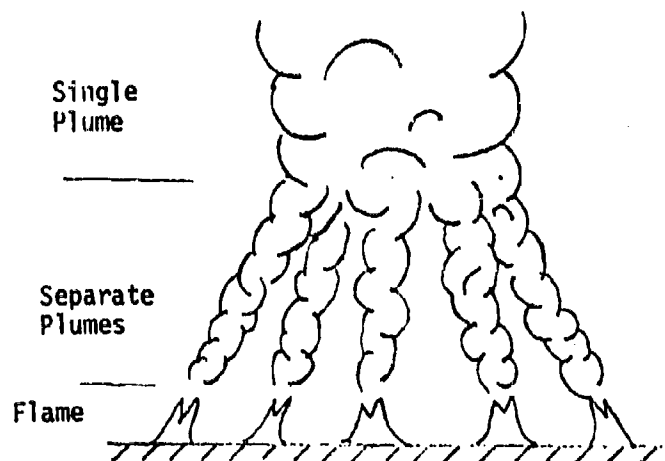


Figure 4-2. Separated small area fires.

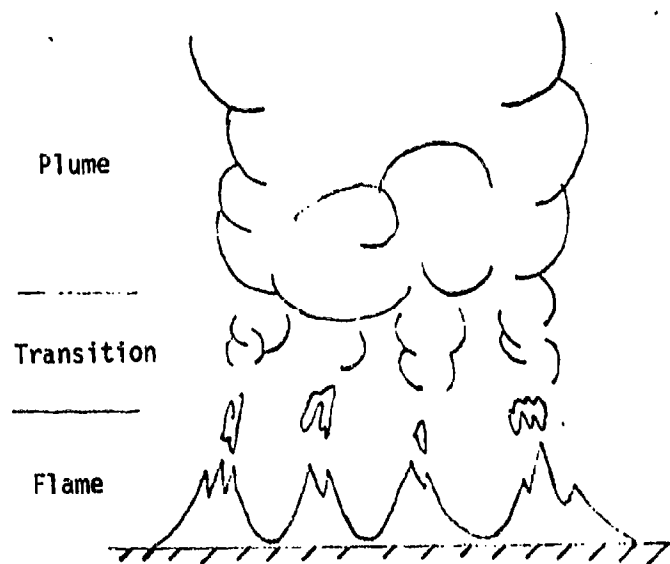


Figure 4-3. Large area fire (spontaneous break-up into separate flame columns). "Countryman Descriptive Model."

a result of fire dynamics. In either case, or in a possible combination of the two, the atmospheric motion and plume character are interactively determined. Plumes as effective sinks of ambient air determine fire winds, but winds affect the plume (or sink) distribution.

The illustrations of Figures 4-2 through 4-4 depict some of the effects of atmospheric fire plumes in the absence of an ambient wind. Both ambient winds and atmospheric stratification can modify the picture. Since we have by no means solved these problems, we describe in the following paragraphs some partial features to illustrate the concept. Most of these features have been incorporated as elements in the interactive demonstration model.

#### 4.3.1 Single Fire Plumes

A single weakly buoyant plume, in a uniform atmosphere and in the absence of wind, approximates the form of a right circular cone. Taking the apex of the cone at the ground, the similarity solution of the buoyant plume (References 26 and 27) requires

$$w = a Z^{-1/3} \quad (4-1)$$

$$Z_B = n r_B ,$$

where  $w$  is the mean upward velocity in the plume and the ratio  $Z_B/r_B$  between the height and radius of the plume has the constant empirical value,  $n = 5.51$ . The constant,  $a$ , is a function of the buoyancy flux in the plume, which is directly related to the heat production rate  $\dot{Q}$  if the plume is fire driven. By assuming  $3w = w_{\max}$ , the plume centerline velocity, the plume measurements of Cox and Chitty (Reference 25) permit computation of the relation



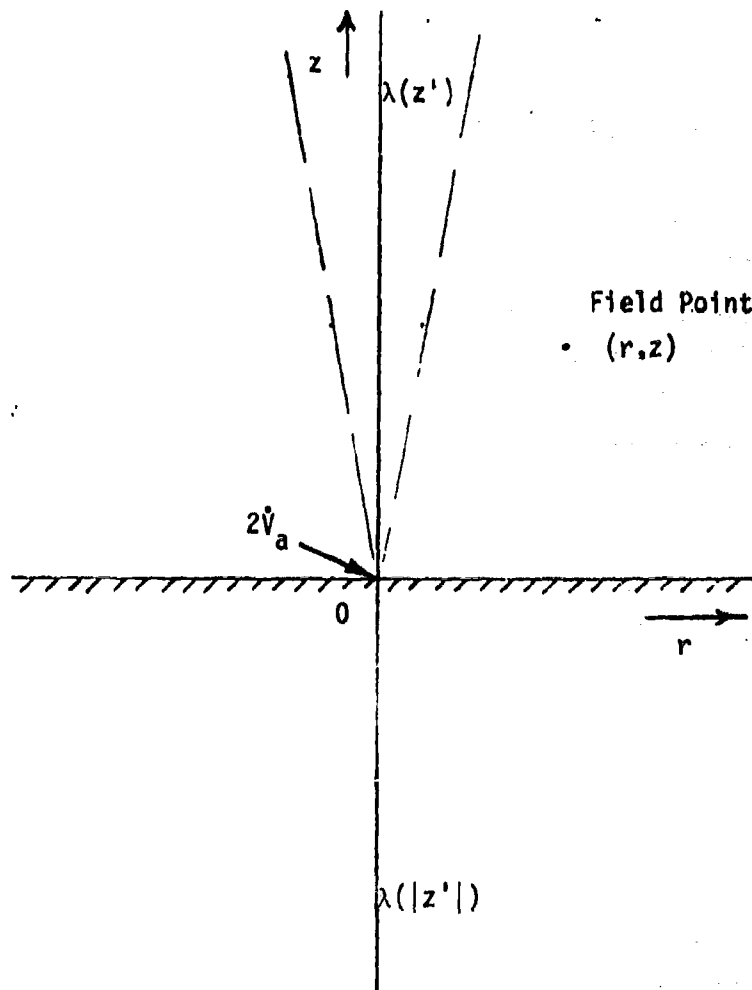


Figure 4-4. Plume geometry and sinks.

$$\alpha = 3.897(10)^{-2} \dot{Q}^{1/3} \quad (4-2)$$

where units are mks and  $\dot{Q}$  is heat production in watts. An entrainment constant  $\alpha$  (defined as the constant of proportionality between the mean upward plume velocity and the indraft velocity of ambient air through the sides of the plume),  $u = \alpha w$ , can be calculated from these relations, by using mass conservation and the assumption of incompressible flow. The result,  $\alpha = 5/(6n) = 0.151$ , does not agree with measured values, which are near 0.1. We use  $\alpha = 0.1$ .

Outside the plume, the ambient air motion may be modeled as the flow induced by a distribution of sinks located along the plume axis. The entrainment sink density  $\lambda$  is

$$\lambda(Z') = \frac{d\dot{V}}{dZ} = -2\pi\alpha\dot{Q}(Z')^{2/3}/n$$

where  $Z'$  is the vertical coordinate of the source point and  $\dot{V}$  ( $\text{m}^3/\text{s}$ ) is volume flow rate. In addition, we account for the air supply necessary for combustion by placing a point sink of magnitude  $\dot{V}_a$  on the ground at the cone apex:

$$\dot{V}_a = -k \dot{Q}/(h_0 \rho_0) = -5.5(10)^{-7} \dot{Q}$$

Here  $h_0$  is the heat of combustion of the fuel (incomplete combustion of wood,  $\sim 1(10)^7$  J/kg),  $k$  is the mass of air required to burn a unit mass of fuel ( $\sim 7-10$  kg-air/kg-fuel) and  $\rho_0 = 1.27$  kg/ $\text{m}^3$ , the ambient air density.  $\dot{Q}$  is the burning intensity in watts.

The plume geometry and sink distribution are shown in Figure 4-4, where in order to fit the boundary condition at the ground (zero

vertical velocity), a below-ground image distribution is added. This doubles  $\dot{V}_a$ , the magnitude of the point sink at the ground.

Before continuing, we note that this model includes only sinks, although one would expect the effect of heat addition to be gas expansion and, hence, a net overall source. The source is present at the plume cap in a developing plume, and must be considered while the plume is being established. Sudden, quasi-explosive increases of burning rate can also produce transient outdrafts by this mechanism. Here we consider a steady, established plume; place the plume cap at infinite height; and neglect its effect.

The velocity field external to the plume is given by integration over the sink densities. In the cylindrical coordinates chosen, the results take the form

$$\begin{aligned} v_r(r, \beta) &= \dot{V}_a / [2\pi r^2(1+\beta^2)^{3/2}] - \alpha a f_r(\beta) / [2 \pi r^{1/3}] \\ v_z(r, \beta) &= \dot{V}_a \beta / [2\pi r^2(1+\beta^2)^{3/2}] + \alpha a f_z(\beta) / [2 \pi r^{1/3}] \end{aligned} \quad (4-3)$$

where  $\beta = Z/r$ , and units are mks throughout. The nondimensional functions  $f_r(\beta)$  and  $f_z(\beta)$ , obtained by integration of the plume sinks between  $Z' = \pm \infty$ , are shown in Figure 4-5. Values of  $\beta$  are restricted to the interval,  $0 < \beta < 5.51$ , the region outside the plume. At fixed  $\beta$ , the atmospheric velocities induced by plume entrainment fall off at the slow rate of  $r^{-1/3}$ , a result of the infinite plume length. The horizontal velocities directed radially inward always exceed vertical velocities except very near the origin where effects of the point sink dominate. Throughout most of the external region, turbulent entrainment by the plume is a far stronger driver of the flow than is the sink of combustion air.

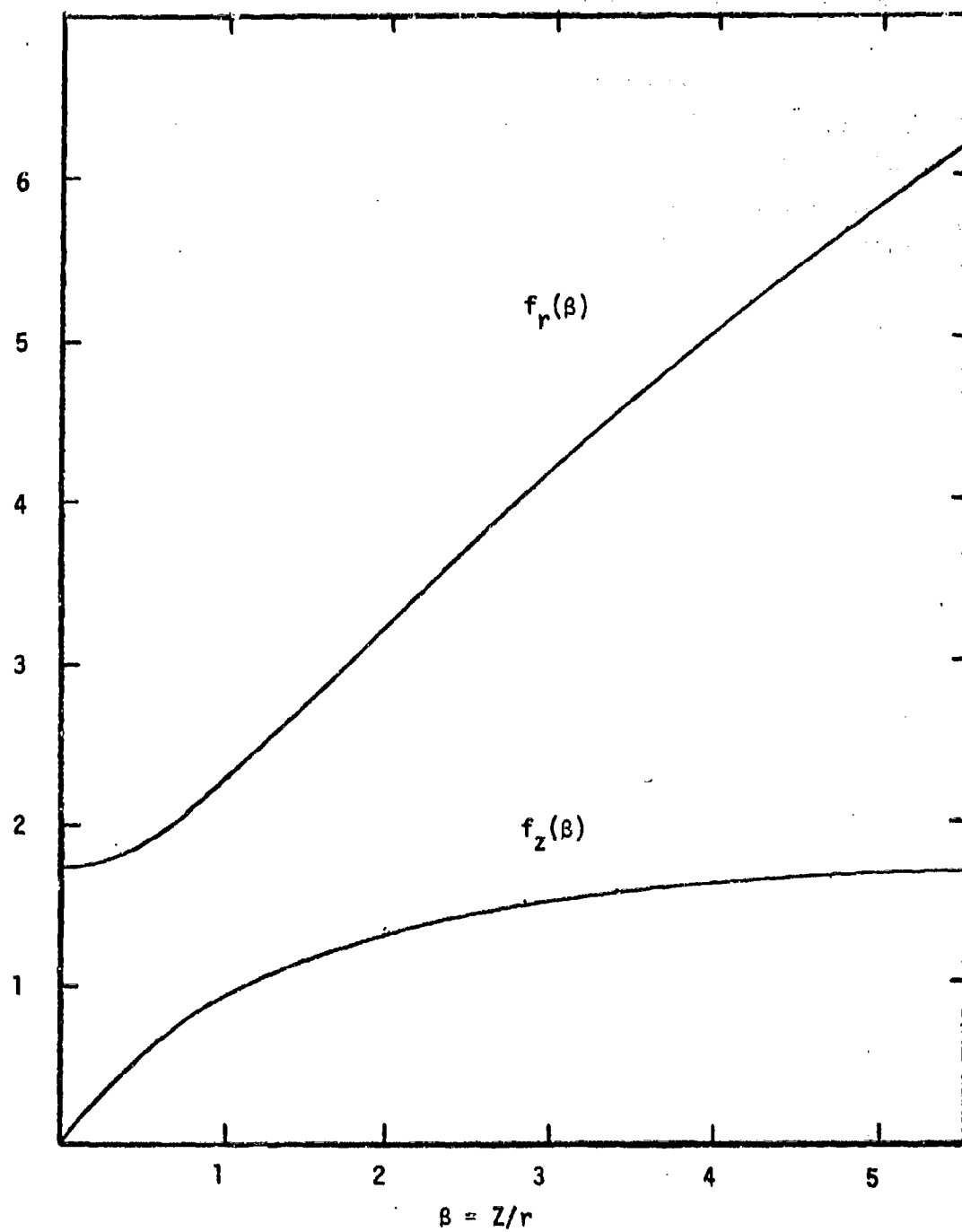


Figure 4-5. Non-dimensional velocity functions of single vertical plume.

This analysis, though very simple, illustrates the technique of calculating induced atmospheric motion from plume parameters. In this case, the sole free parameter is  $\dot{Q}$ , the power of the fire. Clearly, atmospheric stratification, which not only modifies the plume but also, in stable conditions, restricts vertical flow in the ambient atmosphere, would alter these results. Plume bending in a wind, either ambient or induced by other plumes, would change both the magnitude and location of sinks. These questions need to be addressed in a complete model.

A simple algorithm to demonstrate our conceptual approach specializes the above analysis to calculate ground level wind. Each separate fire plume acts as a partial source for the ground level wind and contributes a velocity,

$$v_r(r) = \dot{V}_a / (2\pi r^2) - 0.862 \alpha a / (nr^{1/3}) \quad , \quad (4-4)$$

directed toward the plume origin. The numerical factor 0.862 is half the value of  $f_r(\beta)$  at  $\beta = 0$ . This formula applies to a developed plume of infinite height. To account for the plume formation transient, important in the initial stages, we extend the integral of plume entrainment sinks only over the actual vertical height of the plume. (The source at the cap is still neglected for simplicity.) The height of the plume cap for a steady burning rate starting at  $t=0$  is approximately,

$$Z_c = 0.234 \dot{Q}^{1/4} t^{3/4}$$

again in mks units. A numerical integration over plume sinks to this height introduces a function of  $Z_c/r = \gamma$  in the place of the constant, 0.862. This function is fitted by the approximate formula,

$$0.862 + g(\gamma) = 0.862 \gamma^{1.59} / (1.328 + \gamma^{1.59}) \quad (4-5)$$

which plays the role of a build-up function for the plume-induced surface wind fields. Close to the plume, winds build up to their final steady value more quickly than at larger distances.

#### 4.3.2 Multiple Fire Plumes and Area Fires

If a mass urban fire were to consist of separate point fires of prescribed burning rate whose plumes remained vertical, separate, and independent, the fire-induced ground level wind could be obtained as a superposition of contributions from each fire given by the formulas of the previous section. This, perhaps zeroth order, approximation is in fact the general method used to calculate wind fields in our demonstration model. However, the model does not operate with point fires, but with square grid cells (modeling city blocks), and carries the total burning rate of each cell. A "fire" is defined as a group of contiguous burning cells, separated from other fires by unignited areas. In turn, each fire may be divided, on a geometrical basis, into "sub-fires," the two horizontal dimensions of which are approximately equal. This procedure permits computation of the fire-induced wind by a superposition of effects from each "sub-fire." Outside the sub-fire, its effect is that of an equivalent plume at its center, and the shape of each sub-fire may be approximated as a circle of radius,  $r_f$ .

In order to perform the wind calculation, the number of plumes or, what is the same thing, the number of equivalent point fires in the burning area of the sub-fire must be determined. This is the problem mentioned in Section 4.3 and illustrated in Figures 4-2 and 4-3 relating to the spontaneous breakup of an area fire into separate flame columns and plumes. Its importance stems from the fact that air entrainment into a plume is governed by the factor  $a$  defined in Equation 4-2, which is

proportional to  $\dot{Q}^{1/3}$ . A given total  $\dot{Q}$  of an area fire, divided into  $N$  flame plumes entrains at a rate proportional to  $N(\dot{Q}/N)^{1/3}$ . Entrainment is, thus, proportional to  $N^{2/3}$ . Many separate plumes produce more atmospheric perturbation (fire-induced winds) than does a single fire of the same total power. This reasoning supports the contention that resolution of separate fires and burning areas is essential in a mass fire model. On the basis of these ideas, multiple separated ignitions may be more likely to generate firestorm conditions than area burning.

Our analysis of these features has hardly begun. To implement the demonstration model we estimate the number of plumes,  $N$ , present in a sub-fire of radius  $r_f$  with a total power  $\dot{Q}$  as

$$N = 4.94(10)^3 \dot{Q}^{-2/3} r_f^{5/3} \quad (4-6)$$

This expression has only scant justification, based upon inexact estimates of flow conditions required to minimize pressure gradients, which we do not reproduce here. It is expected that the number of plumes (or flame columns) increase with fire dimensions, and decrease with burning rate. No obviously ridiculous results occur within the ranges of the variables employed.

Each sub-fire is assumed to consist of the number of plumes given by Equation 4-6, which are uniformly distributed over the quasi-circular area of the sub-fire. The effects of each plume, given by terms of the form of Equation 4-4, are superimposed. The total combustion air sink  $\dot{V}_a$  is placed at the fire center, and the weak  $r^{1/3}$  dependence upon distance away from the plume center is neglected inside the sub-fire. There results a simple formula, used in the demonstration model, for the contribution of each sub-fire to the total fire-induced surface wind:

$$\text{for } r > r_f \quad v_r(r) = -\dot{V}_a / (2\pi r^2) - g(\gamma) \dot{Q}^{-1/9} r_f^{10/9} r^{-1/3}$$

$$\text{for } r < r_f \quad v_r(r) = -\dot{V}_a r / (2\pi r_f^3) - g(\gamma) \dot{Q}^{-1/9} r_f^{10/9} r^{-1} \quad (4-7)$$

$$\left\{ \pi - 2 \cos^{-1} \left( \frac{r}{r_f} \right) + \frac{2r}{r_f} \sqrt{1 - \left( \frac{r}{r_f} \right)^2} \right\}$$

where  $\dot{Q}$ ,  $\dot{V}_a$ , and  $r_f$  are the respective total power, combustion air flow, and radius of the sub-fire. The distance  $r$  is the radial distance from the sub-fire center and the build-up function  $g(\gamma)$  is given by Equation 4-5 computed on the basis of the total  $\dot{Q}$  of the largest fire (not sub-fire) in the grid. The total fire-wind at any point is the vector sum of these contributions, each of which is directed toward the center of its sub-fire source.

The fire-induced wind at ground level obtained this way is an overestimate, especially in the region outside of sub-fires, since, in reality, separate plumes coalesce into a single plume whose entrainment is less. (See Figures 4-2 and 4-3.) The far outside region is influenced more by the single plume at high elevations than by the multiple plumes lower down. The reverse effect of the winds upon plume location and entrainment rate is also neglected. By contrast, very near to and inside of sub-fires, the winds may be more realistic. If an ambient wind is present, its velocity is simply added vectorially to the fire-induced wind.

In general, the demonstration model neglects the essential interaction between fire plumes, as well as the effects of plume tilt and atmospheric stratification. These matters require further analysis, but from the foregoing, the necessity of resolving these details and the efficacy of this approach may be appreciated.



#### 4.4 PROPAGATION BY BRANDING

Winds are important because of their influence upon propagation mechanisms. In this section, we develop a simplified branding algorithm, used in the demonstration model, which illustrates the problem areas and general features of fire propagation by branding.

##### 4.4.1 Brand Transport

According to the experiments of Tarifa (Reference 28), the vertical component of firebrand motion can be described by a terminal velocity, with respect to surrounding air, which is a function of time. We approximate the families of curves obtained in his experiments by a simple linear function for the terminal velocity,  $w_T$ ,

$$w_T = w_i - kt$$

where  $w_T$  is parameterized by  $w_i$ , the initial terminal velocity of the brand, which expresses the effect of brand size and geometry. The constant,  $k = 1/12 \text{ m/s}^2$ , is the same for all brands. At  $t_b = w_i/k$ , the terminal velocity is zero, which is taken as the time of brand burnout.

The updraft velocity of a fire plume reaches its maximum,  $w_0$ , in the region of intermittent flaming at a height,  $Z_0$ , after which the velocity decreases as  $w = aZ^{-1/3}$ . The values of  $a$ ,  $Z_0$ , and  $w_0$  are determined by the power of the fire,  $\dot{Q}$ , using the measurements of Cox and Chitty (Reference 25). We assume these relations to apply for the vertical component of plume motion, even in the presence of a wind. In a wind, which is needed for brand transport, both the horizontal plume and brand velocity are taken as equal to the wind velocity. These plume velocities are used as the mechanism for brand lifting. The potentially important-brand lifting mechanism of strong fire whirls is neglected.

In a plume the vertical velocity of a brand is,

$$\dot{Z} = aZ^{-1/3} - (w_i - kt); \quad Z = Z_0 \text{ at } t = 0 \quad (4-8)$$

We take the condition  $\dot{Z} = 0$  as the condition for the brand to fall out of the plume. An integration of this equation would determine the height and time at which a brand leaves the plume or whether it burns out before leaving the plume. Clearly, small brands will burn out inside the plume before the condition is met. An upper limit of brand size is fixed by the lofting condition,  $w_i < w_0$ . The fire parameters determine a range of relevant initial terminal velocities,  $w_{\min} < w_i < w_0$ , of brands that can be both lofted and fall out while still burning.

For expediency, we do not perform the integration. Instead, a series of linear approximations are employed to estimate the time of fallout and the lofting height of the brands. We characterize a brand by the parameter  $n$  defined in terms of its initial terminal velocity and the range of relevant terminal velocities:

$$n = (w_0 - w_i)/(w_0 - w_{\min}) \quad ; \quad 0 < n < 1$$

A brand will stay in the plume for a time  $t_F = nt_T$ , where  $t_T$  is the time of fallout of the smallest brand that falls out. The height of fallout  $Z_F$  is given by linear interpolation of  $Z^{-1/3}$ , on the height  $Z_T$  to which the smallest brand rises,

$$Z_F^{-1/3} = (1 - n) Z_0^{-1/3} + nZ_T^{-1/3}$$

When a brand leaves the plume, its initial terminal velocity for vertical fall through the air is  $w' = w_i - kt_F$ , and for the period of its fall

to the ground, its vertical velocity is  $\dot{Z} = -(w' - kt)$ . The time interval required to fall to the ground from the height  $Z_F$  is

$$\Delta t = \frac{w'}{k} [1 - (1 - f)^{1/2}] ,$$

where  $f = 2kZ_F/(w')^2$ . Provided  $f < 1$ , a real solution exists and the brand reaches the ground before burnout. For the approximations chosen below, this condition is always met for the range of brand sizes, which fall out after lofting.

The total flight time of a brand,  $t_G = t_F + \Delta t$ , is less than its burning time,  $t_B$ . Our simplified algorithm assumes the horizontal transport of a brand takes place in a uniform wind,  $\vec{V}$ , the value of the surface wind field at the point of brand origin. (The result of this approximation can be grossly unrealistic in some cases. One needs to determine the brand trajectory with the complete 3-d wind field.) With this simplification, the brand reaches the ground at a point displaced a distance  $\vec{D} = \vec{V} t_G$  from its point of production.

One would expect the probability for a grounded firebrand to produce a new ignition to depend upon the fuel present and the brand's remaining burning time,  $\tau = t_B - t_G$ . This clearly stochastic event is modeled with the ignition probability

$$P_i = 0.3[1 - \exp(\tau/60)] ,$$

where times are in seconds. We have found no data on this process, so this arbitrary expression is justified only by its reasonableness. In fact, it likely overestimates ignition probability.

#### 4.4.2 Fire Parameters and Brand Production

To implement the transport calculation described above, the values of several quantities must be determined from the fire characteristics. The maximum updraft velocity,  $w_0$ , of each flame column is the decisive quantity for brand lofting. The formula, Equation 4-6, for the number of flame columns in a area fire is employed to determine the burning rate of each flame column in a single burning cell. (We use the burning cells of the model, instead of sub-fires, to compute brand transport.) The plume parameters of each flame column turn out to depend upon the ratio  $q = (\dot{Q}_c/r_c)^{1/3}$ , where  $\dot{Q}_c$  is the power of the cell burning and  $r_c$  is the radius of a circle whose area is equal to the area of the square cell. From the numerical values measured by Cox and Chitty (Reference 25), we compute

$$\begin{aligned}w_0 &= 9.17(10)^{-2} q \\Z_0 &= 4.20(10)^{-4} q^2\end{aligned}\tag{4-9}$$

in mks units. On the basis of a rough approximation to the solution of Equation 4-8, the brand related quantities are

$$\begin{aligned}w_{min} &= 4.74(10)^{-2} q \\Z_T &= 5.82(10)^{-3} q \\t_T &= 4.44(10)^{-1} q\end{aligned}\tag{4-10}$$

again in mks units.

The transport of a brand with parameter,  $\eta_K$ , produced in a burning cell of given  $q$  can be determined with the sequence of calculations outlined in the preceding section. The results of the algebra are

$$\begin{aligned} t_G &= q(0.444\eta_K + 1.100f'_K - 0.975\eta_K f'_K) \\ t_B &= q(1.100 - 0.531\eta_K) \end{aligned} \quad (4-11)$$

where

$$f_K = 4.726(10)^{-4}(1 - 0.887\eta_K)^{-2}(1 - 0.482\eta_K)^{-3}$$

and

$$f'_K = 1 - (1 - f_K)^{1/2}.$$

There remains the critical question of how many, and what size, brands are produced per unit time by the burning cell. Since little is known of this, we assume the number of effective brands produced in the time interval,  $T$ , is proportional to  $T$  and to the burning rate,

$$N = 10^{-11} \dot{Q}_C T$$

where the constant of proportionality is frankly arbitrary, but which, in reality, must be fuel dependent. A brand parameter  $\eta = 1$  corresponds to the smallest relevant brand. Small brands are assumed to be more likely than large ones, so a linear probability distribution of  $\eta$  is postulated:

$$P(\eta)d\eta = 2\eta d\eta \quad ; \quad 0 < \eta < 1.$$

During a time interval  $T$ , the model selects  $N$  values of  $\eta_k$  from this distribution for each burning cell and computes the transport of each brand. If the brand grounds in unignited fuel, ignition at this location either occurs or does not, as determined on the basis of the ignition probability. Should the computed number of brands  $N$  be less than one, the number is interpreted as the probability for producing one brand in the chosen time interval.

#### 4.4.3 Branding Discussion

Stochastic elements play a large role in fire propagation by branding. Their origin is in part physical (random brand shape and size, turbulent fluctuations), but they chiefly originate from areas of ignorance. To a good approximation, given adequate hydrodynamics, brand transport can be modeled deterministically. The simple algorithms developed above demonstrate this. However, both ends of the branding process encounter more serious areas of ignorance--brand production estimation and brand ignition estimation. Limits of resolution of fuel properties and actual lack of knowledge will likely conspire to perpetuate this situation. Any branding model we can imagine will have a significant probabilistic content.

These considerations make it appropriate to emphasize at this point some modeling philosophy, which pertains to branding, but which also applies generally to our total model concept. In the first place, probabilistic elements of a model do not always imply that its overall behavior is random. Provided the basic underlying probability distributions are narrow enough or provided choices from broad probability distributions are made often enough, the overall aggregate results will display only a finite and acceptable scatter. In effect, the results are deterministic.

In the second place, the basic probability distributions governing modeling choices and logic can themselves be conditioned and changed by current values of physical parameters. Partial and qualitative knowledge, even intuition, can in this manner be incorporated with effect, meaning, and interactive potential. Absence of a precise, deterministic description of a process is no license to model it by a rigid and immutable random choice.

#### 4.5 CONTIGUOUS FIRE SPREAD (CONTAGION)

Contiguous fire spread--local spread from ignited fuel to adjacent unignited fuel--is a possible spread mechanism whether branding occurs or not. In the context of wildland fires, the Rothermel model successfully models spread in continuous fuel beds on the basis of local fuel parameters, together with the local terrain slope and wind. The physical framework of the Rothermel model is a spread rate determined by the ratio of emitted heat flux to heat required to ignite new fuel, but the numerical implementation of this idea required extensive tests to quantify fuel characteristics.

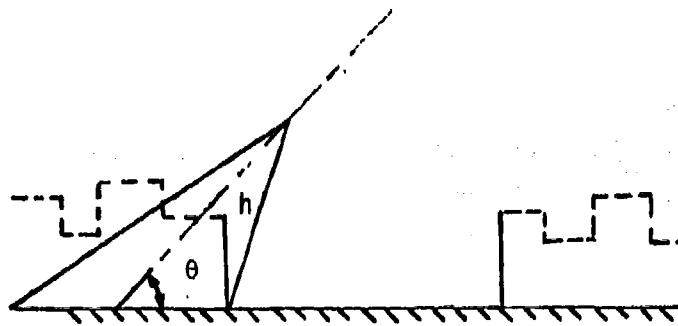
In the urban mass-fire context, fuel types and distributions are probably less well quantified than in wildlands and are certainly distinctly different. Also, building separation and the effect of streets as firebreaks may control spread (even after possible fuel scattering and modification by blast effects). Because of these distinctions, the short-range fire propagation across firebreaks is judged the most important mechanism to be modeled in the urban mass fire context. This process depends upon the local wind field and may be far less dependent upon detailed fuel parameters than spread in continuous fuel beds. These statements outline our conception of the proper modeling approach to contiguous fire spread in the urban mass-fire model.

In the following, we briefly outline the very approximate calculation of contiguous spread which we employ in the demonstration model. Contiguous spread is specialized to spread between city blocks (the basic grid cells of the model) across streets, which are assumed devoid of fuel. No inter-building spread is explicitly modeled, since city blocks are the basic units. Spread between separated buildings within a block needs more investigation, along with several other "sub-grid" effects, which must be parameterized. Minimal cell size is limited by the large area of the simulation. If ignited anywhere, an entire city block in the demonstration model eventually burns. Multiple ignitions of the same block are possible and result in faster burning. The rate of burning is proportional to the number of ignitions of the block.

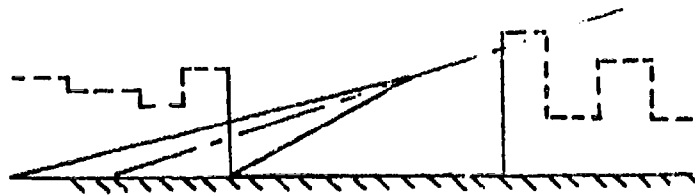
#### 4.5.1 Summary of Contagion Concepts

An important observation of the Flambeau tests (Reference 9) was that no fires were ignited outside the original fuel beds except within the horizontal distance determined by the vertical projection of the flaming volume onto the ground. Hence, ignitions only occurred on the lee side of the fire in a wind. We model spread across streets by estimating the configuration of tilted flame columns in the presence of a wind. Each flame column has the assumed shape of a cone with a circular base whose axis length and tilt are functions of burning rate and wind velocity. Figure 4-6 shows some possible relations of a flame column, burning at the edge of a block, to an open street in the downwind direction. Structures are suggested by the dotted outlines, and the flame column is represented by ground-based triangles. If the flame column does not overlap the adjacent block and its projected axis does not intersect buildings across the street, Figure 4-6(a), no contagion is possible and the adjacent block remains unignited. A finite ignition probability per unit time is calculated for the two cases of Figure 4-6(b) and 4-6(c). Figure 4-6(b) provides a mechanism for propagation between tall buildings separated by

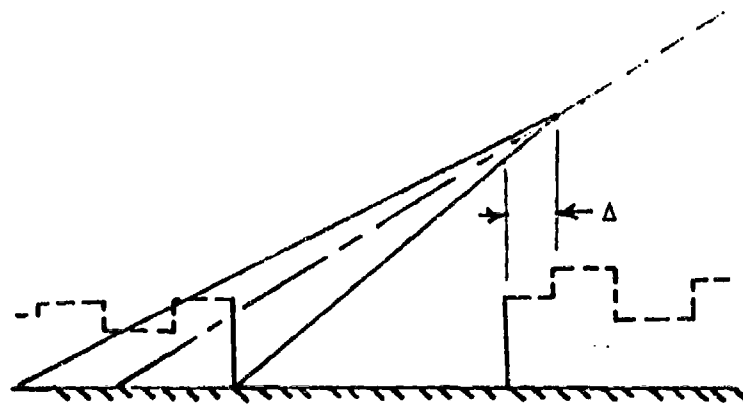




a. No contagion. No overlap. No axis intersection.



b. Contagion probability finite.  
Flame axis intersects buildings across street.



c. Contagion probability finite.  
Flame column overlaps buildings across street.

Figure 4-6. Contagion across streets.

narrow streets, and makes explicit use of building height. The configuration of Figure 4-6(c) allows for propagation in accord with the Flambeau observations, and an ignition probability proportional to the overlap  $\Delta$  is calculated.

The formulas and algorithms used by the demonstration model to implement these concepts are described in detail in Section 5. These methods may require substantial revision, so our summary description here includes only general features to indicate our concept of the physical factors involved.

Given the power  $\dot{Q}$  of a fire and its area,  $A = \pi r_0^2$ , where  $r_0$  is the effective radius of the cone base, the conical flame volume is computed from the air supply required for combustion  $\dot{V}_a \sim \dot{Q}$  and an assumed entrainment velocity 1.0 (m/s) through the lateral surface of the cone. From the volume and base area, the axial slant height,  $h$ , of the cone is computed. The angle  $\theta$  of the cone axis is determined from the ratio of the net vertical force on the flame, its buoyancy, to the net horizontal force. The buoyancy of the flame equals  $V_f g (\rho_a - \rho)$  where  $V_f$  is flame volume,  $g$  is the acceleration of gravity, and  $\rho_a - \rho$  is the difference between ambient air density and flame density. The horizontal force equals  $\rho_a \dot{V}_a v$  where  $\dot{V}_a$  is the total rate of air entrainment and  $v$  is the local wind velocity. These rough estimates establish the flame geometry shown in Figure 4-6.

A problem arises because the model carries only the burning rate  $\dot{Q}$  of an entire city block. If the base area of the single conical flame equals the area of the block, only rarely is  $\dot{Q}$  large enough to result in a flame tip located outside the base area. Here again, we encounter another aspect of the "sub-grid" problem and the need to estimate the number of flame columns in area burning. To resolve this problem

(somewhat inconsistently with procedures of the wind calculation) all the burning is assumed to take place within an area such that  $h > r_0$ . Since, in this case, the location of the burning sub-area within the block is not known, one employs a probability that it is located on the downwind periphery adjacent to unignited cells.

The geometry of the wind direction and the flame column in conjunction with the position of burning cells in relation to unignited ones forms the basis for calculating spread probability. These probabilities are, in fact, probabilities per unit time. Probabilities are computed at time steps internally determined on the basis of burning rate  $\dot{Q}$  and its derivative  $\ddot{Q}$ . Furthermore, these probabilities are accumulated so that when the time integral of the probability per unit time equals one, ignition is certain.

A more physical contagion algorithm, based upon a ratio of heat flux to heat of ignition as in the Rothermel model, might be preferable to the one we have used in the demonstration model. Also, recall that short-range branding may play a major role in contagion. In general, we feel the demonstration model exaggerates spread by contagion. However, it does capture the dependence of this propagation mechanism upon wind speed, wind direction, and upon burning rate.

#### 4.6 CONCEPT SUMMARY

The preceding sections have emphasized the salient aspects of our urban fire behavior concept. Fire development takes place by the principal spread mechanisms of contagion and branding, which are governed by atmospheric motion, a major component of which can be generated by the fire itself. The demonstration model, which has guided the discussion, provides an explicit framework illustrating the implementation of these concepts. The meaning of the demonstration model, we emphasize, does not

extend any farther. Narrowly viewed, it only provides a suitable structure and classifies the areas requiring further refinement.

A measure of uncertainty must be accepted in a model of urban mass fires. Not only are there limits of resolution of basic fuel and structural data, but also there are limits in the understanding of basic mechanisms all the way through the causal chain of events that occur. This circumstance requires a judicious selection and balance of model elements and model structure in order to minimize the uncertainties. The concept presented is our approach to this problem.

## SECTION 5

### DESCRIPTION OF DEMONSTRATION URBAN FIRE SIMULATION

The demonstration version of the Urban Fire Simulation embodies the range of phenomenology together with the logic and data management structures needed to implement the simulation concept described in Section 4. However, the phenomenology models are simplified versions of those described in Section 4. Development of a demonstration version of the simulation concept was undertaken to demonstrate the feasibility of implementing the concept, to qualitatively demonstrate simple regimes of behavior for the concept, and to identify areas in which modeling problems might exist. This section describes the structure and operation of the demonstration simulation. Simulation results are presented in Section 6, and a discussion of modeling problems is included in Section 1.

#### 5.1 DEMONSTRATION SIMULATION STRUCTURE AND OPERATION

The demonstration simulation structure is designed to provide flexibility and simplicity of maintenance. The simulation is modular, event sequenced, and autointeractive. The simulation is asynchronously stepped forward in time through execution of events sequentially selected from an event list. Autointeraction is achieved by allowing each module to insert events in the event list.

The overall structure of the Demonstration Urban Fire Simulation is shown by the block diagram of Figure 5-1. The meanings of the blocks shown in Figure 5-1 are defined below:

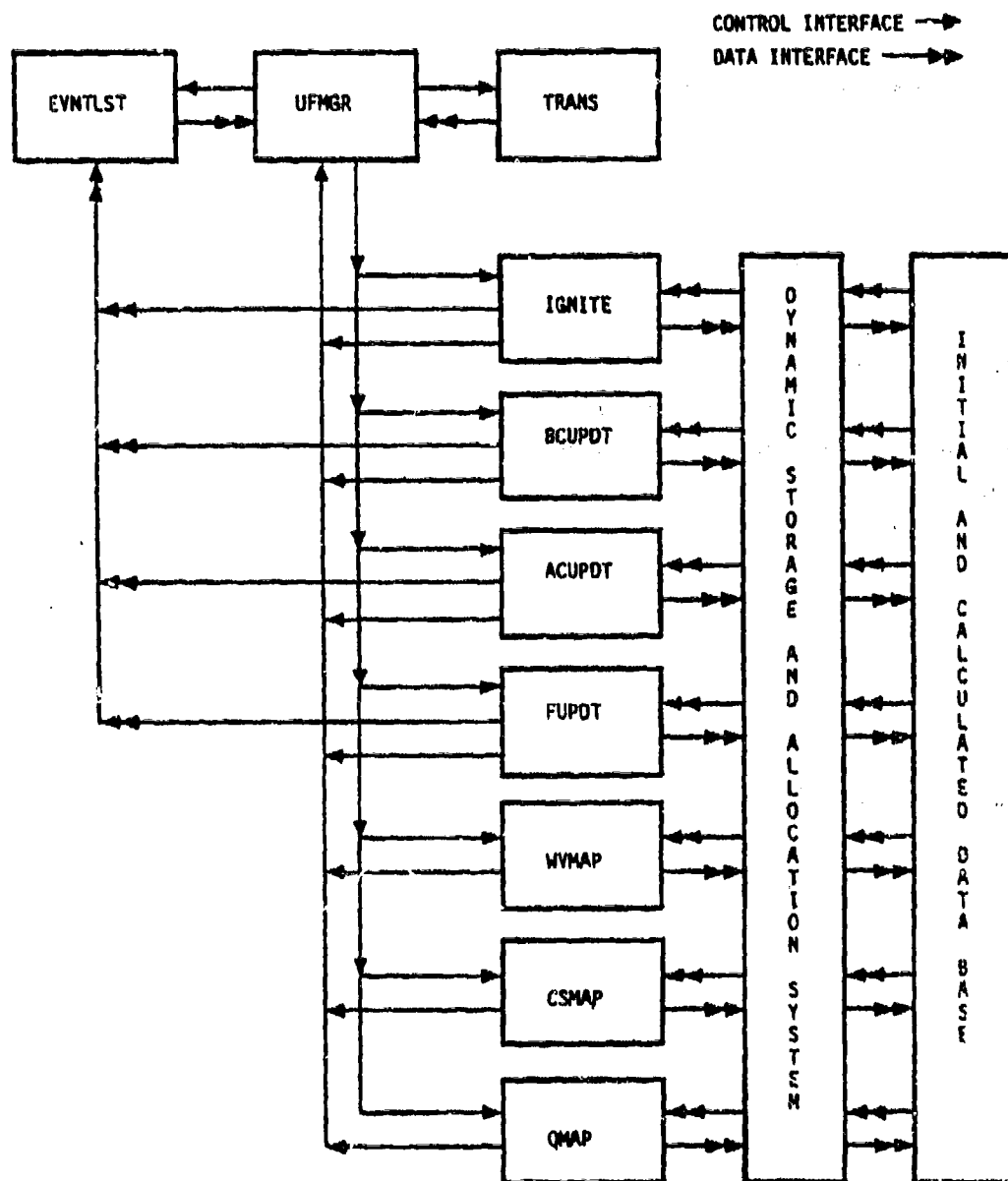


Figure 5-1. Block diagram of demonstration urban fire model.

- ENVTLST - the list (queue) of events to be executed
- UFMGR - the Urban Fire Manager (i.e., the executive structure)
- TRANS - the event module transfer list
- IGNITE - the functional module, which ignites unignited cells
- BCUPDT - the functional module, which updates burning cells
- ACUPDT - the functional module, which updates unignited cells adjacent to ignited cells
- FUPDT - the functional module, which updates the status of fires
- BRNDNG - the functional module, which determines if branding occurs
- WVMAP - the data processing module, which produces wind velocity maps
- CSMAP - the data processing module, which produces cell state maps
- QMAP - the data processing module, which produces heat production maps.

The Dynamic Storage and Allocation System (DSAS) provides for user interface to and management of the Data Base. The Data Base includes input data, interim calculations, and final results. In Figure 5-1, single and double headed arrows are used to indicate interfaces between the blocks. Single headed arrows denote control interfaces and double headed arrows denote data interfaces.

The simulation structure allows a simple executive procedure, which consists largely of two nested sequences of operations as described below. The Urban Fire Manager accesses the Event List and obtains the event in the list having the earliest execution time. With this event, the Urban Fire Manager accesses the Transfer List and obtains the sequence of modules, which must be processed to execute the subject event. The Urban Fire Manager transfers control to the first module in the sequence. The module accesses the Data Base through the Dynamic Storage and Allocation System to obtain its current input data, performs the computations

required by its function, stores an event in the Event List as appropriate, stores the results of its computations in the Data Base, and returns control to the Urban Fire Manager. The Urban Fire Manager continues to transfer control to the modules in sequence until all the modules in the sequence have been processed. When all of the modules in the sequence have been processed, event execution is, by definition, completed. The Urban Fire Manager then accesses the Event List to obtain the event having the earliest execution time and the event execution process is repeated until all events in the Event List have been executed. This executive procedure is both simple and flexible. It allows for altering events, adding events, and adding modules without any coding changes.

The demonstration model computation process is based on a two-dimensional grid structure, which is superimposed on the urban area of interest. The grid partitions the urban area into approximately city block sized square cells (i.e., 150 x 150 meters). As will be seen in the module descriptions, the grid-cell structure provides an organizational medium for the input data, the computational processes, and intermediate and final results. A description of the dynamic data base, which is used by each module, is presented in the next paragraph. This is followed in subsequent paragraphs by descriptions of each of the modules in Figure 5-1.

## **5.2 DYNAMIC DATA BASE DESCRIPTION**

The dynamic data base is keyed to the grid-cell structure and partitioned into data sets consistent with the types of data required or produced by the modules. These data sets are described below.

Grid Data: The grid data are used to define the grid dimensions for a specific simulation execution and can be changed between simulation executions. The grid data are as follows:



1. The cell dimension (assumes square cells)
2. The location of the rectangular coordinate system origin
3. The maximum number of cells in each of the two dimensions.

Cell State Data: Each cell in the grid may, at any time, be in one of the following five states:

1. Unignited
2. Unignited, but adjacent to a burning cell (Adjacent)
3. Ignited and on a fire periphery (Peripheral)
4. Ignited and in a fire interior (Interior)
5. Burned out.

The cell state data are an array containing the state of each cell in the grid. This array is updated each time a cell changes state.

Fuel Data: The fuel within each cell is assumed to be uniform and the fuel type within each cell is identified in terms of an occupancy class. An arbitrary number of occupancy classes can be defined, ranging from heavy industrial through single family residential to parks and unimproved areas. The fuel data specified for each occupancy class are:

1. Fuel loading( kg/cell)
2. Fuel heat content (J/kg)
3. Fuel height (m)
4. No wind combustion rate (m/s)
5. Scale factor for time of maximum heat production.

Event List: The event list is a queue of all the events that have been scheduled for execution and is updated each time an event is taken from or added to the queue.

Burning Cell Data: The burning cell data consist of a sequence of three data sets for each ignited cell. Each cell is assigned a unique identification number (ID) based upon its row-column location in the grid. The cell ID is used to access the cell state data, and the cell state together with cell ID are used to access data for both ignited and unignited cells. The following burning cell data are maintained for each ignited cell:

1. Entry ID (1)
2. Occupancy class (fuel type)
3. Cell topographic height (m)
4. Time of cell ignition (s)
5. Number of times cell has been ignited
6. Cell ID
7. Entry ID (2 or 3)
8. Current cell heat production rate (J/s)
9. Maximum cell heat production rate (J/s)
10. Current cell burn time (s)
11. Time of cell maximum rate of heat production (s)
12. Time at which these data are valid.

Data elements 2 through 6 do not change, and entry ID = 1 denotes this subset of a burning cell data set. Data elements 8 through 12 may change at each calculation time, and this is denoted by entry ID = 2 or 3. Subsets of calculated burning cell data are maintained at two times, which always subtend the simulation time. Data required at any other times are obtained by interpolating between the data stored at these two times. Entry ID = 2 denotes the earlier, and entry ID = 3 denotes the later of these two data subsets.

Adjacent Cell Data: Adjacent cell data consist of a sequence of data sets for each unignited cell that is adjacent to a burning cell. The following information is maintained for each adjacent cell:

1. Entry ID (1)
2. Occupancy class (fuel type)
3. Cell topographic height (m)
4. Time of last cell update
5. Cumulative probability of cell ignition
6. Cell ID

Data for entry ID = 1 are included in this case because the data for an adjacent cell will be used to form the first subset of data for a burning cell. When the cell is ignited, the entry ID = 1 subset will be updated, and subsets for entry levels 2 and 3 will be generated.

Unignited Cell Data: Unignited cell data consist of a sequence of data sets for each unignited cell in the grid that is not adjacent to a burning cell. The following quantities are maintained for each unignited cell:

1. Entry ID (1)
2. Occupancy class (fuel type)
3. Cell topographic height (m).

Data for entry ID = 1 are included in this case because the data for an unignited cell will be used to form the entry ID = 1 subset of data for an adjacent cell when the subject cell becomes adjacent to a burning cell.

Fire Data: A fire is defined to consist of a set of contiguous burning cells. Depending upon its geometry, a fire may be partitioned into subfires that are reasonably symmetrical. This is done because some

of the phenomenology models include assumptions regarding geometric symmetry of the fires they describe. The following data are maintained for each defined fire:

1. Fire ID
2. Location of the effective center of the fire (x,y coordinates - m)
3. Effective radius of the fire (m)
4. Fire heat production rate (J/s)
5. Fire area ( $m^2$ )
6. Volume rate of surface air inflow to fire ( $m^3/s$ )
7. Time at which these data were calculated (s)
8. Number of cells in fire at the time given in (7)
9. List of cells currently in fire.

The use of an effective center and radius for each fire recognizes that the rate of heat production over a fire will generally not be uniform. Each time a cell is added to (ignited) or deleted from (burned out) the fire data, element 9 is updated. The other eight data elements may be updated much less frequently for reasons of computational efficiency.

The data sets described above constitute most of the dynamic data base, which is accessible to and updated by the simulation models. The remaining data consist of flags, constants, and other numerical quantities that are not generally part of the dynamic data base. The following paragraphs describe the logic flow and data interfaces within the modules shown in Figure 5-1.

### 5.3 IGNITE MODULE

The IGNITE module initializes burning in cells that have been determined to have been ignited. As shown in Figure 5-2, the event data

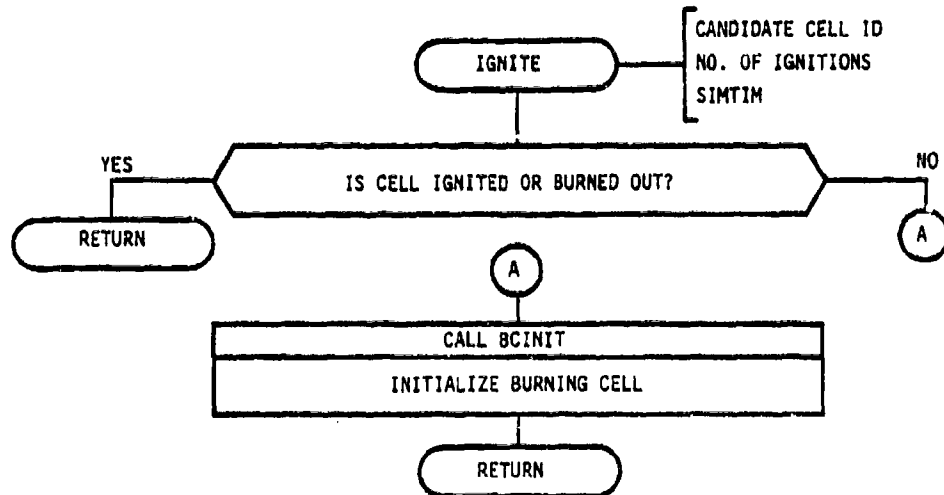


Figure 5-2. Logic flow of IGNITE module.

passed to IGNITE are the identity of the candidate cell, the number of ignitions and the current simulation time (SIMTIM). The candidate cell status is tested to determine if the cell can be ignited. If the cell is already ignited or burned out, it cannot be ignited and IGNITE returns control to UFMGR. If the candidate cell is unignited, the Burning Cell Initialization Subroutine is called and then control is returned to UFMGR.

The Burning Cell Initialization Subroutine (BCINIT) performs the tasks associated with changing the status of a cell from unignited to ignited as shown in Figure 5-3. BCINIT ignites the candidate cell at SIMTIM and changes the cell state from unignited to ignited. While the cell was unignited, the entry ID = 2 and 3 cell data subsets did not exist. The entry ID = 1 cell data subset is initialized at SIMTIM with all zero values. The wind velocity in the just ignited cell is calculated at SIMTIM + 360 seconds by the Wind Velocity Subroutine (WINDV). The entry ID = 2 data subset is initialized at SIMTIM + 360 seconds with values calculated for that time, and a burning cell update event is placed in the event list for execution time at SIMTIM + 360 seconds. Any subroutine requiring data on this cell between the current time and current time plus 360 seconds will obtain it by interpolating between these two data subsets. At current time plus 360 seconds, execution of the burning cell update event will reset data subset ID = 2 to ID = 1, generate a new data subset ID = 2 at a future time dependent upon cell heat production rate, and place an update event in the event list for execution at the same future time. In this way, two data subsets that always subtend SIMTIM are maintained for each burning cell .

The cell state and the fire to which it belongs (if burning) are identified for each of the eight cells adjacent to the just ignited cell. Also, the oldest fire represented among the eight adjacent cells is identified. Fires are assigned unique ID numbers in sequential order, so that older fires have lower ID numbers. When fires are merged, younger

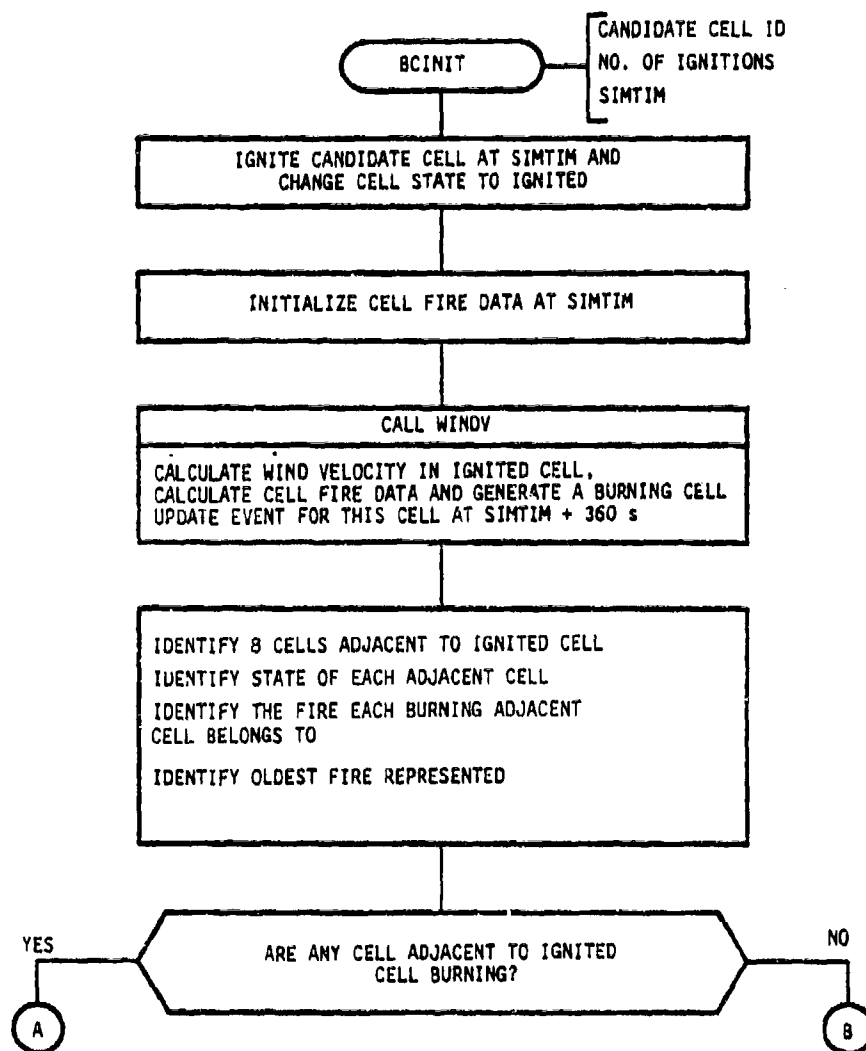


Figure 5-3. Logic flow of burning cell initialization module.

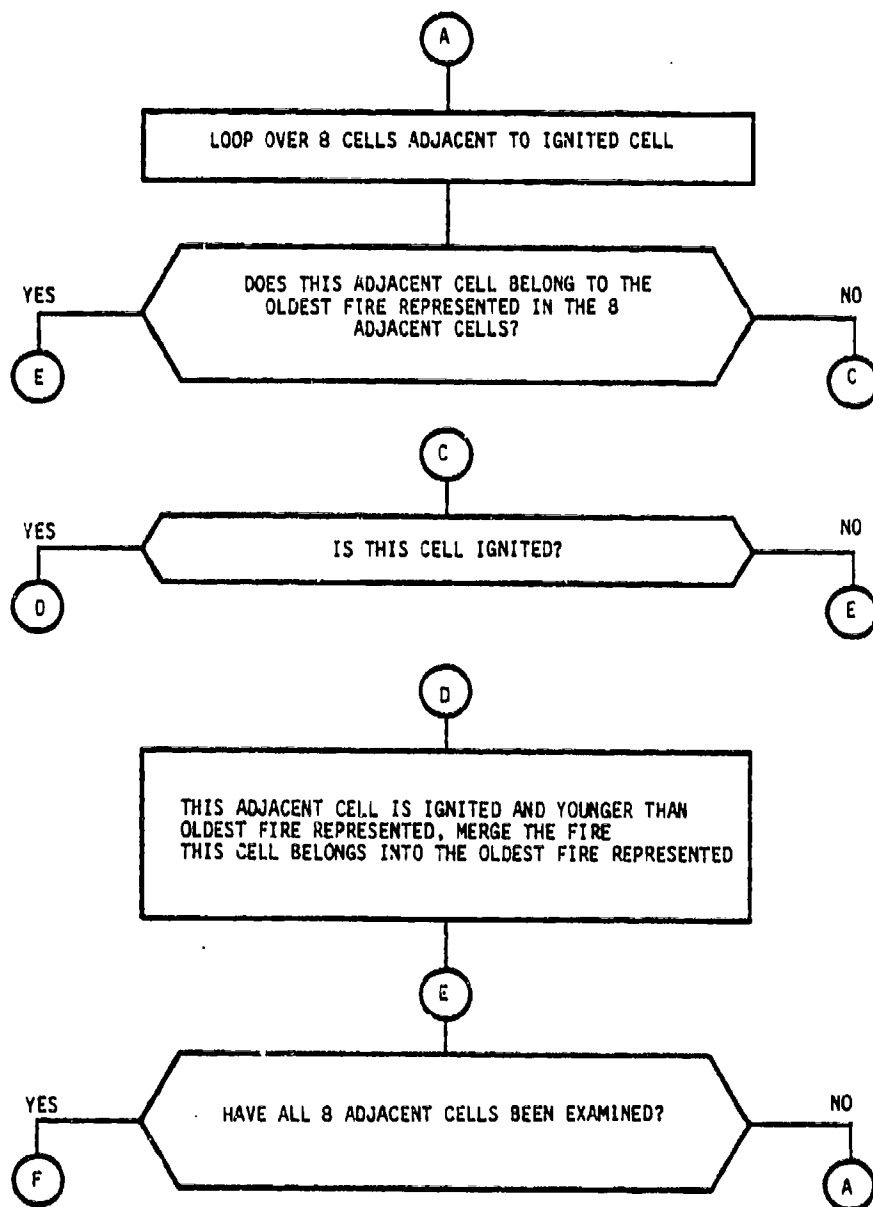


Figure 5-3. Logic flow of burning cell initialization module (continued).



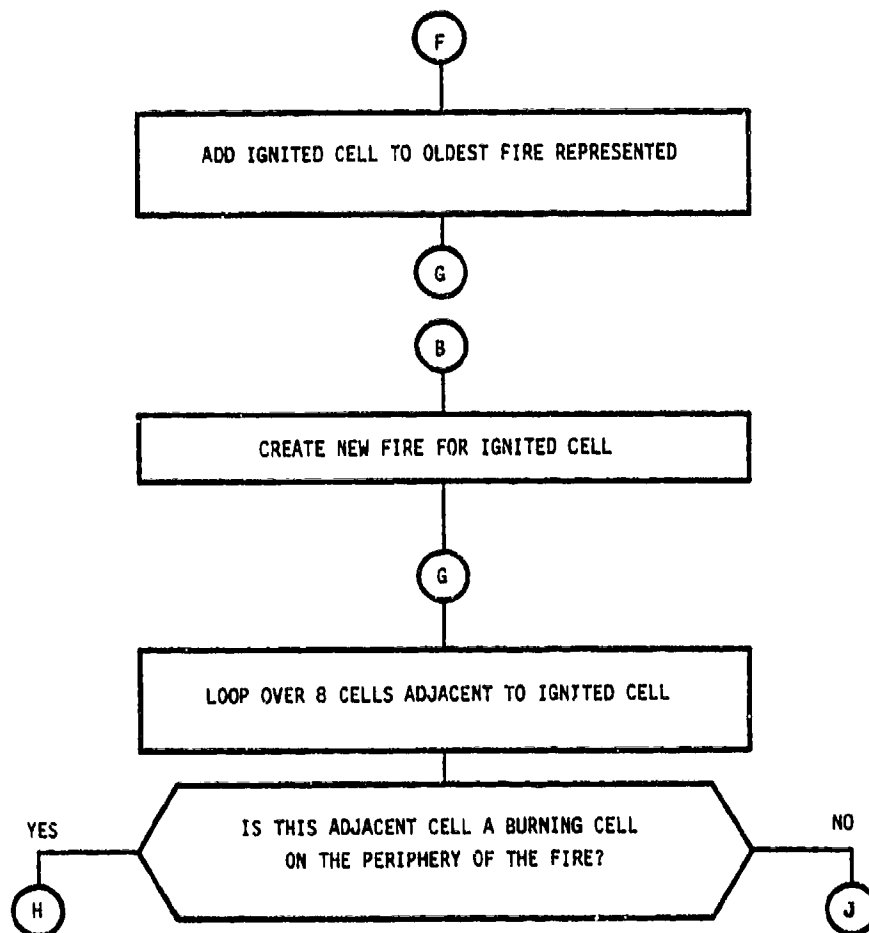


Figure 5-3. Logic flow of burning cell initialization module (continued).

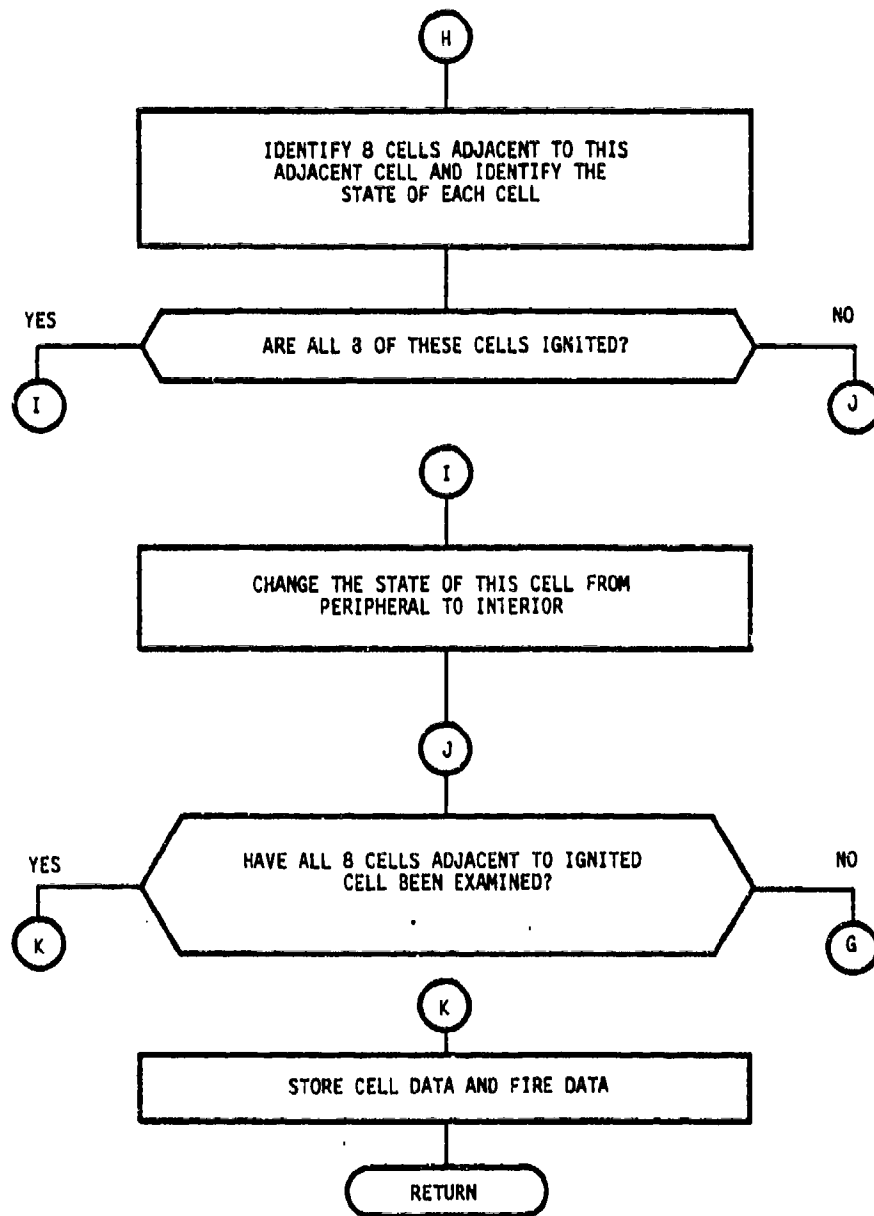


Figure 5-3. Logic flow of burning cell initialization module (concluded).

fires are always merged into older fires to maintain continuity of (older) fire identities.

If at least one cell adjacent to the just ignited cell is burning, BCINIT transfers to label (A), otherwise transfer is to label (B). At label (A), the fire identities of all of the ignited adjacent cells are examined. If the fire ID of an ignited cell is different from the ID of the oldest fire represented among the adjacent cells, transfer is to label (D). At label (D), the fire that the subject burning cell, adjacent to the just ignited cell belongs to, is merged with the oldest fire represented among the eight adjacent cells. Merging the two fires involves combining the burning and adjacent unignited cell lists of the younger fire with the burning and adjacent unignited cell lists of the older fire, updating the fire geometry partitioning, and updating the fire physical data. After all of the required mergers have been performed, the just ignited cell is added to the oldest fire represented among its eight adjacent cells and a transfer is made to label (E).

At label (B), none of the eight cells adjacent to the just ignited cell were found to be ignited. This is the definition of an isolated fire. Thus, a new fire is created for the just ignited cell. This involves assigning to this cell the next fire ID number, creating burning and adjacent unignited cell lists, and initializing the fire physical data.

The Wind Velocity Subroutine (WINDV) calculates the wind velocity at a specified point due to all fires in the grid area and due to the ambient wind. The wind velocity calculation assumes a flux sink at the center of each circularly symmetrical subfire. As mentioned before, fires consist of sets of contiguous burning cells, which are partitioned into subfires that are approximately symmetrical. Thus, each fire, even if not partitioned, includes one subfire (i.e., the whole). As shown in the

logic flowchart of Figure 5-4, WINDV loops over all fires and subfires in the grid and calculates the contribution of each subfire to the fire induced wind velocity at a specified field point. Three cases are considered in this calculation: (1) the field point is located at the center of the subfire under consideration; (2) the field point is inside the subfire under consideration; and (3) the field point is outside of the subfire under consideration. Upon completion of the fire induced wind calculations, the ambient wind velocity is added to the fire induced wind velocity to define the total wind velocity at the specified point.

Calculation of the fire induced wind velocity is based on the following equations.

$$\vec{v}_F(\vec{r}_p) = \sum_{f=1}^N \vec{v}_r(\vec{r}_p) + \sum_{f'=1}^M \vec{v}_f(\vec{r}_p) \quad (5-1)$$

where

$\vec{v}_F(\vec{r}_p)$  = the fire induced wind velocity at the grid point  $\vec{r}_p$ ,

$f=1, N$  are the subfires that do not contain grid point  $\vec{r}_p$ ,

$f'=1, M$  are the subfires that do contain grid point  $\vec{r}_p$ .

The contribution to the fire induced wind at point  $\vec{r}_p$  due to subfire  $f$ , which does not contain grid point  $\vec{r}_p$ , is given by

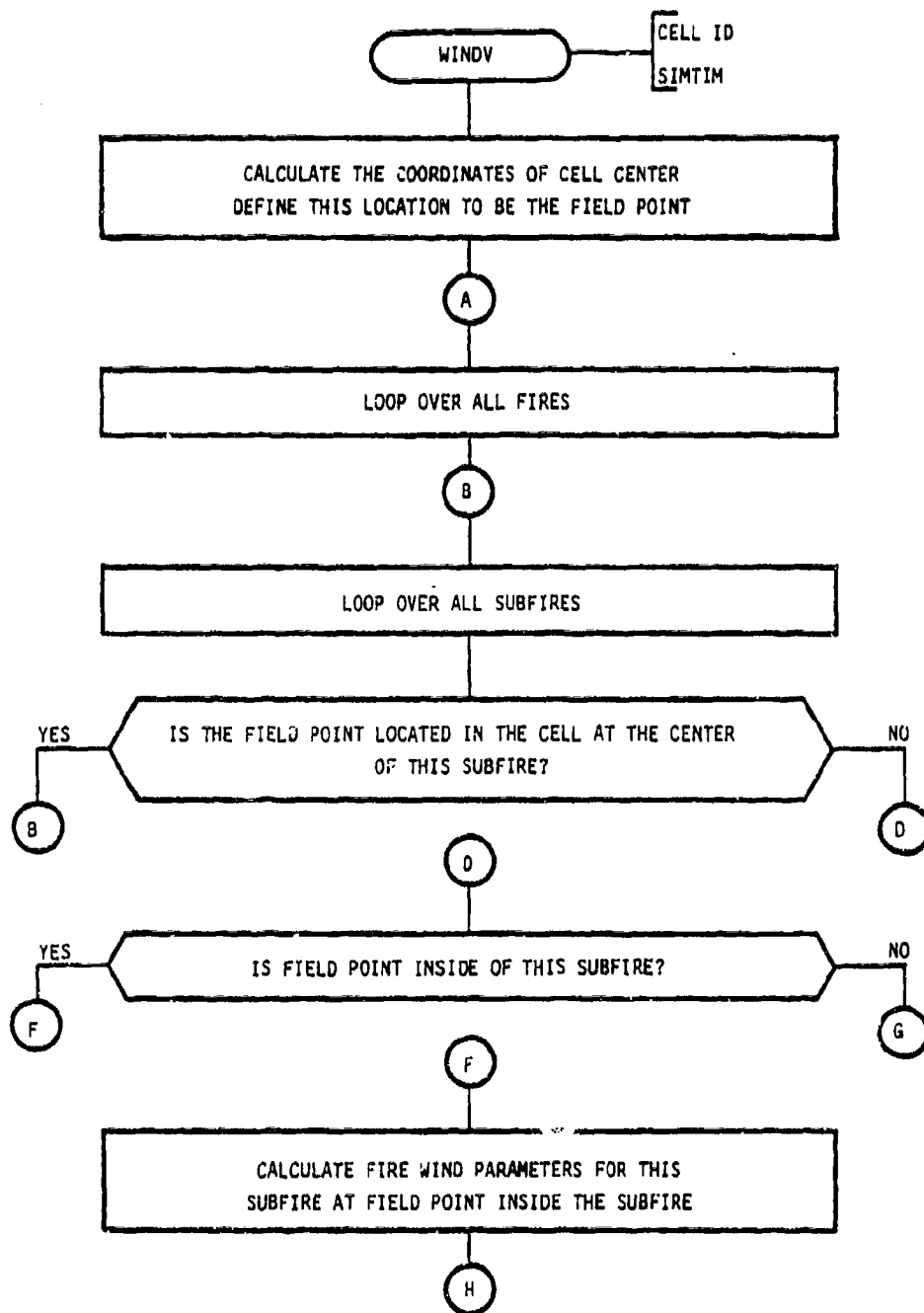


Figure 5-4. Logic flow of wind velocity subroutine.

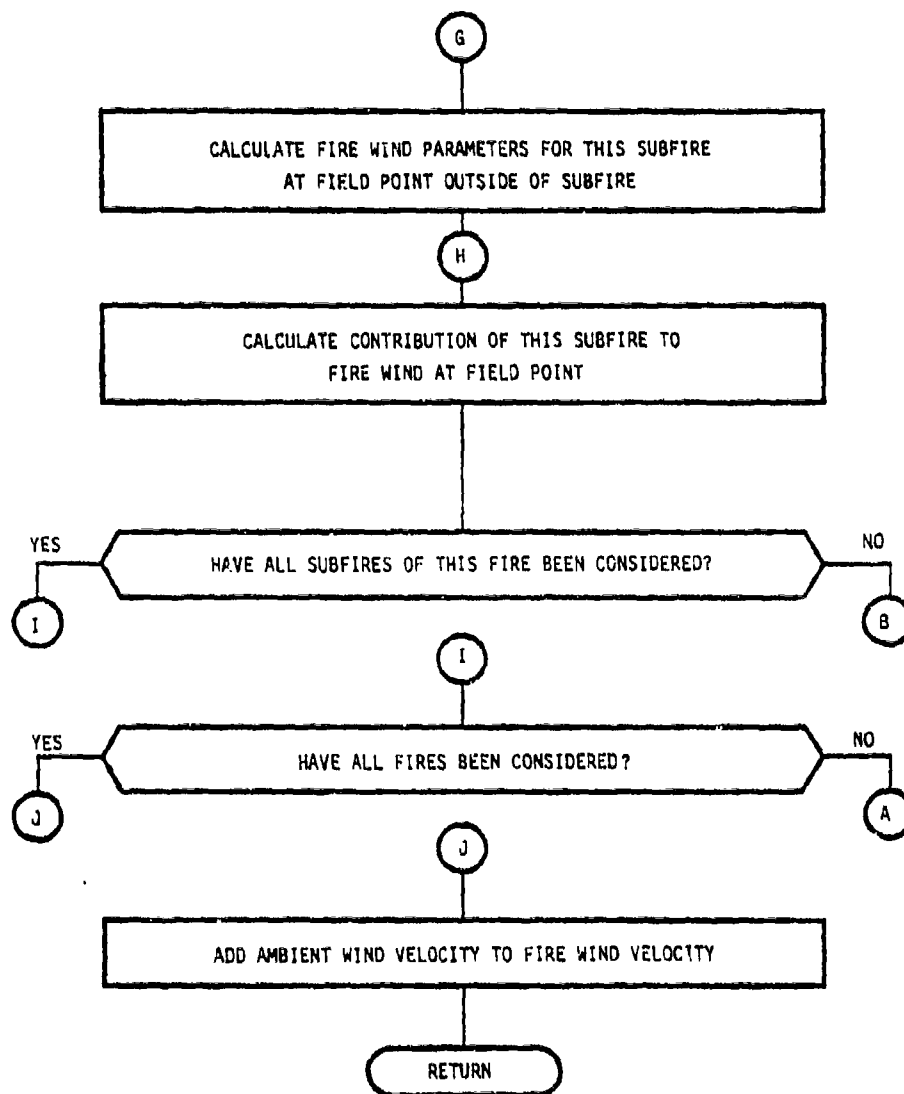


Figure 5-4. Logic flow of wind velocity subroutine (concluded).

$$\vec{v}_f(\vec{r}_p) = \left[ \frac{\dot{V}_f}{2\pi v |\vec{a}_f|^3} + \frac{g(\gamma) \dot{Q}_f^{-1/9} r_f^{10/9}}{|\vec{a}_f|^{4/3}} \right] \vec{a}_f. \quad (5-2)$$

The contribution to the fire induced wind at point  $\vec{r}_p$  due to subfire  $f$ , which does contain grid point  $\vec{r}_p$ , is given by

$$\vec{v}_{f'}(\vec{r}_p) = \left[ \frac{\dot{V}_{f'}}{2\pi r_{f'}^3} + g(W)h \left( \frac{|\vec{a}_{f'}|}{r_{f'}} \right) \dot{Q}_{f'}^{-1/9} r_{f'}^{7/9} \right] \vec{a}_{f'}, \quad (5-3)$$

where

$\dot{V}_{f'}$  = volume rate of air inflow to subfire  $f'$ ,

$\vec{a}_{f'} = \vec{r}_{cf'} - \vec{r}_p$ ,

$\vec{r}_{cf'}$  = location of the effective center of subfire  $f'$ ,

$\dot{Q}_{f'}$  = total energy release rate of subfire  $f'$ ,

$r_{f'}$  = effective radius of subfire  $f'$ .

The function  $g(\gamma)$  is given by

$$g(\gamma) = 0.5298 \gamma^{1.5863} / (1.3285 + \gamma^{1.5863}) \quad (5-4)$$

where

$$\gamma = Z_c / |\vec{a}_f| \quad \text{if} \quad |\vec{a}_f| > r_f \quad \text{or} \quad (5-5)$$

$$Z_c/r_f \quad \text{if } |\vec{a}_f| < r_f ,$$

$$Z_c = 0.23376 \dot{Q}_{mx}^{1/4} t^{3/4} \quad (5-6)$$

$\dot{Q}_{mx}$  = total energy release rate of the largest fire in the grid

t = simulation time.

The function  $h(|\vec{a}_f|/r_f)$  is given by

$$h\left(\frac{|\vec{a}_f|}{r_f}\right) = \pi - 2 \cos^{-1}\left(\frac{|\vec{a}_f|}{r_f}\right) + 2\left(\frac{|\vec{a}_f|}{r_f}\right) \sqrt{1 - \left(\frac{|\vec{a}_f|}{r_f}\right)^2} . \quad (5-7)$$

#### 5.4 BURNING CELL UPDATE (BCUPDT) MODULE

The Burning Cell Update Module maintains dynamic cell data that provide the characteristics of a burning cell. Two dynamic cell data lists are maintained that always subtend SIMTIM. Characteristics at any SIMTIM are determined by interpolating with respect to time between these two data lists.

The energy production rate of a burning cell is defined by

$$\dot{q}_c = \frac{Q_c}{\tau_{mx}} \tau e^{-\tau/\tau_{mx}} \quad (\text{J/s}) \quad (5-8)$$



where

- $\dot{q}_c$  = energy production rate of cell c (J/s)
- $Q_c$  = total energy content of cell (J)
- $t_{mx}$  = cell time of maximum energy production (s)
- $t$  = cell burn time (s).

The total cell energy content is given by

$$Q_c = H_F L_F A_c \quad , \quad (j) \quad (5-9)$$

where

- $H_F$  = fuel heat content (J/kg)
- $L_F$  = fuel loading (kg/m<sup>2</sup>)
- $A_c$  = cell area (m<sup>2</sup>).

The cell heat production rate given by Equation 5-8 rises to a peak value at  $\tau = \tau_{mx}$  and then decays as shown in Figure 5-5.

As shown in the logic flowchart of Figure 5-6, the information transferred to BCUPDT by the update event is the ID of the burning cell and the current SIMTIM.

BCUPDT identifies the fire the burning cell belongs to by referring to the cell state map. In this map, a burning cell is identified by the ID of the fire to which it belongs.

The fraction of the cell that has been burned at current SIMTIM is calculated. As shown in Equation 5-8 and Figure 5-5, the cell combustion function is characterized by a maximum heat production rate  $(\dot{q}_c)_{mx}$ , which occurs at time  $\tau_{mx}$ . Cell burnout is defined to occur at  $\tau = 4 \tau_{mx}$ , at which time the cell is approximately 90 percent

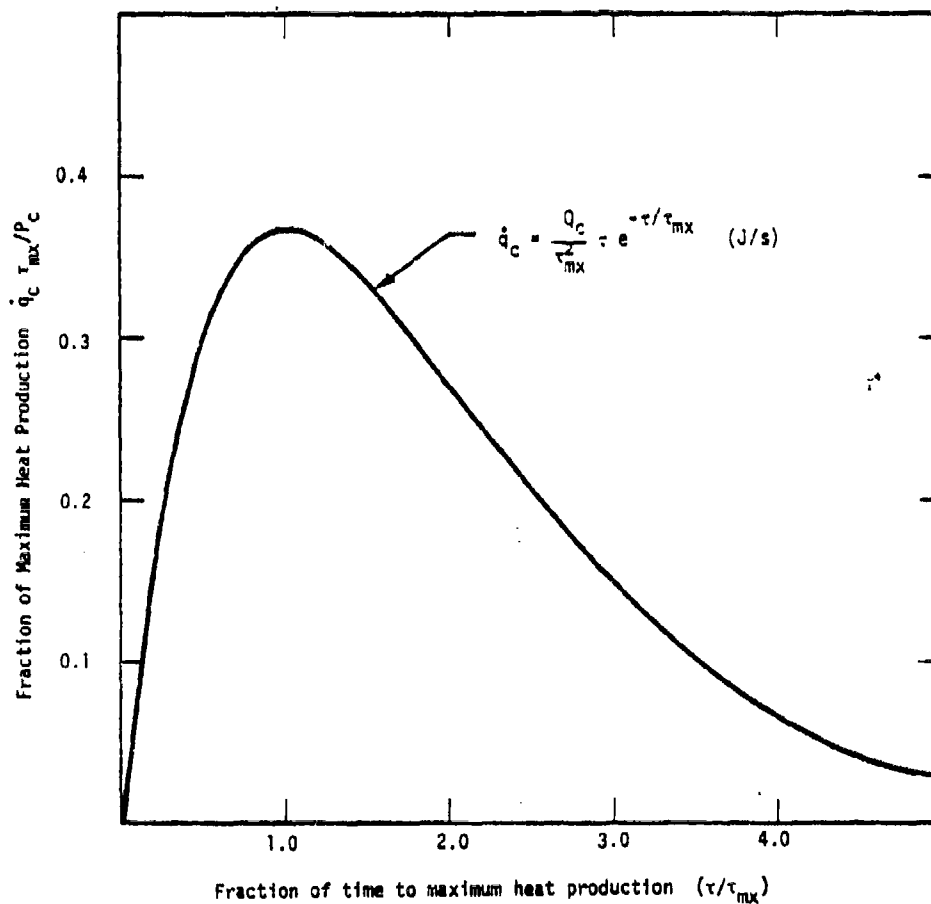


Figure 5-5. Functional form of cell heat production rate.

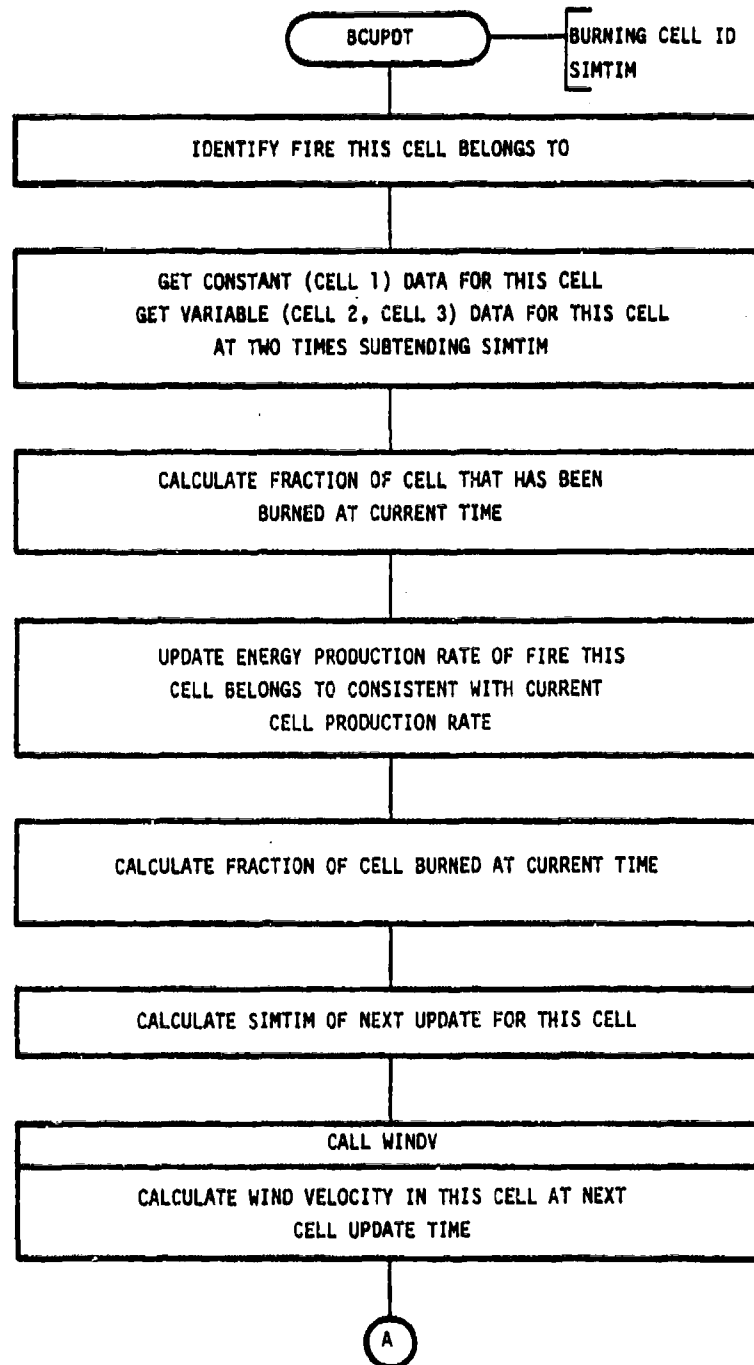


Figure 5-6. Logic flow of burning cell update module.

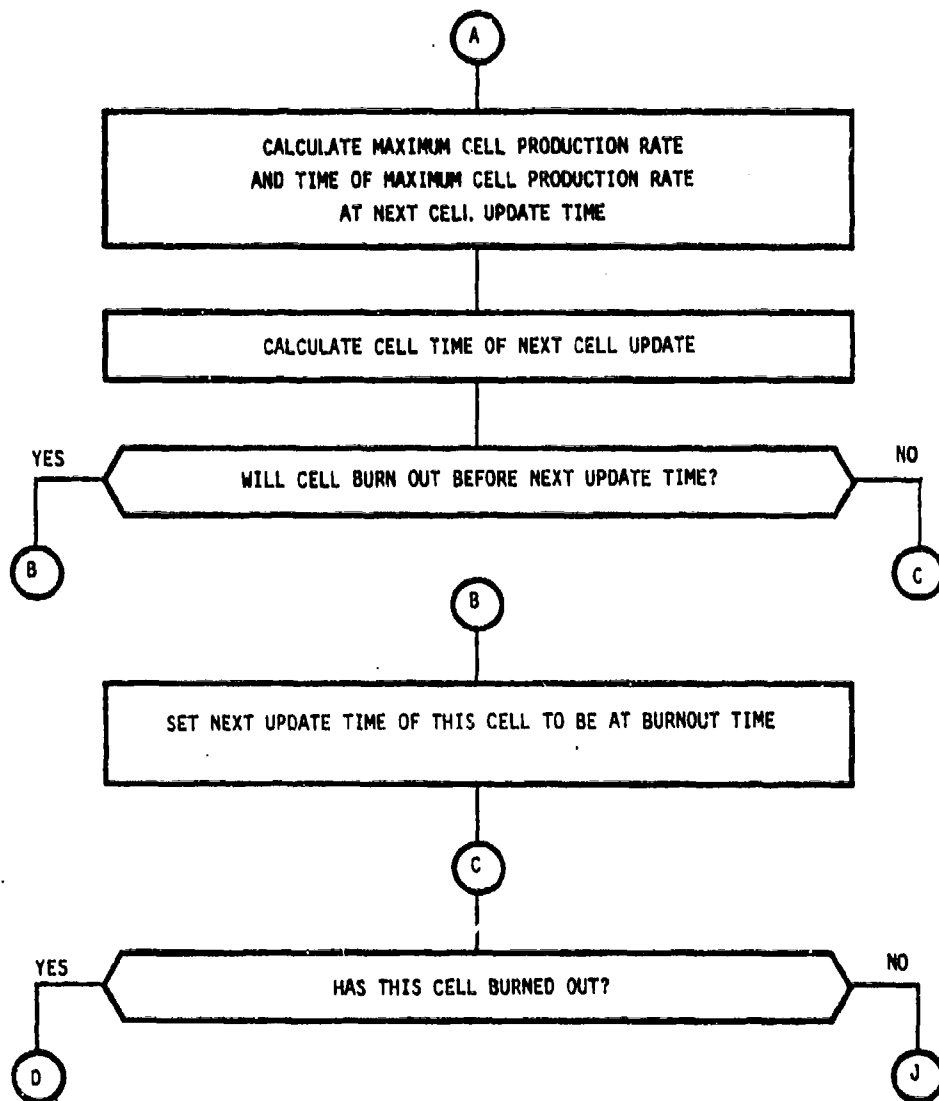


Figure 5-6. Logic flow of burning cell update module (continued).

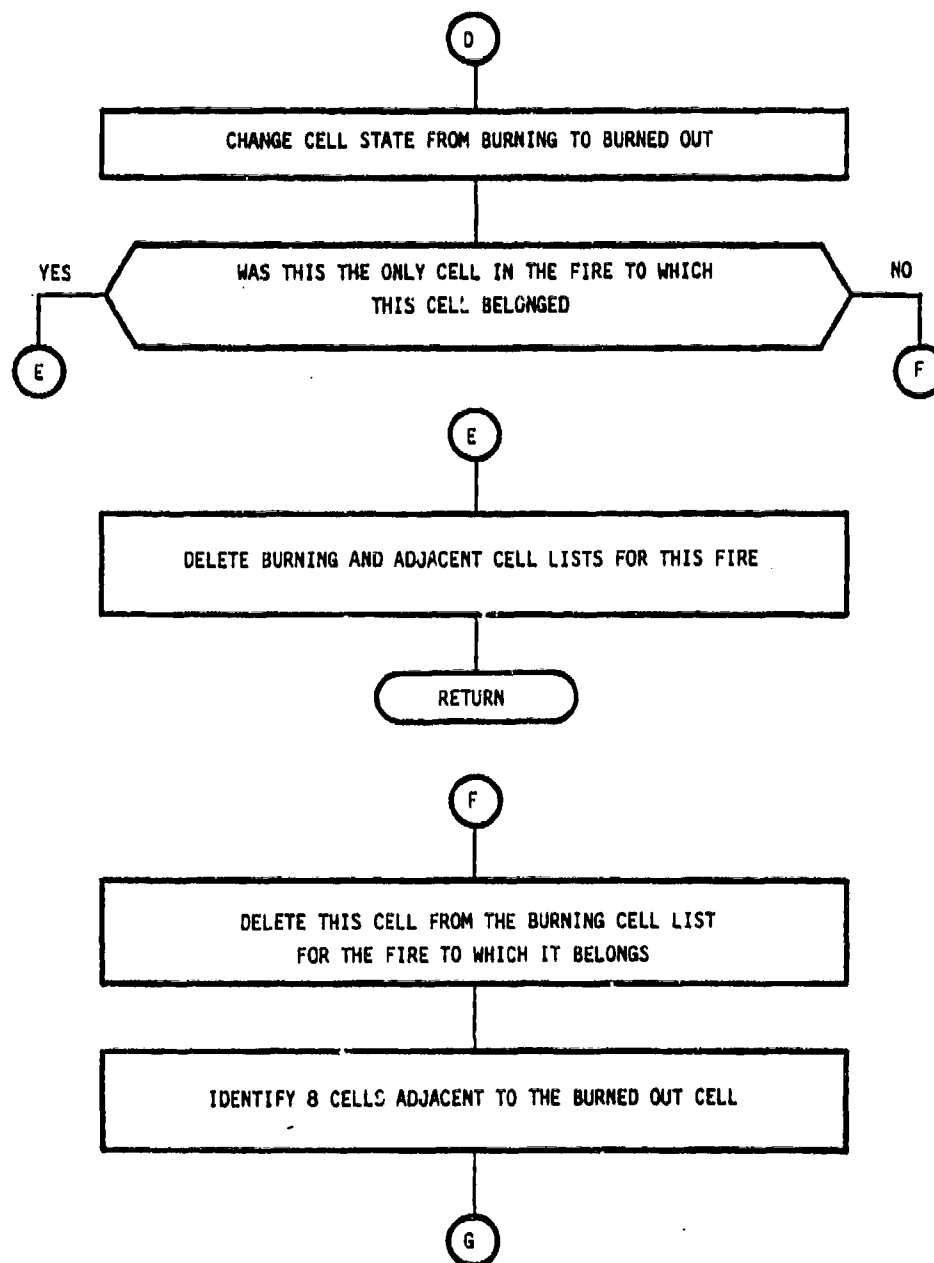


Figure 5-6. Logic flow of burning cell update module (continued).

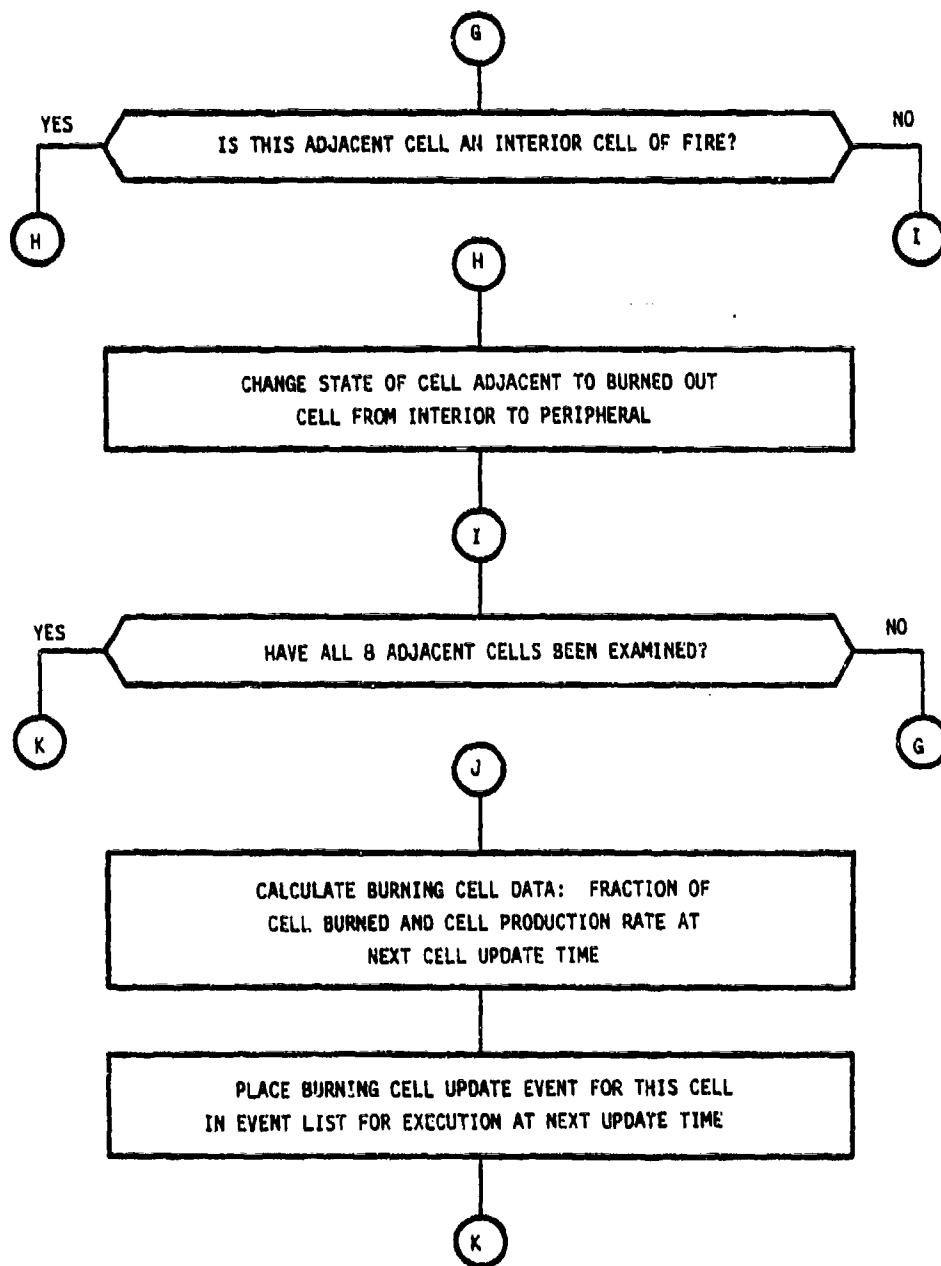


Figure 5-6. Logic flow of burning cell update module (continued).

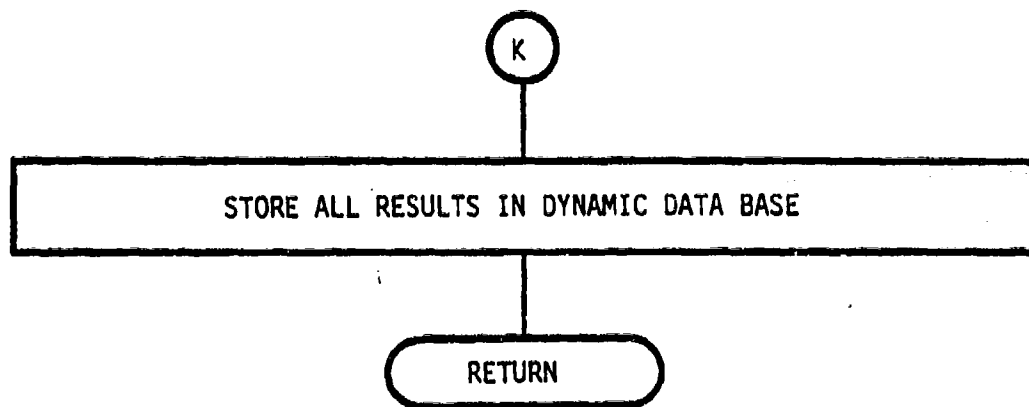


Figure 5-6. Logic flow of burning cell update module (concluded).

consumed, according to Equation 5-8. Thus, a measure of the fraction of the cell that has been burned is given by  $\tau/4\tau_{mx}$ .

The current energy production rate of the cell is calculated from the dynamic cell data. This cell production rate is used to update the energy production rate of the fire to which the cell belongs. In the case of fires (as opposed to cells), only one set of data is maintained to describe the fire status. In between fire update events, the fire state is assumed not to change, except for fire heat production rate, which is adjusted each time one of the fire's constituent cells is updated.

A burning cell update event is always scheduled to occur when SIMTIM is equal to the time of the most recent dynamic set of cell data. A significant function of the burning cell update is to determine the next update time, project dynamic cell data to that time, and arrange for a cell update at that time.

The time to be associated with the new data set and with the next update of the burning cell is based on the current rate of change of cell heat production rate. The time increment to the next update is given by

$$d\tau = 0.5 \tau_{mx} (1 - q/q_0) \quad (s), \quad (5-10)$$

where  $\ddot{q}_0 = \ddot{q}/(t=0)$ . This provides for updates at approximately 2000 second intervals when  $\tau > \tau_{mx}$  and provides more frequent updates when  $\tau < \tau_{mx}$ . The rate of change of cell heat production rate with respect to time ( $q_c$ ) is from Equation 5-8

$$q_c = (Q_c/\tau_{mx}^2)(1 - \tau/\tau_{mx}) e^{-\tau/\tau_{mx}} \quad (5-11)$$



A call is made to WINDV to calculate the wind velocity in the burning cell at  $\tau' = \tau + d\tau$ , the time of the next cell update.

At label (A) of Figure 5-6, the time of maximum cell heat production is calculated from

$$\tau_{mx} = k L_c / (N_{ig} h_f (a + S_w)) \quad (s), \quad (5-12)$$

where

$k$  = fuel constant

$L_c$  = cell dimension (m)

$N_{ig}$  = number of ignitions in cell

$h_f$  = fuel height (m)

$a$  = zero-wind spread rate coefficient (m/s)

$S_w$  = total wind speed in cell (m/s).

The effects of increasing wind speed upon cell combustion are, thus, to increase the maximum cell heat production rate and to cause its occurrence at an earlier time. Maximum cell heat production rate occurs at  $\tau = \tau_{mx}$ , which from Equation 5-8 yields

$$(\dot{q}_c)_{mx} = 0.368 Q_c / \tau_{mx} \quad , \quad (5-13)$$

where  $Q_c$  is defined by Equation 5-9 and  $\tau_{mx}$  by Equation 5-12.

The time of maximum heat production is a function of total wind speed in the cell, which is a function of the geometry and intensity of all the fires in the grid, together with the ambient wind. The wind in the cell may, thus, fluctuate and cause both the time and level of maximum heat production rate to fluctuate. These fluctuations are acceptable and represent an important part of the fire wind interaction.

A change in wind speed affects  $\tau_{mx}$ ,  $(\dot{q}_c)_{mx}$ ,  $q_c$  and burnout time, together with other cell and fire variables. Given a change in  $\tau_{mx}$ , we must, to be physically consistent, require the cumulative heat production to be unchanged. The cumulative heat production rate  $(\dot{Q}_c)$  is, from Equation 5-8, given by

$$\dot{Q}_c(\tau) = \int_0^\tau \dot{q} dt = Q[1 - (1 + \frac{\tau}{\tau_{mx}}) e^{-\tau/\tau_{mx}}] \quad , \quad (5-14)$$

which we write in the form

$$\dot{Q}_c(f) = Q[1 - (1 + f) e^{-f}] \quad , \quad (5-15)$$

where  $f = \tau/\tau_{mx}$  is a measure of the fraction of the cell that has been burned. The cumulative cell heat production is held constant under varying  $\tau_{mx}$  by also varying  $\tau$  so that  $f$  remains constant. The fraction burned at the next cell update time ( $\tau'$ ) with the current value of  $\tau_{mx}$  is

$$f_1 = \tau'/\tau_{mx} \quad . \quad (5-16)$$

The fraction burned at the next cell update time with the value of  $\tau'_{mx}$  at that time is

$$f_2 = \tau'(\tau'_{mx}/\tau_{mx}) \quad . \quad (5-17)$$

Calculate the new value of cell time at the next update ( $\tau''$ ) of this cell as

$$\tau'' = \tau'(\tau'_{mx}/\tau_{mx}) \quad (5-18)$$

by requiring that  $f_1 = f_2$ . The manipulation at cell time is possible without affecting simulation time because the cell time is coupled to SIMTIM only by

$$\text{SIMTIM} = t_{ig} < \tau < 4\tau_{mx} = \text{SIMTIM} \quad . \quad (5-19)$$

Within the limitations imposed by Equation 5-19,  $\tau$  may advance or regress, as required by Equation 5-18, without affecting SIMTIM.

Given the adjusted time of the next cell update ( $\tau''$ ), the test  $\tau'' > 4\tau_{mx}$  is performed. If the update time is after cell burnout, the update time is adjusted at label (B) to coincide with cell burnout.

If  $\tau'' < 4\tau_{mx}$ , transfer is made to label (C). If  $\tau'' = 4\tau_{mx}$ , transfer is to label (D), otherwise transfer is to label (J).

At Label (D), a burned out cell has been identified. The state of the subject cell is changed from burning to burned out, and adjustments are made to the related fire data.

At label (E) the subject cell was the only burning cell in the related fire; thus, the fire is deleted by deleting its burning cell and adjacent cell lists. Processing of this cell is then complete and BCUPDT returns control to UFMGR.

At label (F) the subject cell was not the only burning cell in the related fire; thus, the subject cell is deleted from the burning cell list. The 8 cells adjacent to the subject cell are identified to determine if their state has been changed by the state change of the subject cell. All burning cells are either interior cells or peripheral cells.

An interior cell is one that has 8 burning adjacent cells and a peripheral cell is one that has at least one nonburning (unignited or burned out) adjacent cell. Thus, the only state change possible for a cell adjacent to a newly burned out cell is a change from an interior cell to a peripheral cell. In labels (G) through (I) all adjacent cells of the subject cell that were interior cells are changed to peripheral cells.

At label (J) all fire data manipulations have been completed. The burning cell heat production rate at the adjusted time of next cell update is calculated. A burning cell update event for the subject cell is placed in the event list for execution at the SIMTIM corresponding to the adjusted cell update time. At label (K) the new set of dynamic cell data are stored in the dynamic data base in place of the older of the two existing sets of dynamic cell data for this cell. The data stored are Entry ID, Heat Production Rate, Maximum Heat Production Rate, Cell Time of These Data, Cell Time of Maximum Heat Production Rate, and SIMTIM of these data. After storing these data in the dynamic data base, BCUPDT returns control to UFMGR.

## **5.5 ADJACENT CELL UPDATE (ACUPDT) MODULE**

As shown in Figure 5-7, the information passed to the ACUPDT module by the update event is the current SIMTIM and the ID of the cell to be updated. The cell to be updated is called an adjacent cell because it is adjacent to a fire. We will also be concerned with the eight cells adjacent to the cell to be updated. To prevent confusion, the cell to be updated is referred to here and in Figure 5-7 as the subject cell.

An unignited cell adjacent to a fire may experience a state change by becoming ignited. Ignition may result from branding or from contagion. Branding is defined as ignition due to the physical transport of burning material and will be discussed in a later section. Contagion

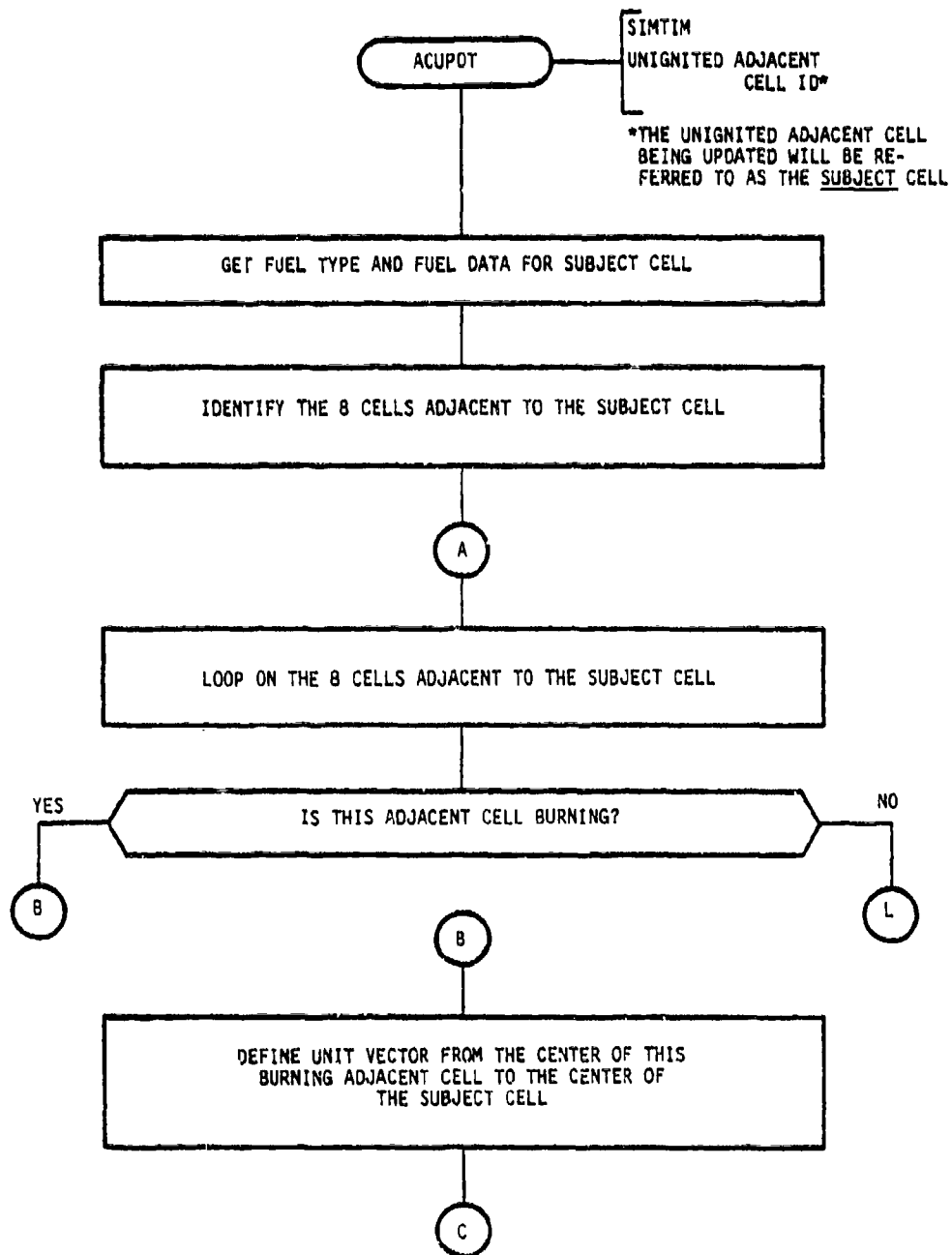


Figure 5-7. Adjacent cell update module.

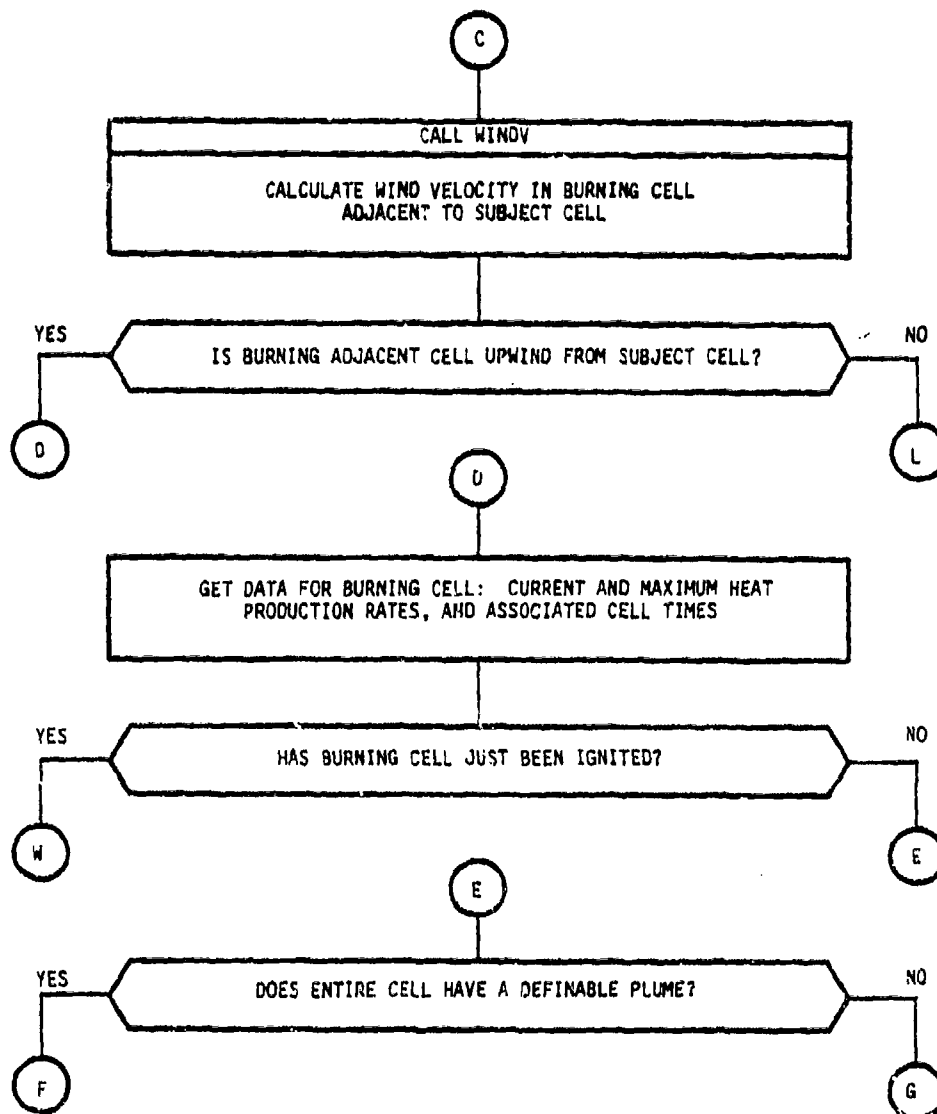


Figure 5-7. Adjacent cell update module (continued).

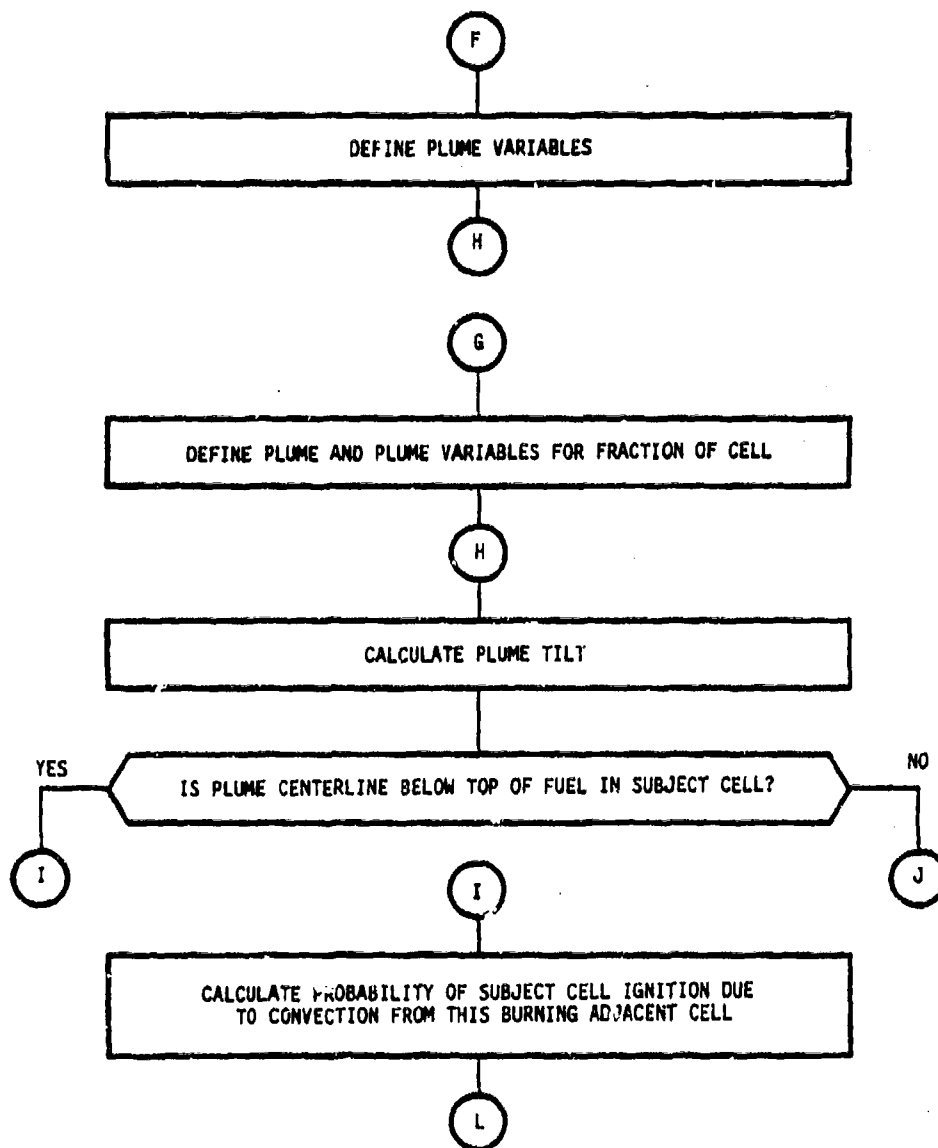


Figure 5-7. Adjacent cell update module (continued).

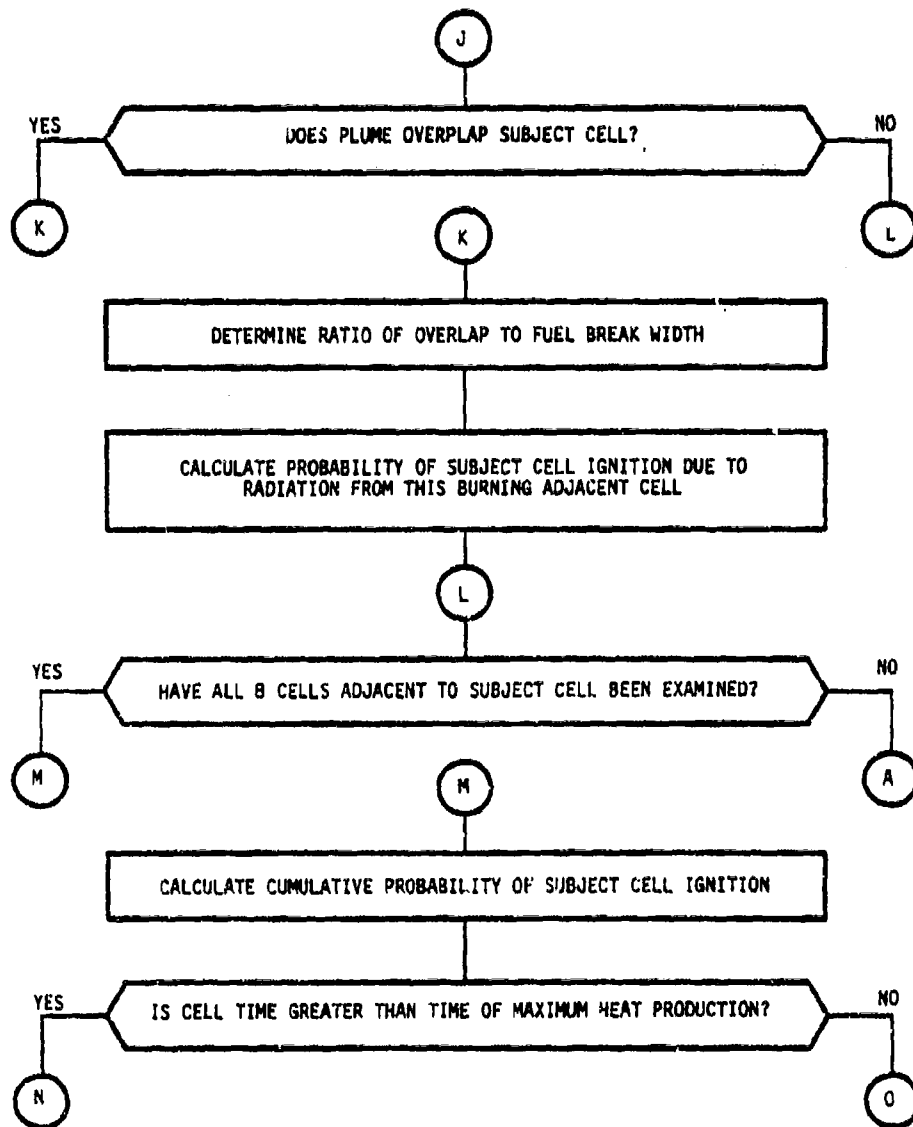


Figure 5-7. Adjacent cell update module (continued).



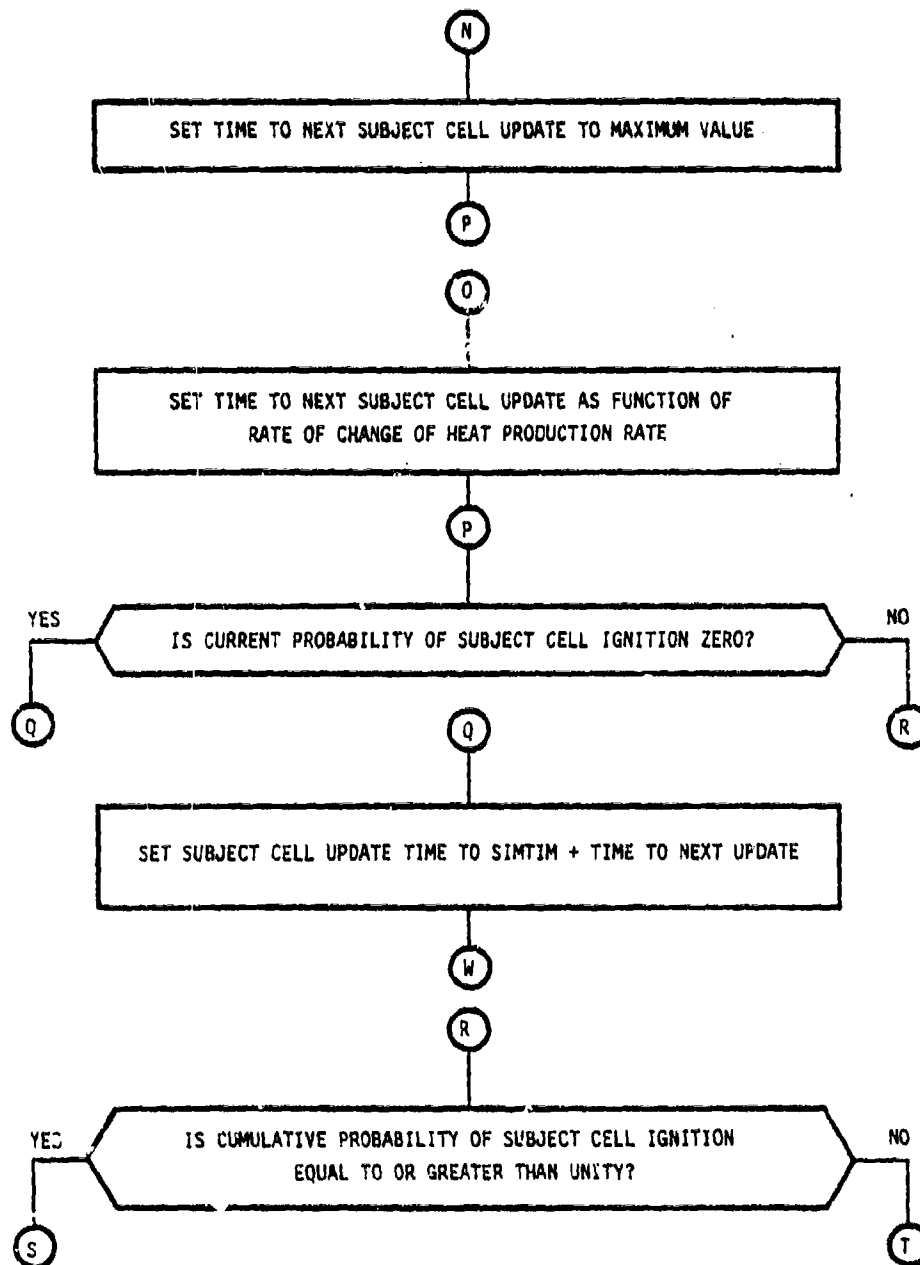


Figure 5-7. Adjacent cell update module (continued).

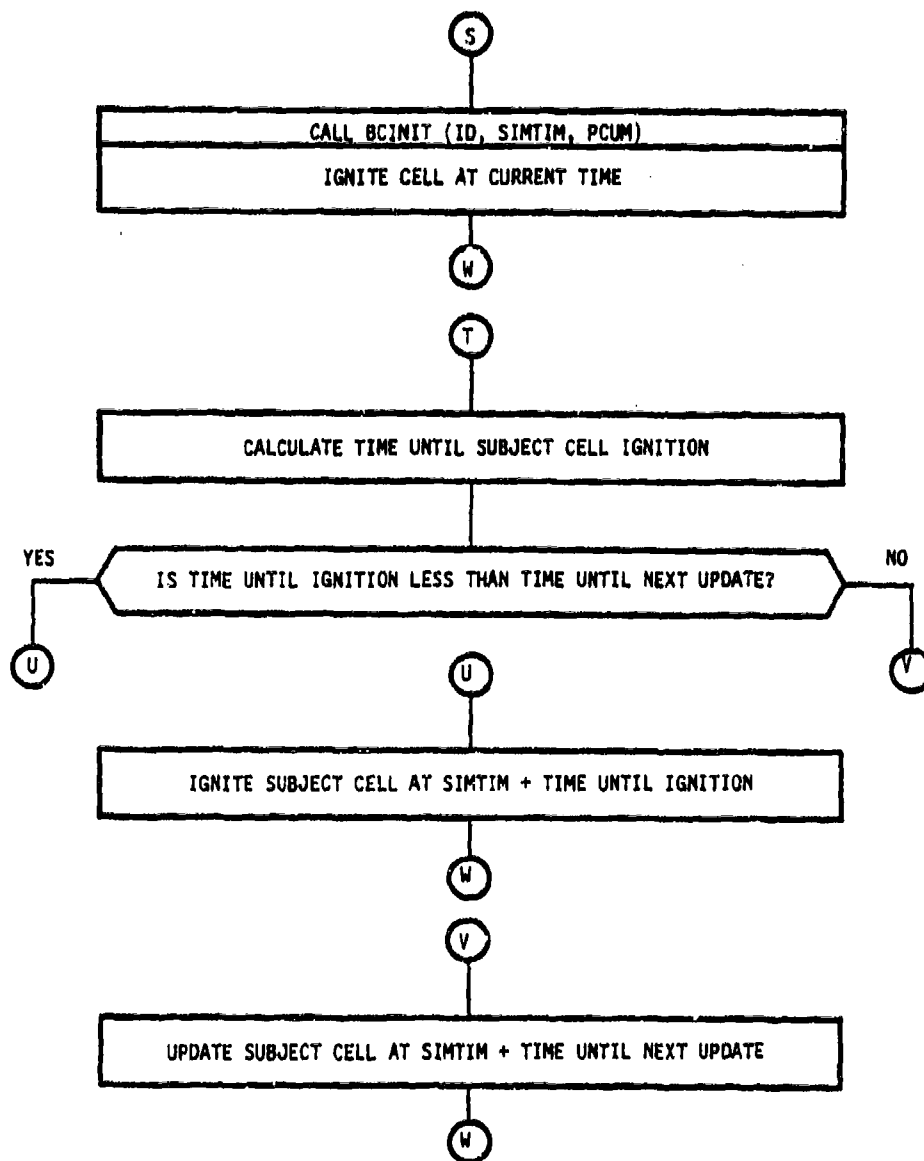


Figure 5-7. Adjacent cell update module (continued).

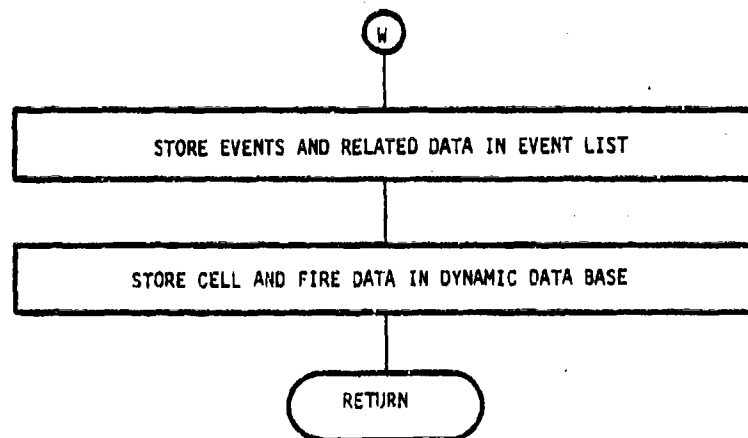


Figure 5-7. Adjacent cell update module (concluded).

is defined as ignition due to the transport of thermal energy by conduction, convection, or radiation. The purpose of ACUPDT is to determine if and when the subject will be ignited by contagion.

The subject cell ID provides access to the appropriate cell data, which contains the cell fuel type ID. The fuel type ID provides access to the fuel characteristics associated with that fuel type. The eight cells adjacent to the subject cell are identified.

Label (A) is the beginning of a loop over the eight cells adjacent to the subject cell in which only burning cells will be examined. Observe that since the subject cell is adjacent to a fire, at least one of its adjacent cells must be ignited. Each adjacent cell is tested (via the cell state matrix) to determine if it is burning. If it is not, the next cell is examined via label (L). If the cell is burning, transfer is to label (B).

At label (B) the unit vector is calculated in the direction from the center of the burning adjacent cell to the center of the subject cell. At label (C) a call is made to WINDV to calculate the wind velocity in the burning adjacent cell. Examination of the scalar product of the unit vector and wind velocity reveals if a wind component exists in the direction from the burning adjacent cell to the subject cell. If there is no wind component in the direction of the subject cell, the next adjacent cell is examined via label (L). If there is a wind component in the direction of the subject cell, transfer is to label (D).

At label (D) the dynamic cell data are accessed for the burning cell adjacent to, and upwind of, the subject cell. If this cell has just been ignited (at the current SIMTIM), its heat production rate is still zero and the next adjacent cell is examined via label (L). If the cell was ignited prior to the current SIMTIM, transfer is to label (E).

At label (E) all of the preliminary conditions have been satisfied for contagion to occur. An ignited cell with nonzero heat production has been identified adjacent to, and upwind of, the subject cell. A test is performed to determine if a plume can be defined for the entire burning cell. The plume test assumes a uniformly burning circular area of radius  $r_0$ , a constant entrainment velocity  $v_e$ , and a conical plume of base radius  $r_0$  and height  $h$ . The volume rate of air entrained by the plume ( $\dot{V}_G$ ) is

$$\dot{V}_G = A_p v_e \quad , \quad (5-20)$$

where the cone area  $A_p$  is given by

$$A_p = \pi r_0 (r_0^2 + h^2)^{1/2} \quad . \quad (5-21)$$

Combine Equations 5-20 and 5-21 and solve for the plume height  $h$  to obtain

$$h = r_0 \left[ \left( \frac{\dot{V}_G}{\pi r_0^2 v_e} \right)^2 - 1 \right]^{1/2} \quad . \quad (5-22)$$

The total heat production  $\dot{Q}_c$  of the cell is

$$\dot{Q}_c = \left( \frac{q_0 \rho_a}{k} \right) \dot{V}_G \quad , \quad (5-23)$$

where

$q_0$  = heat content of fuel (J/kg)

$\rho_a$  = air density (kg/m<sup>3</sup>)

$k$  = mass of air per mass of fuel.

The average heat production rate over the cell ( $\bar{q}$ ) is

$$\bar{q} = \dot{Q}_c / A_c \quad (5-24)$$

where  $A_c$  = base area of conical plume. From Equations 5-23 and 5-24, Equation 5-22 can be written in the form

$$h = r_0 \left[ \left( \frac{k_1 \bar{q}}{v_e} \right)^2 - 1 \right]^{1/2} \quad (5-25)$$

where

$$k_1 = \frac{k}{q_0 \rho_a}$$

$\bar{q}$  = average heat production rate per unit cell area.

The condition for a cell to have a definable plume is that the plume height ( $h$ ) as defined by Equation 5-25 be real valued. For  $h$  to be real, we must have

$$\left( \frac{k_1 \bar{q}}{v_e} \right) > 1 \quad (5-26)$$

If Equation 5-26 is satisfied, transfer is to label (F), else transfer is to label (G).

At label (F) the base area, base radius, and height of the conical plume are defined from Equation 5-25 and the cell area, and transfer is to label (H).

At label (G) a plume cannot be defined for the entire cell. It is assumed that, since the cell is burning, a plume exists and can be defined for some fraction of the cell. The appropriate cell fraction is defined by requiring that the minimum plume height  $h_{mn}$  be equal to the radius of the burning cell fraction responsible for its generation. In terms of a fraction  $f$  of cell area  $A_c = L_c^2$ , Equation 5-25 can be written

$$h_{mn} = r_{mn} \left[ \left( \frac{k_1 \bar{q} L_c^2}{f L_c^2 v_e} \right)^2 - 1 \right]^{1/2}, \quad (5-27)$$

where the effective cell fraction in plume generation is obtained by partitioning  $\bar{q}$  and assuming that  $\dot{q}$  is uniform over the cell. The requirement for  $h_{mn} = r_{mn}$  yields, from Equation 5-27, a definition of the cell fraction  $f$ , which is

$$f = (k_1 \bar{q}) / (2 v_e) \quad (5-28)$$

The plume base area, base radius and height are defined as

$$A_p = f A_c, \quad (5-29)$$

$$r_0 = (A_p/\pi)^{1/2} , \quad (5-30)$$

$$h = r_p , \quad (5-31)$$

respectively, and transfer is to label (H).

At label (H) a plume has been defined, either for the entire cell or for a fraction of the cell, and we desire to calculate the plume tilt resulting from wind velocity in the burning cell adjacent to the subject cell. The horizontal ambient wind force  $F_x$  is given by

$$F_x = \dot{V}_G \rho_a v_e \quad (5-32)$$

and the vertical buoyancy force  $F_z$  is given by

$$F_z = V_p g (\rho_a - \rho_i) , \quad (5-33)$$

where

$\dot{V}_G$  = volume rate of air entrained ( $m^3/s$ )

$v_e$  = entrainment velocity ( $m/s$ )

$\rho_a$  = ambient air density ( $kg/m^3$ )

$V_p$  = plume volume ( $m^3$ )

$g$  = gravitational acceleration ( $m/s^2$ )

$\rho_i$  = air density inside plume ( $kg/m^3$ ) .

The inclination  $\theta$  of the force vector measured from the horizontal is



$$\tan \theta = F_z/F_x = (0.8 V_p g)/(\dot{V}_G v_e) \quad (5-34)$$

where

$$(\rho_a - \rho_i)/\rho_a = 0.8 \quad .$$

The velocity ( $V_p$ ) of a conical plume tilted  $(\pi/2 - \theta)$  radians from the vertical is

$$V_p = (1/3)hA_b \sin \theta \quad (5-35)$$

where

$h$  = cone height (m)

$A_b$  = cone base area (m).

Combine Equations 5-34 and 5-35 to obtain

$$\frac{1}{\cos \theta} = \frac{\tan \theta}{\sin \theta} = \frac{0.8}{3} \frac{hA_b g}{\dot{V}_G v_e} \quad (5-36)$$

Substitution of Equations 5-23, 5-24, and 5-25 into 5-36 and simplifying yields

$$\frac{1}{\cos \theta} = \frac{0.8}{3} \frac{g r_o}{v_e} \left[ \left( \frac{1}{v_e} \right)^2 - \left( \frac{1}{k_1 \frac{r}{q}} \right)^2 \right]^{1/2} \quad (5-37)$$

The angle  $\theta$  given by Equation 5-37 is defined to be the plume tilt angle. It can be seen that Equation 5-37 may be imaginary and that the condition

for Equation 5-37 to be real valued is the same as the condition for Equation 5-25 to be real valued. Thus, the plume definition tests, which define  $h$  to be real valued, also assure that  $\theta$  is real valued.

The cells in the grid are considered to be separated by streets, which are lines of specified width that contain no fuel. The ACUPDT module considers two methods by which heat from a burning cell may ignite an adjacent unignited cell across a street. The method considered depends upon whether the plume centerline lies above (label I) or below (label J) the top of the fuel in the unignited adjacent cell.

At label (I) the plume is tilted sufficiently far from the vertical that the plume centerline lies below the top of the fuel in the adjacent cell. In this case, it is assumed that the plume is blowing directly on the unignited fuel in the adjacent cell, and the probability of ignition of the subject cell is calculated as

$$P_{ig} = \min(\tau/\tau_{mx}, 1.0) \left( \frac{\hat{u} \cdot \vec{v}_G}{|\vec{v}_G|} \right) \left( \frac{\cos(\theta)}{\cos(\theta_{mx})} \right), \quad (5-38)$$

where

$\tau/\tau_{mx}$  = ratio of cell burntime to time of maximum heat production

$\hat{u}$  = unit vector from the burning cell center to the unignited adjacent cell center

$\vec{v}_G$  = wind velocity in the burning cell

$\theta$  = plume tilt angle

$\theta_{mx}$  = angle to the top of fuel in adjacent unignited cell.

Transfer is then made to label (L).

At label (J) the plume is not tilted enough for the plume centerline to lie below the top of the fuel in the subject cell. In this case the plume is required to extend across the intervening street and overlap the fuel in the adjacent cell for ignition to be considered. If overlap occurs, transfer is to label K, else transfer is to label L.

At label (K) the probability of ignition of the subject cell due to radiation from the overlapping plume of the burning cell is calculated as

$$P_{ig} = \min\left(\frac{\tau}{\tau_{mx}}, 1\right) \left(\frac{A_p}{A_c}\right) \left(\frac{\hat{u} \cdot \vec{v}_G}{|\vec{v}_G|}\right) \quad (5-39)$$

where

$A_p/A_c$  = fraction of cell (f) for which plume is defined.

Transfer is then made to label (L).

At label (I) as at label (J), prior to the transfer to label L, the probability of subject cell ignition is calculated by Equations 5-38 and 5-39, respectively and accumulated for each appropriate burning cell adjacent to the subject cell. This accumulation, when performed for all cells adjacent to the subject cell, represents the spatial accumulation of probability of ignition for all burning cells surrounding the subject cell.

At label (L) a test is made to determine if all eight cells adjacent to the subject cell have been examined. If all adjacent cells have not been examined, transfer is to label (A) where the next cell is selected, else transfer is to label (M).

At label (M) the just calculated cumulative probability of ignition over the cells surrounding the subject cell is accumulated to the probability of ignition calculated at the last subject cell update. If the minimum value of  $\tau/\tau_{mx}$  for the eight adjacent cells  $(\tau/\tau_{mx})_{mn}$  is greater than four, transfer is to label (N), else transfer is to label (O).

At label (N),  $(\tau/\tau_{mx})_{mn}$  is greater than four, which means that all burning cells adjacent to the subject cell are beyond the time of burnout. Under these conditions, no increase will occur in the cumulative probability of subject cell ignition. For these reasons, the time interval to the next examination of the subject cell by ACUPDT is set at the maximum allowable value.

At label (O),  $(\tau/\tau_{mx})$  is less than or equal to four. Thus, at least one of the cells adjacent to the subject cell is currently burning. The time interval to the next examination of the subject cell by ACUPDT is scheduled in accordance with the maximum rate of change of the heat production rates of the cells surrounding the subject cell by the relation

$$DT = (1/2)(1 - q_{mx})(\tau_{mx})_{mn} \quad (5-40)$$

where

$$q_{mx} = [(1 - (\tau/\tau_{mx})_{mn})] \exp(\tau/\tau_{mx})_{mn} \quad (5-41)$$

Control is then transferred to label (W).

At label (P) the just calculated probability of cell ignition  $P_{ig}$  is tested. If  $P_{ig}$  is zero, transfer is to label (Q), else transfer is to label (R).

At label (R) the just calculated cumulative probability of cell ignition ( $P_{cum}$ ) is tested. If  $P_{cum}$  is equal to or greater than unity, transfer is to label (S), else transfer is to label (T).

At label (S), ignition is certain and the subject cell is ignited by a call to BCINIT. The cumulative probability of ignition is allowed to exceed unity in cases where ignition conditions are appropriately severe. The value of  $P_{cum}$  is passed to BCINIT in such cases as the number (real valued) of simultaneous ignitions, thus allowing for multiple (fractional) ignitions. The effect of multiple ignitions is to cause the cell to burn hotter and faster than it otherwise would. These effects are implemented as shown in Equations 5-12 by making  $\tau_{mx}$  an inverse function of the number of ignitions  $N_{ig}$  in the cell and in Equation 5-8 by making  $\dot{q}_c$  a function of  $1/\tau_{mx}$ .

At label T the cumulative probability of ignition for the subject cell is greater than zero but not certain. The determination of what to do in this case is based on a definition of the rate of change of cumulative probability of cell ignition per unit time. The cumulative probability of cell ignition  $P_{cum}$  is

$$P_{cum} = \sum_{j=1}^N (P_{ig})_j \quad (5-42)$$

where  $(P_{ig})_j$  is the probability of ignition associated with the  $j$ -th cell update time interval  $\Delta t_j$  and where the time interval  $\Delta T_{cum}$  over which probability of ignition has been accumulated is

$$\Delta T_{cum} = \sum_{j=1}^N \Delta T_j \quad (5-43)$$

The increment of cumulative probability remaining until cell ignition is certain ( $\Delta P'$ ) is given by

$$\Delta P' = 1 - P_{\text{cum}} \quad . \quad (5-44)$$

Denote the time interval until ignition is certain by  $\Delta T'$  and define the average rate of change of cumulative probability of cell ignition  $dP_{\text{cum}}/dt$  over the interval  $\Delta T'$  by

$$\frac{d}{dt} (P_{\text{cum}}) = \frac{\Delta P'}{\Delta T'} \quad . \quad (5-45)$$

Define the current rate of change in cumulative probability of cell ignition in terms of the most recently calculated values as

$$\frac{d(P_{\text{cum}})}{dt} = \frac{(P_{\text{ig}})_N}{\Delta T_N} \quad . \quad (5-46)$$

At the current rate of change, the time interval until cell ignition is certain is given by Equations 5-45 and 5-46 as

$$\Delta T' = \frac{\Delta P'}{(P_{\text{ig}})_N} \Delta T \quad , \quad (5-47)$$

which is called the projected time to ignition. The interval until the next scheduled cell update  $\Delta T_{N+1}$  has already been calculated at either label (N) or label (0). If  $\Delta T'$  is less than  $\Delta T_{N+1}$  transfer is to label (U), else transfer is to label (V).

At label (U) the projected time to ignition is less than the time to the next scheduled update. The cell is, thus, scheduled for ignition at the projected ignition time.

At label (V) the time to the next cell update is less than the projected time to ignition. The cell is, thus, scheduled to be updated at the calculated update time.

At label (W) all events that have been scheduled by ACUPDT are placed in the Event List and all new cell and fire data calculated by ACUPDT are stored in the Dynamic Data Base. Control is then returned by ACUPDT to the UFMGR.

## 5.6 FIRE UPDATE (FUPDT) MODULE

The logical organization of the Fire Update Module (FUPDT) is shown in Figure 5-8. The FUPDT module deals primarily with the problem of scheduling the next update of the subject fire. The mechanics of the update process are performed by the Fire Geometry (FGEOM) and Fire Physical Data (FPHYSD) subroutines, which will be described next.

During initialization, all ignitions need not occur simultaneously, but can be spread over a specified interval. This can initially cause many small independent fires with rapidly changing sizes and heat production rates which can result in the necessity for many fire updates early in the simulation. These updates occur over time intervals that are significant to each fire but are not significant over all of the fires. To satisfy the tradeoff between frequency and significance, all fire updates are constrained by the FUPDT module to occur at intervals that are consistent with significant changes in global fire characteristics.

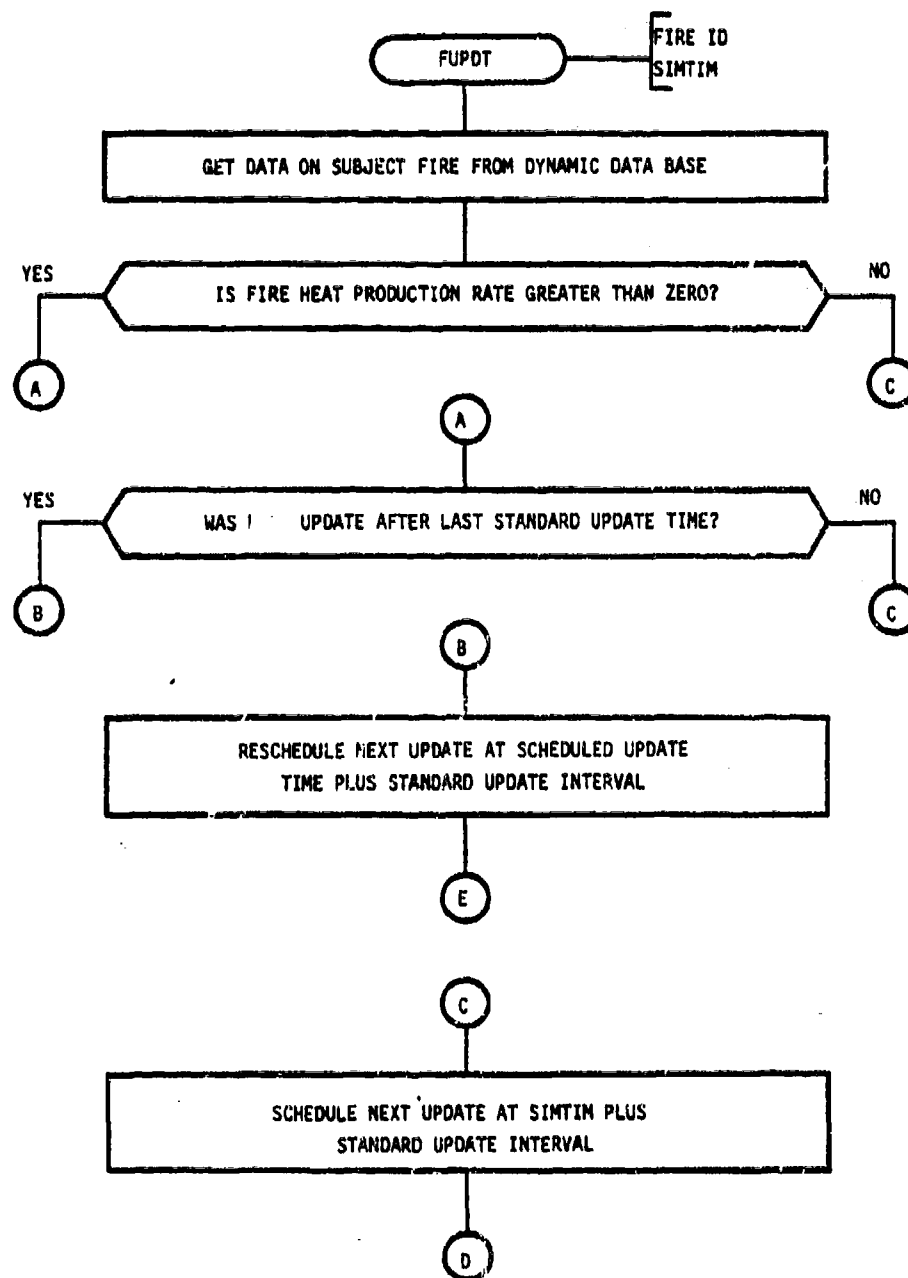


Figure 5-8. Logic flow of fire update module.



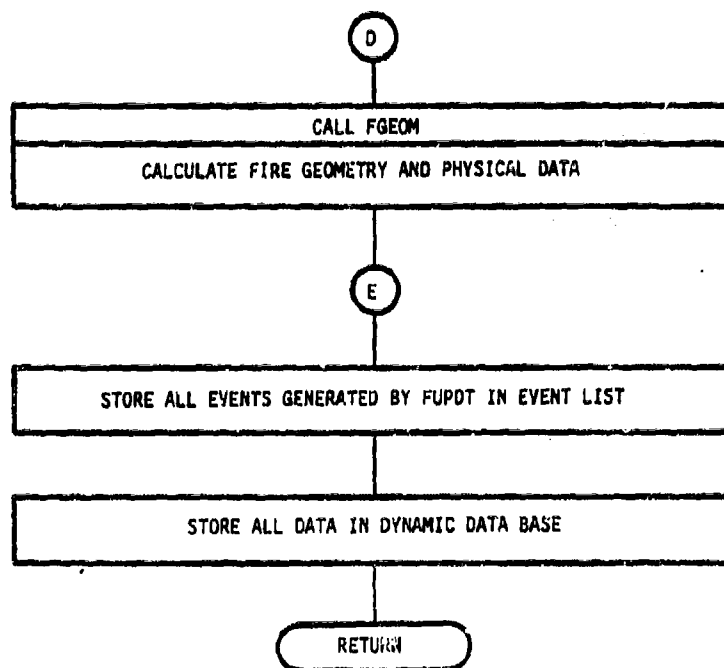


Figure 5-8. Logic flow of fire update module (concluded).

Fire data are treated in two parts, physical data and geometrical data. The fire physical data consist of the burning characteristics of the aggregate of cells that make up the fire. The geometrical data consist of a partitioning of the fire into a set of suitably symmetric subfires. To maintain physically significant fire data, the following fire update criterion are employed:

1. A fire physical update occurs whenever the fire heat production rate has changed by ten percent relative to the value at the last update time.
2. A fire geometry update occurs whenever the fire area has changed by ten percent relative to the area at the last update time.
3. A fire physical data update can occur without an accompanying geometry update.
4. A fire geometry data update must be accompanied by a physical data update.
5. No fire may be updated more frequently than once each 360 seconds.

The period of 360 seconds was chosen as the standard update interval because it represents 10 percent of the minimum time in which an ignited cell can reach maximum rate of heat production.

Fire updates, thus, occur whenever the heat production rate or the size of the fire are changed by ten percent relative to the respective values at the last update. The Burning Cell Update (BCUPDT) module is responsible for maintenance of heat production rate values for burning

cells. It, thus, incrementally changes the heat production rates of fires and determines if a fire update is required under the change in fire heat production-rate criterion. In the process of updating burning cells, the BCUPDT module also identifies cells that burn out. It, thus, decrements fire size as cells burn out, and determines if a fire update is required under the change-in-fire-area criterion. The Ignition (IGNITE) module is responsible for igniting cells. It, thus, increments fire area and determines if a fire update is required under the change-in-fire-area criterion.

Upon entry to the FUPDT module, shown in Figure 5-8, fire data for the subject fire are accessed. If the fire heat production rate is greater than zero, transfer is to label (A), else transfer is to label (C).

At label (A) the most recent update of the subject fire is compared with the last standard update time. If the most recent update was later than the last standard update time, transfer is to label (B), else transfer is to label (C).

At label (B) the fire has been updated since the last standard update time. The current update is, thus, rescheduled to occur at the time of the last update plus the standard fire update interval. Control is transferred to label (E).

At label (C) either the fire heat production rate is zero or the last update was at or before the last standard update. In the first case, the initial update is required and in the second case, the next update is required. In either case, an update is currently required, and the next update is scheduled to occur at SIMTIM plus the standard fire update interval.

At label (D), the geometry and physical data for the fire are calculated by the Fire Geometry subroutine.

At label (E), all events scheduled by the FUPDT module are stored in the Event List, all data are stored in the dynamic data base, and the FUPDT module returns control to the UFMGR module.

#### **5.6.1 Fire Geometry (FGEOM) Subroutine**

The algorithm used for fire induced wind velocity calculations assumes that the fires involved are circular. In the processes of initialization and propagation, high aspect (length-width) ratio fires can be generated, which violate this assumption. The fire geometry subroutine employs a simple pattern recognition algorithm to identify long thin fires and partitions them into sets of approximately square subfires, as a suitable representation of the circular fires expected by the fire induced wind model.

Upon entry to the FGEOM subroutine shown in Figure 5-9, the existing physical and geometrical fire data for the subject fire are deleted. The overall fire physical data are independent of the fire geometry. Thus, the Fire Physical Data (FPHYSD) subroutine is entered to calculate physical data for the entire fire. Upon return from the FPHYSD subroutine, the number of cells in the fire is tested. If the fire contains four or more cells, transfer is to label (A), else transfer is to label (J).

At label (A), the fire has been found to have four or more cells. Fires smaller than four cells are not examined for elongation. This is consistent with the attempt to maintain the aspect ratio of involved fires to be no greater than four. The number of candidate subfires is set to zero (i.e., the entire fire), and all cells in the fire are assigned to this subfire.

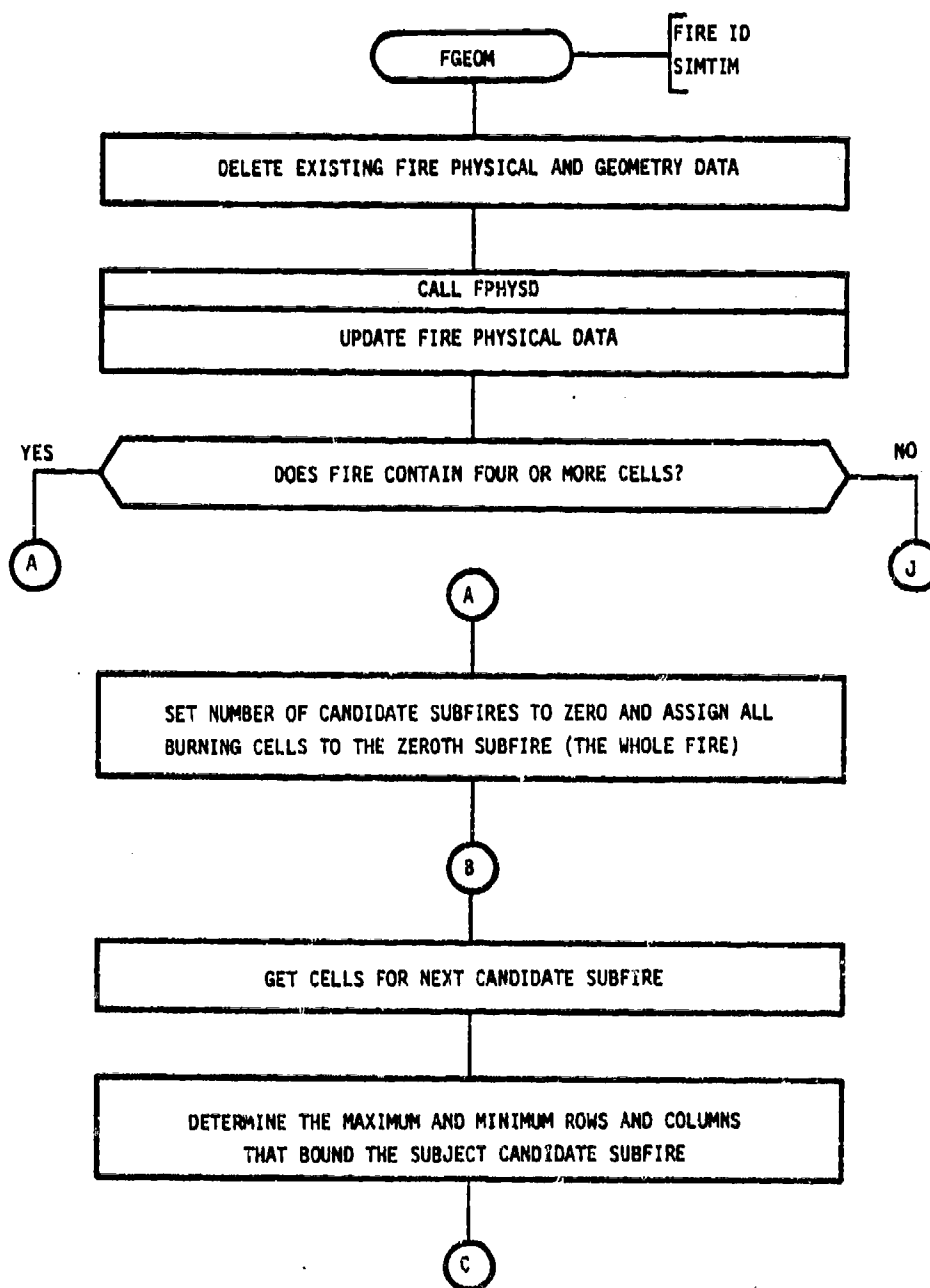


Figure 5-9. Logic flow of fire geometry subroutine.

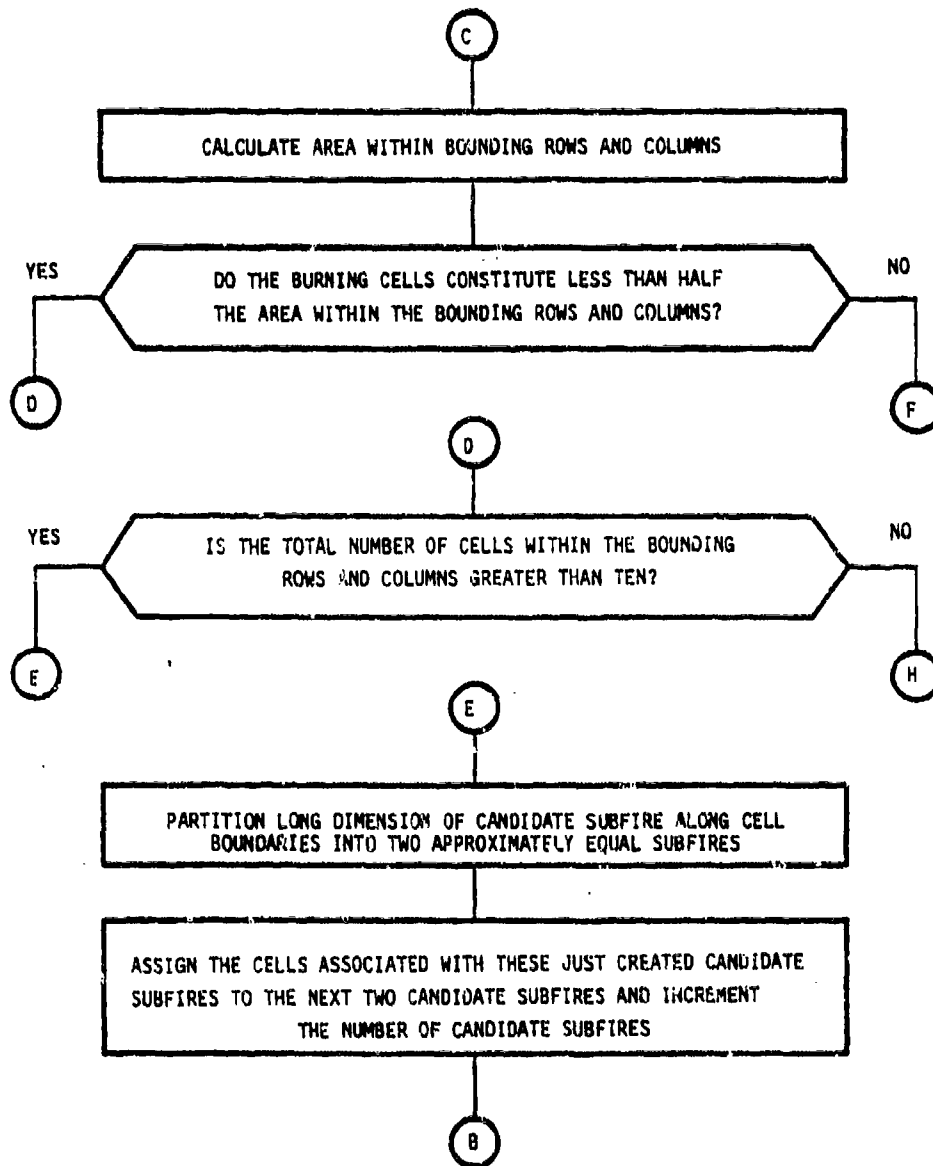


Figure 5-9. Logic flow of fire geometry subroutine (continued).

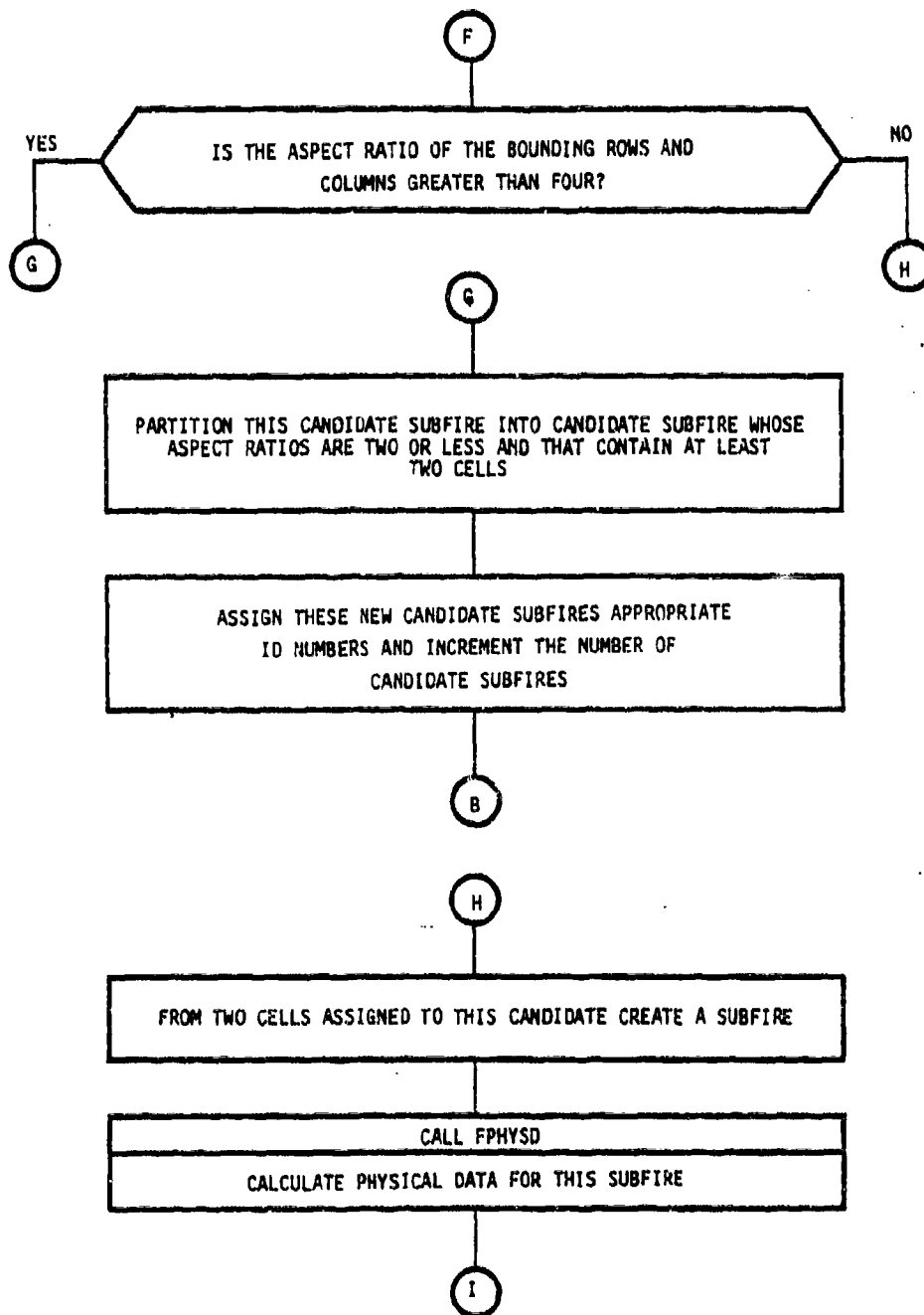


Figure 5-9. Logic flow of fire geometry subroutine (continued).

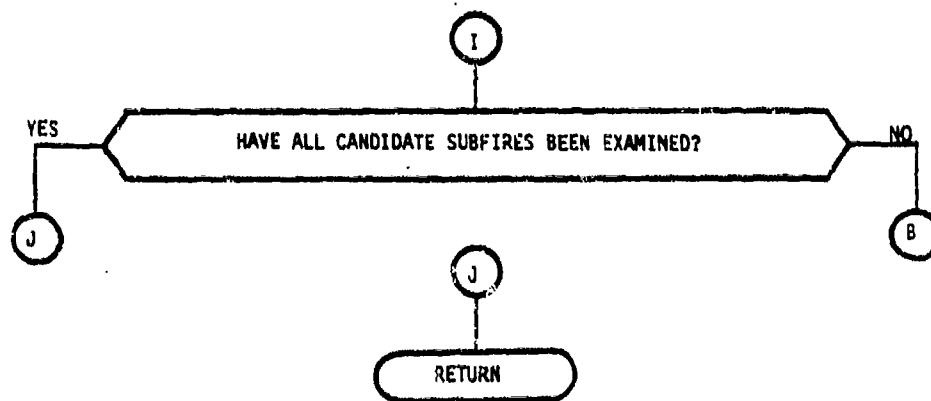


Figure 5-9. Logic flow of fire geometry subroutine (concluded).



At label (B) the cells for the next candidate subfire are accessed. At the first entry to label (B), the only candidate is the whole fire (i.e., zeroth subfire), and all of the cells in the fire are accessed. A subfire consists of a set of contiguous burning cells, cells are identified by their row-column indices, and the rectilinear boundary of a subfire is defined by the maximum and minimum row and column indices exhibited by the set of cells in the candidate subfire. These indices identify the rows and columns that bound the candidate subfire.

At label (C) the area within the bounding rows and columns is calculated. If the burning cells constitute less than half the bounded area, transfer is to label (D), else transfer is to label (F).

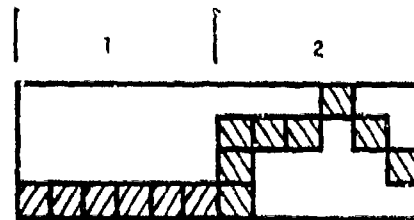
At label (D), if the total number of cells within the bounding rows and columns is greater than ten, transfer is to label (E), else transfer is to label (H).

At label (E) the bounded area is less than half filled by the burning cells and the total number of burning cells is greater than ten. The intent here is to identify subfires represented as sparsely filled bounded areas. The long dimension of these candidate subfires is approximately halved along cell boundaries to create two potentially less sparsely filled subfires. A simple example of such a fire is shown in Figure 5-10, where it can be seen in (a) that the burning cells (shaded) constitute only 30 percent of the bounded cells. The largest dimension of the fire is, thus, partitioned as shown in Figure 5-10(b), creating candidate subfires 1 and 2.

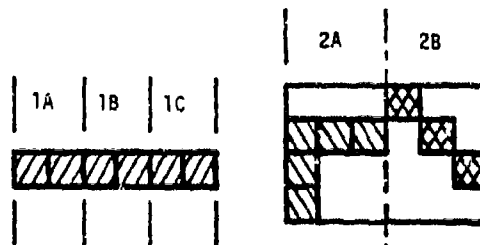
The partitioning of the example fire shown in Figure 5-10 will be described here, although some of the logic will not be encountered



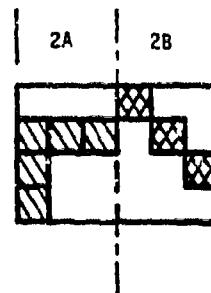
(a) Entire Fire



(b) Subfires 1 and 2



(c) Subfires 1A, 1B, and 1C



(d) Subfires 2A and 2B



(e) Subfire 2A



(f) Subfire 2B

Figure 5-10. Example of fire-subfire partitioning.

until later. One of the reasons for re-examining each newly created candidate subfire by a subsequent entry to label (B) is clearly shown in Figure 5-10(c) and is as follows. As shown in Figure 5-10(b), the burning cells of candidate subfire 1 only occupy 25 percent of its portion of the bounded area. However, when the boundary for candidate subfire 1 is redefined at label (C), the burning cells constitute 100 percent of the bounded area as shown in Figure 5-10(c). Candidate subfire 1 will be identified as an elongated subfire and appropriately subpartitioned. Candidate subfire 2 of Figure 5-10(b) has only 30 percent burning occupancy and is subpartitioned into candidate subfires 2A and 2B. In a subsequent entry to label (B), candidate subfire 2A will be found acceptable with respect to burning cell occupancy and elongation, and will be made into a subfire. Candidate subfire 2B will be found unacceptable with respect to occupancy (33 percent), but too small (less than 10 cells) to subdivide, and will also be made into a subfire.

The candidate subfire under examination has been subpartitioned, the new candidate subfires, thus, created have been assigned IDs, and the total number of subfires included in this fire has been appropriately incremented. At this point, transfer is back to label (B) where the next subfire will be accessed and the above described tests will be repeated.

At label (F) the bounded area of the candidate subfire is 50 percent or more filled with burning cells. The ratio of the longer to the shorter rectilinear boundary lengths (aspect ratio) is calculated for the candidate subfire. If the aspect ratio is greater than four, transfer is to label (G), else transfer is to label (H).

At label (G) an elongated candidate subfire has been identified and the degree of elongation quantified. The candidate subfire is partitioned into subfires each having an aspect ratio no greater than two. An example elongated subfire is shown in Figure 5-10(c) as subfire 1. It can

be seen that subfire 1 has an aspect ratio of six and has been partitioned into three subfires (1A, 1B, and 1C) each having aspect ratios of two. After the new subfires have been defined and the number of subfires appropriately incremented, transfer is back to label (B) where the next subfire is accessed.

At label (H) the candidate subfire has failed the occupancy test at label (C), failed the size test at label (D), or failed the elongation test at label (F). In any of these cases, the candidate requires no further modifications to become a subfire. The cells are assigned to a subfire and physical fire data are calculated by the FPHYSD subroutine for this subfire. Transfer is then to label (I).

At label (I), if all candidate subfires that have been identified have also been examined, transfer is to label (J) where control is returned to the FUPDT module, else transfer is to label (B) where the next subfire is accessed.

#### **5.6.2 Fire Physical Data (FPHYSD) Subroutine**

The Fire Physical Data subroutine calculates current values for the specified physical parameters of a fire or subfire. The fire physical (and geometrical) data are an exception to the rule of maintaining two sets of data subtending current time and interpolating between them to obtain current values of specified variables. It is not possible, in this case, because changes in the fire geometry may not allow correlation between the subfires existing at different times. Fire physical data are, thus, updated more frequently than interpolated data, but are held constant between updates.

The logic flow of the FPHYSD subroutine is shown in Figure 5-11, where it can be seen to be devoid of logic branches and to consist simply

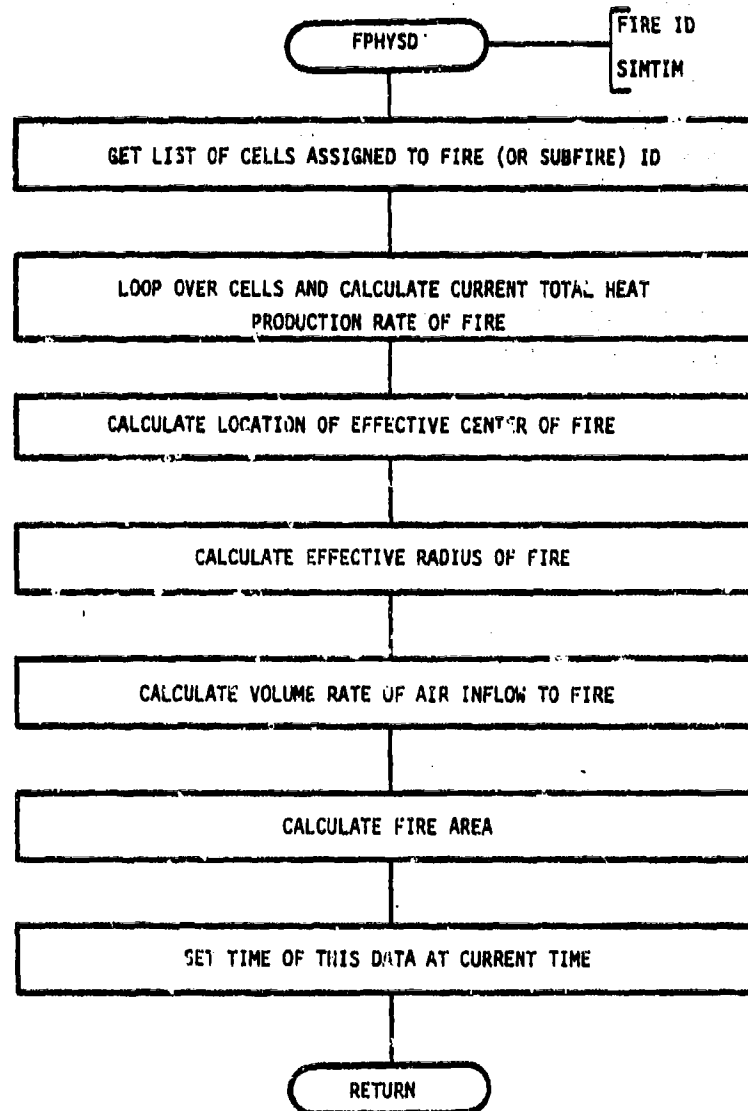


Figure 5-11. Logic flow of fire physical data subroutine.

of a sequence of calculations. Upon entry to the FPHYSO subroutine, the list of cells assigned to the subject fire (or subfire) is accessed and the total heat production rate is calculated from

$$\dot{Q}_k = \sum_{i=1}^{N_k} \dot{q}_i \quad (\text{J/s}) \quad (5-48)$$

where

$\dot{Q}_k$  = total heat production rate of fire k  
 $N_k$  = number of cells in fire k  
 $\dot{q}_i$  = heat production rate of the i-th cell in fire k.

The location of the effective fire center is calculated in terms of the fire extent weighted by local heat production rate, and is used in the fire induced wind velocity calculations. The coordinates of the effective center of fire k,  $(\bar{x}_k, \bar{y}_k)$ , are given by

$$(\bar{x}_k, \bar{y}_k) = \left( \sum_{i=1}^{N_k} \dot{q}_i x_i, \sum_{i=1}^{N_k} \dot{q}_i y_i \right) \quad (\text{m}) \quad (5-49)$$

where  $x_i, y_i$  = coordinates of the center of the i-th cell of fire k.

The effective radius  $(r_o)_k$  of fire k, also used in fire induced wind velocity calculations, is calculated from

$$(r_o)_k = \left\{ \frac{1}{\dot{Q}_k} \sum_{i=1}^{N_k} \left[ (x_i - \bar{x}_k)^2 + (y_i - \bar{y}_k)^2 \right] \dot{q}_i \right\}^{1/2} (\text{m}). \quad (5-50)$$

The volume rate of air inflow  $(\dot{V}_k)$  to fire k is calculated from

$$\dot{V}_k = a\dot{Q}_k/bc \quad (\text{m}^3/\text{sec}) \quad (5-51)$$

where

a = mass of air required to burn a mass of fuel,  
(kg air/kg fuel)

b = heat produced per weight of fuel (J/kg)

c = air density (kg/m<sup>3</sup>).

The area ( $A_k$ ) of fire k is given by

$$A_k = N_k A_c, \quad (5-52)$$

where  $A_c$  is the specified cell area. The cell area cannot be changed during an execution, but may be changed between executions. The time these data were calculated is denoted as SIMTIM, and control is returned to the calling routines.

## 5.7 BRANDING (BRANDG) MODULE

The execution of a burning cell update event consists of sequentially processing the BCUPDT module (Subsection 5.4) and the BRANDG module. Thus, upon entry to the BRANDG model, current BCUPDT data are available.

The logic flow diagram of the BRANDG module is shown in Figure 5-12, where the event data are shown to include the (burning) cell ID, SIMTIM, cell heat production rate, and the time of the next cell update. Only burning cells can launch brands, and this is assured by making the test for branding a part of each burning cell update event. The time of the next cell update is calculated by the BCUPDT module and passed to the BRANDG module.

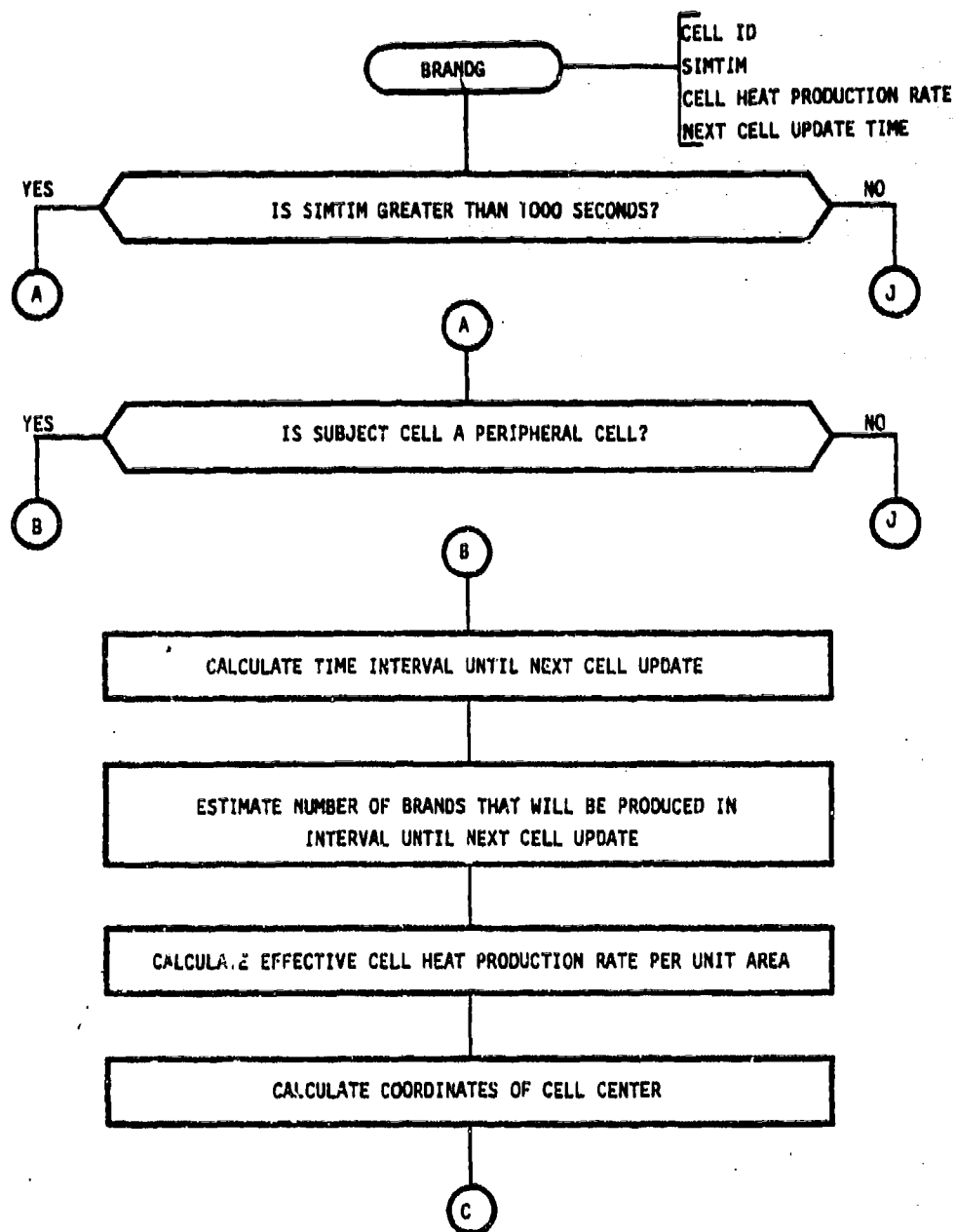


Figure 5-12. Logic flow for branding module.



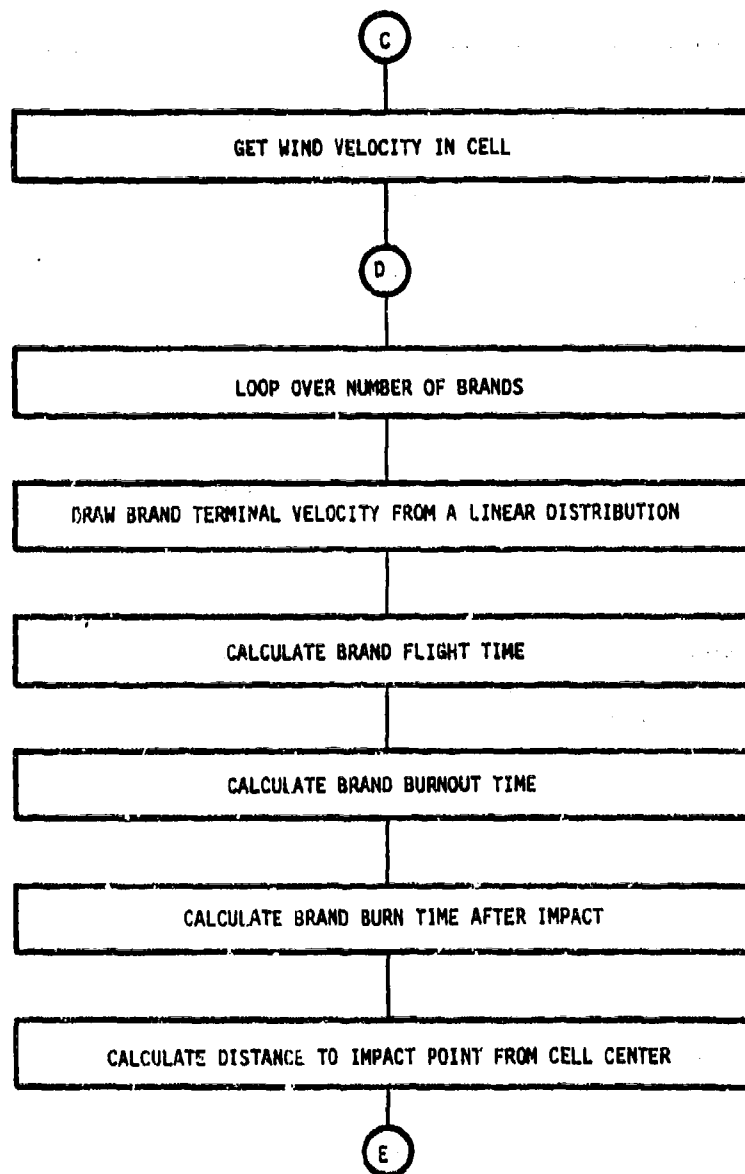


Figure 5-12. Logic flow for branding module (continued).

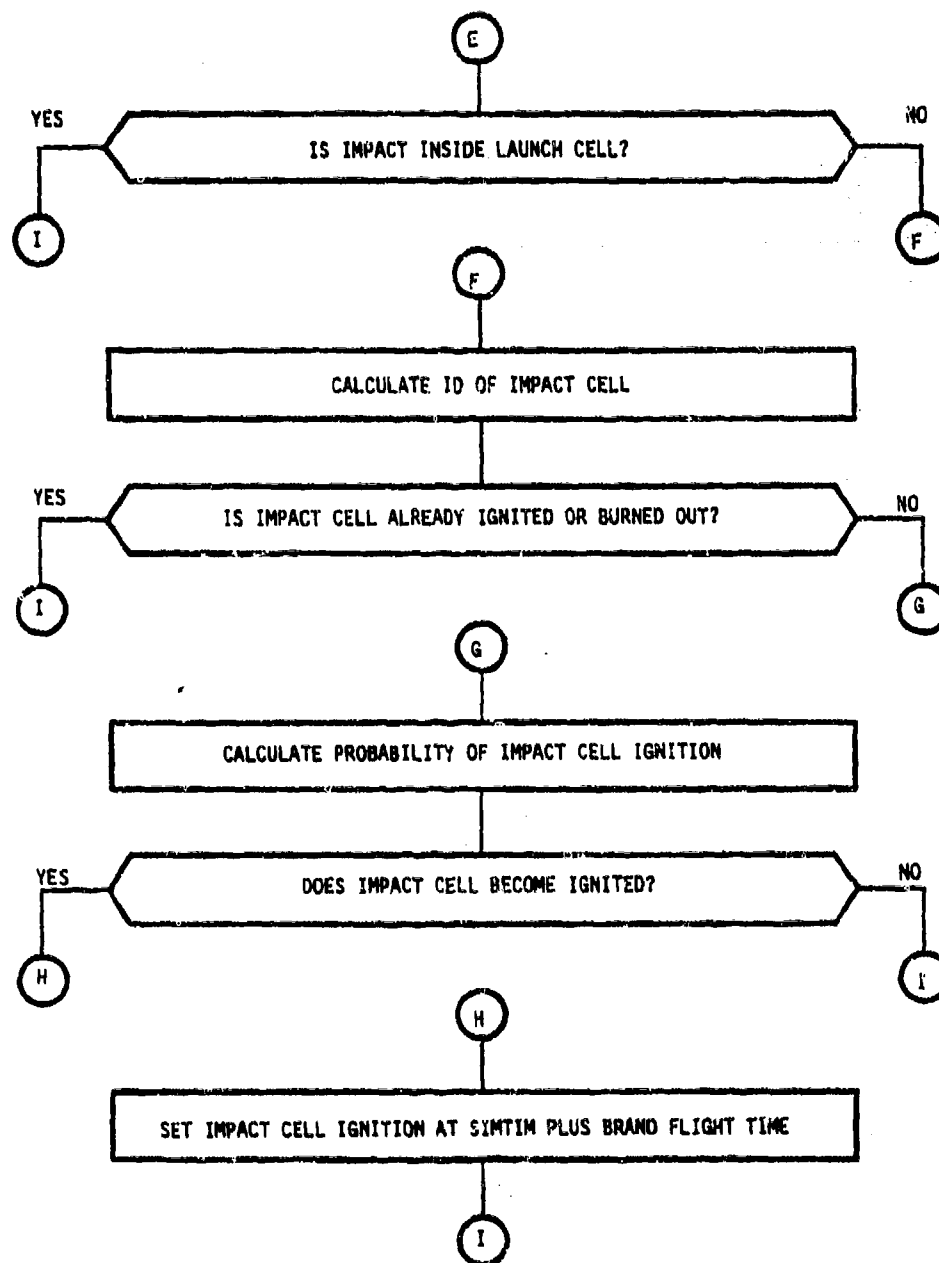


Figure 5-12. Logic flow for branding module (continued).

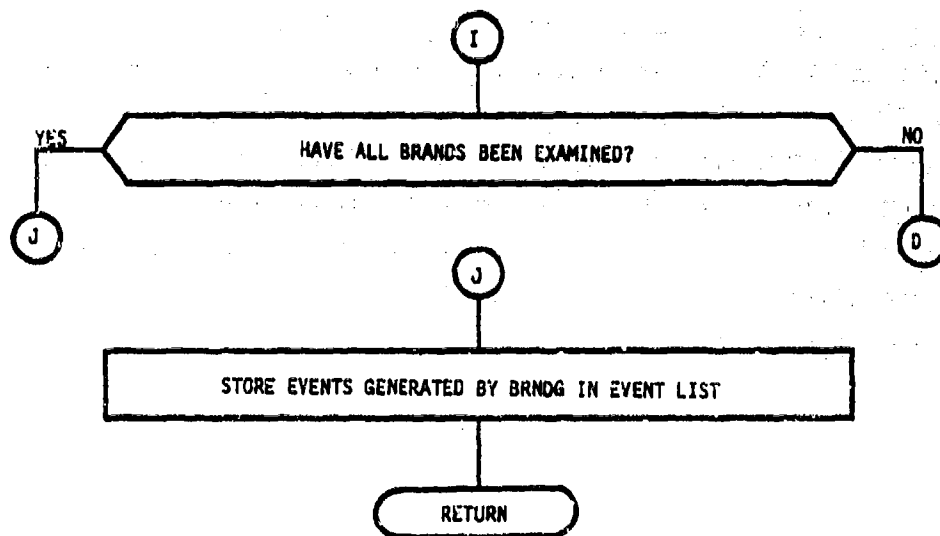


Figure 5-12. Logic flow for branding module (concluded).

Upon entry to the BRANDG module, SIMTIM is tested, and if SIMTIM is greater than 1000 seconds, transfer is to label (A), else transfer is to label (J) where control is returned to the UFMGR. Branding is not allowed for the first 1000 seconds ( $\approx 17$  min) of a simulation for both physical and computational reasons. In the cases that have been run, initialization (i.e., initial ignitions) have been allowed to occur over the first 1000 seconds of simulation time. Thus, cells are being ignited throughout this interval. In general, large numbers of cells are initialized, and all have very low probabilities of branding over the first 1000 seconds. Significant computational resources are saved by not examining these low probability occurrences.

At label (A), if the subject cell is a peripheral cell of the fire to which it belongs, transfer is to label (B), else transfer is to label (J). Only peripheral cells are tested for branding. It is assumed that brands launched by interior cell plumes will, if they fall out, be caught up in, and consumed by the plume of an adjacent burning cell.

At label (B) the time interval until the next cell update  $\Delta t$  is calculated, and the number of brands that will be produced in the interval until the next cell update  $N_B$  is estimated as

$$N_B = \dot{q} \Delta t / (1.63 \times 10^{11}) \quad , \quad (5-53)$$

where  $\dot{q}$  = cell heat production rate. The constant includes the nature of the fuel in the cell, which can be made explicit. The effective heat production rate per unit cell area is calculated from

$$q_A = \left( \frac{\dot{q}}{L_C \pi^{1/2}} \right)^{1/3} \quad , \quad (5-54)$$

where  $L_c$  = the cell linear dimension. From the cell ID, the coordinates of the cell center are calculated.

At label (C) the wind velocity (calculated in the BCUPDT module) is accessed. A loop is formed over the estimated number of brands. Each brand is characterized by its terminal velocity, which is obtained by a random draw from a linear distribution. A linear distribution fits empirical data and produces many more smaller, than larger, brands. From the terminal velocity of the k-th brand  $\eta_k$ , the brand flight time  $T_k$  is calculated as

$$T_k = \dot{q}(0.444 \eta_k + 1.10 f'_k - 0.975 \eta_k f'_k) \quad (s) \quad , \quad (5-55)$$

where

$$f'_k = 1.0 - (1 - f_k)^{1/2} \quad (5-56)$$

and

$$f_k = 4.726 \times 10^{-4} (1 - 0.887 \eta_k)^{-2} (1 - 0.482 \eta_k)^{-3} \quad . \quad (5-57)$$

The time at which the brand will burn out is calculated as

$$T_{BO} = \dot{q}(1.1000 - 0.5314 \eta_k) \quad (s) \quad , \quad (5-58)$$

and the amount of time the brand will burn after impact is given by  $T_{BI} = T_{BO} - T_k$  (s). The distance the brand is transported from the cell center is given by

$$\Delta \vec{r} = \vec{v}_G T_k \quad (m) \quad , \quad (5-59)$$

where  $\vec{v}_G$  = surface wind velocity at cell center.

At label (E), if the brand transport distance,  $|\Delta \vec{r}|$ , is such that impact is within the launch cell, transfer is to label (I), else transfer is to label (F).

At label (F) the impact coordinates and the ID of the impact cell are calculated. If the impact cell is already ignited or burned out, transfer is to label (I), else transfer is to label (G).

At label (G) the probability that the brand will ignite the impact cell is calculated by

$$P_{ig} = 1 - \exp(-T_{BI}/60) \quad . \quad (5-60)$$

If the cell is to be ignited, transfer is to label (H), else transfer is to label (I).

At label (H) an event is added to the Event List, which will ignite the impact cell at  $SIMTIM + T_k$ . At label (I), if all ( $N_B$ ) brands have been tested, transfer is to label (J), else transfer is to label (D) where the terminal velocity is drawn for the next brand. At label (J) events generated by the BRANDG module are stored on the Event List and control is returned to the UFMGR.

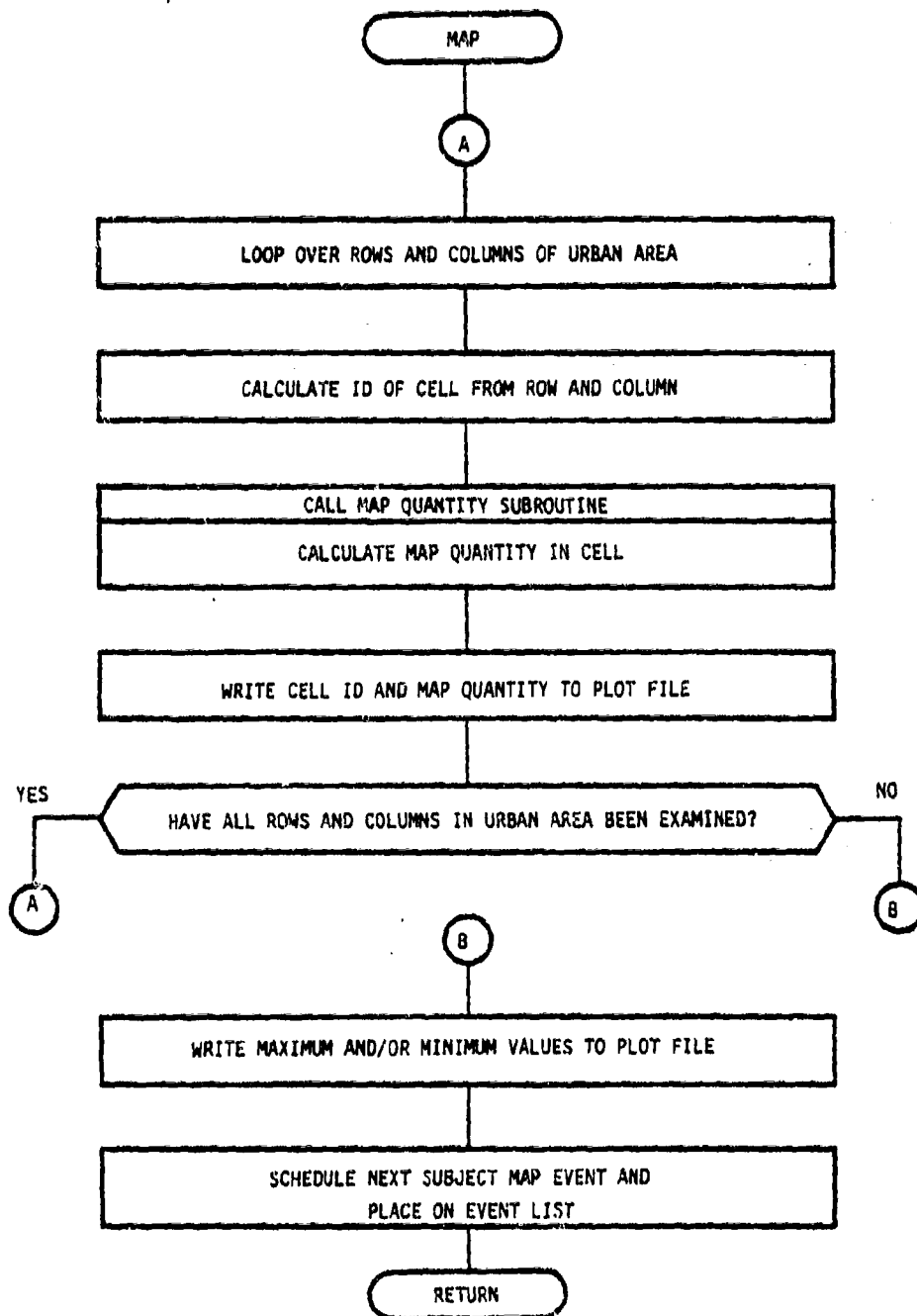


Figure 5-13. Logic flow of typical MAP module.

## 5.8 OUTPUT MODULES (WVMAP, CSMAP, QMAP)

The output modules present the results of the simulation in the form of maps of wind velocity (WVMAP), cell state (CSMAP), and heat production rate (QMAP) over the specified urban area. The logic flow diagrams of these modules are very similar and are, thus, represented in Figure 5-13 by a logic flow diagram typical of the three modules.

At label (A) each cell of the specified urban area (matrix) is identified by row and column. The map quantity (i.e., wind velocity, cell state, or heat production rate) is calculated for the identified cell and written to a plot file. This is continued until a value of the map quantity has been calculated and stored for every cell in the urban area.

At label (B) specified maximum and/or minimum values of the map quantity are written to the plot file. The map module then stores its next update event in the Event List. The update event is timed according to a specified schedule, which may be periodic or aperiodic.



## SECTION 6

### EXAMPLE MODEL RESULTS

Results from the model for eleven example cases are presented in this section. The results for each case presented consist of the following:

1. A description of the initial conditions for the fire
2. Sets of maps depicting these results:
  - a) the state of each cell in the area
  - b) heat production rate contours over the area
  - c) heat production rates of each cell in the area
  - d) wind velocity.

Map results are presented at times of 1000, 1750, 2750, 4750, 8750, 16750, and 32750 seconds after simulation initialization.

Included with the results for each case is a description of the initialization conditions and brief comments on the case results.

Initialization is an important aspect of uncontrolled urban fires in the cases of interest. For this reason, and because of its uncertainty, the model has been designed to accept arbitrary initialization processes. For the example cases presented, the initialization consisted of selecting a candidate set of cells for ignition and igniting them over a 1000 second interval with a uniform random distribution in time and a Poisson distribution of from zero to four ignitions per candidate cell for a specified expected value of ignition.

All example cases are simulated in an urban area that is  $50 \times 50$  city blocks (about  $56.25 \text{ km}^2$ ). Cellulosic fuels loaded at  $40 \text{ kg/m}^2$  are uniformly distributed over the area. The model will allow different fuel types and loadings in each cell; however, for the example cases, it was desired to have the results reflect phenomenology variations instead of fuel variations.

An objective of developing the demonstration model was to demonstrate a model structure capable of integrating the range of variables and variable interactions required to describe the onset and growth of mass fires in an urban setting. Even for demonstration purposes, the model must contain physically based phenomenology models that include most of the variables and variable interactions of interest. In this sense the phenomenology models included in this demonstration urban fire model are considered to be qualitatively appropriate, although it is known that they are, in many cases, quantitatively in error.

In the interest of aiding in model development and in mitigating model maintenance problems, the model structure has been designed to readily allow the introduction of new models and/or processes and for the alteration of existing models and/or processes.

#### **6.1 LARGE AREA FIRE WITH NO AMBIENT WIND**

As shown in Figure 6-1, the central  $35 \times 35$  cells of the  $50 \times 50$  cell urban area are chosen as candidates for ignition, and ignited with a probability of ignition of 0.1. There is initially no ambient wind velocity; however, very strong fire-induced winds are generated, as shown in Figures 6-1(l) and 6-1(m). It is noted that the wind velocities are considered to be excessive in all of the cases presented.

Figures 6-1 through 6-1(g), together with Figures 6-1(j) and 6-1(l), show that the fire, once ignited, tends to propagate inwards, following the inward fire-generated wind flow. These figures also show that, as the fire grows inward, it generates radial "fingers" along the wind velocity stream lines. This is consistent with wildland fire experience, which reveals similar combustion patterns under high wind velocity conditions.

Figures 6-1 and 6-1(c) show a quantitative phenomenology that occurs in other example cases as well. Looking at the upper right hand corner of Figure 6-1, it can be seen that no cells are ignited above row 44. In Figure 6-1(c), it can be seen that a cell has been ignited in row 50. Because this cell is disjoint from any other ignited cell, ignition had to have occurred by branding. However, as shown by Figures 6-1(l) and 6-1(m), the winds are all directed inward toward the center of the urban area. In view of this, the only way the cell in row 50 could have been ignited by branding is for a brand to have been thrown from the lower left corner of the fire all of the way across the burning area. This is clearly erroneous and is an artifact of the simplicity of the brand transport model that is used.

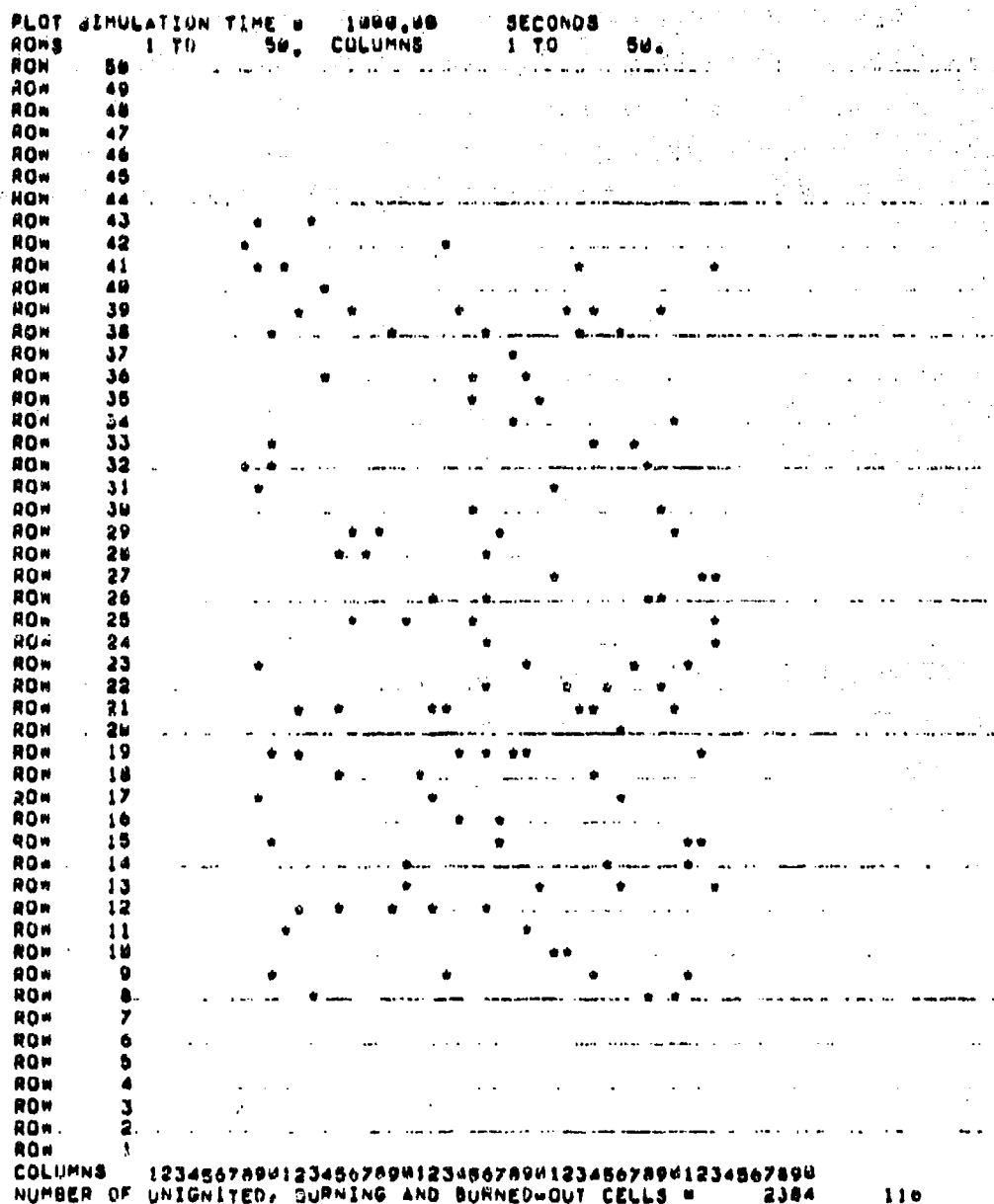


Figure 6-1. Cell state map for area fire.

PLT SIMULATION TIME 1200.00 SECONDS  
 ROWS 1 TO 50, COLUMNS 1 TO 80.  
 ROW 54  
 ROW 49  
 ROW 48

ROW 47  
 ROW 46  
 ROW 45  
 ROW 44  
 ROW 43  
 ROW 42  
 ROW 41  
 ROW 40  
 ROW 39  
 ROW 38  
 ROW 37  
 ROW 36  
 ROW 35  
 ROW 34  
 ROW 33  
 ROW 32  
 ROW 31  
 ROW 30  
 ROW 29  
 ROW 28  
 ROW 27  
 ROW 26  
 ROW 25  
 ROW 24  
 ROW 23  
 ROW 22  
 ROW 21  
 ROW 20  
 ROW 19  
 ROW 18  
 ROW 17  
 ROW 16  
 ROW 15  
 ROW 14  
 ROW 13  
 ROW 12  
 ROW 11  
 ROW 10  
 ROW 9  
 ROW 8  
 ROW 7  
 ROW 6  
 ROW 5  
 ROW 4  
 ROW 3  
 ROW 2  
 ROW 1  
 COLUMNS 12345678901234567890123456789012345678901234567890  
 NUMBER OF UNIGNITED, BURNING AND BURNED-OUT CELLS 2360 132

Figure 6-1(a). Cell state map for area fire.

```

PLOT SIMULATION TIME = 1750.00 SECONDS
ROWS 1 TO 50. COLUMNS 1 TO 50.

ROW 49
ROW 49
ROW 48
ROW 47
ROW 46
ROW 45
ROW 44
ROW 43
ROW 42

ROW 41
ROW 40
ROW 39
ROW 38
ROW 37
ROW 36
ROW 35
ROW 34
ROW 33
ROW 32
ROW 31
ROW 30
ROW 29
ROW 28
ROW 27
ROW 26
ROW 25
ROW 24
ROW 23
ROW 22
ROW 21
ROW 20
ROW 19
ROW 18
ROW 17
ROW 16
ROW 15
ROW 14
ROW 13
ROW 12
ROW 11
ROW 10
ROW 9
ROW 8
ROW 7
ROW 6
ROW 5
ROW 4
ROW 3
ROW 2
ROW 1

COLUMNS 1234567890123456789012345678901234567890
NUMBER OF UNIGNITED, BURNING AND BURNED-OUT CELLS = 2222 278

```

Figure 6-1(b). Cell state map for area fire.

PLOT SIMULATION TIME • 2754.00 SECONDS

ROWS 1 TO 50, COLUMNS 1 TO 50.

ROW 50  
ROW 49  
ROW 48  
ROW 47  
ROW 46  
ROW 45  
ROW 44  
ROW 43  
ROW 42  
ROW 41  
ROW 40  
ROW 39  
ROW 38  
ROW 37  
ROW 36

ROW 35  
ROW 34  
ROW 33  
ROW 32  
ROW 31  
ROW 30  
ROW 29  
ROW 28  
ROW 27  
ROW 26  
ROW 25  
ROW 24  
ROW 23  
ROW 22  
ROW 21  
ROW 20  
ROW 19  
ROW 18  
ROW 17  
ROW 16  
ROW 15  
ROW 14  
ROW 13  
ROW 12  
ROW 11  
ROW 10  
ROW 9  
ROW 8  
ROW 7  
ROW 6  
ROW 5  
ROW 4  
ROW 3  
ROW 2  
ROW 1

COLUMNS 12345678901234567890123456789012345678901234567890

NUMBER OF UNIGNITED, BURNING AND BURNED-OUT CELLS • 1750 750

Figure 6-1(c). Cell state map for area fire.

```

PLOT SIMULATION TIME = 4750.00 SECONDS
ROWS 1 TO 50, COLUMNS 1 TO 50.
ROW 49
ROW 48
ROW 47
ROW 46
ROW 45
ROW 44
ROW 43
ROW 42
ROW 41
ROW 40
ROW 39
ROW 38
ROW 37
ROW 36
ROW 35
ROW 34
ROW 33
ROW 32
ROW 31
ROW 30
ROW 29
ROW 28
ROW 27
ROW 26
ROW 25
ROW 24
ROW 23
ROW 22
ROW 21
ROW 20
ROW 19
ROW 18
ROW 17
ROW 16
ROW 15
ROW 14
ROW 13
ROW 12
ROW 11
ROW 10
ROW 9
ROW 8
ROW 7
ROW 6
ROW 5
ROW 4
ROW 3
ROW 2
ROW 1
COLUMNS 12345678901234567890123456789012345678901234567890
NUMBER OF UNIGNITED, BURNING AND BURNED-OUT CELLS = 1291 1209

```

Figure 6-1(d). Cell state map for area fire.



```

PLOT SIMULATION TIME = 0750.00 SECONDS
ROWS 1 TO 50, COLUMNS 1 TO 50,
ROW 50
ROW 49
ROW 48
ROW 47
ROW 46
ROW 45
ROW 44
ROW 43
ROW 42
ROW 41
ROW 40
ROW 39
ROW 38
ROW 37
ROW 36
ROW 35
ROW 34
ROW 33
ROW 32
ROW 31
ROW 30
ROW 29
ROW 28
ROW 27
ROW 26
ROW 25
ROW 24

```

```

ROW 23
ROW 22
ROW 21
ROW 20
ROW 19
ROW 18
ROW 17
ROW 16
ROW 15
ROW 14
ROW 13
ROW 12
ROW 11
ROW 10
ROW 9
ROW 8
ROW 7
ROW 6
ROW 5
ROW 4
ROW 3
ROW 2
ROW 1
COLUMNS 12345678901234567890123456789012345678901234567890
NUMBER OF UNIGNITED, BURNING AND BURNED-OUT CELLS = 1123 1377

```

Figure 6-1(e). Cell state map for area fire.

```

PLOT SIMULATION TIME = 16750.0 SECONDS
ROWS 1 TO 50, COLUMNS 1 TO 50.
ROW 50
ROW 49
ROW 48
ROW 47
ROW 46
ROW 45
ROW 44
ROW 43
ROW 42
ROW 41
ROW 40
ROW 39
ROW 38
ROW 37
ROW 36
ROW 35
ROW 34
ROW 33
ROW 32
ROW 31
ROW 30
ROW 29
ROW 28
ROW 27
ROW 26
ROW 25
ROW 24
ROW 23
ROW 22
ROW 21
ROW 20
ROW 19
ROW 18

ROW 17
ROW 16
ROW 15
ROW 14
ROW 13
ROW 12
ROW 11
ROW 10
ROW 9
ROW 8
ROW 7
ROW 6
ROW 5
ROW 4
ROW 3
ROW 2
ROW 1

COLUMNS 12345678901234567890123456789012345678901234567890
NUMBER OF UNIGNITED, BURNING AND BURNED-OUT CELLS = 1005 1401 14

```

Figure 6-1(f). Cell state map for area fire.

NUMBER OF UNIGNITED, BURNING AND BURNED-OUT CELLS = 1486 1481

PLOT SIMULATION TIME = 32750.8 SECONDS

ROWS 1 TO 54, COLUMNS 1 TO 50

```

ROW 50 ***
ROW 49 *****
ROW 48 ***
ROW 47 *****
ROW 46 *****
ROW 45 *****
ROW 44 *****
ROW 43 *****
ROW 42 *****
ROW 41 *****
ROW 40 *****
ROW 39 *****
ROW 38 *****
ROW 37 *****
ROW 36 *****
ROW 35 *****
ROW 34 *****
ROW 33 *****
ROW 32 *****
ROW 31 *****
ROW 30 *****
ROW 29 *****
ROW 28 *****
ROW 27 *****
ROW 26 *****
ROW 25 *****
ROW 24 *****
ROW 23 *****
ROW 22 *****
ROW 21 *****
ROW 20 *****
ROW 19 *****
ROW 18 *****
ROW 17 *****
ROW 16 *****
ROW 15 *****
ROW 14 *****
ROW 13 *****
ROW 12 *****

```

```

ROW 11 *****
ROW 10 *****
ROW 9 *****
ROW 8 *****
ROW 7 *****
ROW 6 *****
ROW 5 *****
ROW 4 *****
ROW 3 *****
ROW 2 *****
ROW 1 *****

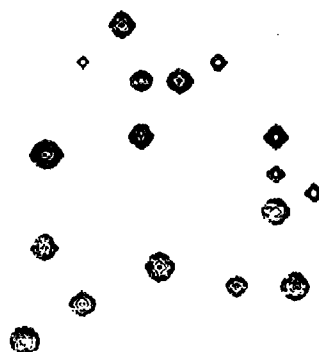
```

COLUMNS 12345678901234567890123456789012345678901234567890

NUMBER OF UNIGNITED, BURNING AND BURNED-OUT CELLS = 891 1487 1;

Figure 6-1(g). Cell state map for area fire.

HEPSON RESEARCH CORPORATION  
 URBAN FIRE MODEL  
 PLAY RELEASE ON TIME = 1000.00  
 TIME 1 TO 100.00  
 WALL GIVE OFF RATE 1.00  
 \*\*\* ONLY DATA FROM WALL GIVE OFF RATES IS PLotted \*\*\*  
 HOT SCALE IS LOGARITHMIC SCALE 10 ( 0-1.00 0-1.013 )



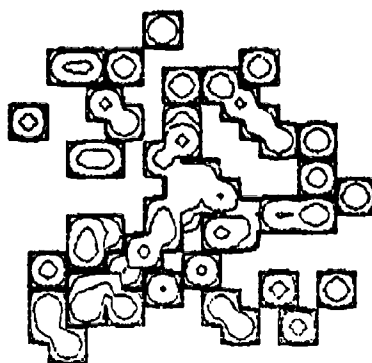
1357913579135791357913579

HEPSON RESEARCH CORPORATION  
 URBAN FIRE MODEL  
 PLAY RELEASE ON TIME = 1000.00  
 TIME 1 TO 100.00  
 WALL GIVE OFF RATE 1.00  
 \*\*\* ONLY DATA FROM WALL GIVE OFF RATES IS PLotted \*\*\*  
 HOT SCALE IS LOGARITHMIC SCALE 10 ( 0-1.00 0-1.013 )



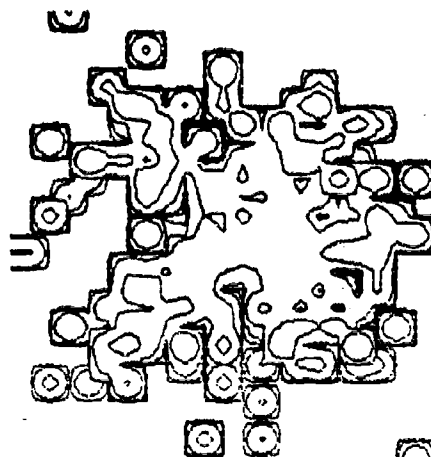
1357913579135791357913579

HEPSON RESEARCH CORPORATION  
 URBAN FIRE MODEL  
 PLAY RELEASE ON TIME = 1000.00  
 TIME 1 TO 100.00  
 WALL GIVE OFF RATE 1.00  
 \*\*\* ONLY DATA FROM WALL GIVE OFF RATES IS PLotted \*\*\*  
 HOT SCALE IS LOGARITHMIC SCALE 10 ( 0-1.00 0-1.013 )



1357913579135791357913579

HEPSON RESEARCH CORPORATION  
 URBAN FIRE MODEL  
 PLAY RELEASE ON TIME = 1000.00  
 TIME 1 TO 100.00  
 WALL GIVE OFF RATE 1.00  
 \*\*\* ONLY DATA FROM WALL GIVE OFF RATES IS PLotted \*\*\*  
 HOT SCALE IS LOGARITHMIC SCALE 10 ( 0-1.00 0-1.013 )



1357913579135791357913579

Figure 6-1(h). Heat production rate contour for area fire.

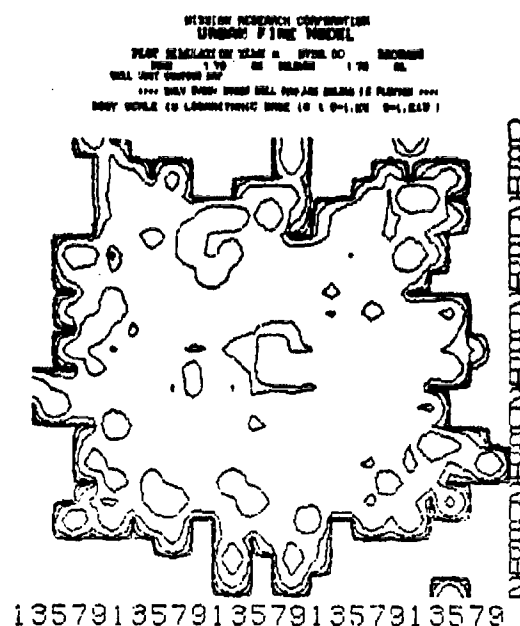
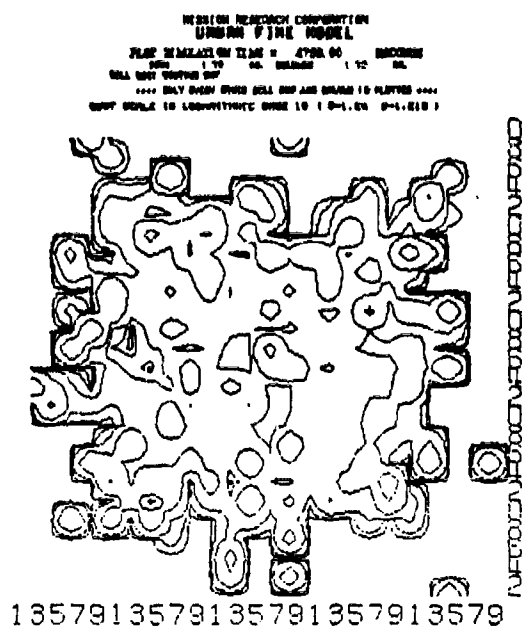
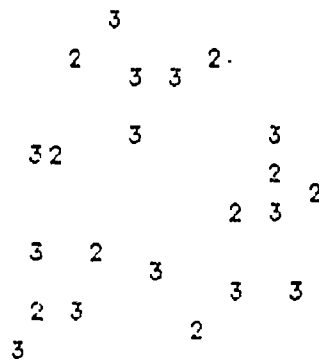


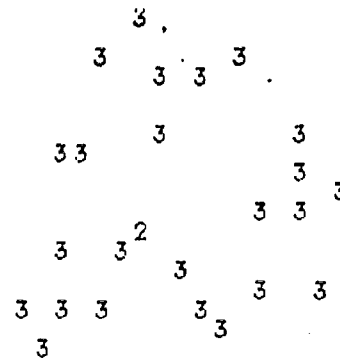
Figure 6-1(i). Heat production rate contour for area fire.

MISSION RESEARCH CORPORATION  
URBAN FIRE MODEL  
PLOT SIMULANT ON TIME = 1000.00 SECONDS  
DATA 1 TO 10 BY COLUMN 1 TO 10  
ONLY HOT: LETTERS A TO Z ARE A RANGE OF HOT VALUES  
ONLY HOT: OTHER OTHER CALL FOR ARE VALUES TO PLOTTER  
HOT SCALE IS LOGARITHMIC BASE 10 ( 0-1.00 0-1.013 )



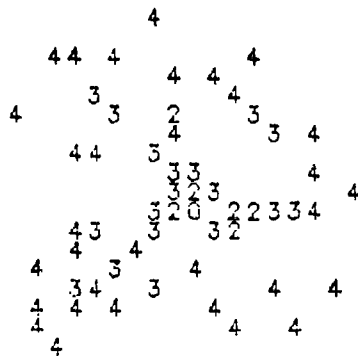
1357913579135791357913579

MISSION RESEARCH CORPORATION  
URBAN FIRE MODEL  
PLOT SIMULANT ON TIME = 1000.00 SECONDS  
DATA 1 TO 10 BY COLUMN 1 TO 10  
ONLY HOT: LETTERS A TO Z ARE A RANGE OF HOT VALUES  
ONLY HOT: OTHER OTHER CALL FOR ARE VALUES TO PLOTTER  
HOT SCALE IS LOGARITHMIC BASE 10 ( 0-1.00 0-1.013 )



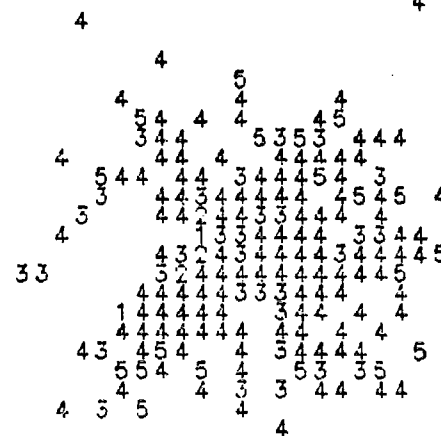
1357913579135791357913579

MISSION RESEARCH CORPORATION  
URBAN FIRE MODEL  
PLOT SIMULANT ON TIME = 1750.00 SECONDS  
DATA 1 TO 10 BY COLUMN 1 TO 10  
ONLY HOT: LETTERS A TO Z ARE A RANGE OF HOT VALUES  
ONLY HOT: OTHER OTHER CALL FOR ARE VALUES TO PLOTTER  
HOT SCALE IS LOGARITHMIC BASE 10 ( 0-1.00 0-1.013 )



1357913579135791357913579

MISSION RESEARCH CORPORATION  
URBAN FIRE MODEL  
PLOT SIMULANT ON TIME = 1750.00 SECONDS  
DATA 1 TO 10 BY COLUMN 1 TO 10  
ONLY HOT: LETTERS A TO Z ARE A RANGE OF HOT VALUES  
ONLY HOT: OTHER OTHER CALL FOR ARE VALUES TO PLOTTER  
HOT SCALE IS LOGARITHMIC BASE 10 ( 0-1.00 0-1.013 )



1357913579135791357913579

Figure 6-1(j). Cell heat production rate map for area fire.

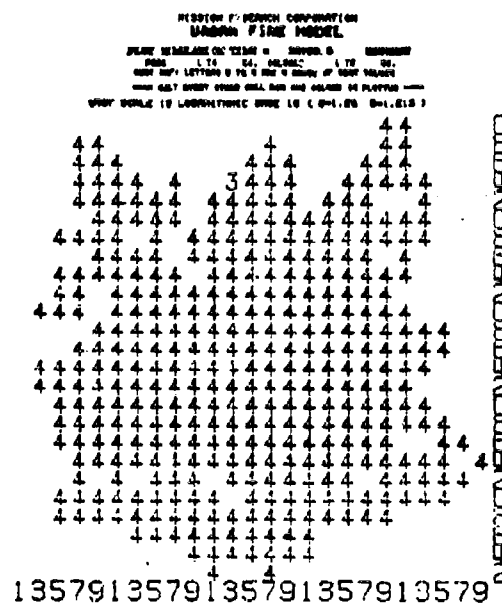
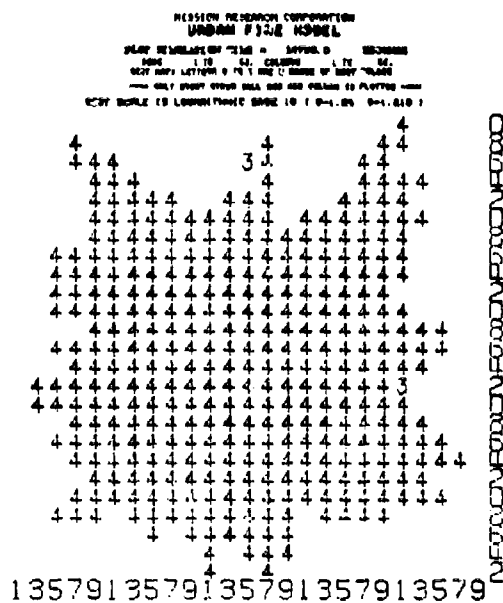
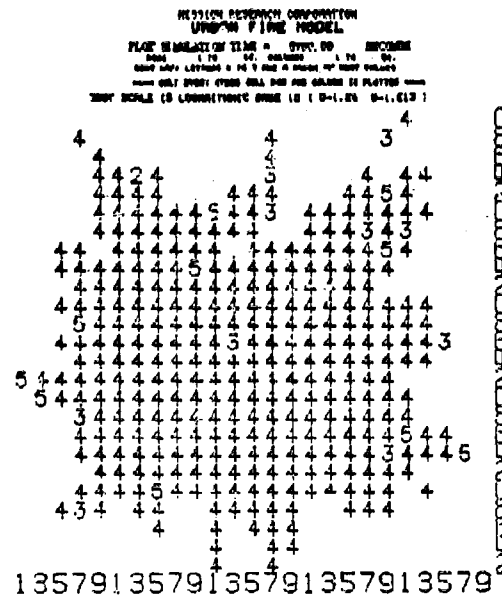
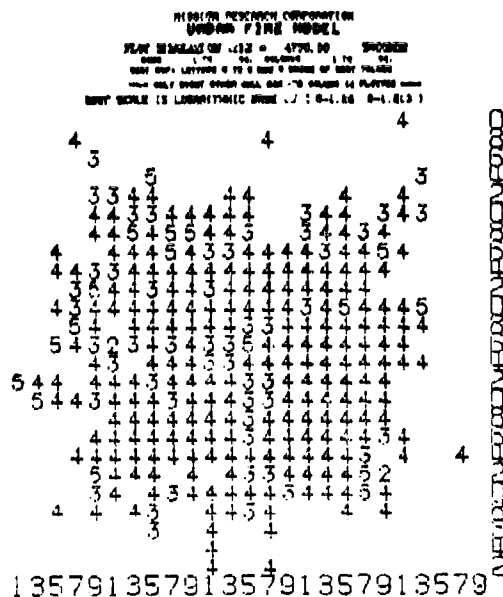


Figure 6-1(k). Cell heat production rate map for area fire.

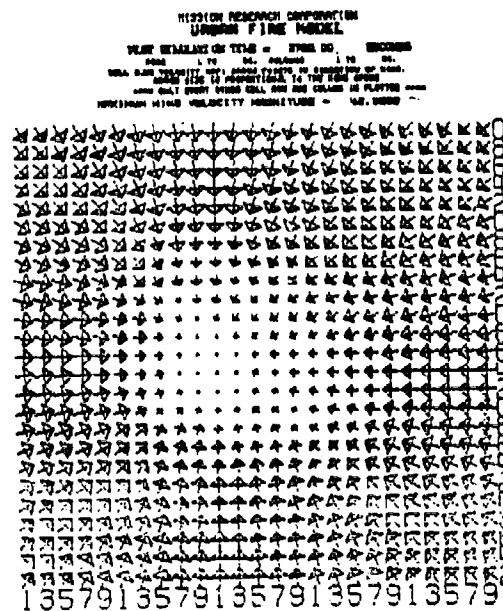
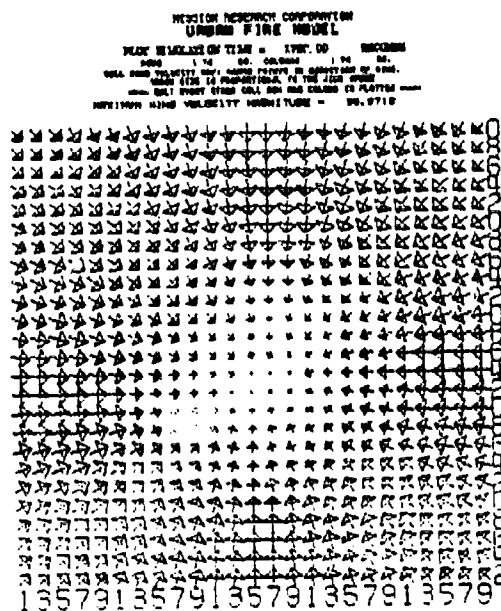
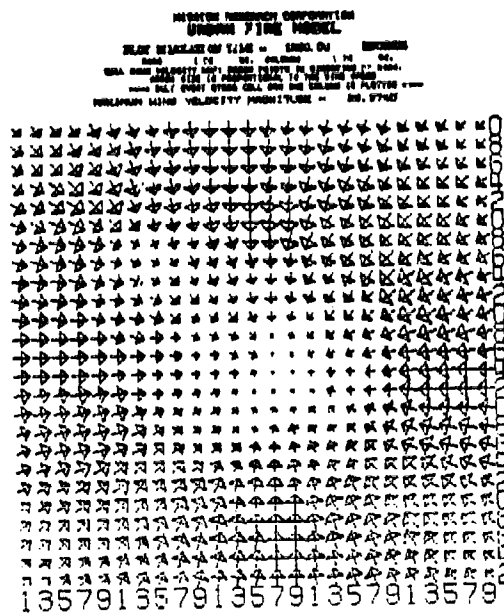
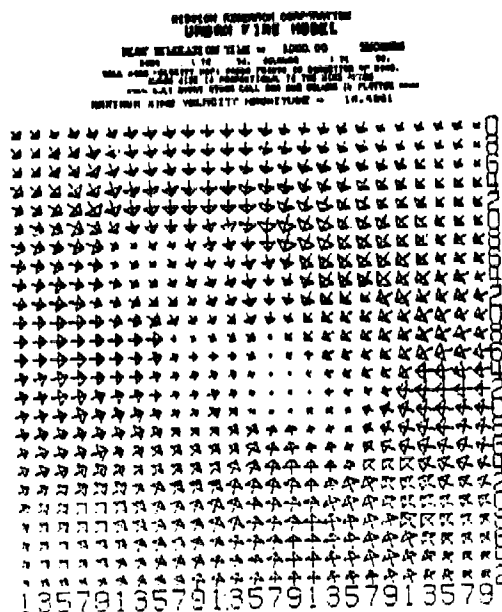
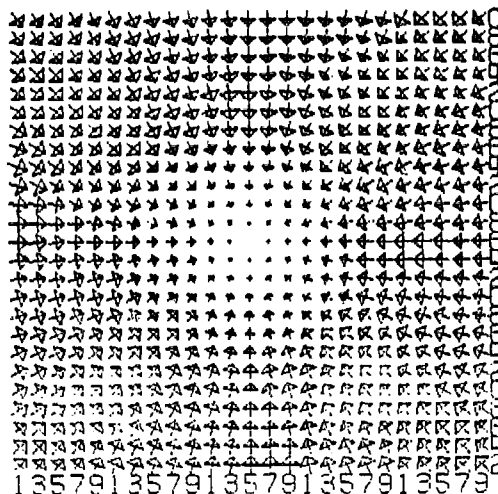


Figure 6-1(1). Cell heat production rate map for area fire.



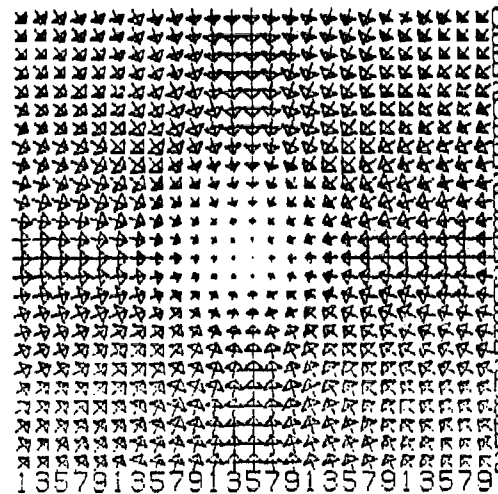
MISSION RESEARCH CORPORATION  
UNIFORM FIRE MODEL

PLAN RELEASED ON TIME = 4700.00  
DATE = 1 74 00.00  
WIND VELOCITY = 10.0000  
WIND DIRECTION = 0.0000  
WIND VELOCITY MAGNITUDE = 10.0000



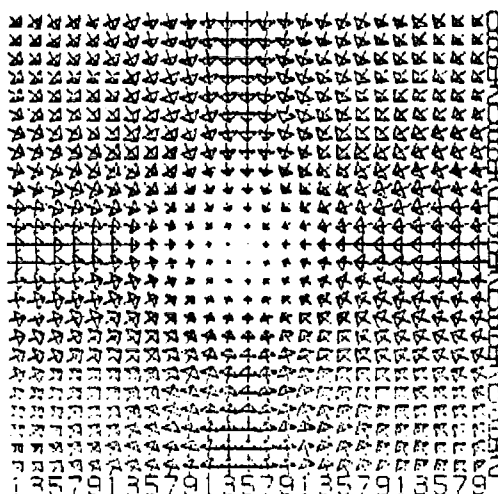
MISSION RESEARCH CORPORATION  
UNIFORM FIRE MODEL

PLAN RELEASED ON TIME = 4700.00  
DATE = 1 74 00.00  
WIND VELOCITY = 11.0000  
WIND DIRECTION = 0.0000  
WIND VELOCITY MAGNITUDE = 11.0000



MISSION RESEARCH CORPORATION  
UNIFORM FIRE MODEL

PLAN RELEASED ON TIME = 4700.00  
DATE = 1 74 00.00  
WIND VELOCITY = 11.0000  
WIND DIRECTION = 0.0000  
WIND VELOCITY MAGNITUDE = 11.0000



MISSION RESEARCH CORPORATION  
UNIFORM FIRE MODEL

PLAN RELEASED ON TIME = 4700.00  
DATE = 1 74 00.00  
WIND VELOCITY = 12.0000  
WIND DIRECTION = 0.0000  
WIND VELOCITY MAGNITUDE = 12.0000

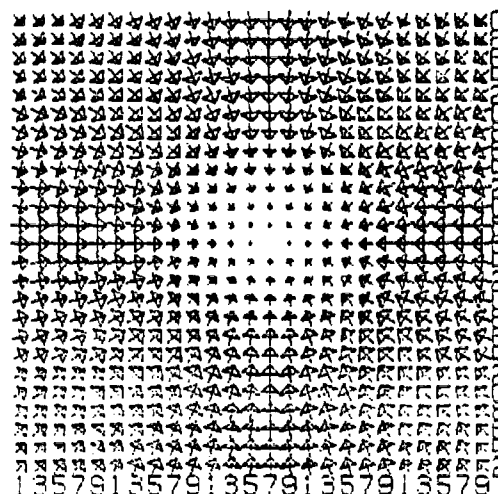


Figure 6-1(m). Wind velocity map for area fire.

## 6.2 LARGE AREA FIRE WITH 10 M/SEC AMBIENT WIND VELOCITY

The initial fire geometry in this case is exactly the same as in Case 6.1. The ambient wind is 10 m/sec, and directed from the lower left corner to the upper right corner. Figures 6-2 through 6-2(g) show that the fire burns very similarly to that of Case 6.1. The spread is slightly more rapid and tends to follow the wind direction more than in Case 6.1. The reason the fires are so similar is because the fire induced winds are a factor of from two to four times as large as the ambient wind. Propagation effects, which are strongly related to wind velocity, are thus dominated by the fire induced winds. Figures 6-2(l) and 6-2(m) show the interactions between the ambient and fire induced winds.

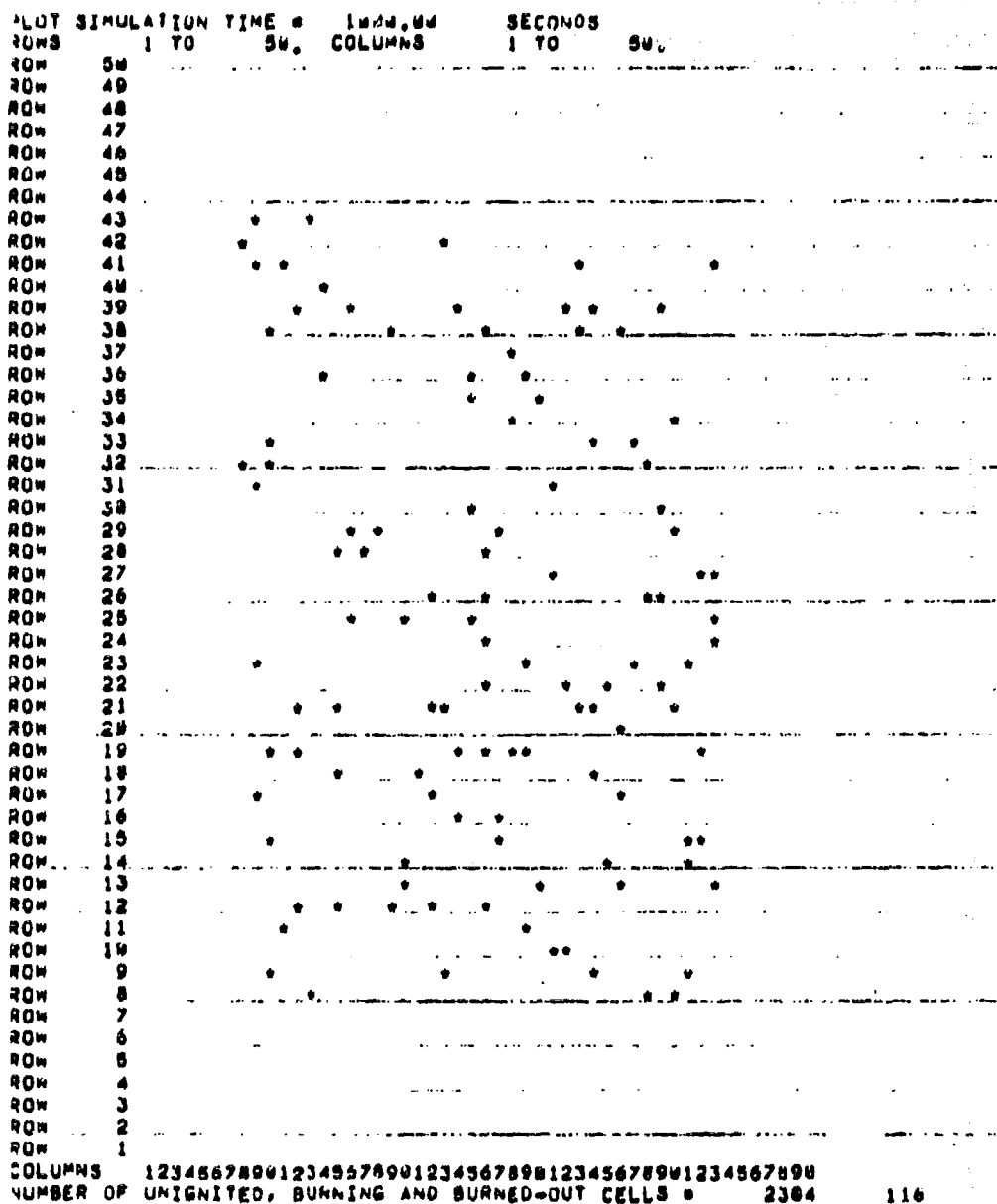
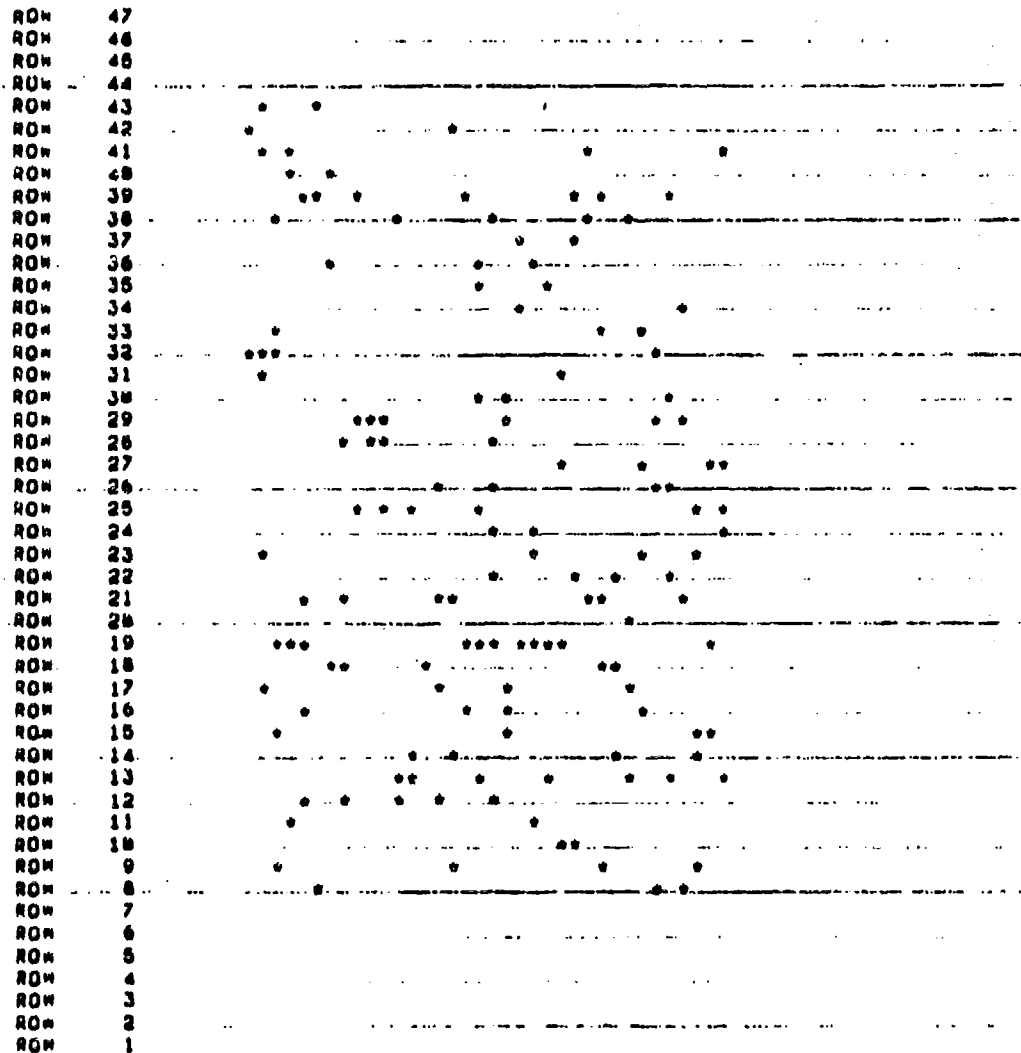


Figure 6-2. Cell state map for area fire with 10 m/s ambient wind.

PLOT SIMULATION TIME = 1260.00 SECONDS

ROWS 1 TO 50, COLUMNS 1 TO 50.

ROW 50  
ROW 49  
ROW 48



COLUMNS 1234567890123456789012345678901234567890

NUMBER OF UNIGNITED, BURNING AND BURNED-OUT CELLS = 2389

141

Figure 6-2(a). Cell state map for area fire with .10 m/s ambient wind.

```

PLOT SIMULATION TIME = 1754.00 SECONDS
ROWS 1 TO 50, COLUMNS 1 TO 80.

ROW 50
ROW 49
ROW 48
ROW 47
ROW 46
ROW 45
ROW 44
ROW 43
ROW 42

ROW 41
ROW 40
ROW 39
ROW 38
ROW 37
ROW 36
ROW 35
ROW 34
ROW 33
ROW 32
ROW 31
ROW 30
ROW 29
ROW 28
ROW 27
ROW 26
ROW 25
ROW 24
ROW 23
ROW 22
ROW 21
ROW 20
ROW 19
ROW 18
ROW 17
ROW 16
ROW 15
ROW 14
ROW 13
ROW 12
ROW 11
ROW 10
ROW 9
ROW 8
ROW 7
ROW 6
ROW 5
ROW 4
ROW 3
ROW 2
ROW 1
COLUMNS 12345678901234567890123456789012345678901234567890
NUMBER OF UNIGNITED, BURNING AND BURNED-OUT CELLS = 2233 267 0

```

Figure 6-2(b). Cell state map for area fire with .10 m/s ambient wind.

PLOT SIMULATION TIME = 2750.00 SECONDS  
 ROWS 1 TO 50. COLUMNS 1 TO 50.

```

ROW 50
ROW 49
ROW 48
ROW 47
ROW 46
ROW 45
ROW 44
ROW 43
ROW 42
ROW 41
ROW 40
ROW 39
ROW 38
ROW 37
ROW 36
  
```

```

ROW 35
ROW 34
ROW 33
ROW 32
ROW 31
ROW 30
ROW 29
ROW 28
ROW 27
ROW 26
ROW 25
ROW 24
ROW 23
ROW 22
ROW 21
ROW 20
ROW 19
ROW 18
ROW 17
ROW 16
ROW 15
ROW 14
ROW 13
ROW 12
ROW 11
ROW 10
ROW 9
ROW 8
ROW 7
ROW 6
ROW 5
ROW 4
ROW 3
ROW 2
ROW 1
  
```

COLUMNS 1234567890123456789012345678901234567890  
 NUMBER OF UNIGNITED, BURNING AND BURNED-OUT CELLS = 176 740

Figure 6-2(c). Cell state map for area fire with .10 m/s ambient wind.

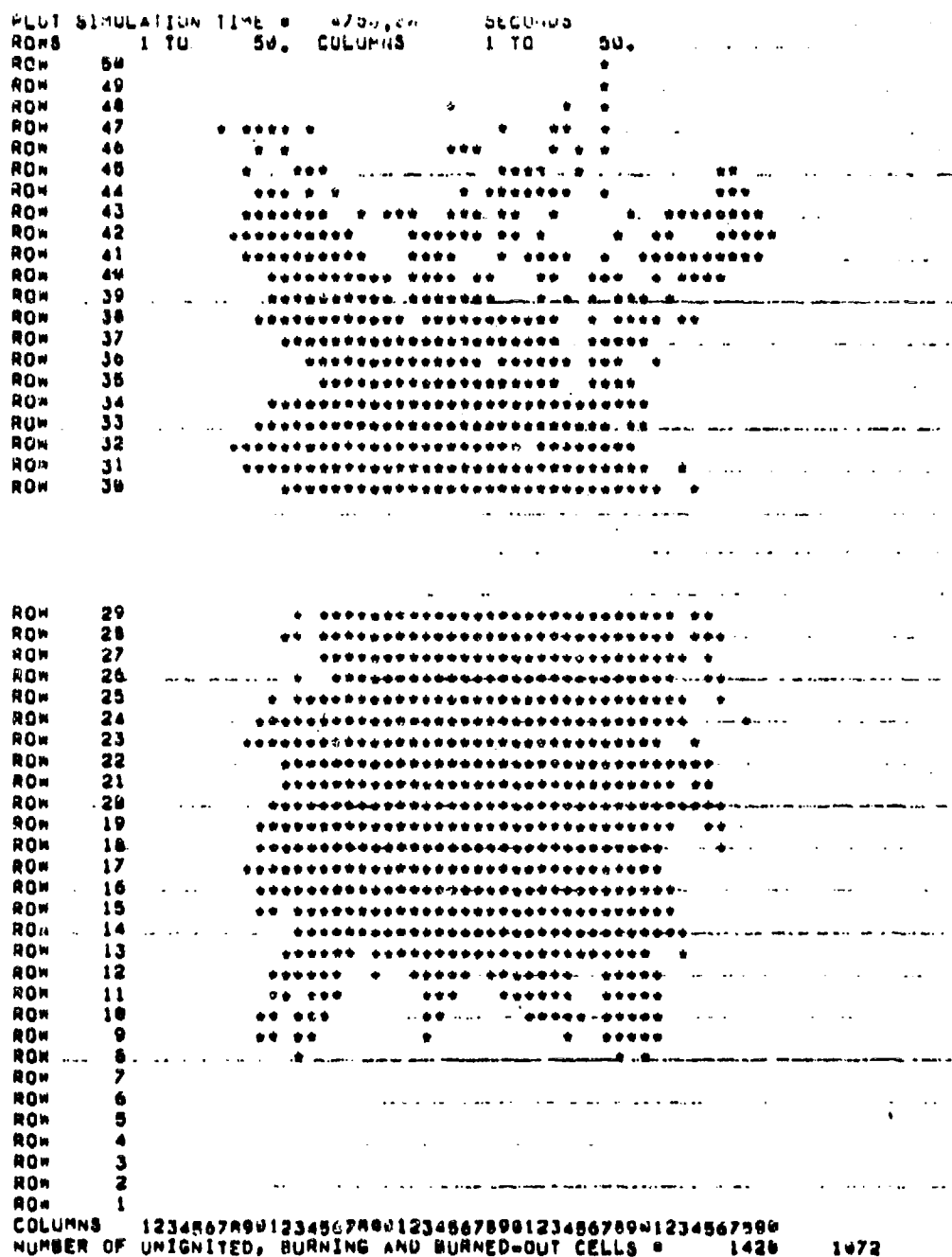


Figure 6-2(d). Cell state map for area fire with .10 m/s ambient wind.

```

PLOT SIMULATION TIME = 0752.00 SECONDS
ROWS 1 TO 50, COLUMNS 1 TO 50.
ROW 50
ROW 49
ROW 48 *****
ROW 47 *****
ROW 46 *****
ROW 45 *****
ROW 44 *****
ROW 43 *****
ROW 42 *****
ROW 41 *****
ROW 40 *****
ROW 39 *****
ROW 38 *****
ROW 37 *****
ROW 36 *****
ROW 35 *****
ROW 34 *****
ROW 33 *****
ROW 32 *****
ROW 31 *****
ROW 30 *****
ROW 29 *****
ROW 28 *****
ROW 27 *****
ROW 26 *****
ROW 25 *****
ROW 24 *****

ROW 23 *****
ROW 22 *****
ROW 21 *****
ROW 20 *****
ROW 19 *****
ROW 18 *****
ROW 17 *****
ROW 16 *****
ROW 15 *****
ROW 14 *****
ROW 13 *****
ROW 12 *****
ROW 11 *****
ROW 10 *****
ROW 9 *****
ROW 8 *****
ROW 7 *****
ROW 6 *****
ROW 5 *****
ROW 4 *****
ROW 3 *****
ROW 2 *****
ROW 1 *****
COLUMNS 12345678901234567890123456789012345678901234567890
NUMBER OF UNIGNITED, BURNING AND BURNED-OUT CELLS = 1246 1254

```

Figure 6-2(e). Cell state map for area fire with .10 m/s ambient wind.



```

PLU1 SIMULATION TIME = 1075.00 SECONDS
ROWS 1 TO 50, COLUMNS 1 TO 50.
ROW 50 *****
ROW 49 *****
ROW 48 *****
ROW 47 *****
ROW 46 *****
ROW 45 *****
ROW 44 *****
ROW 43 *****
ROW 42 *****
ROW 41 *****
ROW 40 *****
ROW 39 *****
ROW 38 *****
ROW 37 *****
ROW 36 *****
ROW 35 *****
ROW 34 *****
ROW 33 *****
ROW 32 *****
ROW 31 *****
ROW 30 *****
ROW 29 *****
ROW 28 *****
ROW 27 *****
ROW 26 *****
ROW 25 *****
ROW 24 *****
ROW 23 *****
ROW 22 *****
ROW 21 *****
ROW 20 *****
ROW 19 *****
ROW 18 *****

ROW 17 *****
ROW 16 *****
ROW 15 *****
ROW 14 *****
ROW 13 *****
ROW 12 *****
ROW 11 *****
ROW 10 *****
ROW 9 *****
ROW 8 *****
ROW 7 *****
ROW 6 *****
ROW 5 *****
ROW 4 *****
ROW 3 *****
ROW 2 *****
ROW 1 *****

COLUMNS 1234567890123456789012345678901234567890
NUMBER OF UNIGNITED, BURNING AND BURNED-OUT CELLS = 1003 1412 9

```

Figure 6-2(f). Cell state map for area fire with .10 m/s ambient wind.

```

PLOT SIMULATION TIME = 3275.0 SECONDS
ROW# 1 TO 50 COLUMNS 1 TO 50
ROW 50 .....
ROW 49 .....
ROW 48 .....
ROW 47 .....
ROW 46 .....
ROW 45 .....
ROW 44 .....
ROW 43 .....
ROW 42 .....
ROW 41 .....
ROW 40 .....
ROW 39 .....
ROW 38 .....
ROW 37 .....
ROW 36 .....
ROW 35 .....
ROW 34 .....
ROW 33 .....
ROW 32 .....
ROW 31 .....
ROW 30 .....
ROW 29 .....
ROW 28 .....
ROW 27 .....
ROW 26 .....
ROW 25 .....
ROW 24 .....
ROW 23 .....
ROW 22 .....
ROW 21 .....
ROW 20 .....
ROW 19 .....
ROW 18 .....
ROW 17 .....
ROW 16 .....
ROW 15 .....
ROW 14 .....
ROW 13 .....
ROW 12 .....

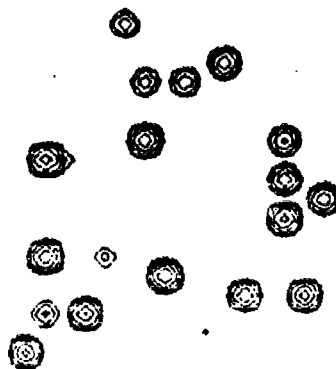
ROW 11 .....
ROW 10 .....
ROW 9 .....
ROW 8 .....
ROW 7 .....
ROW 6 .....
ROW 5 .....
ROW 4 .....
ROW 3 .....
ROW 2 .....
ROW 1 .....

COLUMNS 1234567890123456789012345678901234567890
NUMBER OF UNIGNITED, BURNING AND BURNED-OUT CELLS = 931 1469 110

```

Figure 6-2(g). Cell state map for area fire with .10 m/s ambient wind.

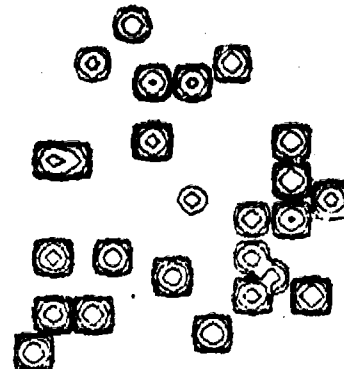
MISSION RESEARCH CORPORATION  
UPDOWN FIRE MODEL  
PLAY SEQUENCE ON TIME = 0000.00  
TIME 1 TO 10.0000 1 TO 10.0000  
WALL NOT COVERED BY  
\*\*\* ONLY EVERY OTHER BALL AND RELAX IS PLAYED \*\*\*  
BODY SCALE IS LOGARITHMIC (BASE 10) (0-1.00 0-1.010)



MISSION RESEARCH CORPORATION

1357913579135791357913579

MISSION RESEARCH CORPORATION  
UPDOWN FIRE MODEL  
PLAY SEQUENCE ON TIME = 0000.00  
TIME 1 TO 10.0000 1 TO 10.0000  
WALL NOT COVERED BY  
\*\*\* ONLY EVERY OTHER BALL AND RELAX IS PLAYED \*\*\*  
BODY SCALE IS LOGARITHMIC (BASE 10) (0-1.00 0-1.010)



MISSION RESEARCH CORPORATION

1357913579135791357913579

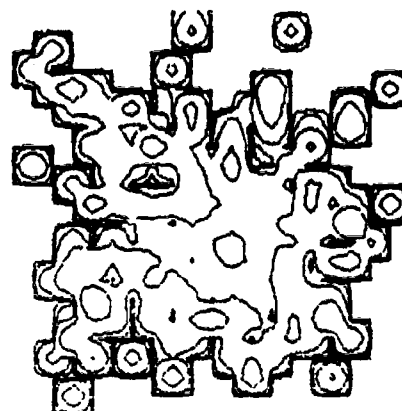
MISSION RESEARCH CORPORATION  
UPDOWN FIRE MODEL  
PLAY SEQUENCE ON TIME = 0000.00  
TIME 1 TO 10.0000 1 TO 10.0000  
WALL NOT COVERED BY  
\*\*\* ONLY EVERY OTHER BALL AND RELAX IS PLAYED \*\*\*  
BODY SCALE IS LOGARITHMIC (BASE 10) (0-1.00 0-1.010)



MISSION RESEARCH CORPORATION

1357913579135791357913579

MISSION RESEARCH CORPORATION  
UPDOWN FIRE MODEL  
PLAY SEQUENCE ON TIME = 0000.00  
TIME 1 TO 10.0000 1 TO 10.0000  
WALL NOT COVERED BY  
\*\*\* ONLY EVERY OTHER BALL AND RELAX IS PLAYED \*\*\*  
BODY SCALE IS LOGARITHMIC (BASE 10) (0-1.00 0-1.010)



MISSION RESEARCH CORPORATION

1357913579135791357913579

Figure 6-2(h). Heat production rate contour for area fire with .10 m/s ambient wind.

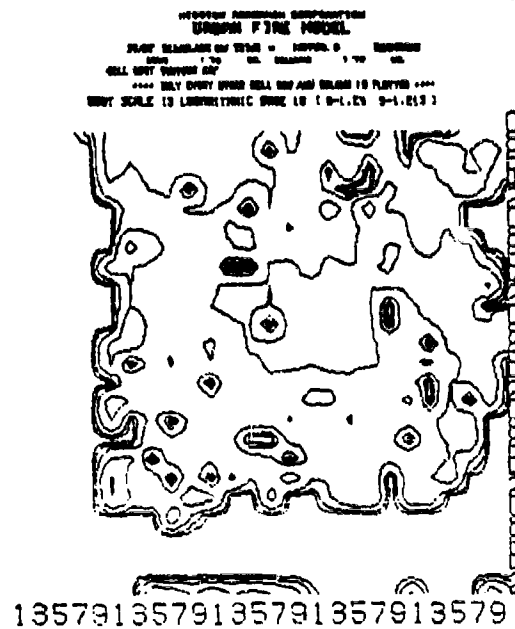
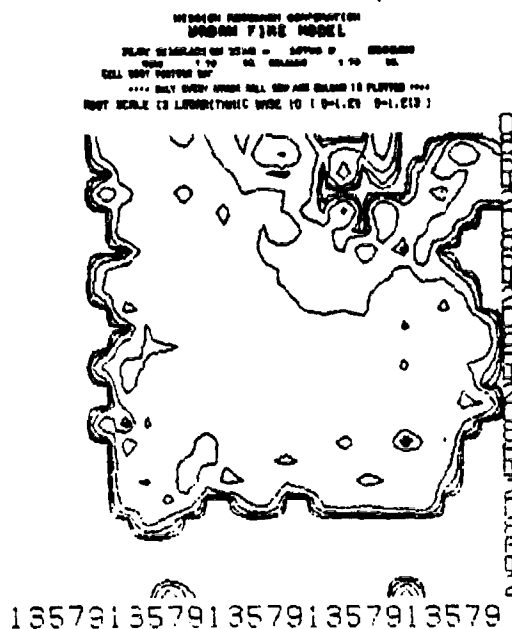
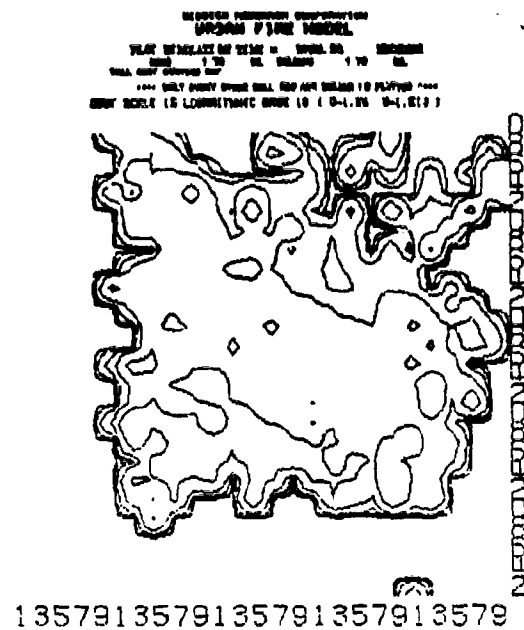
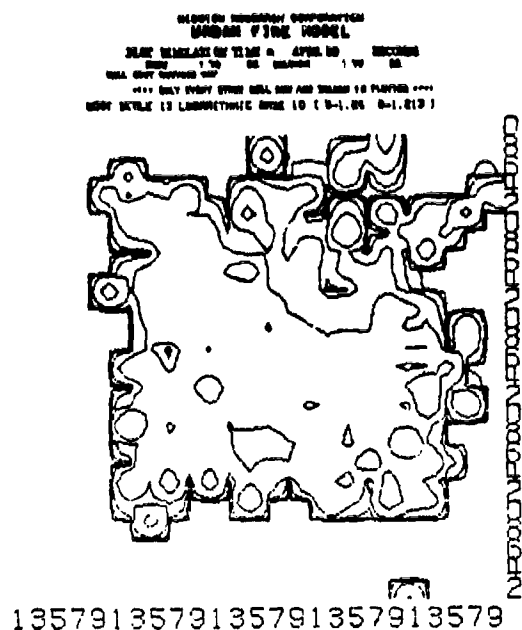


Figure 6-2(1). Heat production rate contour for area fire with .10 m/s ambient wind.





[illegible]

A 10x10 grid of 100 small, stylized, black and white images, each depicting a different animal or creature, arranged in a grid pattern. The images are small and detailed, showing various species of birds, mammals, and reptiles. The grid is organized into 10 rows and 10 columns, with each cell containing a unique illustration. The overall effect is a dense, organized collection of diverse animal life.

[illegible]

1	2	3	4	5	6	7	8	9	10	11	12	13	14	15	16	17	18	19	20	21	22	23	24	25	26	27	28	29	30	31	32	33	34	35	36	37	38	39	40	41	42	43	44	45	46	47	48	49	50	51	52	53	54	55	56	57	58	59	60	61	62	63	64	65	66	67	68	69	70	71	72	73	74	75	76	77	78	79	80	81	82	83	84	85	86	87	88	89	90	91	92	93	94	95	96	97	98	99	100
1	2	3	4	5	6	7	8	9	10	11	12	13	14	15	16	17	18	19	20	21	22	23	24	25	26	27	28	29	30	31	32	33	34	35	36	37	38	39	40	41	42	43	44	45	46	47	48	49	50	51	52	53	54	55	56	57	58	59	60	61	62	63	64	65	66	67	68	69	70	71	72	73	74	75	76	77	78	79	80	81	82	83	84	85	86	87	88	89	90	91	92	93	94	95	96	97	98	99	100
1	2	3	4	5	6	7	8	9	10	11	12	13	14	15	16	17	18	19	20	21	22	23	24	25	26	27	28	29	30	31	32	33	34	35	36	37	38	39	40	41	42	43	44	45	46	47	48	49	50	51	52	53	54	55	56	57	58	59	60	61	62	63	64	65	66	67	68	69	70	71	72	73	74	75	76	77	78	79	80	81	82	83	84	85	86	87	88	89	90	91	92	93	94	95	96	97	98	99	100
1	2	3	4	5	6	7	8	9	10	11	12	13	14	15	16	17	18	19	20	21	22	23	24	25	26	27	28	29	30	31	32	33	34	35	36	37	38	39	40	41	42	43	44	45	46	47	48	49	50	51	52	53	54	55	56	57	58	59	60	61	62	63	64	65	66	67	68	69	70	71	72	73	74	75	76	77	78	79	80	81	82	83	84	85	86	87	88	89	90	91	92	93	94	95	96	97	98	99	100
1	2	3	4	5	6	7	8	9	10	11	12	13	14	15	16	17	18	19	20	21	22	23	24	25	26	27	28	29	30	31	32	33	34	35	36	37	38	39	40	41	42	43	44	45	46	47	48	49	50	51	52	53	54	55	56	57	58	59	60	61	62	63	64	65	66	67	68	69	70	71	72	73	74	75	76	77	78	79	80	81	82	83	84	85	86	87	88	89	90	91	92	93	94	95	96	97	98	99	100
1	2	3	4	5	6	7	8	9	10	11	12	13	14	15	16	17	18	19	20	21	22	23	24	25	26	27	28	29	30	31	32	33	34	35	36	37	38	39	40	41	42	43	44	45	46	47	48	49	50	51	52	53	54	55	56	57	58	59	60	61	62	63	64	65	66	67	68	69	70	71	72	73	74	75	76	77	78	79	80	81	82	83	84	85	86	87	8												

191





### 6.3 LINE FIRE WITH NO AMBIENT WIND

As shown in Figure 6-3, the central  $3 \times 35$  cells were ignited with a probability of ignition of 0.5. Fire induced winds are generated ranging from 7 to 18 m/s as shown in Figures 6-3(l) and 6-3(m). This is not sufficient wind speed to cause a significant amount of fire propagation. The ignited area does, however, partially fill in, due primarily to contagion. The "dumbbell" appearance shown in Figures 6-3(f) and 6-3(g) is an artifact of brands being tossed completely across the fire as described in Case 6.1.

PLOT SIMULATION TIME = 1440.00 SECONDS  
 ROWS 1 TO 50, COLUMNS 1 TO 50,

ROW	50
ROW	49
ROW	48
ROW	47
ROW	46
ROW	45
ROW	44
ROW	43
ROW	42
ROW	41
ROW	40
ROW	39
ROW	38
ROW	37
ROW	36
ROW	35
ROW	34
ROW	33
ROW	32
ROW	31
ROW	30
ROW	29
ROW	28
ROW	27
ROW	26
ROW	25
ROW	24
ROW	23
ROW	22
ROW	21
ROW	20
ROW	19
ROW	18
ROW	17
ROW	16
ROW	15
ROW	14
ROW	13
ROW	12
ROW	11
ROW	10
ROW	9
ROW	8
ROW	7
ROW	6
ROW	5
ROW	4
ROW	3
ROW	2
ROW	1

COLUMNS 1234567890123456789012345678901234567890  
 NUMBER OF UNIGNITED, BURNING AND BURNED-OUT CELLS = 2462 38 0

Figure 6-3. Cell state map for line fire.

```

PLOT SIMULATION TIME = 1250.00 SECONDS
ROWS 1 TO 50. COLUMNS 1 TO 50.
ROW 50
ROW 49
ROW 48

ROW 47
ROW 46
ROW 45
ROW 44
ROW 43
ROW 42
ROW 41
ROW 40
ROW 39
ROW 38
ROW 37
ROW 36
ROW 35
ROW 34
ROW 33
ROW 32
ROW 31
ROW 30
ROW 29
ROW 28
ROW 27
ROW 26
ROW 25
ROW 24
ROW 23
ROW 22
ROW 21
ROW 20
ROW 19
ROW 18
ROW 17
ROW 16
ROW 15
ROW 14
ROW 13
ROW 12
ROW 11
ROW 10
ROW 9
ROW 8
ROW 7
ROW 6
ROW 5
ROW 4
ROW 3
ROW 2
ROW 1
COLUMNS 12345678901234567890123456789012345678901234567890
NUMBER OF UNIGNITED, BURNING AND BURNED-OUT CELLS = 2461 39 0

```

The figure displays a 50x50 grid representing a cell state map. The rows are labeled from 1 to 50, and the columns are labeled from 1 to 50. A horizontal line of burning cells is visible across rows 24, 25, and 26. The cells in this line are marked with dots, indicating a burning state. The rest of the grid is empty, representing unignited cells.

Figure 6-3(a). Cell state map for line fire.

```

PLOT SIMULATION TIME = 1754.00 SECONDS
ROWS 1 TO 50 COLUMNS 1 TO 50
ROW 50
ROW 49
ROW 48
ROW 47
ROW 46
ROW 45
ROW 44
ROW 43
ROW 42

ROW 41
ROW 40
ROW 39
ROW 38
ROW 37
ROW 36
ROW 35
ROW 34
ROW 33
ROW 32
ROW 31
ROW 30
ROW 29
ROW 28
ROW 27
ROW 26
ROW 25
ROW 24
ROW 23
ROW 22
ROW 21
ROW 20
ROW 19
ROW 18
ROW 17
ROW 16
ROW 15
ROW 14
ROW 13
ROW 12
ROW 11
ROW 10
ROW 9
ROW 8
ROW 7
ROW 6
ROW 5
ROW 4
ROW 3
ROW 2
ROW 1
COLUMNS 12345678901234567890123456789012345678901234567890
NUMBER OF UNIGNITED, BURNING AND BURNED-OUT CELLS = 2456 44

```

Figure 6-3(b). Cell state map for line fire.

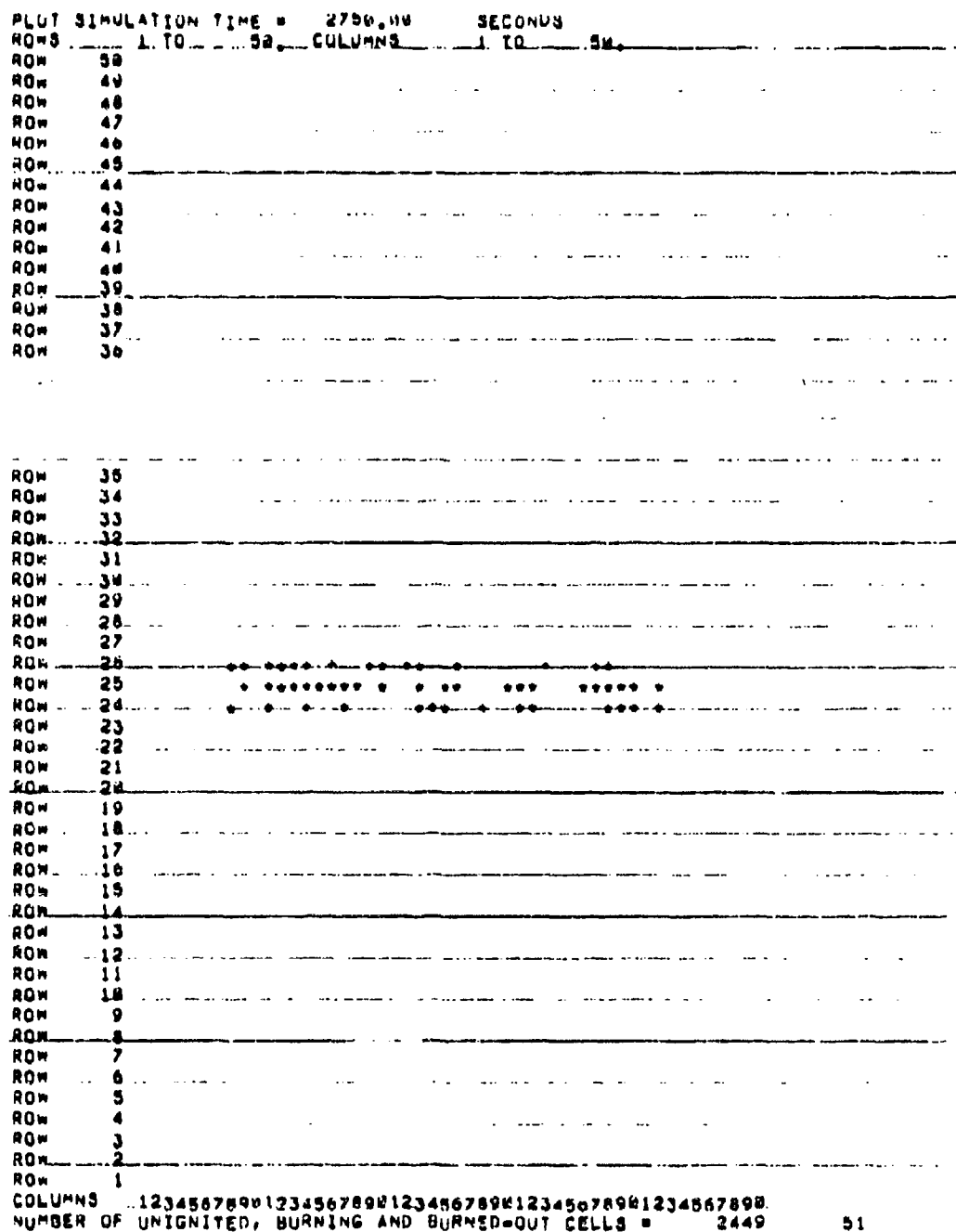


Figure 6-3(c). Cell state map for line fire.

```

PLOT SIMULATION TIME = 4750.00 SECONDS
ROWS 1 TO 50, COLUMNS 1 TO 50.

ROW 50
ROW 49
ROW 48
ROW 47
ROW 46
ROW 45
ROW 44
ROW 43
ROW 42
ROW 41
ROW 40
ROW 39
ROW 38
ROW 37
ROW 36
ROW 35
ROW 34
ROW 33
ROW 32
ROW 31
ROW 30

ROW 29
ROW 28
ROW 27
ROW 26 .....
ROW 25 .....
ROW 24 .....
ROW 23 .....
ROW 22 .....
ROW 21 .....
ROW 20 .....
ROW 19 .....
ROW 18 .....
ROW 17 .....
ROW 16 .....
ROW 15 .....
ROW 14 .....
ROW 13 .....
ROW 12 .....
ROW 11 .....
ROW 10 .....
ROW 9 .....
ROW 8 .....
ROW 7 .....
ROW 6 .....
ROW 5 .....
ROW 4 .....
ROW 3 .....
ROW 2 .....
ROW 1 .....

COLUMNS 1234567890123456789012345678901234567890
NUMBER OF UNIGNITED, BURNING AND BURNED-OUT CELLS = 2443 57

```

Figure 6-3(d). Cell state map for line fire.

```

PLOT SIMULATION TIME = 5752.54 SECONDS
ROWS 1 TO 50 COLUMNS 1 TO 80
ROW 50
ROW 49
ROW 48
ROW 47
ROW 46
ROW 45
ROW 44
ROW 43
ROW 42
ROW 41
ROW 40
ROW 39
ROW 38
ROW 37
ROW 36
ROW 35
ROW 34
ROW 33
ROW 32
ROW 31
ROW 30
ROW 29
ROW 28
ROW 27
ROW 26 *****
ROW 25 *****
ROW 24 *****

ROW 23
ROW 22
ROW 21
ROW 20
ROW 19
ROW 18
ROW 17
ROW 16
ROW 15
ROW 14
ROW 13
ROW 12
ROW 11
ROW 10
ROW 9
ROW 8
ROW 7
ROW 6
ROW 5
ROW 4
ROW 3
ROW 2
ROW 1
COLUMNS 12345678901234567890123456789012345678901234567890
NUMBER OF UNIGNITED, BURNING AND BURNED-OUT CELLS = 2418 02

```

Figure 6-3(e). Cell state map for line fire.

```

PLOT SIMULATION TIME = 10750.4 SECONDS
ROWS 1 TO 50 COLUMNS 1 TO 50
ROW 50
ROW 49
ROW 48
ROW 47
ROW 46
ROW 45
ROW 44
ROW 43
ROW 42
ROW 41
ROW 40
ROW 39
ROW 38
ROW 37
ROW 36
ROW 35
ROW 34
ROW 33
ROW 32
ROW 31
ROW 30
ROW 29
ROW 28
ROW 27
ROW 26
ROW 25
ROW 24
ROW 23
ROW 22
ROW 21
ROW 20
ROW 19
ROW 18

```

```

ROW 17
ROW 16
ROW 15
ROW 14
ROW 13
ROW 12
ROW 11
ROW 10
ROW 9
ROW 8
ROW 7
ROW 6
ROW 5
ROW 4
ROW 3
ROW 2
ROW 1
COLUMNS 1234567890123456789012345678901234567890
NUMBER OF UNIGNITED, BURNING AND BURNED-OUT CELLS = 2400 100

```

Figure 6-3(f). Cell state map for line fire.



```

PLOT SIMULATION TIME = 32769.0 SECONDS
ROWS - 1-TO - 50, COLUMNS - 1-TO - 50,
ROW 50
ROW 49
ROW 48
ROW 47
ROW 46
ROW 45
ROW 44
ROW 43
ROW 42
ROW 41
ROW 40
ROW 39
ROW 38
ROW 37
ROW 36
ROW 35
ROW 34
ROW 33
ROW 32
ROW 31
ROW 30
ROW 29
ROW 28
ROW 27
ROW 26
ROW 25
ROW 24
ROW 23
ROW 22
ROW 21
ROW 20
ROW 19
ROW 18
ROW 17
ROW 16
ROW 15
ROW 14
ROW 13
ROW 12

ROW 11
ROW 10
ROW 9
ROW 8
ROW 7
ROW 6
ROW 5
ROW 4
ROW 3
ROW 2
ROW 1
COLUMNS. 12345678901234567890123456789012345678901234567890
NUMBER OF UNIGNITED, BURNING AND BURNED-OUT CELLS = 2369 120 1

```

Figure 6-3(g). Cell state map for line fire.

MISSION RESEARCH CORPORATION  
URBAN FIRE MODEL  
PLAY SIMULATION TIME = 3400.00  
TIME 1 TO 24.0000 1 TO 24.0000  
CELL NOT COVERED BY  
\*\*\* ONLY EVERY OTHER CELL NOT AND CELLS IS PLAYED \*\*\*  
BODY STYLE (S LOGARITHMIC) BODY (S (0-1.00 0-1.00))



135791357913579135791357913579

MISSION RESEARCH CORPORATION  
URBAN FIRE MODEL  
PLAY SIMULATION TIME = 3700.00  
TIME 1 TO 24.0000 1 TO 24.0000  
CELL NOT COVERED BY  
\*\*\* ONLY EVERY OTHER CELL NOT AND CELLS IS PLAYED \*\*\*  
BODY STYLE (S LOGARITHMIC) BODY (S (0-1.00 0-1.00))



135791357913579135791357913579

MISSION RESEARCH CORPORATION  
URBAN FIRE MODEL  
PLAY SIMULATION TIME = 3800.00  
TIME 1 TO 24.0000 1 TO 24.0000  
CELL NOT COVERED BY  
\*\*\* ONLY EVERY OTHER CELL NOT AND CELLS IS PLAYED \*\*\*  
BODY STYLE (S LOGARITHMIC) BODY (S (0-1.00 0-1.00))



135791357913579135791357913579

MISSION RESEARCH CORPORATION  
URBAN FIRE MODEL  
PLAY SIMULATION TIME = 3700.00  
TIME 1 TO 24.0000 1 TO 24.0000  
CELL NOT COVERED BY  
\*\*\* ONLY EVERY OTHER CELL NOT AND CELLS IS PLAYED \*\*\*  
BODY STYLE (S LOGARITHMIC) BODY (S (0-1.00 0-1.00))



135791357913579135791357913579

Figure 6-3(h). Heat production rate contour for line fire.

MISSION RESEARCH CORPORATION  
URBAN FIRE MODEL  
PLOT RELEASE ON TIME = 47.70 SE SECONDS  
RMS 1 TO 10.0000 1 TO 10  
CELL SIZE 0.00000000  
\*\*\* ONLY EVERY OTHER CELL SIZE AND RELEASE IS PLOTTED \*\*\*  
COPY SCALE IS LOGARITHMIC SCALE IS 1 0-1.25 0-1.25



1357913579135791357913579

MISSION RESEARCH CORPORATION  
URBAN FIRE MODEL  
PLOT RELEASE ON TIME = 47.70 SE SECONDS  
RMS 1 TO 10.0000 1 TO 10  
CELL SIZE 0.00000000  
\*\*\* ONLY EVERY OTHER CELL SIZE AND RELEASE IS PLOTTED \*\*\*  
COPY SCALE IS LOGARITHMIC SCALE IS 1 0-1.25 0-1.25



1357913579135791357913579

MISSION RESEARCH CORPORATION  
URBAN FIRE MODEL  
PLOT RELEASE ON TIME = 47.70 SE SECONDS  
RMS 1 TO 10.0000 1 TO 10  
CELL SIZE 0.00000000  
\*\*\* ONLY EVERY OTHER CELL SIZE AND RELEASE IS PLOTTED \*\*\*  
COPY SCALE IS LOGARITHMIC SCALE IS 1 0-1.25 0-1.25



1357913579135791357913579

MISSION RESEARCH CORPORATION  
URBAN FIRE MODEL  
PLOT RELEASE ON TIME = 47.70 SE SECONDS  
RMS 1 TO 10.0000 1 TO 10  
CELL SIZE 0.00000000  
\*\*\* ONLY EVERY OTHER CELL SIZE AND RELEASE IS PLOTTED \*\*\*  
COPY SCALE IS LOGARITHMIC SCALE IS 1 0-1.25 0-1.25



1357913579135791357913579

Figure 6-3(i). Heat production rate contour for line fire.

MISSION RESEARCH CORPORATION  
URBAN FIRE MODEL  
PLAN SIMULATION TIME = 1000.00 SECONDS  
DATA 1 TO 99: 00000000 1 TO 99:  
ONLY HOT: LETTERS 0 TO 9 ARE A PART OF HOT: VALUE  
ONLY HOT: OTHER CELL ARE ARE 00000000 IN PLATES  
HOT: SCALE IS LOGARITHMIC SCALE 10 ( 0-1.00 0-1.010 )

22 23 22 22  
2 2 22 22

135791357913579135791357913579

MISSION RESEARCH CORPORATION  
URBAN FIRE MODEL  
PLAN SIMULATION TIME = 1700.00 SECONDS  
DATA 1 TO 99: 00000000 1 TO 99:  
ONLY HOT: LETTERS 0 TO 9 ARE A PART OF HOT: VALUE  
ONLY HOT: OTHER CELL ARE ARE 00000000 IN PLATES  
HOT: SCALE IS LOGARITHMIC SCALE 10 ( 0-1.00 0-1.010 )

43 33 33 43  
3 3 33 4 3

135791357913579135791357913579

MISSION RESEARCH CORPORATION  
URBAN FIRE MODEL  
PLAN SIMULATION TIME = 1200.00 SECONDS  
DATA 1 TO 99: 00000000 1 TO 99:  
ONLY HOT: LETTERS 0 TO 9 ARE A PART OF HOT: VALUE  
ONLY HOT: OTHER CELL ARE ARE 00000000 IN PLATES  
HOT: SCALE IS LOGARITHMIC SCALE 10 ( 0-1.00 0-1.010 )

23 33 23 33  
2 3 23 3

135791357913579135791357913579

MISSION RESEARCH CORPORATION  
URBAN FIRE MODEL  
PLAN SIMULATION TIME = 1700.00 SECONDS  
DATA 1 TO 99: 00000000 1 TO 99:  
ONLY HOT: LETTERS 0 TO 9 ARE A PART OF HOT: VALUE  
ONLY HOT: OTHER CELL ARE ARE 00000000 IN PLATES  
HOT: SCALE IS LOGARITHMIC SCALE 10 ( 0-1.00 0-1.010 )

153 33 33 43  
4 3 33 4 3

135791357913579135791357913579

Figure 6-3(j). Cell heat production rate map for line fire.

MISSION RESEARCH CORPORATION  
URBAN FIRE MODEL  
PLOT SIMULATION TIME = 4790.00 SECONDS  
GRID 1 TO 100, COLUMNS 1 TO 100  
ONLY MAP: LETTERS A TO Z ARE A RANGE OF GRID VALUES  
ONLY EVERY OTHER CELL HAS AND COLUMN IS PLOTTED  
ONLY SCALE IS LOGARITHMIC SCALE (0-1.00 0-1.00)

4 5 4 4 4 4 4 4  
4 3 4 4 4 4 4 4

1357913579135791357913579

MISSION RESEARCH CORPORATION  
URBAN FIRE MODEL  
PLOT SIMULATION TIME = 10790.0 SECONDS  
GRID 1 TO 100, COLUMNS 1 TO 100  
ONLY MAP: LETTERS A TO Z ARE A RANGE OF GRID VALUES  
ONLY EVERY OTHER CELL HAS AND COLUMN IS PLOTTED  
ONLY SCALE IS LOGARITHMIC SCALE (0-1.00 0-1.00)

4 4 4 4 4 4 4 4 4 4 4 4 4 4  
4 4 5 4 4 4 4 4 4 4 4 4 4 4

1357913579135791357913579

MISSION RESEARCH CORPORATION  
URBAN FIRE MODEL  
PLOT SIMULATION TIME = 5790.00 SECONDS  
GRID 1 TO 100, COLUMNS 1 TO 100  
ONLY MAP: LETTERS A TO Z ARE A RANGE OF GRID VALUES  
ONLY EVERY OTHER CELL HAS AND COLUMN IS PLOTTED  
ONLY SCALE IS LOGARITHMIC SCALE (0-1.00 0-1.00)

4 5 4 4 4 4 3 4 4 3 4 4 5  
4 4 3 4 4 4 4 4 3 4 4 4 5

1357913579135791357913579

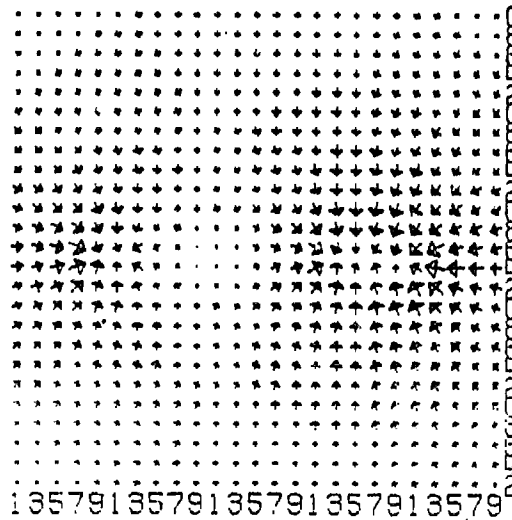
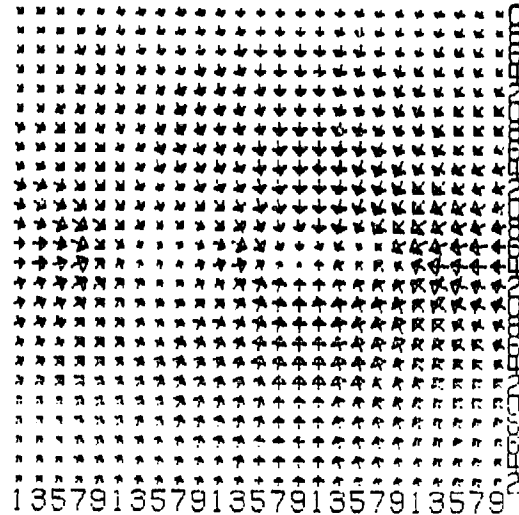
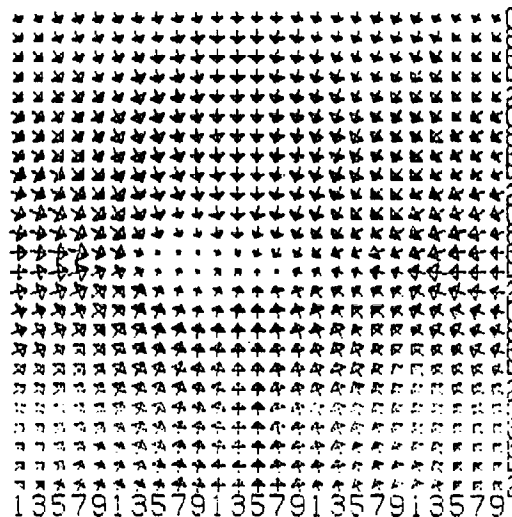
MISSION RESEARCH CORPORATION  
URBAN FIRE MODEL  
PLOT SIMULATION TIME = 20790.0 SECONDS  
GRID 1 TO 100, COLUMNS 1 TO 100  
ONLY MAP: LETTERS A TO Z ARE A RANGE OF GRID VALUES  
ONLY EVERY OTHER CELL HAS AND COLUMN IS PLOTTED  
ONLY SCALE IS LOGARITHMIC SCALE (0-1.00 0-1.00)

4 4 4 4 4 4 4 4 4 4 4 4 4 4  
4 4 4 4 4 3 4 4 4 4 4 4 4 4  
4 4 4 4 4 4 4 4 4 4 4 4 4 4

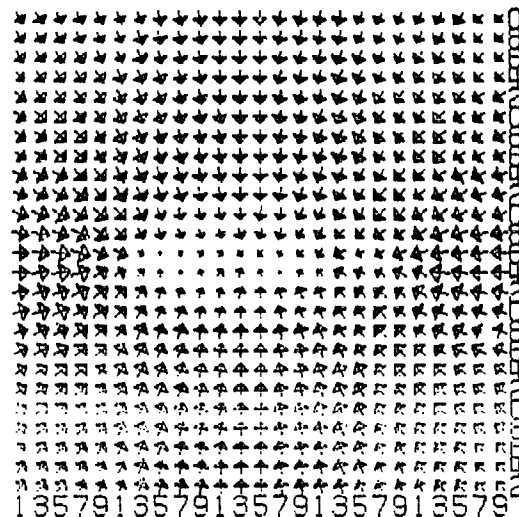
1357913579135791357913579

Figure 6-3(k). Cell heat production rate map for line fire.

BLAST EMULATION TIME = 1000.00 HOURS  
 0000 1 TO 00. 000000 1 TO 00.  
 WMA 0000 VELOCITY 000. 000000 000000 IN QUANTITY OF 0000.  
 000000 0000 0000 0000 0000 0000 0000 0000 0000 0000  
 0000 0000 0000 0000 0000 0000 0000 0000 0000 0000  
 000000 0000 VELOCITY 000000 000000 = 0.000000

[illegible][illegible]

PLAN RELEASED BY TIME = 0700.00 SOURCE  
0000 1 TO 01. COLUMN 1 TO 01.  
WILL SEND VELOCITY AND RANGE DATA IN DEPENDENT OF 0000.  
0000 0100 14 00000000 14 00 00000000  
ONLY 0000 OTHER CALL AND 0000 0000 0000 0000  
00000000 0000 VELOCITY 00000000 = 11.0000



**Figure 6-3(1). Wind velocity map for line fire.**

[illegible]

1	2	3	4	5	6	7	8	9	10	11	12	13	14	15	16	17	18	19	20	21	22	23	24	25	26	27	28	29	30	31	32	33	34	35	36	37	38	39	40	41	42	43	44	45	46	47	48	49	50	51	52	53	54	55	56	57	58	59	60	61	62	63	64	65	66	67	68	69	70	71	72	73	74	75	76	77	78	79	80	81	82	83	84	85	86	87	88	89	90	91	92	93	94	95	96	97	98	99	100
---	---	---	---	---	---	---	---	---	----	----	----	----	----	----	----	----	----	----	----	----	----	----	----	----	----	----	----	----	----	----	----	----	----	----	----	----	----	----	----	----	----	----	----	----	----	----	----	----	----	----	----	----	----	----	----	----	----	----	----	----	----	----	----	----	----	----	----	----	----	----	----	----	----	----	----	----	----	----	----	----	----	----	----	----	----	----	----	----	----	----	----	----	----	----	----	----	----	----	-----

[illegible]

1	2	3	4	5	6	7	8	9	10	11	12	13	14	15	16	17	18	19	20	21	22	23	24	25	26	27	28	29	30	31	32	33	34	35	36	37	38	39	40	41	42	43	44	45	46	47	48	49	50	51	52	53	54	55	56	57	58	59	60	61	62	63	64	65	66	67	68	69	70	71	72	73	74	75	76	77	78	79	80	81	82	83	84	85	86	87	88	89	90	91	92	93	94	95	96	97	98	99	100
1	2	3	4	5	6	7	8	9	10	11	12	13	14	15	16	17	18	19	20	21	22	23	24	25	26	27	28	29	30	31	32	33	34	35	36	37	38	39	40	41	42	43	44	45	46	47	48	49	50	51	52	53	54	55	56	57	58	59	60	61	62	63	64	65	66	67	68	69	70	71	72	73	74	75	76	77	78	79	80	81	82	83	84	85	86	87	88	89	90	91	92	93	94	95	96	97	98	99	100
1	2	3	4	5	6	7	8	9	10	11	12	13	14	15	16	17	18	19	20	21	22	23	24	25	26	27	28	29	30	31	32	33	34	35	36	37	38	39	40	41	42	43	44	45	46	47	48	49	50	51	52	53	54	55	56	57	58	59	60	61	62	63	64	65	66	67	68	69	70	71	72	73	74	75	76	77	78	79	80	81	82	83	84	85	86	87	88	89	90	91	92	93	94	95	96	97	98	99	100
1	2	3	4	5	6	7	8	9	10	11	12	13	14	15	16	17	18	19	20	21	22	23	24	25	26	27	28	29	30	31	32	33	34	35	36	37	38	39	40	41	42	43	44	45	46	47	48	49	50	51	52	53	54	55	56	57	58	59	60	61	62	63	64	65	66	67	68	69	70	71	72	73	74	75	76	77	78	79	80	81	82	83	84	85	86	87	88	89	90	91	92	93	94	95	96	97	98	99	100
1	2	3	4	5	6	7	8	9	10	11	12	13	14	15	16	17	18	19	20	21	22	23	24	25	26	27	28	29	30	31	32	33	34	35	36	37	38	39	40	41	42	43	44	45	46	47	48	49	50	51	52	53	54	55	56	57	58	59	60	61	62	63	64	65	66	67	68	69	70	71	72	73	74	75	76	77	78	79	80	81	82	83	84	85	86	87	88	89	90	91	92	93	94	95	96	97	98	99	100
1	2	3	4	5	6	7	8	9	10	11	12	13	14	15	16	17	18	19	20	21	22	23	24	25	26	27	28	29	30	31	32	33	34	35	36	37	38	39	40	41	42	43	44	45	46	47	48	49	50	51	52	53	54	55	56	57	58	59	60	61	62	63	64	65	66	67	68	69	70	71	72	73	74	75	76	77	78	79	80	81	82	83	84	85	86	87	8												

207

#### 6.4 LINE FIRE WITH 10 M/SEC AMBIENT WIND

The ignition geometry is the same as for case 6.3; however, the location of the candidate cells was moved to the lower left corner. This was done so that the fire would have room to propagate along the wind direction from the lower left corner to the upper right corner. Figures 6-4 to 6-4(g) show that the fire propagates much more rapidly than in Case 6.3 and that the propagation is along the wind stream lines. Comparison of the wind maps for Cases 6.3 and 6.4 shows that the ratio of the fire induced to the ambient winds is such that the 10 m/s ambient winds would be expected to cause the fire to burn significantly differently than in the case with no ambient wind.



```

PLOT SIMULATION TIME = 1000.00 SECONDS
ROWS 1 TO 50, COLUMNS 1 TO 50.
ROW 50
ROW 49
ROW 48
ROW 47
ROW 46
ROW 45
ROW 44
ROW 43
ROW 42
ROW 41
ROW 40
ROW 39
ROW 38
ROW 37
ROW 36
ROW 35
ROW 34
ROW 33
ROW 32
ROW 31
ROW 30
ROW 29
ROW 28
ROW 27
ROW 26
ROW 25
ROW 24
ROW 23
ROW 22
ROW 21
ROW 20
ROW 19
ROW 18
ROW 17
ROW 16
ROW 15
ROW 14
ROW 13
ROW 12
ROW 11
ROW 10
ROW 9
ROW 8
ROW 7
ROW 6
ROW 5
ROW 4
ROW 3
ROW 2
ROW 1

```

```

COLUMNS 12345678901234567890123456789012345678901234567890
NUMBER OF UNIGNITED, BURNING AND BURNED-OUT CELLS = 2485 15

```

Figure 6-4. Cell state map for line fire with .10 m/s ambient wind.

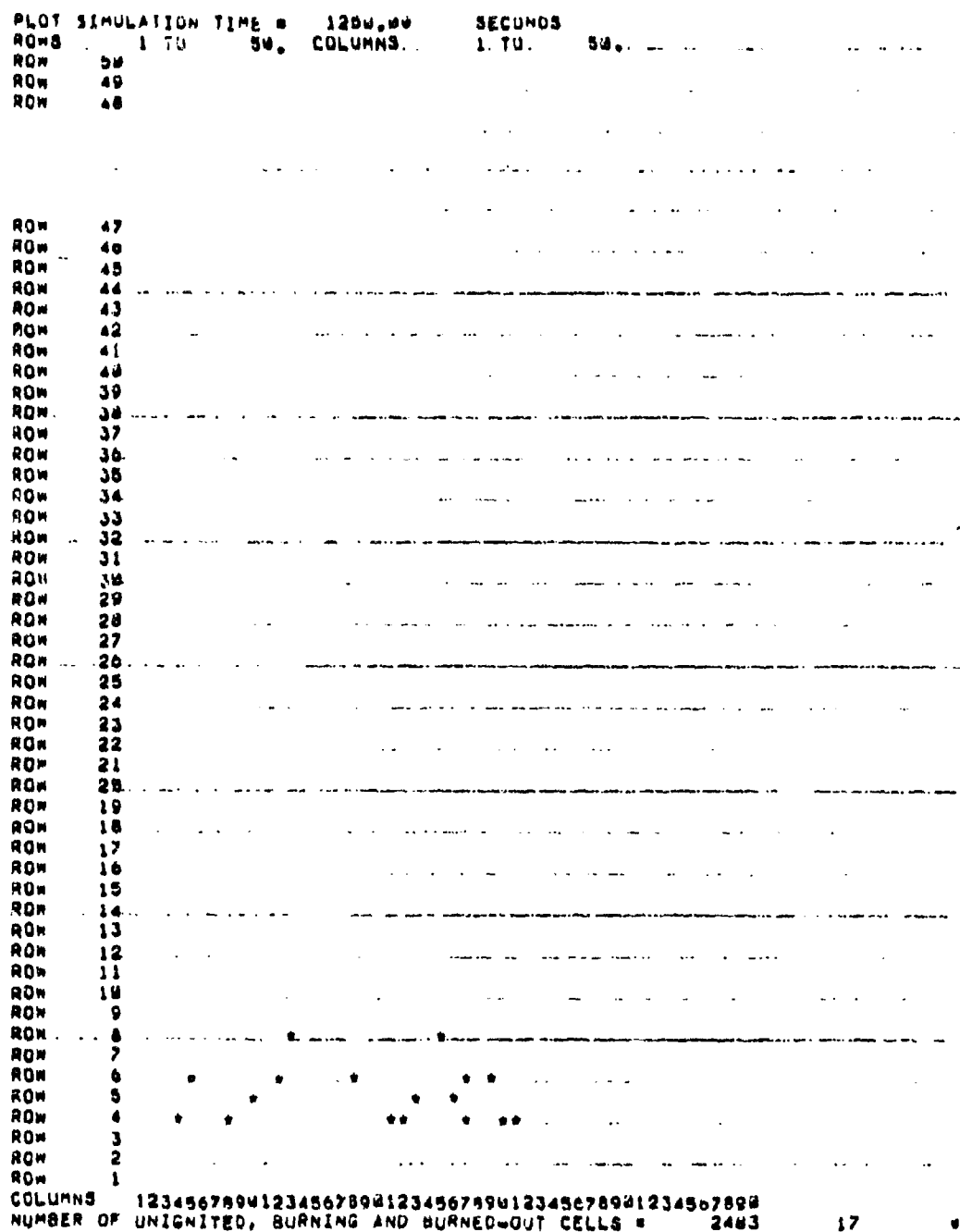


Figure 6-4(a). Cell state map for line fire with .10 m/s ambient wind.



PLOT SIMULATION TIME = 2750.00 SECONDS  
 ROWS 1 TO 50, COLUMNS 1 TO 50.

ROW	50
ROW	49
ROW	48
ROW	47
ROW	46
ROW	45
ROW	44
ROW	43
ROW	42
ROW	41
ROW	40
ROW	39
ROW	38
ROW	37
ROW	36
ROW	35
ROW	34
ROW	33
ROW	32
ROW	31
ROW	30
ROW	29
ROW	28
ROW	27
ROW	26
ROW	25
ROW	24
ROW	23
ROW	22
ROW	21
ROW	20
ROW	19
ROW	18
ROW	17
ROW	16
ROW	15
ROW	14
ROW	13
ROW	12
ROW	11
ROW	10
ROW	9
ROW	8
ROW	7
ROW	6
ROW	5
ROW	4
ROW	3
ROW	2
ROW	1

COLUMNS 1234567890123456789012345678901234567890  
 NUMBER OF UNIGNITED, BURNING AND BURNED-OUT CELLS = 2400 34

Figure 6-4(c). Cell state map for line fire with .10 m/s ambient wind.

NUMBER OF UNIGNITED, BURNING AND BURIED-OUT CELLS • 2400 3-

PLOT SIMULATION TIME • 4785.00 SECONDS

ROWS 1 TO 50, COLUMNS 1 TO 50.

ROW 50  
ROW 49  
ROW 48  
ROW 47  
ROW 46  
ROW 45  
ROW 44  
ROW 43  
ROW 42  
ROW 41  
ROW 40  
ROW 39  
ROW 38  
ROW 37  
ROW 36  
ROW 35  
ROW 34  
ROW 33  
ROW 32  
ROW 31  
ROW 30

ROW 29  
ROW 28  
ROW 27  
ROW 26  
ROW 25  
ROW 24  
ROW 23  
ROW 22  
ROW 21  
ROW 20  
ROW 19  
ROW 18  
ROW 17  
ROW 16  
ROW 15  
ROW 14  
ROW 13  
ROW 12  
ROW 11  
ROW 10  
ROW 9  
ROW 8  
ROW 7  
ROW 6  
ROW 5  
ROW 4  
ROW 3  
ROW 2  
ROW 1

COLUMNS 1234567890123456789012345678901234567890

NUMBER OF UNIGNITED, BURNING AND BURIED-OUT CELLS • 2422 78

Figure 6-4(d). Cell state map for line fire with .10 m/s ambient wind.

Figure 6-4(e). Cell state map for line fire with .10 m/s ambient wind.

PLOT SIMULATION TIME • 10750.0 SECONDS  
 ROWS 1 TO 50, COLUMNS 1 TO 50

ROW 50  
 ROW 49  
 ROW 48  
 ROW 47  
 ROW 46  
 ROW 45  
 ROW 44  
 ROW 43  
 ROW 42  
 ROW 41  
 ROW 40  
 ROW 39  
 ROW 38  
 ROW 37  
 ROW 36  
 ROW 35  
 ROW 34  
 ROW 33  
 ROW 32  
 ROW 31  
 ROW 30  
 ROW 29  
 ROW 28  
 ROW 27  
 ROW 26  
 ROW 25  
 ROW 24  
 ROW 23  
 ROW 22  
 ROW 21  
 ROW 20  
 ROW 19  
 ROW 18

ROW 17  
 ROW 16  
 ROW 15  
 ROW 14  
 ROW 13  
 ROW 12  
 ROW 11  
 ROW 10  
 ROW 9  
 ROW 8  
 ROW 7  
 ROW 6  
 ROW 5  
 ROW 4  
 ROW 3  
 ROW 2  
 ROW 1

COLUMNS 12345678901234567890123456789012345678901234567890  
 NUMBER OF UNIGNITED, BURNING AND BURNED-OUT CELLS • 2282 218 0

Figure 6-4(f). Cell state map for line fire with .10 m/s ambient wind.



Figure 6-4(g). Cell state map for line fire with .10 m/s ambient wind.



MISSION RESEARCH CORPORATION  
URBAN FIRE MODEL  
PLAY SIMULATION TIME = 0000.00 SECONDS  
STEP 1 TO 99. RELEASE 1 TO 99  
CELL NOT OUTSIDE 99  
\*\*\* ONLY EVERY OTHER CELL AND RELEASE IS PLAYED \*\*\*  
BEST SCALE IS LOGARITHMIC SCALE (0-1.00 0-1.00)



1357913579135791357913579

MISSION RESEARCH CORPORATION  
URBAN FIRE MODEL  
PLAY SIMULATION TIME = 0700.00 SECONDS  
STEP 1 TO 99. RELEASE 1 TO 99  
CELL NOT OUTSIDE 99  
\*\*\* ONLY EVERY OTHER CELL AND RELEASE IS PLAYED \*\*\*  
BEST SCALE IS LOGARITHMIC SCALE (0-1.00 0-1.00)



1357913579135791357913579

MISSION RESEARCH CORPORATION  
URBAN FIRE MODEL  
PLAY SIMULATION TIME = 0000.00 SECONDS  
STEP 1 TO 99. RELEASE 1 TO 99  
CELL NOT OUTSIDE 99  
\*\*\* ONLY EVERY OTHER CELL AND RELEASE IS PLAYED \*\*\*  
BEST SCALE IS LOGARITHMIC SCALE (0-1.00 0-1.00)



1357913579135791357913579

MISSION RESEARCH CORPORATION  
URBAN FIRE MODEL  
PLAY SIMULATION TIME = 0700.00 SECONDS  
STEP 1 TO 99. RELEASE 1 TO 99  
CELL NOT OUTSIDE 99  
\*\*\* ONLY EVERY OTHER CELL AND RELEASE IS PLAYED \*\*\*  
BEST SCALE IS LOGARITHMIC SCALE (0-1.00 0-1.00)



1357913579135791357913579

Figure 6-4(h). Heat production rate contour map for line fire with .10 m/s ambient wind.

MISSION PERFORMANCE COMPARISON  
 URBAN FIRE MODEL  
 PLOT SIMULATION TIME = 4750.0 SECONDS  
 CASE 1 TO 1000 1 TO 1000  
 CASE 1001 TO 2000 1 TO 1000  
 \*\*\* ONLY EVERY OTHER CELL AND SHOWN IS PLOTTED \*\*\*  
 MAP SCALE IS LOGARITHMIC (0-1.00 0-1.00)



1357913579135791357913579

MISSION PERFORMANCE COMPARISON  
 URBAN FIRE MODEL  
 PLOT SIMULATION TIME = 10750.0 SECONDS  
 CASE 1 TO 1000 1 TO 1000  
 CASE 1001 TO 2000 1 TO 1000  
 \*\*\* ONLY EVERY OTHER CELL AND SHOWN IS PLOTTED \*\*\*  
 MAP SCALE IS LOGARITHMIC (0-1.00 0-1.00)



1357913579135791357913579

MISSION PERFORMANCE COMPARISON  
 URBAN FIRE MODEL  
 PLOT SIMULATION TIME = 4750.0 SECONDS  
 CASE 1 TO 1000 1 TO 1000  
 CASE 1001 TO 2000 1 TO 1000  
 \*\*\* ONLY EVERY OTHER CELL AND SHOWN IS PLOTTED \*\*\*  
 MAP SCALE IS LOGARITHMIC (0-1.00 0-1.00)



1357913579135791357913579

MISSION PERFORMANCE COMPARISON  
 URBAN FIRE MODEL  
 PLOT SIMULATION TIME = 10750.0 SECONDS  
 CASE 1 TO 1000 1 TO 1000  
 CASE 1001 TO 2000 1 TO 1000  
 \*\*\* ONLY EVERY OTHER CELL AND SHOWN IS PLOTTED \*\*\*  
 MAP SCALE IS LOGARITHMIC (0-1.00 0-1.00)



1357913579135791357913579

Figure 6-4(1). Heat production rate contour map for line fire with .10 m/s ambient wind.

MISSION RESEARCH CORPORATION  
URBAN FIRE MODEL  
PLOT RELEASES OF TIME = 0000.00  
ROWS 1 TO 60, COLUMNS 1 TO 60  
ONLY HOT LETTERS A TO Z ARE A PART OF HOT PLACES  
ONLY HOT LETTERS A TO Z ARE A PART OF HOT PLACES  
ONLY HOT LETTERS A TO Z ARE A PART OF HOT PLACES  
ONLY HOT LETTERS A TO Z ARE A PART OF HOT PLACES

2 3 3 2  
3 3 2  
1357913579135791357913579

MISSION RESEARCH CORPORATION  
URBAN FIRE MODEL  
PLOT RELEASES OF TIME = 1700.00  
ROWS 1 TO 60, COLUMNS 1 TO 60  
ONLY HOT LETTERS A TO Z ARE A PART OF HOT PLACES  
ONLY HOT LETTERS A TO Z ARE A PART OF HOT PLACES  
ONLY HOT LETTERS A TO Z ARE A PART OF HOT PLACES  
ONLY HOT LETTERS A TO Z ARE A PART OF HOT PLACES

3 3 3 3 3 3  
4 4 3  
1357913579135791357913579

MISSION RESEARCH CORPORATION  
URBAN FIRE MODEL  
PLOT RELEASES OF TIME = 0000.00  
ROWS 1 TO 60, COLUMNS 1 TO 60  
ONLY HOT LETTERS A TO Z ARE A PART OF HOT PLACES  
ONLY HOT LETTERS A TO Z ARE A PART OF HOT PLACES  
ONLY HOT LETTERS A TO Z ARE A PART OF HOT PLACES  
ONLY HOT LETTERS A TO Z ARE A PART OF HOT PLACES

3 2 2 3 3 3  
3 3 3 3  
1357913579135791357913579

MISSION RESEARCH CORPORATION  
URBAN FIRE MODEL  
PLOT RELEASES OF TIME = 0700.00  
ROWS 1 TO 60, COLUMNS 1 TO 60  
ONLY HOT LETTERS A TO Z ARE A PART OF HOT PLACES  
ONLY HOT LETTERS A TO Z ARE A PART OF HOT PLACES  
ONLY HOT LETTERS A TO Z ARE A PART OF HOT PLACES  
ONLY HOT LETTERS A TO Z ARE A PART OF HOT PLACES

4 3 4 3 3 3 4 3  
4 4 4 4  
1357913579135791357913579

Figure 6-4(j). Cell heat production rate map for line fire with .10 m/s ambient wind.

MISSION RESEARCH CORPORATION  
URBAN FIRE MODEL  
PLAY SIMULATION TIME = 00:00:00  
TIME 1 TO 24 HOURS 1 TO 24 HOURS  
SHOT MAP: LETTERS A TO Z ARE A SCALE OF SHOT VALUES  
NOTE: ONLY SHOT VALUES ARE SHOWN IN PLAYERS AREA  
SHOT SCALE IS LOGARITHMIC SCALE (0 = 1.00 9 = 1.019)

42 44 3  
3 4 3 4 3  
4 4 4 4 3  
1357913579135791357913579

MISSION RESEARCH CORPORATION  
URBAN FIRE MODEL  
PLAY SIMULATION TIME = 00:00:00  
TIME 1 TO 24 HOURS 1 TO 24 HOURS  
SHOT MAP: LETTERS A TO Z ARE A SCALE OF SHOT VALUES  
NOTE: ONLY SHOT VALUES ARE SHOWN IN PLAYERS AREA  
SHOT SCALE IS LOGARITHMIC SCALE (0 = 1.00 9 = 1.019)

4 4 3  
3 4 4 4 3  
4 4 4 4 3  
4 4 4 4 3  
1357913579135791357913579

MISSION RESEARCH CORPORATION  
URBAN FIRE MODEL  
PLAY SIMULATION TIME = 00:00:00  
TIME 1 TO 24 HOURS 1 TO 24 HOURS  
SHOT MAP: LETTERS A TO Z ARE A SCALE OF SHOT VALUES  
NOTE: ONLY SHOT VALUES ARE SHOWN IN PLAYERS AREA  
SHOT SCALE IS LOGARITHMIC SCALE (0 = 1.00 9 = 1.019)

4 4 4 4 3 4 3 3  
4 4 4 4 4 4 4 4 4  
4 4 4 4 4 4 4 4 4  
4 4 4 4 4 4 4 4 4  
1357913579135791357913579

MISSION RESEARCH CORPORATION  
URBAN FIRE MODEL  
PLAY SIMULATION TIME = 00:00:00  
TIME 1 TO 24 HOURS 1 TO 24 HOURS  
SHOT MAP: LETTERS A TO Z ARE A SCALE OF SHOT VALUES  
NOTE: ONLY SHOT VALUES ARE SHOWN IN PLAYERS AREA  
SHOT SCALE IS LOGARITHMIC SCALE (0 = 1.00 9 = 1.019)

4 4 4 4 4 4 4 4 4  
4 4 4 4 4 4 4 4 4  
4 4 4 4 4 4 4 4 4  
4 4 4 4 4 4 4 4 4  
1357913579135791357913579

Figure 6-4(k). Cell heat production rate map for line fire with .10 m/s ambient wind.



[illegible][illegible]

222

## 6.5 RING FIRE WITH NO AMBIENT WIND

As shown in Figure 6-5, a four-cell wide annulus, 42 cells in diameter, was initially ignited with a probability of ignition of 0.5. There was no initial wind velocity; however, strong, inward-directed fire induced winds resulted in heavy branding and contagion in the interior of the annulus. It is clear in all of the cases that fire spread is much too rapid. However, this is graphically shown by the marked increase in the number of ignited cells in the 1000 seconds (from 1750 to 2750 seconds), as shown in Figures 6-5(b) and 6-5(c). The "tails" shown in Figures 6-5(d) through 6-5(g) are artifacts of the erroneous branding process described in Case 6.1.

PLOT SIMULATION TIME = 1440.00 SECONDS	
ROWS	COLUMNS
1 TO 50	1 TO 50
ROW 50	
ROW 49	
ROW 48	
ROW 47	
ROW 46	
ROW 45	
ROW 44	
ROW 43	
ROW 42	
ROW 41	
ROW 40	
ROW 39	
ROW 38	
ROW 37	
ROW 36	
ROW 35	
ROW 34	
ROW 33	
ROW 32	
ROW 31	
ROW 30	
ROW 29	
ROW 28	
ROW 27	
ROW 26	
ROW 25	
ROW 24	
ROW 23	
ROW 22	
ROW 21	
ROW 20	
ROW 19	
ROW 18	
ROW 17	
ROW 16	
ROW 15	
ROW 14	
ROW 13	
ROW 12	
ROW 11	
ROW 10	
ROW 9	
ROW 8	
ROW 7	
ROW 6	
ROW 5	
ROW 4	
ROW 3	
ROW 2	
ROW 1	

COLUMNS 12345678901234567890123456789012345678901234567890  
 NUMBER OF UNIGNITED, BURNING AND BURNED-OUT CELLS = 2363 137

Figure 6-5. Cell state map for ring fire.



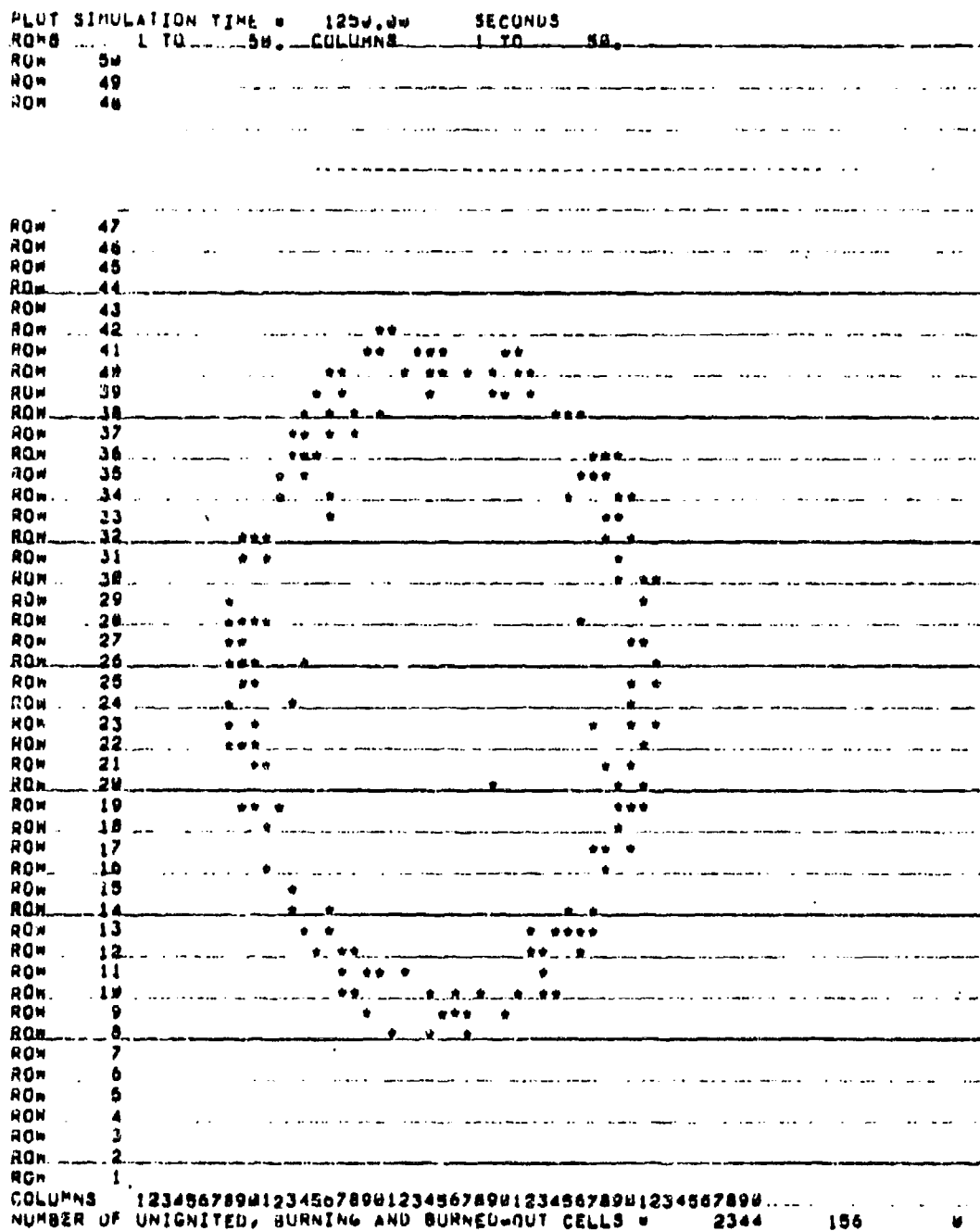


Figure 6-5(a). Cell state map for ring fire.

```

PLUT SIMULATION TIME 1700.00 SECONDS
ROWS 1 TO 50 COLUMNS 1 TO 50
ROW 49
ROW 48
ROW 47
ROW 46
ROW 45
ROW 44
ROW 43
ROW 42

ROW 41
ROW 40
ROW 39
ROW 38
ROW 37
ROW 36
ROW 35
ROW 34
ROW 33
ROW 32
ROW 31
ROW 30
ROW 29
ROW 28
ROW 27
ROW 26
ROW 25
ROW 24
ROW 23
ROW 22
ROW 21
ROW 20
ROW 19
ROW 18
ROW 17
ROW 16
ROW 15
ROW 14
ROW 13
ROW 12
ROW 11
ROW 10
ROW 9
ROW 8
ROW 7
ROW 6
ROW 5
ROW 4
ROW 3
ROW 2
ROW 1
COLUMNS 12345678901234567890123456789012345678901234567890
NUMBER OF UNIGNITED, BURNING AND BURNED-OUT CELLS 2150 350 0

```

Figure 6-5(b). Cell state map for ring fire.

```

PLOT SIMULATION TIME = 2700.00 SECONDS
ROWS 1 TO 50 COLUMNS 1 TO 50
ROW 50
ROW 49
ROW 48
ROW 47
ROW 46
ROW 45
ROW 44
ROW 43
ROW 42
ROW 41
ROW 40
ROW 39
ROW 38
ROW 37
ROW 36

```

```

ROW 35
ROW 34
ROW 33
ROW 32
ROW 31
ROW 30
ROW 29
ROW 28
ROW 27
ROW 26
ROW 25
ROW 24
ROW 23
ROW 22
ROW 21
ROW 20
ROW 19
ROW 18
ROW 17
ROW 16
ROW 15
ROW 14
ROW 13
ROW 12
ROW 11
ROW 10
ROW 9
ROW 8
ROW 7
ROW 6
ROW 5
ROW 4
ROW 3
ROW 2
ROW 1
COLUMNS 12345678901234567890123456789012345678901234567890
NUMBER OF UNIGNITED, BURNING AND BURNED-OUT CELLS = 1727 773

```

Figure 6-5(c). Cell state map for ring fire.



```

PLOT SIMULATION TIME = 8750.00 SECONDS
ROWS 1 TO 50 COLUMNS 1 TO 50
ROW 50
ROW 49
ROW 48
ROW 47
ROW 46
ROW 45
ROW 44
ROW 43
ROW 42
ROW 41
ROW 40
ROW 39
ROW 38
ROW 37
ROW 36
ROW 35
ROW 34
ROW 33
ROW 32
ROW 31
ROW 30
ROW 29
ROW 28
ROW 27
ROW 26
ROW 25
ROW 24

ROW 23
ROW 22
ROW 21
ROW 20
ROW 19
ROW 18
ROW 17
ROW 16
ROW 15
ROW 14
ROW 13
ROW 12
ROW 11
ROW 10
ROW 9
ROW 8
ROW 7
ROW 6
ROW 5
ROW 4
ROW 3
ROW 2
ROW 1
COLUMNS 12345678901234567890123456789012345678901234567890
NUMBER OF UNIGNITED, BURNING AND BURNED-OUT CELLS = 1558 942

```

Figure 6-5(e). Cell state map for ring fire.

NUMBER OF UNIGNITED, BURNING AND BURNED-OUT CELLS = 1558 942

PLOT SIMULATION TIME = 10750.0 SECONDS  
 ROWS 1 TO 50 COLUMNS 1 TO 50

ROW	50	
ROW	49	*
ROW	48	**
ROW	47	***
ROW	46	****
ROW	45	*****
ROW	44	*****
ROW	43	*****
ROW	42	*****
ROW	41	*****
ROW	40	*****
ROW	39	*****
ROW	38	*****
ROW	37	*****
ROW	36	*****
ROW	35	*****
ROW	34	*****
ROW	33	*****
ROW	32	*****
ROW	31	*****
ROW	30	*****
ROW	29	*****
ROW	28	*****
ROW	27	*****
ROW	26	*****
ROW	25	*****
ROW	24	*****
ROW	23	*****
ROW	22	*****
ROW	21	*****
ROW	20	*****
ROW	19	*****
ROW	18	*****

ROW	17	*****
ROW	16	*****
ROW	15	*****
ROW	14	*****
ROW	13	*****
ROW	12	*****
ROW	11	*****
ROW	10	*****
ROW	9	*****
ROW	8	*****
ROW	7	*****
ROW	6	*****
ROW	5	*****
ROW	4	*****
ROW	3	*****
ROW	2	*****
ROW	1	*****

COLUMNS 12345678901234567890123456789012345678901234567890  
 NUMBER OF UNIGNITED, BURNING AND BURNED-OUT CELLS = 1528 970

Figure 6-5(f). Cell state map for ring fire.

```

FUEL SIMULATION TIME = 32750.0 SECONDS
ROWS = 1 TO 50, COLUMNS = 1 TO 50.
ROW 50
ROW 49
ROW 48
ROW 47
ROW 46
ROW 45
ROW 44
ROW 43
ROW 42
ROW 41
ROW 40
ROW 39
ROW 38
ROW 37
ROW 36
ROW 35
ROW 34
ROW 33
ROW 32
ROW 31
ROW 30
ROW 29
ROW 28
ROW 27
ROW 26
ROW 25
ROW 24
ROW 23
ROW 22
ROW 21
ROW 20
ROW 19
ROW 18
ROW 17
ROW 16
ROW 15
ROW 14
ROW 13
ROW 12

ROW 11
ROW 10
ROW 9
ROW 8
ROW 7
ROW 6
ROW 5
ROW 4
ROW 3
ROW 2
ROW 1
COLUMNS 12345678901234567890123456789012345678901234567890
NUMBER OF UNIGNITED, BURNING AND BURNED-OUT CELLS = 1490 934 75

```

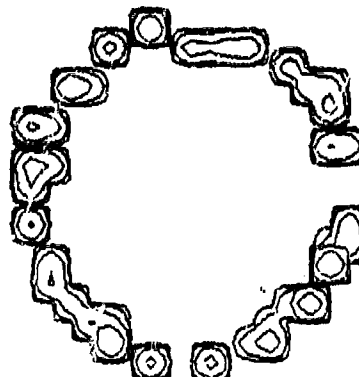
Figure 6-5(g). Cell state map for ring fire.

HYDRO RESEARCH CORPORATION  
 OPEN FIRE MODEL  
 PLAC RELEASES BY TIME = 0000.00  
 1 TO 1000.00  
 1 TO 1000.00  
 ALL DATA COVERED BY  
 \*\*\* ONLY DATA OTHER THAN RELEASE IS PLOTTED \*\*\*  
 UNIT SCALE (IS LOGARITHMIC) 10 (0-1.00 0-1.010)



1357913579135791357913579

HYDRO RESEARCH CORPORATION  
 OPEN FIRE MODEL  
 PLAC RELEASES BY TIME = 0000.00  
 1 TO 1000.00  
 1 TO 1000.00  
 ALL DATA COVERED BY  
 \*\*\* ONLY DATA OTHER THAN RELEASE IS PLOTTED \*\*\*  
 UNIT SCALE (IS LOGARITHMIC) 10 (0-1.00 0-1.010)



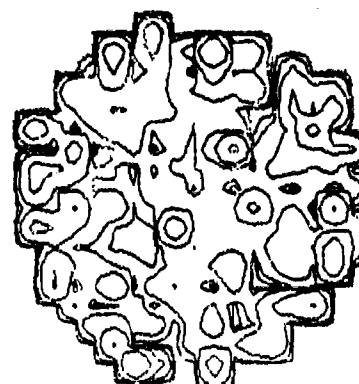
1357913579135791357913579

HYDRO RESEARCH CORPORATION  
 OPEN FIRE MODEL  
 PLAC RELEASES BY TIME = 0000.00  
 1 TO 1000.00  
 1 TO 1000.00  
 ALL DATA COVERED BY  
 \*\*\* ONLY DATA OTHER THAN RELEASE IS PLOTTED \*\*\*  
 UNIT SCALE (IS LOGARITHMIC) 10 (0-1.00 0-1.010)



1357913579135791357913579

HYDRO RESEARCH CORPORATION  
 OPEN FIRE MODEL  
 PLAC RELEASES BY TIME = 0000.00  
 1 TO 1000.00  
 1 TO 1000.00  
 ALL DATA COVERED BY  
 \*\*\* ONLY DATA OTHER THAN RELEASE IS PLOTTED \*\*\*  
 UNIT SCALE (IS LOGARITHMIC) 10 (0-1.00 0-1.010)

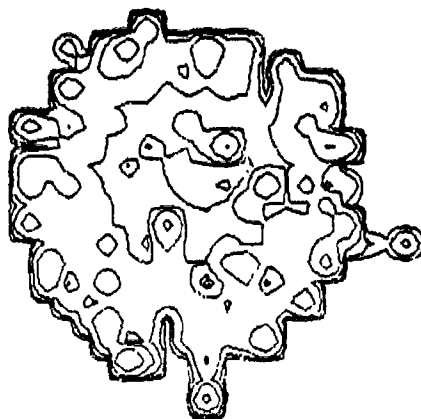


1357913579135791357913579

Figure 6-5(h). Heat production rate contour map for ring fire.

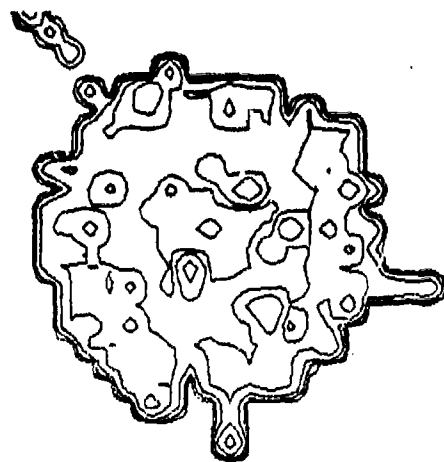


HEWLETT PACKARD CORPORATION  
UNIFORM FIRE MODEL  
PLAY SCENARIO ON TIME = 4000.00  
TIME 1 TO 1000.00 1 TO 1000.00  
ALL DATA POINTS ARE  
\*\*\* ONLY DATA POINTS ARE AND ARE PLOTTED \*\*\*  
GRID SCALE IS LOGARITHMIC (BASE 10) (0-1.00 0-1.010)



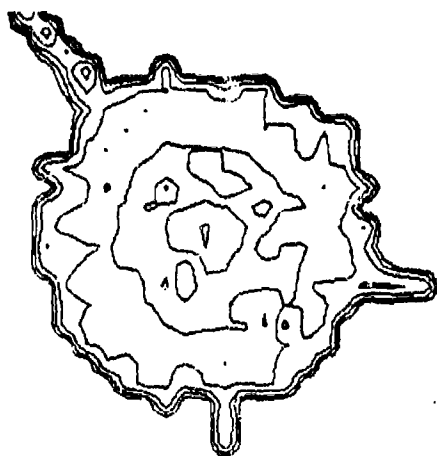
1357913579135791357913579

HEWLETT PACKARD CORPORATION  
UNIFORM FIRE MODEL  
PLAY SCENARIO ON TIME = 4000.00  
TIME 1 TO 1000.00 1 TO 1000.00  
ALL DATA POINTS ARE  
\*\*\* ONLY DATA POINTS ARE AND ARE PLOTTED \*\*\*  
GRID SCALE IS LOGARITHMIC (BASE 10) (0-1.00 0-1.010)



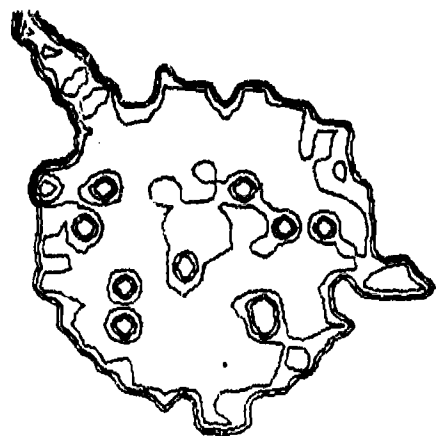
1357913579135791357913579

HEWLETT PACKARD CORPORATION  
UNIFORM FIRE MODEL  
PLAY SCENARIO ON TIME = 4000.00  
TIME 1 TO 1000.00 1 TO 1000.00  
ALL DATA POINTS ARE  
\*\*\* ONLY DATA POINTS ARE AND ARE PLOTTED \*\*\*  
GRID SCALE IS LOGARITHMIC (BASE 10) (0-1.00 0-1.010)



1357913579135791357913579

HEWLETT PACKARD CORPORATION  
UNIFORM FIRE MODEL  
PLAY SCENARIO ON TIME = 4000.00  
TIME 1 TO 1000.00 1 TO 1000.00  
ALL DATA POINTS ARE  
\*\*\* ONLY DATA POINTS ARE AND ARE PLOTTED \*\*\*  
GRID SCALE IS LOGARITHMIC (BASE 10) (0-1.00 0-1.010)



1357913579135791357913579

Figure 6-5(1). Heat production rate contour map for ring fire.



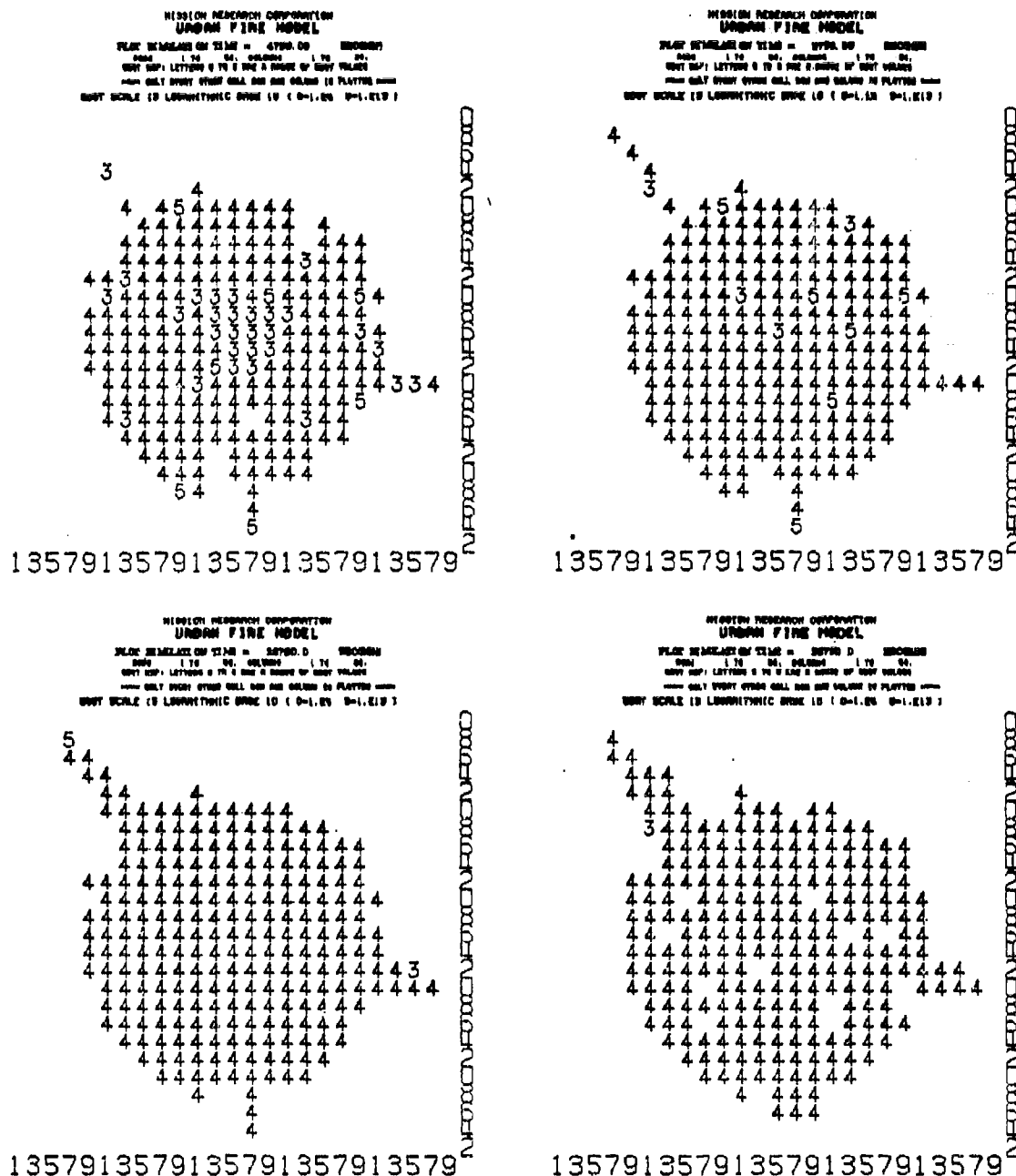


Figure 6-5(k). Cell heat production rate map for ring fire.

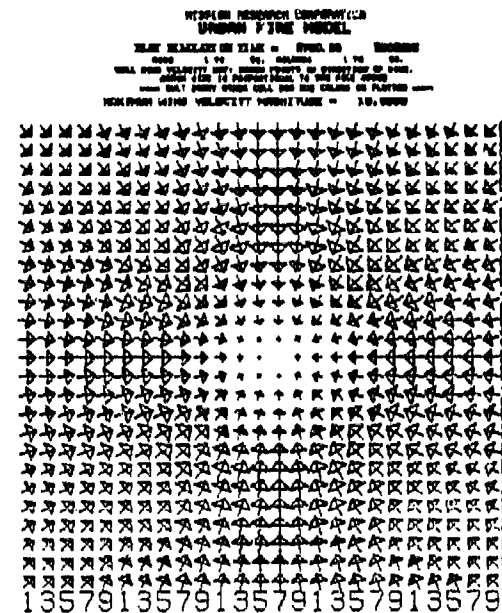
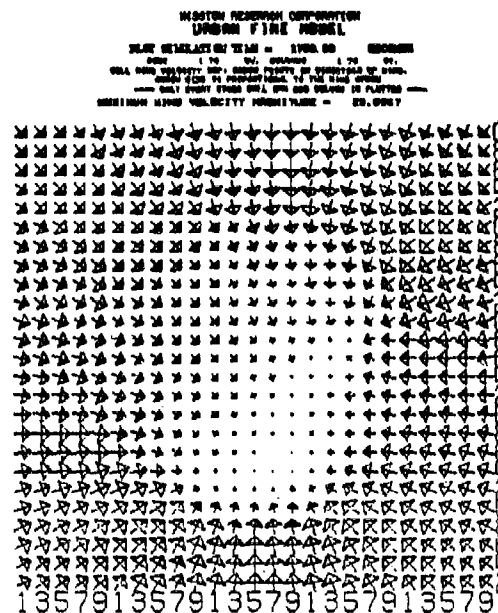
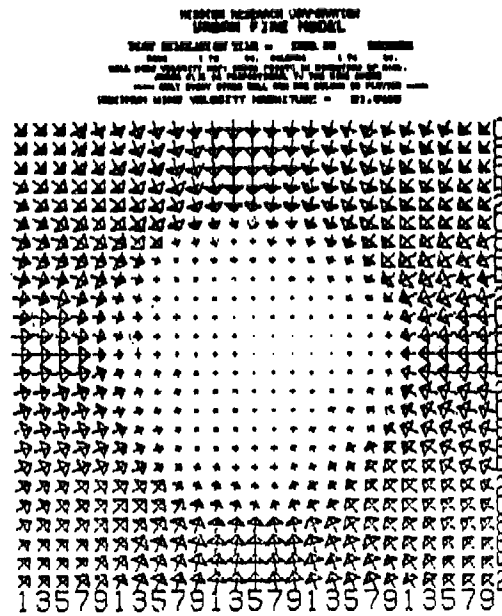
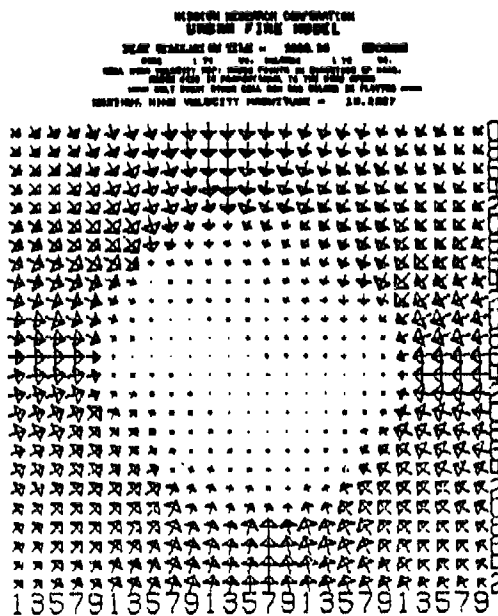
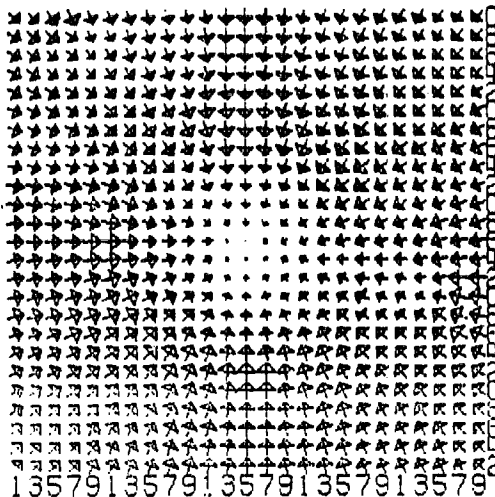
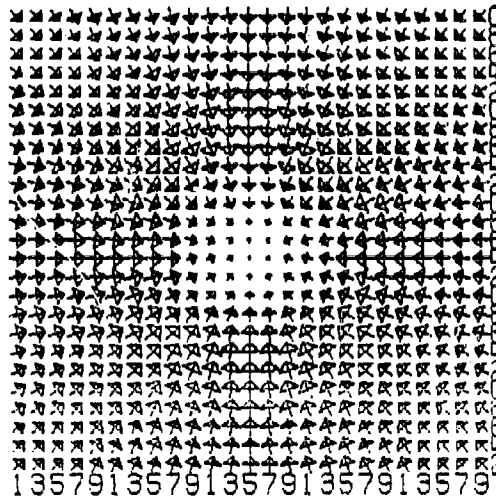


Figure 6-5(1). Wind velocity map for ring fire.

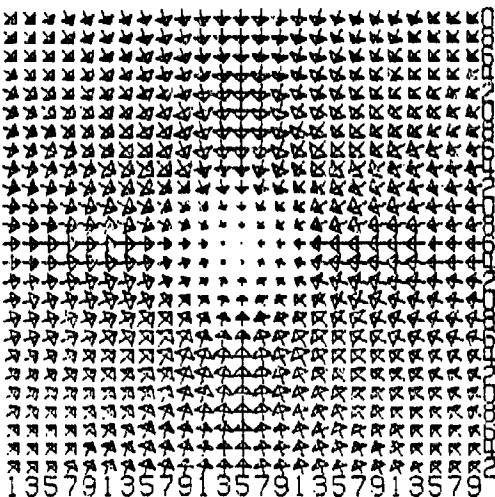
MISSION RESEARCH CORPORATION  
UNIFORM FIRE MODEL  
PLAT RELEASED AT TIME = 4700.00  
SPEED 1 TO 99.000000 1 TO 99.000000  
ALL DATA POINTS ARE IN THE PLATEAU OF THE  
PLATEAU OF THE PLATEAU OF THE PLATEAU OF THE  
PLATEAU OF THE PLATEAU OF THE PLATEAU OF THE  
MISSION RESEARCH CORPORATION  
UNIFORM FIRE MODEL  
PLAT RELEASED AT TIME = 4700.00  
SPEED 1 TO 99.000000 1 TO 99.000000  
ALL DATA POINTS ARE IN THE PLATEAU OF THE  
PLATEAU OF THE PLATEAU OF THE PLATEAU OF THE  
PLATEAU OF THE PLATEAU OF THE PLATEAU OF THE



MISSION RESEARCH CORPORATION  
UNIFORM FIRE MODEL  
PLAT RELEASED AT TIME = 4700.00  
SPEED 1 TO 99.000000 1 TO 99.000000  
ALL DATA POINTS ARE IN THE PLATEAU OF THE  
PLATEAU OF THE PLATEAU OF THE PLATEAU OF THE  
PLATEAU OF THE PLATEAU OF THE PLATEAU OF THE  
MISSION RESEARCH CORPORATION  
UNIFORM FIRE MODEL  
PLAT RELEASED AT TIME = 4700.00  
SPEED 1 TO 99.000000 1 TO 99.000000  
ALL DATA POINTS ARE IN THE PLATEAU OF THE  
PLATEAU OF THE PLATEAU OF THE PLATEAU OF THE  
PLATEAU OF THE PLATEAU OF THE PLATEAU OF THE



MISSION RESEARCH CORPORATION  
UNIFORM FIRE MODEL  
PLAT RELEASED AT TIME = 4700.00  
SPEED 1 TO 99.000000 1 TO 99.000000  
ALL DATA POINTS ARE IN THE PLATEAU OF THE  
PLATEAU OF THE PLATEAU OF THE PLATEAU OF THE  
PLATEAU OF THE PLATEAU OF THE PLATEAU OF THE  
MISSION RESEARCH CORPORATION  
UNIFORM FIRE MODEL  
PLAT RELEASED AT TIME = 4700.00  
SPEED 1 TO 99.000000 1 TO 99.000000  
ALL DATA POINTS ARE IN THE PLATEAU OF THE  
PLATEAU OF THE PLATEAU OF THE PLATEAU OF THE  
PLATEAU OF THE PLATEAU OF THE PLATEAU OF THE



MISSION RESEARCH CORPORATION  
UNIFORM FIRE MODEL  
PLAT RELEASED AT TIME = 4700.00  
SPEED 1 TO 99.000000 1 TO 99.000000  
ALL DATA POINTS ARE IN THE PLATEAU OF THE  
PLATEAU OF THE PLATEAU OF THE PLATEAU OF THE  
PLATEAU OF THE PLATEAU OF THE PLATEAU OF THE  
MISSION RESEARCH CORPORATION  
UNIFORM FIRE MODEL  
PLAT RELEASED AT TIME = 4700.00  
SPEED 1 TO 99.000000 1 TO 99.000000  
ALL DATA POINTS ARE IN THE PLATEAU OF THE  
PLATEAU OF THE PLATEAU OF THE PLATEAU OF THE  
PLATEAU OF THE PLATEAU OF THE PLATEAU OF THE

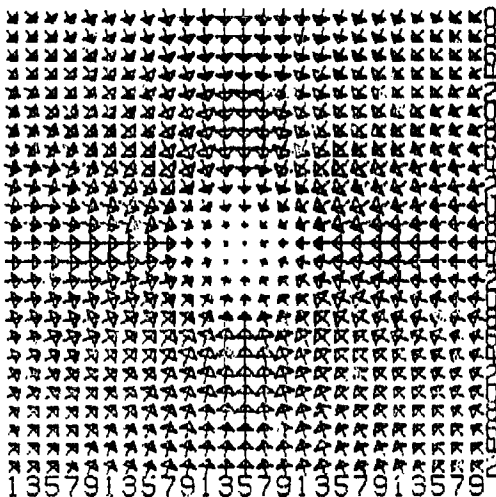


Figure 6-5(m). Wind velocity map for ring fire.

## 6.6 THREE SMALL FIRES WITH NO AMBIENT WIND

As shown in Figure 6-6, three centrally located  $5 \times 5$  candidate sets of cells were ignited with probability of ignition of 0.5. Figures 6-6 through 6-6(g) show that none of the fires spread outwardly, although each fire filled in some. The wind velocity maps of Figure 6-6(l) and 6-6(m) show the reason for this. The fire induced wind speeds generated by these fires were high enough to cause only slight contagion and insufficient to cause branding. Since these winds were essentially directed inward toward the center of the three fires, no outward spread was possible. Only inward spread and filling in could have occurred.

```

PLOT SIMULATION TIME = 1848.00 SECONDS
ROWS 1 TO 50, COLUMNS 1 TO 50.
ROW 50
ROW 49
ROW 48
ROW 47
ROW 46
ROW 45
ROW 44
ROW 43
ROW 42
ROW 41
ROW 40
ROW 39
ROW 38
ROW 37
ROW 36
ROW 35
ROW 34
ROW 33
ROW 32
ROW 31
ROW 30
ROW 29
ROW 28
ROW 27
ROW 26
ROW 25
ROW 24
ROW 23
ROW 22
ROW 21
ROW 20
ROW 19
ROW 18
ROW 17
ROW 16
ROW 15
ROW 14
ROW 13
ROW 12
ROW 11
ROW 10
ROW 9
ROW 8
ROW 7
ROW 6
ROW 5
ROW 4
ROW 3
ROW 2
ROW 1
COLUMNS 12345678901234567890123456789012345678901234567890
NUMBER OF UNIGNITED, BURNING AND BURNED-OUT CELLS = 2452 48

```

Figure 6-6. Cell state map for three clamp fires.

NUMBER OF UNIGNITED, BURNING AND BURNED-OUT CELLS = 2452 40

PLOT SIMULATION TIME = 1250.00 SECONDS  
 ROWS 1 TO 50 COLUMNS 1 TO 50

ROW	50
ROW	49
ROW	48
ROW	47
ROW	46
ROW	45
ROW	44
ROW	43
ROW	42
ROW	41
ROW	40
ROW	39
ROW	38
ROW	37
ROW	36
ROW	35
ROW	34
ROW	33
ROW	32
ROW	31
ROW	30
ROW	29
ROW	28
ROW	27
ROW	26
ROW	25
ROW	24
ROW	23
ROW	22
ROW	21
ROW	20
ROW	19
ROW	18
ROW	17
ROW	16
ROW	15
ROW	14
ROW	13
ROW	12
ROW	11
ROW	10
ROW	9
ROW	8
ROW	7
ROW	6
ROW	5
ROW	4
ROW	3
ROW	2
ROW	1

COLUMNS 1234567890123456789012345678901234567890  
 NUMBER OF UNIGNITED, BURNING AND BURNED-OUT CELLS = 2449 51

Figure 6-6(a). Cell state map for three clump fires.



```

PLOT SIMULATION TIME = 1754.00 SECONDS
ROWS 1 TO 50 COLUMNS 1 TO 50
ROW 50
ROW 49
ROW 48
ROW 47
ROW 46
ROW 45
ROW 44
ROW 43
ROW 42

ROW 41
ROW 40
ROW 39
ROW 38
ROW 37
ROW 36
ROW 35
ROW 34
ROW 33
ROW 32
ROW 31
ROW 30
ROW 29
ROW 28
ROW 27
ROW 26
ROW 25
ROW 24
ROW 23
ROW 22
ROW 21
ROW 20
ROW 19
ROW 18
ROW 17
ROW 16
ROW 15
ROW 14
ROW 13
ROW 12
ROW 11
ROW 10
ROW 9
ROW 8
ROW 7
ROW 6
ROW 5
ROW 4
ROW 3
ROW 2
ROW 1
COLUMNS 1234567890123456789012345678901234567890
NUMBER OF UNIGNITED, BURNING AND BURNED-OUT CELLS = 2448 52

```

Figure 6-6(b). Cell state map for three clump fires.

```

PLOT SIMULATION TIME = 2/50.00 SECONDS
ROWS 1 TO 50 COLUMNS 1 TO 50
ROW 50
ROW 49
ROW 48
ROW 47
ROW 46
ROW 45
ROW 44
ROW 43
ROW 42
ROW 41
ROW 40
ROW 39
ROW 38
ROW 37
ROW 36

ROW 35
ROW 34
ROW 33
ROW 32
ROW 31
ROW 30
ROW 29
ROW 28
ROW 27
ROW 26
ROW 25
ROW 24
ROW 23
ROW 22
ROW 21
ROW 20
ROW 19
ROW 18
ROW 17
ROW 16
ROW 15
ROW 14
ROW 13
ROW 12
ROW 11
ROW 10
ROW 9
ROW 8
ROW 7
ROW 6
ROW 5
ROW 4
ROW 3
ROW 2
ROW 1
COLUMNS 1234567890123456789012345678901234567890
NUMBER OF UNIGNITED, BURNING AND BURNED-OUT CELLS = 2446 54

```

Figure 6-6(c). Cell state map for three clump fires.

```

PLOT SIMULATION TIME = 4750.00 SECONDS
ROWS 1 TO 52, COLUMNS 1 TO 50
ROW 50
ROW 49
ROW 48
ROW 47
ROW 46
ROW 45
ROW 44
ROW 43
ROW 42
ROW 41
ROW 40
ROW 39
ROW 38
ROW 37
ROW 36
ROW 35
ROW 34
ROW 33
ROW 32
ROW 31
ROW 30
ROW 29
ROW 28
ROW 27
ROW 26
ROW 25
ROW 24
ROW 23
ROW 22
ROW 21
ROW 20
ROW 19
ROW 18
ROW 17
ROW 16
ROW 15
ROW 14
ROW 13
ROW 12
ROW 11
ROW 10
ROW 9
ROW 8
ROW 7
ROW 6
ROW 5
ROW 4
ROW 3
ROW 2
ROW 1
COLUMNS 1234567890123456789012345678901234567890
NUMBER OF UNIGNITED, BURNING AND BURNED-OUT CELLS = 2441 59

```

Figure 6-6(d). Cell state map for three clump fires.

```

PLOT SIMULATION TIME = 0756.00 SECONDS
ROWS 1 TO 50 COLUMNS 1 TO 50
ROW 50
ROW 49
ROW 48
ROW 47
ROW 46
ROW 45
ROW 44
ROW 43
ROW 42
ROW 41
ROW 40
ROW 39
ROW 38
ROW 37
ROW 36
ROW 35
ROW 34
ROW 33
ROW 32
ROW 31
ROW 30
ROW 29
ROW 28
ROW 27
ROW 26
ROW 25
ROW 24

ROW 23
ROW 22
ROW 21
ROW 20
ROW 19
ROW 18
ROW 17
ROW 16
ROW 15
ROW 14
ROW 13
ROW 12
ROW 11
ROW 10
ROW 9
ROW 8
ROW 7
ROW 6
ROW 5
ROW 4
ROW 3
ROW 2
ROW 1
COLUMNS 1234567890123456789012345678901234567890
NUMBER OF UNIGNITED, BURNING AND BURNED-OUT CELLS = 2441 69

```

Figure 6-6(e). Cell state map for three clump fires.

```

PLCT SIMULATION TIME = 10753.4 SECONDS
ROWS 1 TO 50 COLUMNS 1 TO 50
ROW 50
ROW 49
ROW 48
ROW 47
ROW 46
ROW 45
ROW 44
ROW 43
ROW 42
ROW 41
ROW 40
ROW 39
ROW 38
ROW 37
ROW 36
ROW 35
ROW 34
ROW 33
ROW 32
ROW 31
ROW 30
ROW 29
ROW 28
ROW 27
ROW 26
ROW 25
ROW 24
ROW 23
ROW 22
ROW 21
ROW 20
ROW 19
ROW 18

```

ROW 17 \*\*\*\*\*  
 ROW 16 \*\*\*\*\*  
 ROW 15 \*\*\*\*\*  
 ROW 14 \*\*\*\*\*  
 ROW 13 \*\*\*\*\*  
 ROW 12 \*\*\*\*\*  
 ROW 11 \*\*\*\*\*  
 ROW 10 \*\*\*\*\*  
 ROW 9 \*\*\*\*\*  
 ROW 8 \*\*\*\*\*  
 ROW 7 \*\*\*\*\*  
 ROW 6 \*\*\*\*\*  
 ROW 5 \*\*\*\*\*  
 ROW 4 \*\*\*\*\*  
 ROW 3 \*\*\*\*\*  
 ROW 2 \*\*\*\*\*  
 ROW 1 \*\*\*\*\*

```

COLUMNS 12345678901234567890123456789012345678901234567890
NUMBER OF UNIGNITED, BURNING AND BURNED-OUT CELLS = 2440 60

```

Figure 6-6(f). Cell state map for three clump fires.

```

PLOT SIMULATION TIME = 32750.0 SECONDS
ROWS 1 TO 50, COLUMNS 1 TO 50,
ROW 50
ROW 49
ROW 48
ROW 47
ROW 46
ROW 45
ROW 44
ROW 43
ROW 42
ROW 41
ROW 40
ROW 39
ROW 38
ROW 37
ROW 36
ROW 35
ROW 34
ROW 33
ROW 32
ROW 31
ROW 30
ROW 29
ROW 28
ROW 27
ROW 26
ROW 25
ROW 24
ROW 23
ROW 22
ROW 21
ROW 20
ROW 19
ROW 18
ROW 17
ROW 16
ROW 15
ROW 14
ROW 13
ROW 12

ROW 11
ROW 10
ROW 9
ROW 8
ROW 7
ROW 6
ROW 5
ROW 4
ROW 3
ROW 2
ROW 1
COLUMNS 12345678901234567890123456789012345678901234567890
NUMBER OF UNIGNITED, BURNING AND BURNED-OUT CELLS = 2440 57

```

Figure 6-6(g). Cell state map for three clump fires.

MISSION RESEARCH CORPORATION  
 UNKNOWN FIRE MODEL  
 PLANT SIMULATION TIME = 3000.00  
 TIME 1 TO 00.00000 1 TO 00.00000  
 WILL NOT OUTPUT ANY  
 \*\*\* ONLY EVERY OTHER WILL BE AND OTHER IS PLAYING \*\*\*  
 UNIT SCALE IS LOGARITHMIC SCALE IS ( 0-1.00 0-1.010 )



135791357913579135791357913579

MISSION RESEARCH CORPORATION  
 UNKNOWN FIRE MODEL  
 PLANT SIMULATION TIME = 3000.00  
 TIME 1 TO 00.00000 1 TO 00.00000  
 WILL NOT OUTPUT ANY  
 \*\*\* ONLY EVERY OTHER WILL BE AND OTHER IS PLAYING \*\*\*  
 UNIT SCALE IS LOGARITHMIC SCALE IS ( 0-1.00 0-1.010 )



135791357913579135791357913579

MISSION RESEARCH CORPORATION  
 UNKNOWN FIRE MODEL  
 PLANT SIMULATION TIME = 3000.00  
 TIME 1 TO 00.00000 1 TO 00.00000  
 WILL NOT OUTPUT ANY  
 \*\*\* ONLY EVERY OTHER WILL BE AND OTHER IS PLAYING \*\*\*  
 UNIT SCALE IS LOGARITHMIC SCALE IS ( 0-1.00 0-1.010 )



135791357913579135791357913579

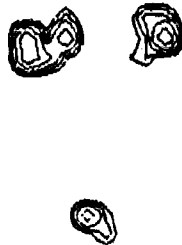
MISSION RESEARCH CORPORATION  
 UNKNOWN FIRE MODEL  
 PLANT SIMULATION TIME = 3000.00  
 TIME 1 TO 00.00000 1 TO 00.00000  
 WILL NOT OUTPUT ANY  
 \*\*\* ONLY EVERY OTHER WILL BE AND OTHER IS PLAYING \*\*\*  
 UNIT SCALE IS LOGARITHMIC SCALE IS ( 0-1.00 0-1.010 )



135791357913579135791357913579

Figure 6-6(h). Heat production rate contour for three clump fires.

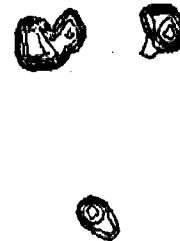
MISSION RESEARCH CORPORATION  
UNBURN FINE MODEL  
PLAY REPEATS ON TIME = 4700.00 RECORDS  
TIME 1 TO 10 10 10 10 10 10  
WALL COPY OFFSIDE OFF  
\*\*\* ONLY COPY OFFSIDE WALL COPY AND COLOR IS PLAYED \*\*\*  
COPY WALL IS LUMINOUS COPY IS ( 0-1.00 0-1.00 )



MISSION RESEARCH CORPORATION

1357913579135791357913579

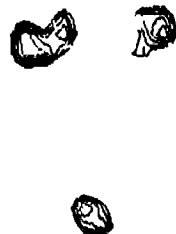
MISSION RESEARCH CORPORATION  
UNBURN FINE MODEL  
PLAY REPEATS ON TIME = 4700.00 RECORDS  
TIME 1 TO 10 10 10 10 10 10  
WALL COPY OFFSIDE OFF  
\*\*\* ONLY COPY OFFSIDE WALL COPY AND COLOR IS PLAYED \*\*\*  
COPY WALL IS LUMINOUS COPY IS ( 0-1.00 0-1.00 )



MISSION RESEARCH CORPORATION

1357913579135791357913579

MISSION RESEARCH CORPORATION  
UNBURN FINE MODEL  
PLAY REPEATS ON TIME = 4700.00 RECORDS  
TIME 1 TO 10 10 10 10 10 10  
WALL COPY OFFSIDE OFF  
\*\*\* ONLY COPY OFFSIDE WALL COPY AND COLOR IS PLAYED \*\*\*  
COPY WALL IS LUMINOUS COPY IS ( 0-1.00 0-1.00 )



MISSION RESEARCH CORPORATION

1357913579135791357913579

MISSION RESEARCH CORPORATION  
UNBURN FINE MODEL  
PLAY REPEATS ON TIME = 4700.00 RECORDS  
TIME 1 TO 10 10 10 10 10 10  
WALL COPY OFFSIDE OFF  
\*\*\* ONLY COPY OFFSIDE WALL COPY AND COLOR IS PLAYED \*\*\*  
COPY WALL IS LUMINOUS COPY IS ( 0-1.00 0-1.00 )



MISSION RESEARCH CORPORATION

1357913579135791357913579

Figure 6-6(i). Heat production rate contour for three clump fires.



MISSION RESEARCH CORPORATION  
UNIFORM FIRE MODEL  
PLATE REVEALATION TIME = 1000.00 SECONDS  
DATE 1 TO 99. COLUMN 1 TO 99.  
BODY ONLY: LETTERS A TO Z ARE A RANGE OF BODY VALUES  
ONLY BODY OTHER THAN 000 AND 000 ARE VALUES IN PLAYERS  
BODY VALUE IS LABOUR FORCE VALUE TO ( 0-1.00 0-1.00 )

222 32  
323 332  
323 332

22

135791357913579135791357913579

MISSION RESEARCH CORPORATION  
UNIFORM FIRE MODEL  
PLATE REVEALATION TIME = 1000.00 SECONDS  
DATE 1 TO 99. COLUMN 1 TO 99.  
BODY ONLY: LETTERS A TO Z ARE A RANGE OF BODY VALUES  
ONLY BODY OTHER THAN 000 AND 000 ARE VALUES IN PLAYERS  
BODY VALUE IS LABOUR FORCE VALUE TO ( 0-1.00 0-1.00 )

433 333  
434 334  
433 333

43

135791357913579135791357913579

MISSION RESEARCH CORPORATION  
UNIFORM FIRE MODEL  
PLATE REVEALATION TIME = 1000.00 SECONDS  
DATE 1 TO 99. COLUMN 1 TO 99.  
BODY ONLY: LETTERS A TO Z ARE A RANGE OF BODY VALUES  
ONLY BODY OTHER THAN 000 AND 000 ARE VALUES IN PLAYERS  
BODY VALUE IS LABOUR FORCE VALUE TO ( 0-1.00 0-1.00 )

333 333  
334 334  
333 333

33

135791357913579135791357913579

MISSION RESEARCH CORPORATION  
UNIFORM FIRE MODEL  
PLATE REVEALATION TIME = 1000.00 SECONDS  
DATE 1 TO 99. COLUMN 1 TO 99.  
BODY ONLY: LETTERS A TO Z ARE A RANGE OF BODY VALUES  
ONLY BODY OTHER THAN 000 AND 000 ARE VALUES IN PLAYERS  
BODY VALUE IS LABOUR FORCE VALUE TO ( 0-1.00 0-1.00 )

433 444  
434 444  
433 444

433

135791357913579135791357913579

Figure 6-6(j). Cell heat production rate map for three clump fires.

MISSION RESEARCH CORPORATION  
URBAN FIRE MODEL  
PLAY RECALCULATION TIME = 4790.00 SECONDS  
DATA 1 TO 99, 000000 1 TO 99  
ONLY HOT: LETTERS A TO Z ARE A RANGE OF HOT VALUES  
ONLY HOT: OTHER THAN A-Z ARE HOT VALUES TO PLAYERS ONLY  
ONLY WIDE IS LOGARITHMIC SCALE (0 = 0-1.00 0-1.010)

4 4 4  
4 4 3 3 4 4  
3 4 4

4 3  
3 4

135791357913579135791357913579

MISSION RESEARCH CORPORATION  
URBAN FIRE MODEL  
PLAY RECALCULATION TIME = 4070.00 SECONDS  
DATA 1 TO 99, 000000 1 TO 99  
ONLY HOT: LETTERS A TO Z ARE A RANGE OF HOT VALUES  
ONLY HOT: OTHER THAN A-Z ARE HOT VALUES TO PLAYERS ONLY  
ONLY WIDE IS LOGARITHMIC SCALE (0 = 0-1.00 0-1.010)

4 4  
4 4 4 4 4 4  
4 4 4 4 4

4 4  
4 4

135791357913579135791357913579

MISSION RESEARCH CORPORATION  
URBAN FIRE MODEL  
PLAY RECALCULATION TIME = 4790.00 SECONDS  
DATA 1 TO 99, 000000 1 TO 99  
ONLY HOT: LETTERS A TO Z ARE A RANGE OF HOT VALUES  
ONLY HOT: OTHER THAN A-Z ARE HOT VALUES TO PLAYERS ONLY  
ONLY WIDE IS LOGARITHMIC SCALE (0 = 0-1.00 0-1.010)

4 4 4  
4 4 4 3 4 4  
3 4 4

4 4  
4 4

135791357913579135791357913579

MISSION RESEARCH CORPORATION  
URBAN FIRE MODEL  
PLAY RECALCULATION TIME = 4070.00 SECONDS  
DATA 1 TO 99, 000000 1 TO 99  
ONLY HOT: LETTERS A TO Z ARE A RANGE OF HOT VALUES  
ONLY HOT: OTHER THAN A-Z ARE HOT VALUES TO PLAYERS ONLY  
ONLY WIDE IS LOGARITHMIC SCALE (0 = 0-1.00 0-1.010)

4 4  
4 4 4 4 4 4  
4 4 4 4 4

4 4  
4 4

135791357913579135791357913579

Figure 6-6(k). Cell heat production rate map for three clump fires.

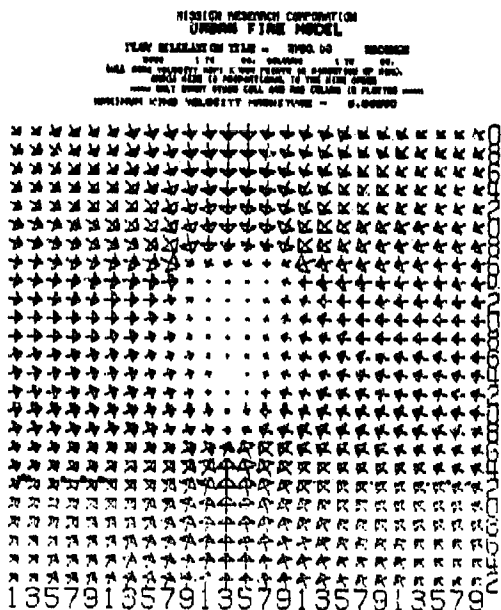
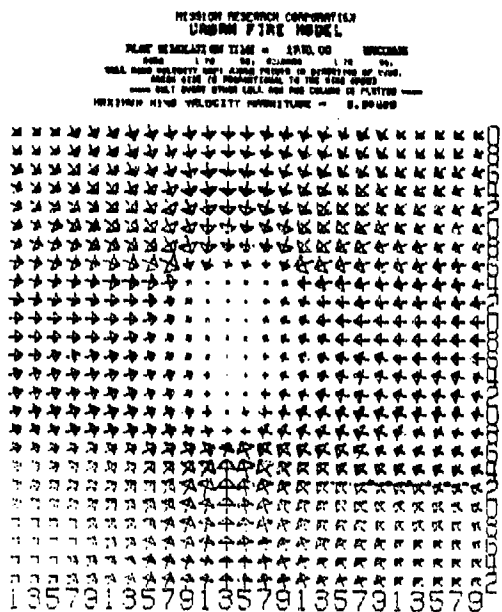
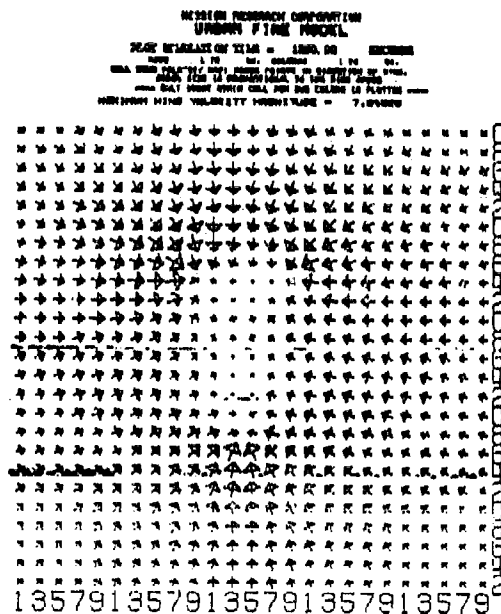
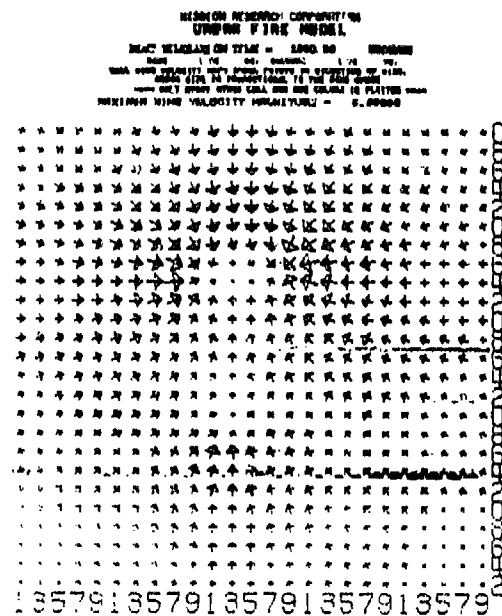


Figure 6-6(1). Wind velocity map for three clump fires.

[illegible][illegible][illegible]

1	2	3	4	5	6	7	8	9	10	11	12	13	14	15	16	17	18	19	20	21	22	23	24	25	26	27	28	29	30	31	32	33	34	35	36	37	38	39	40	41	42	43	44	45	46	47	48	49	50	51	52	53	54	55	56	57	58	59	60	61	62	63	64	65	66	67	68	69	70	71	72	73	74	75	76	77	78	79	80	81	82	83	84	85	86	87	88	89	90	91	92	93	94	95	96	97	98	99	100
---	---	---	---	---	---	---	---	---	----	----	----	----	----	----	----	----	----	----	----	----	----	----	----	----	----	----	----	----	----	----	----	----	----	----	----	----	----	----	----	----	----	----	----	----	----	----	----	----	----	----	----	----	----	----	----	----	----	----	----	----	----	----	----	----	----	----	----	----	----	----	----	----	----	----	----	----	----	----	----	----	----	----	----	----	----	----	----	----	----	----	----	----	----	----	----	----	----	----	-----

252

## 6.7 SMALL AREA FIRE WITH AMBIENT WINDS

As shown in Figure 6-7, a  $10 \times 10$  cell candidate set of cells in the lower left corner of the urban area was ignited with probability of ignition of 0.1. This location was chosen because the effects of wind velocities directed from the lower left to the upper right at speeds of 10, 20, 30, 40, and 50 m/s, were examined and are shown in Figures 6-7, 6-8, 6-9, 6-10, and 6-11, respectively.

These cases depict the sensitivity of propagation to local wind velocity. There are also the first cases in which significant collections of cells are seen to reach burnout. The effects of this are clearly shown in all of the maps at 32,750 seconds, but are best seen in the heat production rate contour maps.

```

PLOT SIMULATION TIME = 1040.00 SECONDS
ROWS 1 TO 50. COLUMNS 1 TO 50.
ROW 50
ROW 49
ROW 48
ROW 47
ROW 46
ROW 45
ROW 44
ROW 43
ROW 42
ROW 41
ROW 40
ROW 39
ROW 38
ROW 37
ROW 36
ROW 35
ROW 34
ROW 33
ROW 32
ROW 31
ROW 30
ROW 29
ROW 28
ROW 27
ROW 26
ROW 25
ROW 24
ROW 23
ROW 22
ROW 21
ROW 20
ROW 19
ROW 18
ROW 17
ROW 16
ROW 15
ROW 14
ROW 13
ROW 12
ROW 11
ROW 10
ROW 9
ROW 8
ROW 7
ROW 6
ROW 5
ROW 4
ROW 3
ROW 2
ROW 1
COLUMNS 12345678901234567890123456789012345678901234567890
NUMBER OF UNIGNITED, BURNING AND BURNED-OUT CELLS = 2491 9

```

Figure 6-7. Cell state map for small area fire with ambient wind = 10 m/s.

PLOT SIMULATION TIME = 1250.0 SECONDS  
 ROWS 1 TO 50. COLUMNS 1 TO 50.

ROW	47
ROW	46
ROW	45
ROW	44
ROW	43
ROW	42
ROW	41
ROW	40
ROW	39
ROW	38
ROW	37
ROW	36
ROW	35
ROW	34
ROW	33
ROW	32
ROW	31
ROW	30
ROW	29
ROW	28
ROW	27
ROW	26
ROW	25
ROW	24
ROW	23
ROW	22
ROW	21
ROW	20
ROW	19
ROW	18
ROW	17
ROW	16
ROW	15
ROW	14
ROW	13
ROW	12
ROW	11
ROW	10
ROW	9
ROW	8
ROW	7
ROW	6
ROW	5
ROW	4
ROW	3
ROW	2
ROW	1

COLUMNS 1234567890123456789012345678901234567890  
 NUMBER OF UNIGNITED, BURNING AND BURNED-OUT CELLS = 2451 9 0

Figure 6-7(a). Cell state map for small area fire with ambient wind  
 = 10 m/s.

PLUT SIMULATION TIME = 1750.00 SECONDS

ROWS 1 TO 50, COLUMNS 1 TO 50.

ROW 50

ROW 49

ROW 48

ROW 47

ROW 46

ROW 45

ROW 44

ROW 43

ROW 42

ROW 41

ROW 40

ROW 39

ROW 38

ROW 37

ROW 36

ROW 35

ROW 34

ROW 33

ROW 32

ROW 31

ROW 30

ROW 29

ROW 28

ROW 27

ROW 26

ROW 25

ROW 24

ROW 23

ROW 22

ROW 21

ROW 20

ROW 19

ROW 18

ROW 17

ROW 16

ROW 15

ROW 14

ROW 13

ROW 12

ROW 11

ROW 10

ROW 9

ROW 8

ROW 7

ROW 6

ROW 5

ROW 4

ROW 3

ROW 2

ROW 1

COLUMNS 12345678901234567890123456789012345678901234567890

NUMBER OF UNIGNITED, BURNING AND BURNED-OUT CELLS = 2487 13

Figure 6-7(b). Cell state map for small area fire with ambient wind = 10 m/s.



PLOT SIMULATION TIME = 2750.00 SECONDS  
 ROWS L TO 50, COLUMNS 1 TO 80

ROW	50
ROW	49
ROW	48
ROW	47
ROW	46
ROW	45
ROW	44
ROW	43
ROW	42
ROW	41
ROW	40
ROW	39
ROW	38
ROW	37
ROW	36

ROW	35
ROW	34
ROW	33
ROW	32
ROW	31
ROW	30
ROW	29
ROW	28
ROW	27
ROW	26
ROW	25
ROW	24
ROW	23
ROW	22
ROW	21
ROW	20
ROW	19
ROW	18
ROW	17
ROW	16
ROW	15
ROW	14
ROW	13
ROW	12
ROW	11
ROW	10
ROW	9
ROW	8
ROW	7
ROW	6
ROW	5
ROW	4
ROW	3
ROW	2
ROW	1

COLUMNS 12345678901234567890123456789012345678901234567890  
 NUMBER OF UNIGNITED, BURNING AND BURNED-OUT CELLS = 2461 19

Figure 6-7(c). Cell state map for small area fire with ambient wind = 10 m/s.

PLOT SIMULATION TIME = 4750.00 SECONDS

ROWS 1 TO 50, COLUMNS 1 TO 50

ROW 50  
ROW 49  
ROW 48  
ROW 47  
ROW 46  
ROW 45  
ROW 44  
ROW 43  
ROW 42  
ROW 41  
ROW 40  
ROW 39  
ROW 38  
ROW 37  
ROW 36  
ROW 35  
ROW 34  
ROW 33  
ROW 32  
ROW 31  
ROW 30

ROW 29  
ROW 28  
ROW 27  
ROW 26  
ROW 25  
ROW 24  
ROW 23  
ROW 22  
ROW 21  
ROW 20  
ROW 19  
ROW 18  
ROW 17  
ROW 16  
ROW 15  
ROW 14  
ROW 13  
ROW 12  
ROW 11  
ROW 10  
ROW 9  
ROW 8  
ROW 7  
ROW 6  
ROW 5  
ROW 4  
ROW 3  
ROW 2  
ROW 1

COLUMNS 1234567890123456789012345678901234567890

NUMBER OF UNIGNITED, BURNING AND BURNED-OUT CELLS = 2459 41

Figure 6-7(d). Cell state map for small area fire with ambient wind = 10 m/s.

```

PLOT SIMULATION TIME = 8750.00 SECONDS
ROWS 1 TO 50, COLUMNS 1 TO 50.
ROW 50
ROW 49
ROW 48
ROW 47
ROW 46
ROW 45
ROW 44
ROW 43
ROW 42
ROW 41
ROW 40
ROW 39
ROW 38
ROW 37
ROW 36
ROW 35
ROW 34
ROW 33
ROW 32
ROW 31
ROW 30
ROW 29
ROW 28
ROW 27
ROW 26
ROW 25
ROW 24

```

```

ROW 23
ROW 22
ROW 21
ROW 20
ROW 19
ROW 18
ROW 17
ROW 16
ROW 15
ROW 14
ROW 13
ROW 12
ROW 11
ROW 10
ROW 9
ROW 8
ROW 7
ROW 6
ROW 5
ROW 4
ROW 3
ROW 2
ROW 1
COLUMNS 1234567890123456789012345678901234567890
NUMBER OF UNIGNITED, BURNING AND BURNED-OUT CELLS = 2438 62

```

Figure 6-7(e). Cell state map for small area fire with ambient wind = 10 m/s.

NUMBER OF UNIGNITED, BURNING AND BURNED-OUT CELLS = 2449 92

PLOT SIMULATION TIME = 10750.0 SECONDS

ROWS 1 TO 50, COLUMNS 1 TO 50

```

ROW 50
ROW 49
ROW 48
ROW 47
ROW 46
ROW 45
ROW 44
ROW 43
ROW 42
ROW 41
ROW 40
ROW 39
ROW 38
ROW 37
ROW 36
ROW 35
ROW 34
ROW 33
ROW 32
ROW 31
ROW 30
ROW 29
ROW 28
ROW 27
ROW 26
ROW 25
ROW 24
ROW 23
ROW 22
ROW 21
ROW 20
ROW 19
ROW 18

```

```

ROW 17
ROW 16
ROW 15
ROW 14
ROW 13
ROW 12
ROW 11
ROW 10
ROW 9
ROW 8
ROW 7
ROW 6
ROW 5
ROW 4
ROW 3
ROW 2
ROW 1

```

COLUMNS 1234567890123456789012345678901234567890

NUMBER OF UNIGNITED, BURNING AND BURNED-OUT CELLS = 2449 91

Figure 6-7(f). Cell state map for small area fire with ambient wind = 10 m/s.

```

PLOT SIMULATION TIME = 32756.0 SECONDS
ROWS 1 TO 50, COLUMNS 1 TO 50,
ROW 50
ROW 49
ROW 48
ROW 47
ROW 46
ROW 45
ROW 44
ROW 43
ROW 42
ROW 41
ROW 40
ROW 39
ROW 38
ROW 37
ROW 36
ROW 35
ROW 34
ROW 33
ROW 32
ROW 31
ROW 30
ROW 29
ROW 28
ROW 27
ROW 26
ROW 25
ROW 24
ROW 23
ROW 22
ROW 21
ROW 20
ROW 19
ROW 18
ROW 17
ROW 16
ROW 15
ROW 14
ROW 13
ROW 12

```

```

ROW 11
ROW 10
ROW 9
ROW 8
ROW 7
ROW 6
ROW 5
ROW 4
ROW 3
ROW 2
ROW 1
COLUMNS 12345678901234567890123456789012345678901234567890
NUMBER OF UNIGNITED, BURNING AND BURNED-OUT CELLS = 2363 143

```

Figure 6-7(g). Cell state map for small area fire with ambient wind = 10 m/s.

MISSION RESEARCH CORPORATION  
URBAN FIRE MODEL  
PLOT RELEASE ON TIME = 2000.00 SECONDS  
PLOT 1 TO 100.00 RELEASE 1 TO 100.00  
CELL NOT CONTAINING  
\*\*\* ONLY EVERY OTHER CELL AND COLUMN IS PLOTTED \*\*\*  
BODY SCALE IS LOGARITHMIC SCALE (0-1.00 0-1.00)

MISSION RESEARCH CORPORATION  
URBAN FIRE MODEL  
PLOT RELEASE ON TIME = 2000.00 SECONDS  
PLOT 1 TO 100.00 RELEASE 1 TO 100.00  
CELL NOT CONTAINING  
\*\*\* ONLY EVERY OTHER CELL AND COLUMN IS PLOTTED \*\*\*  
BODY SCALE IS LOGARITHMIC SCALE (0-1.00 0-1.00)

135791357913579135791357913579

135791357913579135791357913579

MISSION RESEARCH CORPORATION  
URBAN FIRE MODEL  
PLOT RELEASE ON TIME = 2700.00 SECONDS  
PLOT 1 TO 100.00 RELEASE 1 TO 100.00  
CELL NOT CONTAINING  
\*\*\* ONLY EVERY OTHER CELL AND COLUMN IS PLOTTED \*\*\*  
BODY SCALE IS LOGARITHMIC SCALE (0-1.00 0-1.00)

MISSION RESEARCH CORPORATION  
URBAN FIRE MODEL  
PLOT RELEASE ON TIME = 2700.00 SECONDS  
PLOT 1 TO 100.00 RELEASE 1 TO 100.00  
CELL NOT CONTAINING  
\*\*\* ONLY EVERY OTHER CELL AND COLUMN IS PLOTTED \*\*\*  
BODY SCALE IS LOGARITHMIC SCALE (0-1.00 0-1.00)

135791357913579135791357913579

135791357913579135791357913579

Figure 6-7(h). Heat production rate contour for small area fire with ambient wind = 10 m/s.

MISSION RESEARCH CORPORATION  
URBAN FIRE MODEL  
PLOT SIMULATION TIME = 4790.00 SECONDS  
CELL NOT OUTSIDE MAP  
\*\*\* ONLY EVERY OTHER CELL NOW AND BELONG IS PLOTTED \*\*\*  
ROOT STYLE IS LOGARITHMIC SCALE 10 ( 0-1.25 0-1.25 )



1357913579135791357913579

MISSION RESEARCH CORPORATION  
URBAN FIRE MODEL  
PLOT SIMULATION TIME = 5790.00 SECONDS  
CELL NOT OUTSIDE MAP  
\*\*\* ONLY EVERY OTHER CELL NOW AND BELONG IS PLOTTED \*\*\*  
ROOT STYLE IS LOGARITHMIC SCALE 10 ( 0-1.25 0-1.25 )



1357913579135791357913579

MISSION RESEARCH CORPORATION  
URBAN FIRE MODEL  
PLOT SIMULATION TIME = 1790.00 SECONDS  
CELL NOT OUTSIDE MAP  
\*\*\* ONLY EVERY OTHER CELL NOW AND BELONG IS PLOTTED \*\*\*  
ROOT STYLE IS LOGARITHMIC SCALE 10 ( 0-1.25 0-1.25 )



1357913579135791357913579

MISSION RESEARCH CORPORATION  
URBAN FIRE MODEL  
PLOT SIMULATION TIME = 2790.00 SECONDS  
CELL NOT OUTSIDE MAP  
\*\*\* ONLY EVERY OTHER CELL NOW AND BELONG IS PLOTTED \*\*\*  
ROOT STYLE IS LOGARITHMIC SCALE 10 ( 0-1.25 0-1.25 )



1357913579135791357913579

Figure 6-7(1). Heat production rate contour for small area fire with ambient wind = 10 m/s.

MISSION RESEARCH CORPORATION  
URBAN FIRE MODEL  
PLAY REPEAT ON TIME = 9800.00 RECOVER  
DATA 1 TO 99. COLUMN 1 TO 99.  
ONLY SPOT LETTERS 0 TO 9 ARE A PART OF SPOT VALUE  
ONLY SPOT OTHER CALLS ARE ARE ALARM IS PLATED FROM  
SPOT SCALE IS LOGARITHMIC SCALE 10 (0-1.00 0-1.010)

3  
3  
135791357913579135791357913579

MISSION RESEARCH CORPORATION  
URBAN FIRE MODEL  
PLAY REPEAT ON TIME = 9700.00 RECOVER  
DATA 1 TO 99. COLUMN 1 TO 99.  
ONLY SPOT LETTERS 0 TO 9 ARE A PART OF SPOT VALUE  
ONLY SPOT OTHER CALLS ARE ARE ALARM IS PLATED FROM  
SPOT SCALE IS LOGARITHMIC SCALE 10 (0-1.00 0-1.010)

3 4  
4  
135791357913579135791357913579

MISSION RESEARCH CORPORATION  
URBAN FIRE MODEL  
PLAY REPEAT ON TIME = 1800.00 RECOVER  
DATA 1 TO 99. COLUMN 1 TO 99.  
ONLY SPOT LETTERS 0 TO 9 ARE A PART OF SPOT VALUE  
ONLY SPOT OTHER CALLS ARE ARE ALARM IS PLATED FROM  
SPOT SCALE IS LOGARITHMIC SCALE 10 (0-1.00 0-1.010)

3  
3  
135791357913579135791357913579

MISSION RESEARCH CORPORATION  
URBAN FIRE MODEL  
PLAY REPEAT ON TIME = 9700.00 RECOVER  
DATA 1 TO 99. COLUMN 1 TO 99.  
ONLY SPOT LETTERS 0 TO 9 ARE A PART OF SPOT VALUE  
ONLY SPOT OTHER CALLS ARE ARE ALARM IS PLATED FROM  
SPOT SCALE IS LOGARITHMIC SCALE 10 (0-1.00 0-1.010)

2 2  
4 4  
3 4  
135791357913579135791357913579

Figure 6-7(j). Cell heat production rate map for small area fire with ambient wind = 10 m/s.



3  
4 4 3  
4 4 2  
4 4  
4

COULDS: VICE PRESIDENT

[illegible]

00000000000000000000000000000000

[illegible]

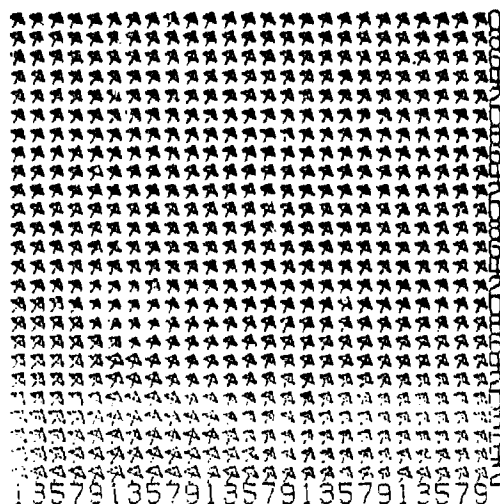
**REGISTRATION INFORMATION**

3  
4  
4  
4  
4  
3 4  
4 4  
4 4  
4 4  
4 4  
4 4  
4 4  
4 4  
4 4  
4 4  
4 4

1. 2. 3. 4. 5. 6. 7. 8. 9. 10. 11. 12. 13. 14. 15. 16. 17. 18. 19. 20. 21. 22. 23. 24. 25. 26. 27. 28. 29. 30. 31. 32. 33. 34. 35. 36. 37. 38. 39. 40. 41. 42. 43. 44. 45. 46. 47. 48. 49. 50. 51. 52. 53. 54. 55. 56. 57. 58. 59. 60. 61. 62. 63. 64. 65. 66. 67. 68. 69. 70. 71. 72. 73. 74. 75. 76. 77. 78. 79. 80. 81. 82. 83. 84. 85. 86. 87. 88. 89. 90. 91. 92. 93. 94. 95. 96. 97. 98. 99. 100. 101. 102. 103. 104. 105. 106. 107. 108. 109. 110. 111. 112. 113. 114. 115. 116. 117. 118. 119. 120. 121. 122. 123. 124. 125. 126. 127. 128. 129. 130. 131. 132. 133. 134. 135. 136. 137. 138. 139. 140. 141. 142. 143. 144. 145. 146. 147. 148. 149. 150. 151. 152. 153. 154. 155. 156. 157. 158. 159. 160. 161. 162. 163. 164. 165. 166. 167. 168. 169. 170. 171. 172. 173. 174. 175. 176. 177. 178. 179. 180. 181. 182. 183. 184. 185. 186. 187. 188. 189. 190. 191. 192. 193. 194. 195. 196. 197. 198. 199. 200. 201. 202. 203. 204. 205. 206. 207. 208. 209. 210. 211. 212. 213. 214. 215. 216. 217. 218. 219. 220. 221. 222. 223. 224. 225. 226. 227. 228. 229. 230. 231. 232. 233. 234. 235. 236. 237. 238. 239. 240. 241. 242. 243. 244. 245. 246. 247. 248. 249. 250. 251. 252. 253. 254. 255. 256. 257. 258. 259. 260. 261. 262. 263. 264. 265. 266. 267. 268. 269. 270. 271. 272. 273. 274. 275. 276. 277. 278. 279. 280. 281. 282. 283. 284. 285. 286. 287. 288. 289. 290. 291. 292. 293. 294. 295. 296. 297. 298. 299. 300. 301. 302. 303. 304. 305. 306. 307. 308. 309. 310. 311. 312. 313. 314. 315. 316. 317. 318. 319. 320. 321. 322. 323. 324. 325. 326. 327. 328. 329. 330. 331. 332. 333. 334. 335. 336. 337. 338. 339. 340. 341. 342. 343. 344. 345. 346. 347. 348. 349. 350. 351. 352. 353. 354. 355. 356. 357. 358. 359. 360. 361. 362. 363. 364. 365. 366. 367. 368. 369. 370. 371. 372. 373. 374. 375. 376. 377. 378. 379. 380. 381. 382. 383. 384. 385. 386. 387. 388. 389. 390. 391. 392. 393. 394. 395. 396. 397. 398. 399. 400. 401. 402. 403. 404. 405. 406. 407. 408. 409. 410. 411. 412. 413. 414. 415. 416. 417. 418. 419. 420. 421. 422. 423. 424. 425. 426. 427. 428. 429. 430. 431. 432. 433. 434. 435. 436. 437. 438. 439. 440. 441. 442. 443. 444. 445. 446. 447. 448. 449. 450. 451. 452. 453. 454. 455. 456. 457. 458. 459. 460. 461. 462. 463. 464. 465. 466. 467. 468. 469. 470. 471. 472. 473. 474. 475. 476. 477. 478. 479. 480. 481. 482. 483. 484. 485. 486. 487. 488. 489. 490. 491. 492. 493. 494. 495. 496. 497. 498. 499. 500. 501. 502. 503. 504. 505. 506. 507. 508. 509. 510. 511. 512. 513. 514. 515. 516. 517. 518. 519. 520. 521. 522. 523. 524. 525. 526. 527. 528. 529. 530. 531. 532. 533. 534. 535. 536. 537. 538. 539. 540. 541. 542. 543. 544. 545. 546. 547. 548. 549. 550. 551. 552. 553. 554. 555. 556. 557. 558. 559. 560. 561. 562. 563. 564. 565. 566. 567. 568. 569. 570. 571. 572. 573. 574. 575. 576. 577. 578. 579. 580. 581. 582. 583. 584. 585. 586. 587. 588. 589. 590. 591. 592. 593. 594. 595. 596. 597. 598. 599. 600. 601. 602. 603. 604. 605. 606. 607. 608. 609. 610. 611. 612. 613. 614. 615. 616. 617. 618. 619. 620. 621. 622. 623. 624. 625. 626. 627. 628. 629. 630. 631. 632. 633. 634. 635. 636. 637. 638. 639. 640. 641. 642. 643. 644. 645. 646. 647. 648. 649. 650. 651. 652. 653. 654. 655. 656. 657. 658. 659. 660. 661. 662. 663. 664. 665. 666. 667. 668. 669. 670. 671. 672. 673. 674. 675. 676. 677. 678. 679. 680. 681. 682. 683. 684. 685. 686. 687. 688. 689. 690. 691. 692. 693. 694. 695. 696. 697. 698. 699. 700. 701. 702. 703. 704. 705. 706. 707. 708. 709. 710. 711. 712. 713. 714. 715. 716. 717. 718. 719. 720. 721. 722. 723. 724. 725. 726. 727. 728. 729. 730. 731. 732. 733. 734. 735. 736. 737. 738. 739. 740. 741. 742. 743. 744. 745. 746. 747. 748. 749. 750. 751. 752. 753. 754. 755. 756. 757. 758. 759. 760. 761. 762. 763. 764. 765. 766. 767. 768. 769. 770. 771. 772. 773. 774. 775. 776. 777. 778. 779. 780. 781. 782. 783. 784. 785. 786. 787. 788. 789. 790. 791. 792. 793. 794. 795. 796. 797. 798. 799. 800. 801. 802. 803. 804. 805. 806. 807. 808. 809. 810. 811. 812. 813. 814. 815. 816. 817. 818. 819. 820. 821. 822. 823. 824. 825. 826. 827. 828. 829. 830. 831. 832. 833. 834. 835. 836. 837. 838. 839. 840.

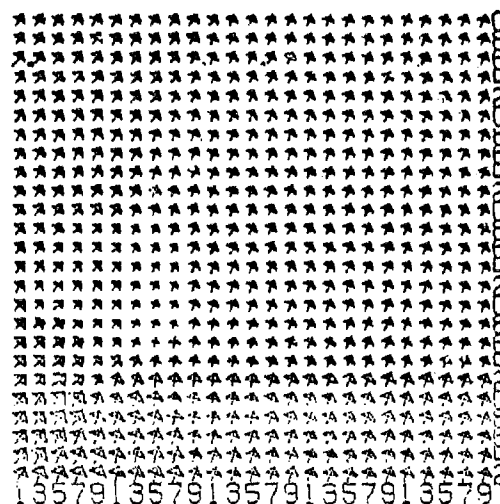
# HYDRO FIBREX CORPORATION UPPER FIRE MODEL

PLAN VIEW: SCALE = 1:1000  
 DATE: 1/10/80  
 BY: J. L. BROWN  
 FOR: HYDRO FIBREX CORPORATION  
 FROM: J. L. BROWN  
 ONLY FOR USE IN THE UPPER FIRE MODEL  
 ONLY FOR USE IN THE UPPER FIRE MODEL



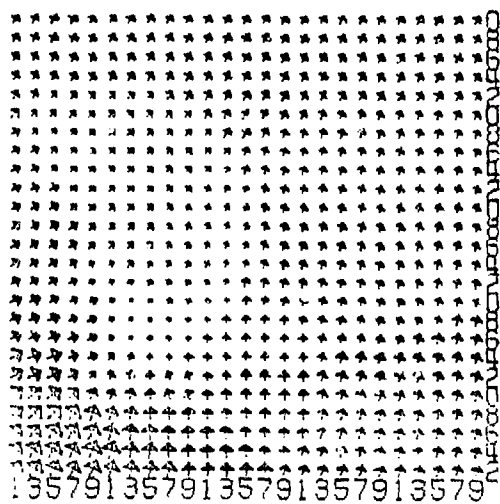
# HYDRO FIBREX CORPORATION UPPER FIRE MODEL

PLAN VIEW: SCALE = 1:1000  
 DATE: 1/10/80  
 BY: J. L. BROWN  
 FOR: HYDRO FIBREX CORPORATION  
 FROM: J. L. BROWN  
 ONLY FOR USE IN THE UPPER FIRE MODEL  
 ONLY FOR USE IN THE UPPER FIRE MODEL



# HYDRO FIBREX CORPORATION UPPER FIRE MODEL

PLAN VIEW: SCALE = 1:1000  
 DATE: 1/10/80  
 BY: J. L. BROWN  
 FOR: HYDRO FIBREX CORPORATION  
 FROM: J. L. BROWN  
 ONLY FOR USE IN THE UPPER FIRE MODEL  
 ONLY FOR USE IN THE UPPER FIRE MODEL



# HYDRO FIBREX CORPORATION UPPER FIRE MODEL

PLAN VIEW: SCALE = 1:1000  
 DATE: 1/10/80  
 BY: J. L. BROWN  
 FOR: HYDRO FIBREX CORPORATION  
 FROM: J. L. BROWN  
 ONLY FOR USE IN THE UPPER FIRE MODEL  
 ONLY FOR USE IN THE UPPER FIRE MODEL

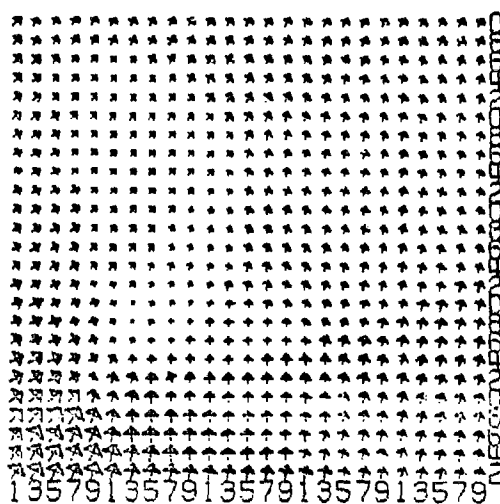


Figure 6-7(1). Wind velocity map for small area fire with ambient wind = 10 m/s.

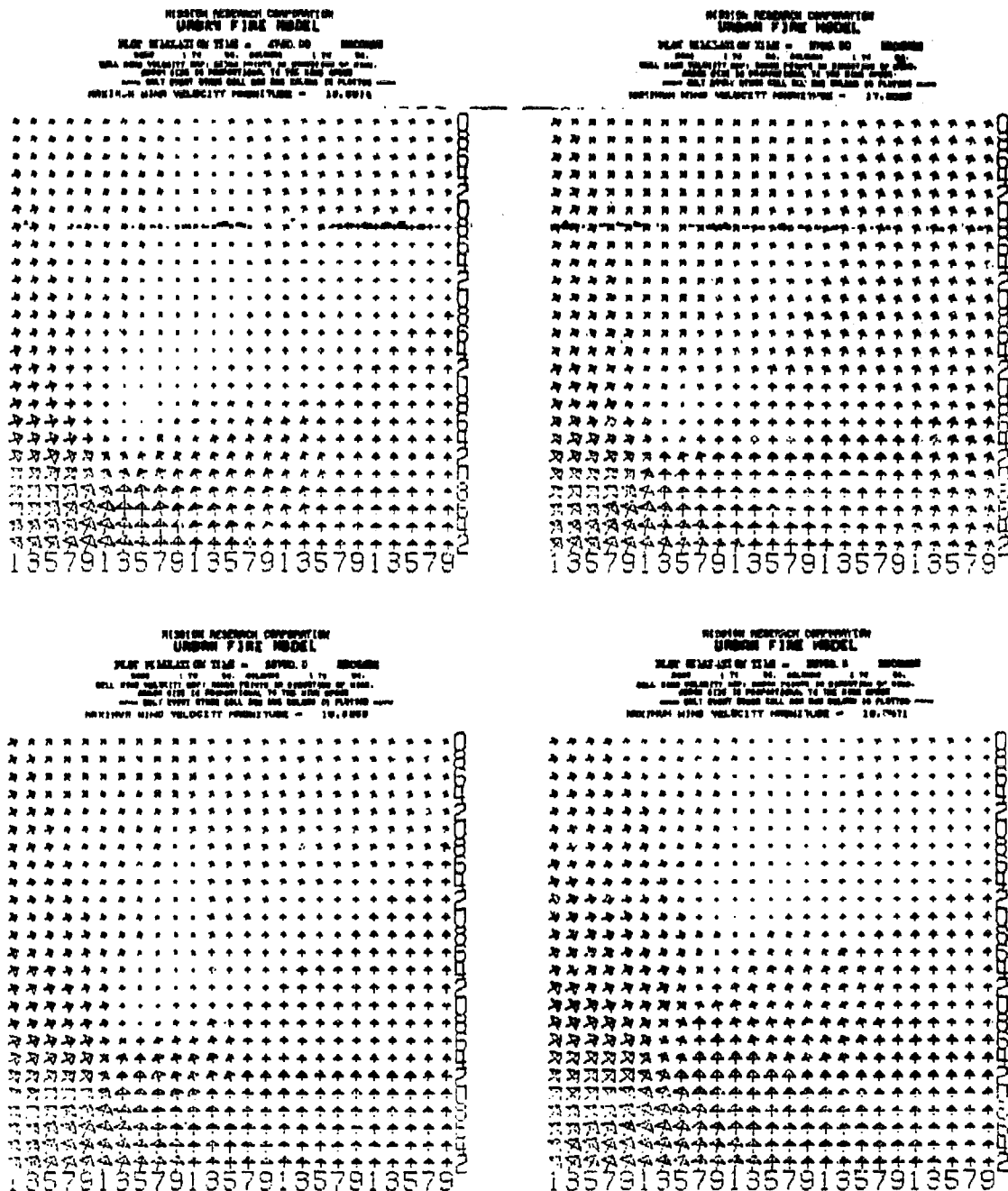


Figure 6-7(m). Wind velocity map for small area fire with ambient wind = 10 m/s.

```

PLOT SIMULATION TIME IN 1000.00 SECONDS
ROWS 1 TO 50, COLUMNS 1 TO 50.
ROW 50
ROW 49
ROW 48
ROW 47
ROW 46
ROW 45
ROW 44
ROW 43
ROW 42
ROW 41
ROW 40
ROW 39
ROW 38
ROW 37
ROW 36
ROW 35
ROW 34
ROW 33
ROW 32
ROW 31
ROW 30
ROW 29
ROW 28
ROW 27
ROW 26
ROW 25
ROW 24
ROW 23
ROW 22
ROW 21
ROW 20
ROW 19
ROW 18
ROW 17
ROW 16
ROW 15
ROW 14
ROW 13
ROW 12
ROW 11
ROW 10
ROW 9
ROW 8
ROW 7
ROW 6
ROW 5
ROW 4
ROW 3
ROW 2
ROW 1
COLUMNS 12345678901234567890123456789012345678901234567890
NUMBER OF UNIGNITED, BURNING AND BURNED-OUT CELLS = 2491

```

Figure 5-8. Cell state map for small area fire, ambient wind = 20 m/s.

PLUT SIMULATION TIME = 1250.00 SECONDS  
 ROWS 1 TO 50, COLUMNS 1 TO 50.

|     |    |
|-----|----|
| ROW | 50 |
| ROW | 49 |
| ROW | 48 |
| ROW | 47 |
| ROW | 46 |
| ROW | 45 |
| ROW | 44 |
| ROW | 43 |
| ROW | 42 |
| ROW | 41 |
| ROW | 40 |
| ROW | 39 |
| ROW | 38 |
| ROW | 37 |
| ROW | 36 |
| ROW | 35 |
| ROW | 34 |
| ROW | 33 |
| ROW | 32 |
| ROW | 31 |
| ROW | 30 |
| ROW | 29 |
| ROW | 28 |
| ROW | 27 |
| ROW | 26 |
| ROW | 25 |
| ROW | 24 |
| ROW | 23 |
| ROW | 22 |
| ROW | 21 |
| ROW | 20 |
| ROW | 19 |
| ROW | 18 |
| ROW | 17 |
| ROW | 16 |
| ROW | 15 |
| ROW | 14 |
| ROW | 13 |
| ROW | 12 |
| ROW | 11 |
| ROW | 10 |
| ROW | 9  |
| ROW | 8  |
| ROW | 7  |
| ROW | 6  |
| ROW | 5  |
| ROW | 4  |
| ROW | 3  |
| ROW | 2  |
| ROW | 1  |

COLUMNS 1234567890123456789012345678901234567890  
 NUMBER OF UNIGNITED, BURNING AND BURNED-OUT CELLS = 2490 10

Figure 6-8(a). Cell state map for small area fire, ambient wind  
 = 20 m/s.

```

PLOT SIMULATION TIME = 1752.00 SECONDS
ROWS 1 TO 52, COLUMNS 1 TO 54.
ROW 50
ROW 49
ROW 48
ROW 47
ROW 46
ROW 45
ROW 44
ROW 43
ROW 42

ROW 41
ROW 40
ROW 39
ROW 38
ROW 37
ROW 36
ROW 35
ROW 34
ROW 33
ROW 32
ROW 31
ROW 30
ROW 29
ROW 28
ROW 27
ROW 26
ROW 25
ROW 24
ROW 23
ROW 22
ROW 21
ROW 20
ROW 19
ROW 18
ROW 17
ROW 16
ROW 15
ROW 14
ROW 13
ROW 12
ROW 11
ROW 10
ROW 9
ROW 8
ROW 7
ROW 6
ROW 5
ROW 4
ROW 3
ROW 2
ROW 1
COLUMNS 12345678901234567890123456789012345678901234567890
NUMBER OF UNIGNITED, BURNING AND BURNED-OUT CELLS = 2481 12

```

Figure 6-8(b). Cell state map for small area fire, ambient wind = 20 m/s.

```

PLOT SIMULATION TIME = 2750.00 SECONDS
ROWS 1 TO 50, COLUMNS 1 TO 50,
ROW 50
ROW 49
ROW 48
ROW 47
ROW 46
ROW 45
ROW 44
ROW 43
ROW 42
ROW 41
ROW 40
ROW 39
ROW 38
ROW 37
ROW 36

ROW 35
ROW 34
ROW 33
ROW 32
ROW 31
ROW 30
ROW 29
ROW 28
ROW 27
ROW 26
ROW 25
ROW 24
ROW 23
ROW 22
ROW 21
ROW 20
ROW 19
ROW 18
ROW 17
ROW 16
ROW 15
ROW 14
ROW 13
ROW 12
ROW 11
ROW 10
ROW 9
ROW 8
ROW 7
ROW 6
ROW 5
ROW 4
ROW 3
ROW 2
ROW 1
COLUMNS 12345678901234567890123456789012345678901234567890
NUMBER OF UNIGNITED, BURNING AND BURNED-OUT CELLS = 2443 57

```

Figure 6-8(c). Cell state map for small area fire, ambient wind = 20 m/s.







```

PLOT SIMULATION TIME = 16750.4 SECONDS
ROWS 1 TO 50, COLUMNS 1 TO 84.
ROW 50 ..
ROW 49 .....
ROW 48 .....
ROW 47 .....
ROW 46 .....
ROW 45 .....
ROW 44 .....
ROW 43 .....
ROW 42 .....
ROW 41 .....
ROW 40 .....
ROW 39 .....
ROW 38 .....
ROW 37 .....
ROW 36 .....
ROW 35 .....
ROW 34 .....
ROW 33 .....
ROW 32 .....
ROW 31 .....
ROW 30 .....
ROW 29 .....
ROW 28 .....
ROW 27 .....
ROW 26 .....
ROW 25 .....
ROW 24 .....
ROW 23 .....
ROW 22 .....
ROW 21 .....
ROW 20 .....
ROW 19 .....
ROW 18 .....

ROW 17 .....
ROW 16 .....
ROW 15 .....
ROW 14 .....
ROW 13 .....
ROW 12 .....
ROW 11 .....
ROW 10 .....
ROW 9 .....
ROW 8 .....
ROW 7 .....
ROW 6 .....
ROW 5 .....
ROW 4 .....
ROW 3 .....
ROW 2 .....
ROW 1 .....
COLUMNS 12345678901234567890123456789012345678901234567890
NUMBER OF UNIGNITED, BURNING AND BURNED-OUT CELLS = 2157 336

```

Figure 6-8(f). Cell state map for small area fire, ambient wind = 20 m/s.

```

PLOT SIMULATION TIME = 32750.0 SECONDS
ROWS 1 TO 50, COLUMNS 1 TO 50.
ROW 50 .....
ROW 49 .....
ROW 48 .....
ROW 47 .....
ROW 46 .....
ROW 45 .....
ROW 44 .....
ROW 43 .....
ROW 42 .....
ROW 41 .....
ROW 40 .....
ROW 39 .....
ROW 38 .....
ROW 37 .....
ROW 36 .....
ROW 35 .....
ROW 34 .....
ROW 33 .....
ROW 32 .....
ROW 31 .....
ROW 30 .....
ROW 29 .....
ROW 28 .....
ROW 27 .....
ROW 26 .....
ROW 25 .....
ROW 24 .....
ROW 23 .....
ROW 22 .....
ROW 21 .....
ROW 20 .....
ROW 19 .....
ROW 18 .....
ROW 17 .....
ROW 16 .....
ROW 15 .....
ROW 14 .....
ROW 13 .....
ROW 12 .....

ROW 11 .....
ROW 10 .....
ROW 9 .....
ROW 8 .....
ROW 7 .....
ROW 6 .....
ROW 5 .....
ROW 4 .....
ROW 3 .....
ROW 2 .....
ROW 1 .....

COLUMNS 1234567890123456789012345678901234567890
NUMBER OF UNIGNITED, BURNING AND BURNED-OUT CELLS = 2020 300 11

```

Figure 6-8(g). Cell state map for area small fire, ambient wind = 20 m/s.

MISSION RESEARCH CORPORATION  
UNDER FIRE MODEL  
PLAY SIMULATION TIME = 1000.00 SECONDS  
TIME 1 TO 1000.00 SECONDS 1 TO 1000.00  
CELL NOT CONTROLLED  
\*\*\* ONLY EVERY OTHER CELL HAS AN OUTLINE IS PLAYED \*\*\*  
SHOT SCALE IS LOGARITHMIC SCALE IS (0-1.00 0-1.00)

MISSION RESEARCH CORPORATION  
UNDER FIRE MODEL  
PLAY SIMULATION TIME = 1000.00 SECONDS  
TIME 1 TO 1000.00 SECONDS 1 TO 1000.00  
CELL NOT CONTROLLED  
\*\*\* ONLY EVERY OTHER CELL HAS AN OUTLINE IS PLAYED \*\*\*  
SHOT SCALE IS LOGARITHMIC SCALE IS (0-1.00 0-1.00)

135791357913579135791357913579

135791357913579135791357913579

MISSION RESEARCH CORPORATION  
UNDER FIRE MODEL  
PLAY SIMULATION TIME = 1000.00 SECONDS  
TIME 1 TO 1000.00 SECONDS 1 TO 1000.00  
CELL NOT CONTROLLED  
\*\*\* ONLY EVERY OTHER CELL HAS AN OUTLINE IS PLAYED \*\*\*  
SHOT SCALE IS LOGARITHMIC SCALE IS (0-1.00 0-1.00)

MISSION RESEARCH CORPORATION  
UNDER FIRE MODEL  
PLAY SIMULATION TIME = 1000.00 SECONDS  
TIME 1 TO 1000.00 SECONDS 1 TO 1000.00  
CELL NOT CONTROLLED  
\*\*\* ONLY EVERY OTHER CELL HAS AN OUTLINE IS PLAYED \*\*\*  
SHOT SCALE IS LOGARITHMIC SCALE IS (0-1.00 0-1.00)

135791357913579135791357913579

135791357913579135791357913579

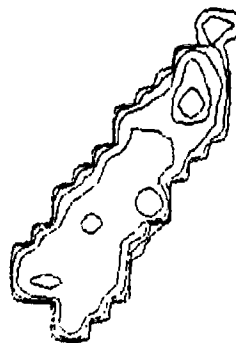
Figure 6-8(h). Heat production rate contour for small area fire,  
ambient wind = 20 m/s.

MISSION RESEARCH CORPORATION  
URBAN FIRE MODEL  
PLOT RELEASE ON TIME = 4700.00 SECONDS  
HWS 1 TO 00. RELEASE 1 TO 00  
CELL NOT CONTAINING 000  
\*\*\* ONLY EVERY OTHER CELL NOW AND RELEASE IS PLOTTED \*\*\*  
SHOT SCALE IS LOGARITHMIC TYPE (0 (0-1.0) 0-1.010)



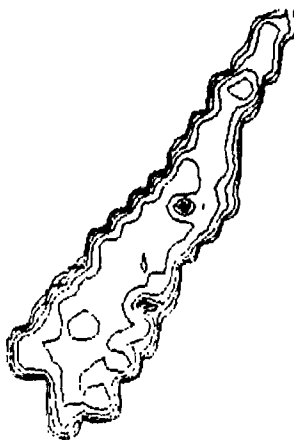
1357913579135791357913579

MISSION RESEARCH CORPORATION  
URBAN FIRE MODEL  
PLOT RELEASE ON TIME = 5700.00 SECONDS  
HWS 1 TO 00. RELEASE 1 TO 00  
CELL NOT CONTAINING 000  
\*\*\* ONLY EVERY OTHER CELL NOW AND RELEASE IS PLOTTED \*\*\*  
SHOT SCALE IS LOGARITHMIC TYPE (0 (0-1.0) 0-1.010)



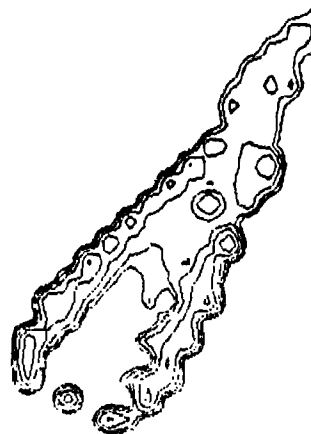
1357913579135791357913579

MISSION RESEARCH CORPORATION  
URBAN FIRE MODEL  
PLOT RELEASE ON TIME = 6700.00 SECONDS  
HWS 1 TO 00. RELEASE 1 TO 00  
CELL NOT CONTAINING 000  
\*\*\* ONLY EVERY OTHER CELL NOW AND RELEASE IS PLOTTED \*\*\*  
SHOT SCALE IS LOGARITHMIC TYPE (0 (0-1.0) 0-1.010)



1357913579135791357913579

MISSION RESEARCH CORPORATION  
URBAN FIRE MODEL  
PLOT RELEASE ON TIME = 8700.00 SECONDS  
HWS 1 TO 00. RELEASE 1 TO 00  
CELL NOT CONTAINING 000  
\*\*\* ONLY EVERY OTHER CELL NOW AND RELEASE IS PLOTTED \*\*\*  
SHOT SCALE IS LOGARITHMIC TYPE (0 (0-1.0) 0-1.010)



1357913579135791357913579

Figure 6-8(1). Heat production rate contour for small area fire,  
ambient wind = 20 m/s.

MISSION RESEARCH CORPORATION  
URBAN FIRE MODEL  
PLOT SIMULATION TIME = 3000.00 SECONDS  
ROWS 1 TO 90, COLUMNS 1 TO 90  
ONLY MAP: LETTERS A TO Z ARE A MAP OF CITY PLACES  
ONLY MAP: OTHER CELL ARE ARE COLUMNS TO PLACES  
ONLY SCALE IS LOGARITHMIC BASE 10 ( 0=1.00 9=1.00 )

MISSION RESEARCH CORPORATION  
URBAN FIRE MODEL  
PLOT SIMULATION TIME = 3000.00 SECONDS  
ROWS 1 TO 90, COLUMNS 1 TO 90  
ONLY MAP: LETTERS A TO Z ARE A MAP OF CITY PLACES  
ONLY MAP: OTHER CELL ARE ARE COLUMNS TO PLACES  
ONLY SCALE IS LOGARITHMIC BASE 10 ( 0=1.00 9=1.00 )

4  
5  
135791357913579135791357913579

4  
4  
135791357913579135791357913579

MISSION RESEARCH CORPORATION  
URBAN FIRE MODEL  
PLOT SIMULATION TIME = 3000.00 SECONDS  
ROWS 1 TO 90, COLUMNS 1 TO 90  
ONLY MAP: LETTERS A TO Z ARE A MAP OF CITY PLACES  
ONLY MAP: OTHER CELL ARE ARE COLUMNS TO PLACES  
ONLY SCALE IS LOGARITHMIC BASE 10 ( 0=1.00 9=1.00 )

MISSION RESEARCH CORPORATION  
URBAN FIRE MODEL  
PLOT SIMULATION TIME = 3000.00 SECONDS  
ROWS 1 TO 90, COLUMNS 1 TO 90  
ONLY MAP: LETTERS A TO Z ARE A MAP OF CITY PLACES  
ONLY MAP: OTHER CELL ARE ARE COLUMNS TO PLACES  
ONLY SCALE IS LOGARITHMIC BASE 10 ( 0=1.00 9=1.00 )

4  
4  
135791357913579135791357913579

43  
34  
4 4  
34  
4  
135791357913579135791357913579

Figure 6-8(j). Cell production rate map for small area fire,  
ambient wind = 20 m/s.

[illegible]

COOPERATION WITH THE POLICE

**CORRECTION**

1. **Introduction**

A large number 4 is formed by a grid of smaller 4s. The grid is roughly 10 units wide and 10 units high. In the center of the grid, where the horizontal and vertical lines of 4s intersect, there is a single digit 5.

CONFERENCER: NANCY L. M. BARNETT

279

[illegible]

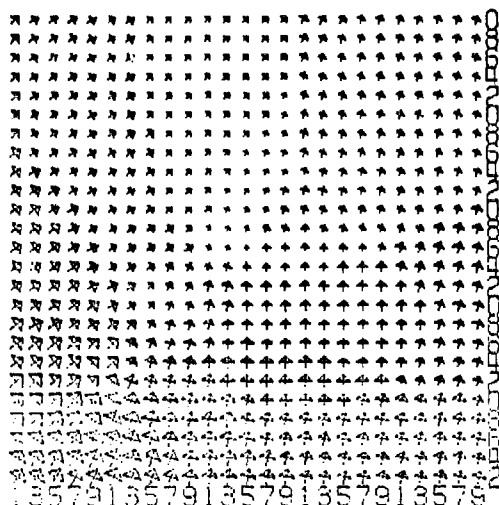
|   |   |   |   |   |   |   |   |   |    |    |    |    |    |    |    |    |    |    |    |    |    |    |    |    |    |    |    |    |    |    |    |    |    |    |    |    |    |    |    |    |    |    |    |    |    |    |    |    |    |    |    |    |    |    |    |    |    |    |    |    |    |    |    |    |    |    |    |    |    |    |    |    |    |    |    |    |    |    |    |    |    |    |    |    |    |    |    |    |    |    |    |    |    |    |    |    |    |    |     |
|---|---|---|---|---|---|---|---|---|----|----|----|----|----|----|----|----|----|----|----|----|----|----|----|----|----|----|----|----|----|----|----|----|----|----|----|----|----|----|----|----|----|----|----|----|----|----|----|----|----|----|----|----|----|----|----|----|----|----|----|----|----|----|----|----|----|----|----|----|----|----|----|----|----|----|----|----|----|----|----|----|----|----|----|----|----|----|----|----|----|----|----|----|----|----|----|----|----|----|-----|
| 1 | 2 | 3 | 4 | 5 | 6 | 7 | 8 | 9 | 10 | 11 | 12 | 13 | 14 | 15 | 16 | 17 | 18 | 19 | 20 | 21 | 22 | 23 | 24 | 25 | 26 | 27 | 28 | 29 | 30 | 31 | 32 | 33 | 34 | 35 | 36 | 37 | 38 | 39 | 40 | 41 | 42 | 43 | 44 | 45 | 46 | 47 | 48 | 49 | 50 | 51 | 52 | 53 | 54 | 55 | 56 | 57 | 58 | 59 | 60 | 61 | 62 | 63 | 64 | 65 | 66 | 67 | 68 | 69 | 70 | 71 | 72 | 73 | 74 | 75 | 76 | 77 | 78 | 79 | 80 | 81 | 82 | 83 | 84 | 85 | 86 | 87 | 88 | 89 | 90 | 91 | 92 | 93 | 94 | 95 | 96 | 97 | 98 | 99 | 100 |
|---|---|---|---|---|---|---|---|---|----|----|----|----|----|----|----|----|----|----|----|----|----|----|----|----|----|----|----|----|----|----|----|----|----|----|----|----|----|----|----|----|----|----|----|----|----|----|----|----|----|----|----|----|----|----|----|----|----|----|----|----|----|----|----|----|----|----|----|----|----|----|----|----|----|----|----|----|----|----|----|----|----|----|----|----|----|----|----|----|----|----|----|----|----|----|----|----|----|----|-----|

280



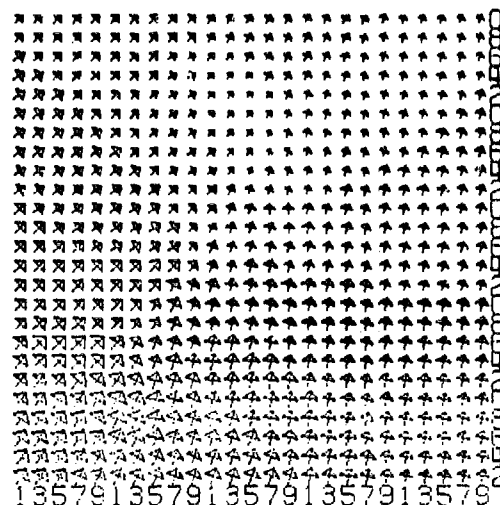
MISSION RESEARCH CORPORATION  
URBAN FIRE MODEL

PLAT RELEASE ON TIME = 4900.00  
DATE 1 TO 00. 00.000000 1 TO 00.000000  
WILL HAVE VELOCITY AND DIRECTION DATA IN DIRECTION OF WIND.  
WIND SIZE IS PROPORTIONAL TO THE SIZE OF THE  
ONLY EVERY OTHER CELL AND ONE COLUMN IS PLATED  
MAXIMUM WIND VELOCITY MAGNITUDE = 01.0000



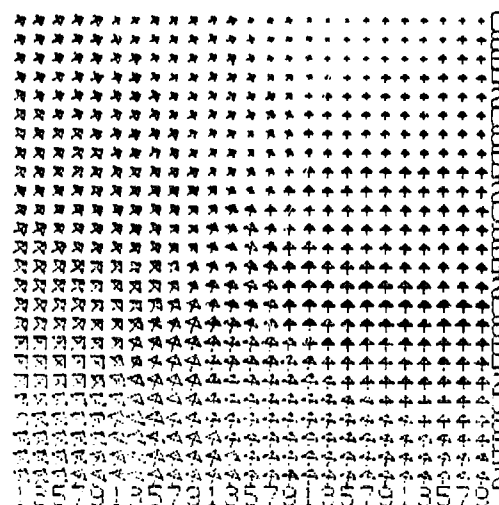
MISSION RESEARCH CORPORATION  
URBAN FIRE MODEL

PLAT RELEASE ON TIME = 4900.00  
DATE 1 TO 00. 00.000000 1 TO 00.000000  
WILL HAVE VELOCITY AND DIRECTION DATA IN DIRECTION OF WIND.  
WIND SIZE IS PROPORTIONAL TO THE SIZE OF THE  
ONLY EVERY OTHER CELL AND ONE COLUMN IS PLATED  
MAXIMUM WIND VELOCITY MAGNITUDE = 01.0000



MISSION RESEARCH CORPORATION  
URBAN FIRE MODEL

PLAT RELEASE ON TIME = 4900.00  
DATE 1 TO 00. 00.000000 1 TO 00.000000  
WILL HAVE VELOCITY AND DIRECTION DATA IN DIRECTION OF WIND.  
WIND SIZE IS PROPORTIONAL TO THE SIZE OF THE  
ONLY EVERY OTHER CELL AND ONE COLUMN IS PLATED  
MAXIMUM WIND VELOCITY MAGNITUDE = 01.0000



MISSION RESEARCH CORPORATION  
URBAN FIRE MODEL

PLAT RELEASE ON TIME = 4900.00  
DATE 1 TO 00. 00.000000 1 TO 00.000000  
WILL HAVE VELOCITY AND DIRECTION DATA IN DIRECTION OF WIND.  
WIND SIZE IS PROPORTIONAL TO THE SIZE OF THE  
ONLY EVERY OTHER CELL AND ONE COLUMN IS PLATED  
MAXIMUM WIND VELOCITY MAGNITUDE = 01.0000

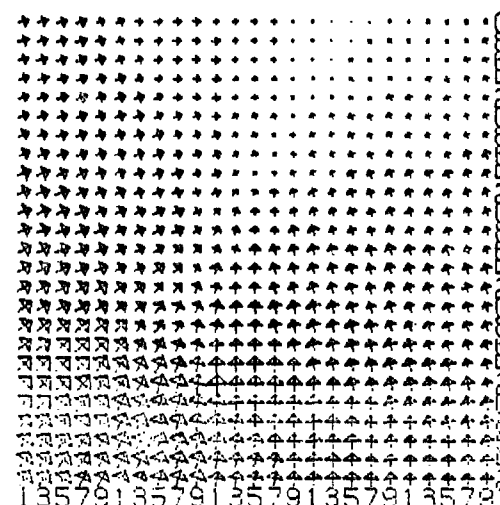


Figure 6-8(m). Wind velocity map for small area fire,  
ambient wind = 20 m/s.

```

PLOT SIMULATION TIME = 1440.00 SECONDS
ROWS 1 TO 50, COLUMNS 1 TO 50.
ROW 50
ROW 49
ROW 48
ROW 47
ROW 46
ROW 45
ROW 44
ROW 43
ROW 42
ROW 41
ROW 40
ROW 39
ROW 38
ROW 37
ROW 36
ROW 35
ROW 34
ROW 33
ROW 32
ROW 31
ROW 30
ROW 29
ROW 28
ROW 27
ROW 26
ROW 25
ROW 24
ROW 23
ROW 22
ROW 21
ROW 20
ROW 19
ROW 18
ROW 17
ROW 16
ROW 15
ROW 14
ROW 13
ROW 12
ROW 11
ROW 10
ROW 9
ROW 8
ROW 7
ROW 6
ROW 5
ROW 4
ROW 3
ROW 2
ROW 1
COLUMNS 12345678901234567890123456789012345678901234567890
NUMBER OF UNIGNITED, BURNING AND BURNED-OUT CELLS = 2491 9

```

Figure 6-9. Cell state map for small area fire, ambient wind = 30 m/s.

```

PLOT SIMULATION TIME = 1254.84 SECONDS
ROWS 1 TO 54, COLUMNS 1 TO 50,
ROW 54
ROW 49
ROW 48

ROW 47
ROW 46
ROW 45
ROW 44
ROW 43
ROW 42
ROW 41
ROW 40
ROW 39
ROW 38
ROW 37
ROW 36
ROW 35
ROW 34
ROW 33
ROW 32
ROW 31
ROW 30
ROW 29
ROW 28
ROW 27
ROW 26
ROW 25
ROW 24
ROW 23
ROW 22
ROW 21
ROW 20
ROW 19
ROW 18
ROW 17
ROW 16
ROW 15
ROW 14
ROW 13
ROW 12
ROW 11
ROW 10
ROW 9
ROW 8
ROW 7
ROW 6
ROW 5
ROW 4
ROW 3
ROW 2
ROW 1
COLUMNS 1234567890123456789012345678901234567890
NUMBER OF UNIGNITED, BURNING AND BURNED-OUT CELLS = 2489 11

```

Figure 6-9(a). Cell state map for small area fire, ambient wind = 30 m/s.

```

PLOT SIMULATION TIME = 1750.00 SECONDS
ROWS 1 TO 54 COLUMNS 1 TO 54
ROW 53
ROW 49
ROW 48
ROW 47
ROW 46
ROW 45
ROW 44
ROW 43
ROW 42

ROW 41
ROW 40
ROW 39
ROW 38
ROW 37
ROW 36
ROW 35
ROW 34
ROW 33
ROW 32
ROW 31
ROW 30
ROW 29
ROW 28
ROW 27
ROW 26
ROW 25
ROW 24
ROW 23
ROW 22
ROW 21
ROW 20
ROW 19
ROW 18
ROW 17
ROW 16
ROW 15
ROW 14
ROW 13
ROW 12
ROW 11
ROW 10
ROW 9
ROW 8
ROW 7
ROW 6
ROW 5
ROW 4
ROW 3
ROW 2
ROW 1
COLUMNS 12345678901234567890123456789012345678901234567890
NUMBER OF UNIGNITED, BURNING AND BURNED-OUT CELLS = 2479 30

```

Figure 6-9(b) Cell state map for small area fire, ambient wind = 30 m/s.

```

PLOT SIMULATION TIME = 2750.00 SECONDS
ROWS 1 TO 50, COLUMNS 1 TO 50.

ROW 50
ROW 49
ROW 48
ROW 47
ROW 46
ROW 45
ROW 44
ROW 43
ROW 42
ROW 41
ROW 40
ROW 39
ROW 38
ROW 37
ROW 36

ROW 35
ROW 34
ROW 33
ROW 32
ROW 31
ROW 30
ROW 29
ROW 28
ROW 27
ROW 26
ROW 25
ROW 24
ROW 23
ROW 22
ROW 21
ROW 20
ROW 19
ROW 18
ROW 17
ROW 16
ROW 15
ROW 14
ROW 13
ROW 12
ROW 11
ROW 10
ROW 9
ROW 8
ROW 7
ROW 6
ROW 5
ROW 4
ROW 3
ROW 2
ROW 1

COLUMNS 12345678901234567890123456789012345678901234567890
NUMBER OF UNIGNITED, BURNING AND BURNED-OUT CELLS = 2415 85

```

Figure 6-9(c). Cell state map for small area fire, ambient wind = 30 m/s

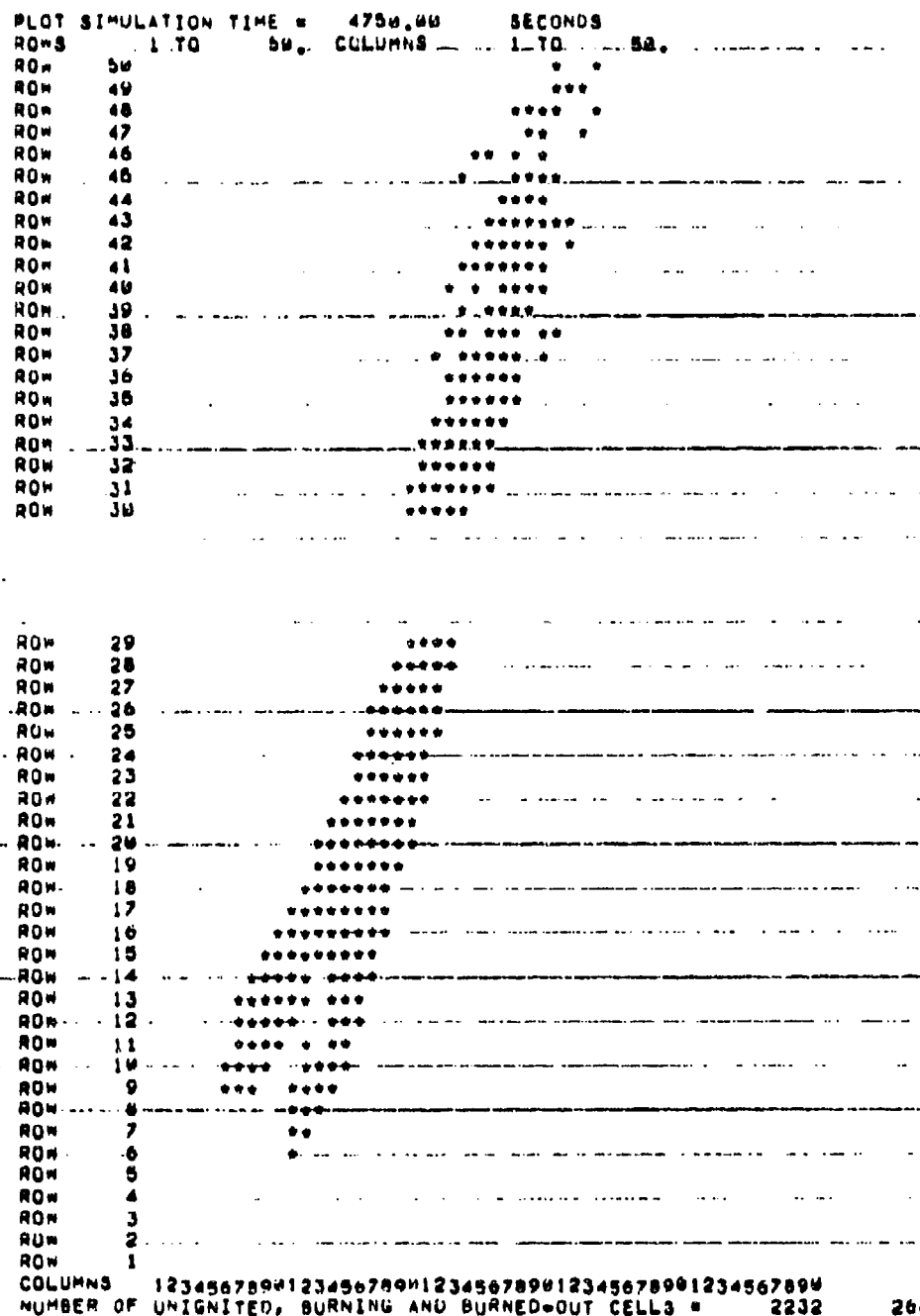


Figure 6-9(d). Cell state map for small area fire, ambient wind = 30 m/s.

```

PLOT SIMULATION TIME = 4750.00 SECONDS
ROWS 1 TO 50, COLUMNS 1 TO 50.
ROW 50 *****
ROW 49 *****
ROW 48 *****
ROW 47 *****
ROW 46 *****
ROW 45 *****
ROW 44 *****
ROW 43 *****
ROW 42 *****
ROW 41 *****
ROW 40 *****
ROW 39 *****
ROW 38 *****
ROW 37 *****
ROW 36 *****
ROW 35 *****
ROW 34 *****
ROW 33 *****
ROW 32 *****
ROW 31 *****
ROW 30 *****
ROW 29 *****
ROW 28 *****
ROW 27 *****
ROW 26 *****
ROW 25 *****
ROW 24 *****

ROW 23 *****
ROW 22 *****
ROW 21 *****
ROW 20 *****
ROW 19 *****
ROW 18 *****
ROW 17 *****
ROW 16 *****
ROW 15 *****
ROW 14 *****
ROW 13 *****
ROW 12 *****
ROW 11 *****
ROW 10 *****
ROW 9 *****
ROW 8 *****
ROW 7 *****
ROW 6 *****
ROW 5 *****
ROW 4 *****
ROW 3 *****
ROW 2 *****
ROW 1 *****
COLUMNS 12345678901234567890123456789012345678901234567890
NUMBER OF UNIGNITED, BURNING AND BURNED-OUT CELLS = 2000 420

```

Figure 6-9(e). Cell state map for small area fire, ambient wind = 30 m/s.

```

PLOT SIMULATION TIME = 10754.0 SECONDS
ROWS 1 TO 50, COLUMNS 1 TO 50,
ROW 50 *****
ROW 49 *****
ROW 48 *****
ROW 47 *****
ROW 46 *****
ROW 45 *****
ROW 44 *****
ROW 43 *****
ROW 42 *****
ROW 41 *****
ROW 40 *****
ROW 39 *****
ROW 38 *****
ROW 37 *****
ROW 36 *****
ROW 35 *****
ROW 34 *****
ROW 33 *****
ROW 32 *****
ROW 31 *****
ROW 30 *****
ROW 29 *****
ROW 28 *****
ROW 27 *****
ROW 26 *****
ROW 25 *****
ROW 24 *****
ROW 23 *****
ROW 22 *****
ROW 21 *****
ROW 20 *****
ROW 19 *****
ROW 18 *****

ROW 17 *****
ROW 16 *****
ROW 15 *****
ROW 14 *****
ROW 13 *****
ROW 12 *****
ROW 11 *****
ROW 10 *****
ROW 9 *****
ROW 8 *****
ROW 7 *****
ROW 6 *****
ROW 5 *****
ROW 4 *****
ROW 3 *****
ROW 2 *****
ROW 1 *****
COLUMNS 12345678901234567890123456789012345678901234567890
NUMBER OF UNIGNITED, BURNING AND BURNED-OUT CELLS = 1903 561 1

```

Figure 6-9(f). Cell state map for small area fire, ambient wind = 30 m/s.



```

PLOT SIMULATION TIME = 3275.00 SECONDS
ROWS 1 TO 50, COLUMNS 1 TO 50.
ROW 50 .....
ROW 49 .....
ROW 48 .....
ROW 47 .....
ROW 46 .....
ROW 45 .....
ROW 44 .....
ROW 43 .....
ROW 42 .....
ROW 41 .....
ROW 40 .....
ROW 39 .....
ROW 38 .....
ROW 37 .....
ROW 36 .....
ROW 35 .....
ROW 34 .....
ROW 33 .....
ROW 32 .....
ROW 31 .....
ROW 30 .....
ROW 29 .....
ROW 28 .....
ROW 27 .....
ROW 26 .....
ROW 25 .....
ROW 24 .....
ROW 23 .....
ROW 22 .....
ROW 21 .....
ROW 20 .....
ROW 19 .....
ROW 18 .....
ROW 17 .....
ROW 16 .....
ROW 15 .....
ROW 14 .....
ROW 13 .....
ROW 12 .....

ROW 11 *RRRRRRRRRRRRRR*
ROW 10 RRRRRRRRRRRRR*
ROW 9  RRRRRRRRRRR*
ROW 8   RRRRRRR*
ROW 7    RRRRR*
ROW 6     RR*
ROW 5
ROW 4
ROW 3
ROW 2
ROW 1

COLUMNS 1234567890123456789012345678901234567890
NUMBER OF UNIGNITED, BURNING AND BURNED-OUT CELLS = 1662 521 29

```

Figure 6-9(g). Cell state map for small area fire, ambient wind = 30 m/s.

MISSION RESEARCH CORPORATION  
URBAN FIRE MODEL  
PLOT SIMULATION TIME = 1000.00 SECONDS  
PDR 1 TO 99 COLUMNS 1 TO 99  
CELL NOT CONTAINING FIRE  
\*\*\* ONLY EVERY OTHER CELL ROW AND COLUMN IS PLOTTED \*\*\*  
GROSS SCALE IS LOGARITHMIC SCALE TO ( 0-1.25 0-1.25 )



1357913579135791357913579

MISSION RESEARCH CORPORATION  
URBAN FIRE MODEL  
PLOT SIMULATION TIME = 1000.00 SECONDS  
PDR 1 TO 99 COLUMNS 1 TO 99  
CELL NOT CONTAINING FIRE  
\*\*\* ONLY EVERY OTHER CELL ROW AND COLUMN IS PLOTTED \*\*\*  
GROSS SCALE IS LOGARITHMIC SCALE TO ( 0-1.25 0-1.25 )



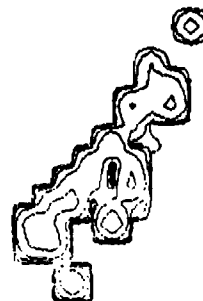
1357913579135791357913579

MISSION RESEARCH CORPORATION  
URBAN FIRE MODEL  
PLOT SIMULATION TIME = 1750.00 SECONDS  
PDR 1 TO 99 COLUMNS 1 TO 99  
CELL NOT CONTAINING FIRE  
\*\*\* ONLY EVERY OTHER CELL ROW AND COLUMN IS PLOTTED \*\*\*  
GROSS SCALE IS LOGARITHMIC SCALE TO ( 0-1.25 0-1.25 )



1357913579135791357913579

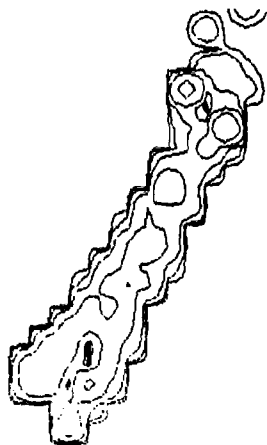
MISSION RESEARCH CORPORATION  
URBAN FIRE MODEL  
PLOT SIMULATION TIME = 2750.00 SECONDS  
PDR 1 TO 99 COLUMNS 1 TO 99  
CELL NOT CONTAINING FIRE  
\*\*\* ONLY EVERY OTHER CELL ROW AND COLUMN IS PLOTTED \*\*\*  
GROSS SCALE IS LOGARITHMIC SCALE TO ( 0-1.25 0-1.25 )



1357913579135791357913579

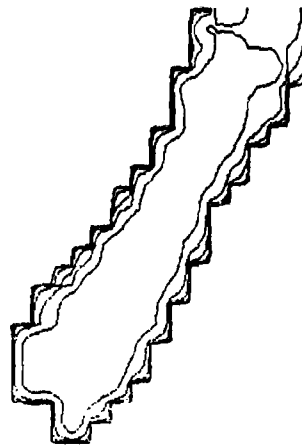
Figure 6-9(h). Heat production rate contour for small area fire,  
ambient wind = 30 m/s.

MISSION RESEARCH CORPORATION  
URBAN FIRE MODEL  
FLOW SIMULATION TIME = 4700.00 SECONDS  
WIND 1 TO 50.00 M/S. 1 TO 50.00  
WALL HEAT CONDUCTION ON  
\*\*\* ONLY EVERY OTHER WALL HEAT AND WIND IS PLOTTED \*\*\*  
ROOT SCALE IS LOGARITHMIC DIFF 10 ( 0-1.2% 0-1.210 )



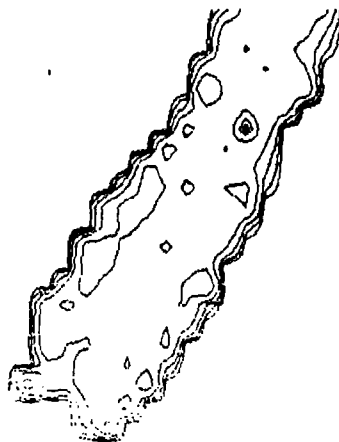
1357913579135791357913579

MISSION RESEARCH CORPORATION  
URBAN FIRE MODEL  
FLOW SIMULATION TIME = 5700.00 SECONDS  
WIND 1 TO 50.00 M/S. 1 TO 50.00  
WALL HEAT CONDUCTION ON  
\*\*\* ONLY EVERY OTHER WALL HEAT AND WIND IS PLOTTED \*\*\*  
ROOT SCALE IS LOGARITHMIC DIFF 10 ( 0-1.2% 0-1.210 )



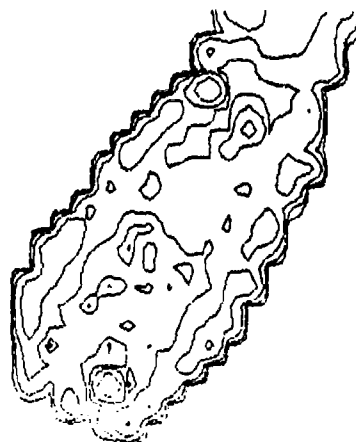
1357913579135791357913579

MISSION RESEARCH CORPORATION  
URBAN FIRE MODEL  
FLOW SIMULATION TIME = 10700.0 SECONDS  
WIND 1 TO 50.00 M/S. 1 TO 50.00  
WALL HEAT CONDUCTION ON  
\*\*\* ONLY EVERY OTHER WALL HEAT AND WIND IS PLOTTED \*\*\*  
ROOT SCALE IS LOGARITHMIC DIFF 10 ( 0-1.2% 0-1.210 )



1357913579135791357913579

MISSION RESEARCH CORPORATION  
URBAN FIRE MODEL  
FLOW SIMULATION TIME = 11700.0 SECONDS  
WIND 1 TO 50.00 M/S. 1 TO 50.00  
WALL HEAT CONDUCTION ON  
\*\*\* ONLY EVERY OTHER WALL HEAT AND WIND IS PLOTTED \*\*\*  
ROOT SCALE IS LOGARITHMIC DIFF 10 ( 0-1.2% 0-1.210 )



1357913579135791357913579

Figure 6-9(1). Heat production rate contour for small area fire, ambient wind = 30 m/s.

4

4

!357913579135791357913579

3  
3 4  
4  
1357913579135791357913579

4  
3 4  
3 4  
4 4  
4 4  
4

1357913579135791357913579

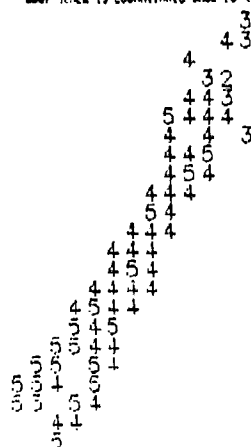
3  
3  
3 3  
4 3 3 4  
4 3 3  
4 4 3  
4 4 2 4 3  
4 4 4 4  
4 4 4  
4 4

5

1357913579135791357913579

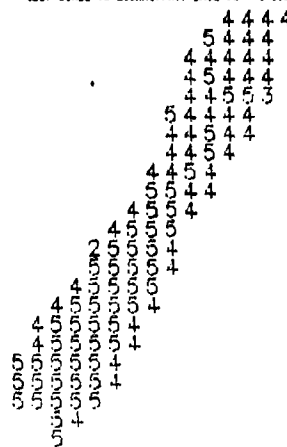
292

MISSION RESEARCH CORPORATION  
URBAN FIRE MODEL  
PLOT SIMULATION TIME = 4790.00 SECONDS  
DATE 1 10 84, 10:00:00, 1 10 84  
NOTE: MAP, LATTITUDE 0 10 0 AND 0 DEGREE OF SLOPE VALUES  
--- ONLY FIRST STIR CELL AND ONE COLUMN IS PLOTTED ---  
GRID SCALE IS LOGARITHMIC GRID 10 1 0-1.00 0-1.010



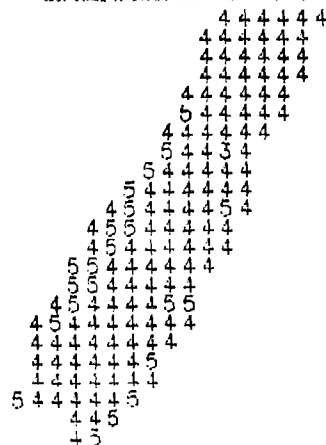
135791357913579135791357913579

MISSION RESEARCH CORPORATION  
URBAN FIRE MODEL  
PLOT SIMULATION TIME = 4790.00 SECONDS  
DATE 1 10 84, 10:00:00, 1 10 84  
NOTE: MAP, LATTITUDE 0 10 0 AND 0 DEGREE OF SLOPE VALUES  
--- ONLY FIRST STIR CELL AND ONE COLUMN IS PLOTTED ---  
GRID SCALE IS LOGARITHMIC GRID 10 1 0-1.00 0-1.010



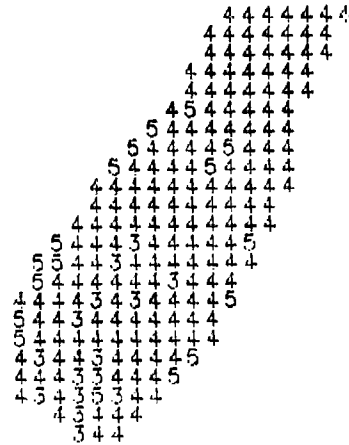
135791357913579135791357913579

MISSION RESEARCH CORPORATION  
URBAN FIRE MODEL  
PLOT SIMULATION TIME = 4790.00 SECONDS  
DATE 1 10 84, 10:00:00, 1 10 84  
NOTE: MAP, LATTITUDE 0 10 0 AND 0 DEGREE OF SLOPE VALUES  
--- ONLY FIRST STIR CELL AND ONE COLUMN IS PLOTTED ---  
GRID SCALE IS LOGARITHMIC GRID 10 1 0-1.00 0-1.010



135791357913579135791357913579

MISSION RESEARCH CORPORATION  
URBAN FIRE MODEL  
PLOT SIMULATION TIME = 4790.00 SECONDS  
DATE 1 10 84, 10:00:00, 1 10 84  
NOTE: MAP, LATTITUDE 0 10 0 AND 0 DEGREE OF SLOPE VALUES  
--- ONLY FIRST STIR CELL AND ONE COLUMN IS PLOTTED ---  
GRID SCALE IS LOGARITHMIC GRID 10 1 0-1.00 0-1.010



135791357913579135791357913579

Figure 6-9(k). Cell heat production rate map for small area fire, ambient wind = 30 m/s.

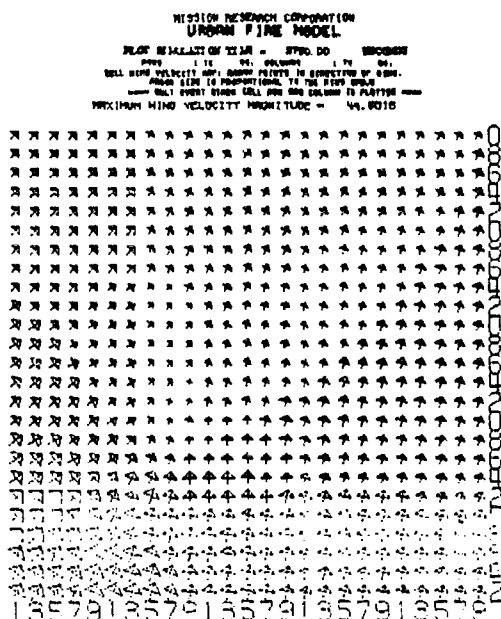
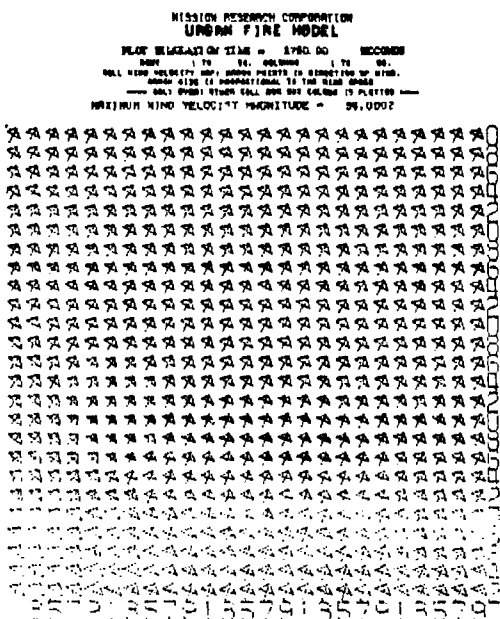
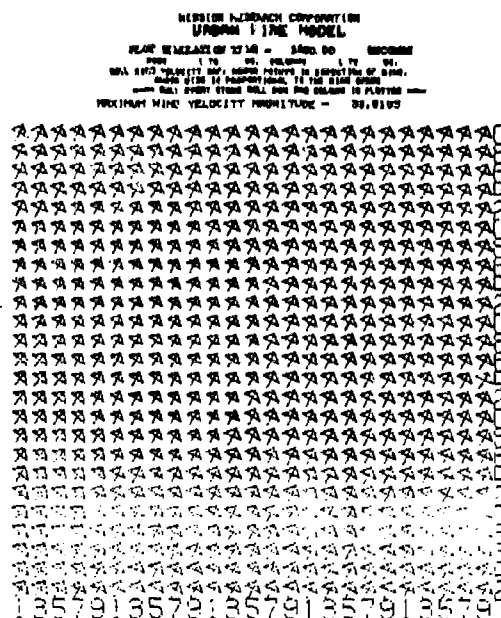
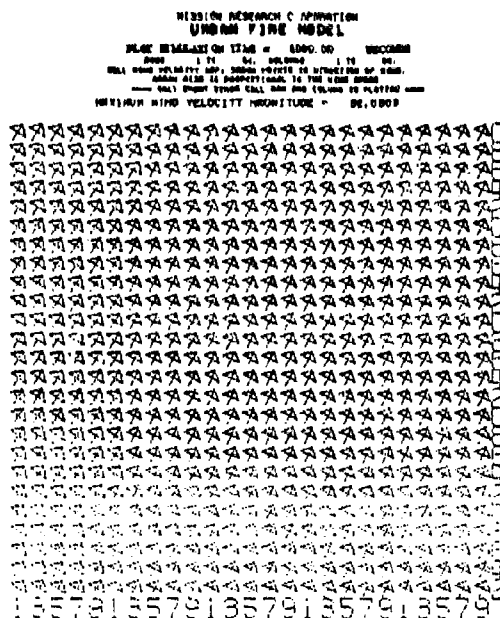


Figure 6-9(1). Wind velocity map for small area fire, ambient wind = 30 m/s.

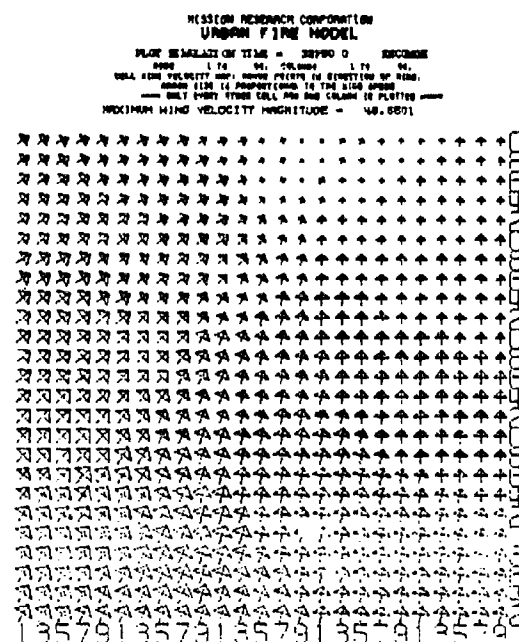
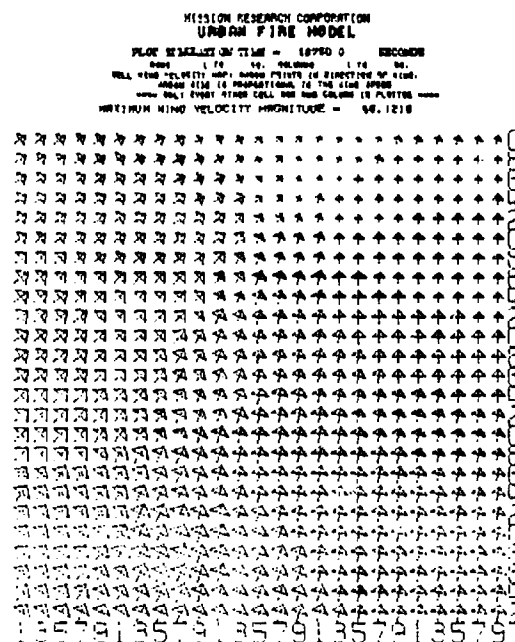
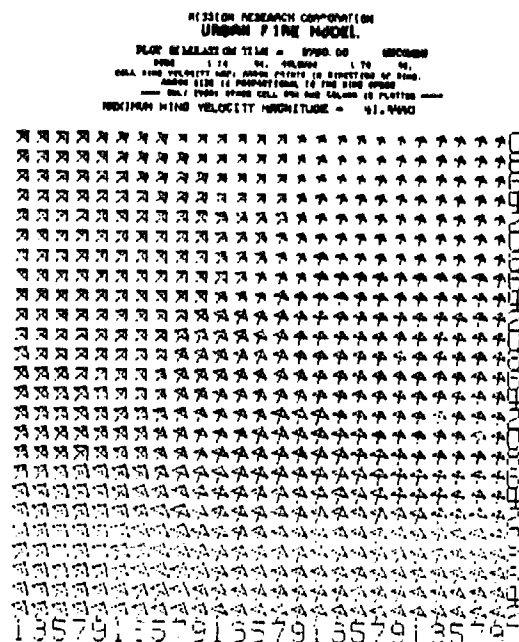
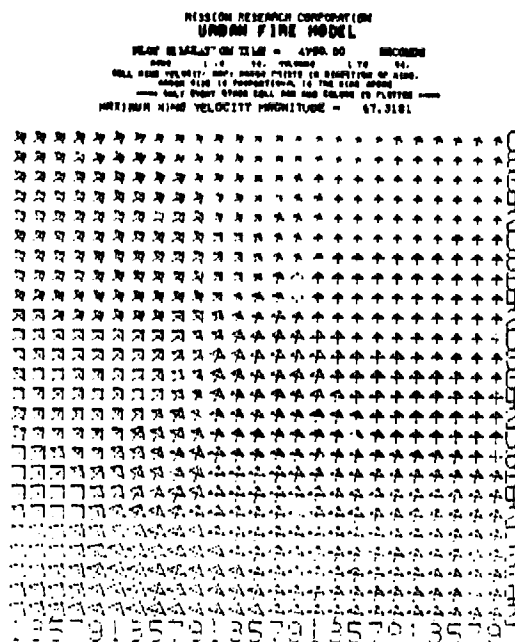


Figure 6-9(m). Wind velocity map for small area fire, ambient wind = 30 m/s.

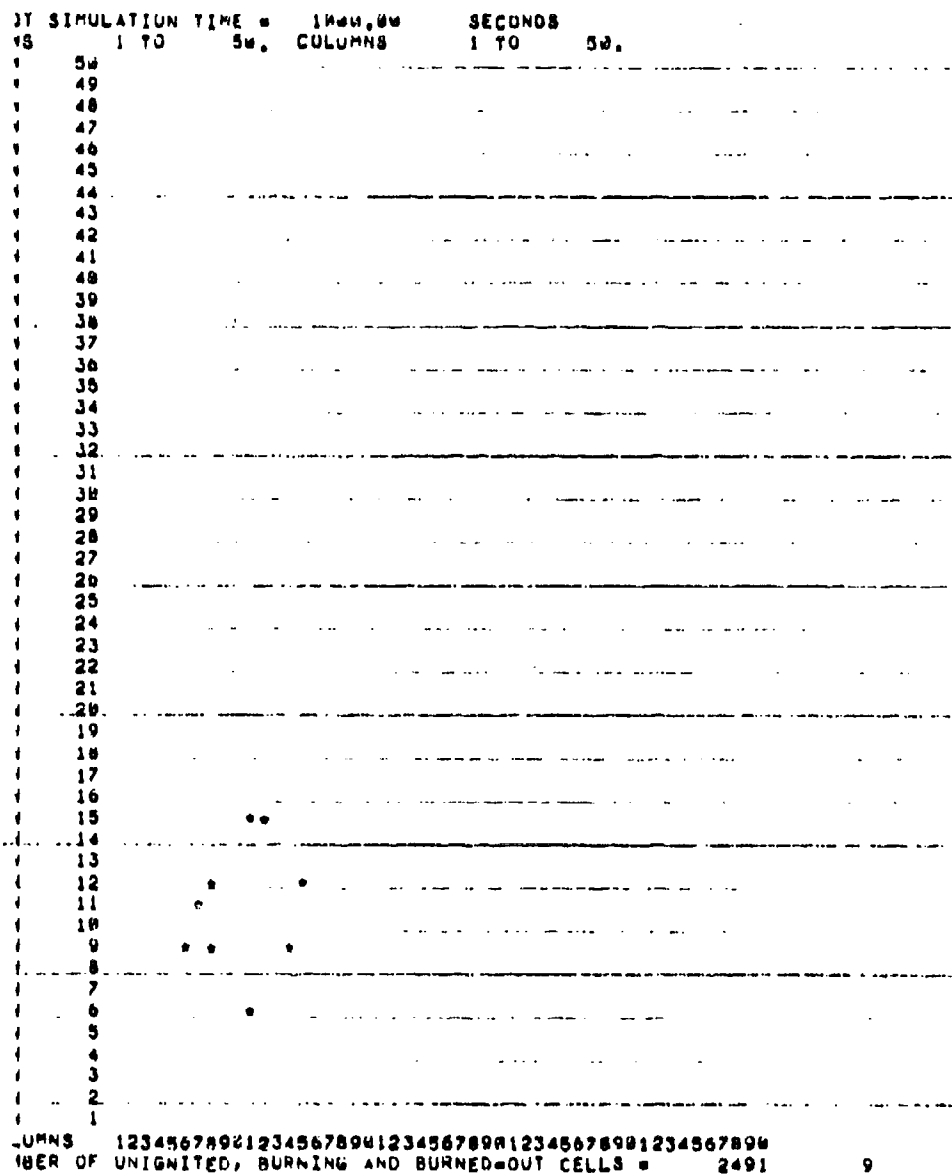


Figure 6-10. Cell state map for small area fire, ambient wind = 40 m/s.



•

IS 1 TO 50, COLUMNS 1 TO 50.

|   |    |
|---|----|
| 1 | 30 |
| 1 | 49 |
| 1 | 48 |

|   |    |
|---|----|
| 1 | 47 |
| 1 | 46 |
| 1 | 45 |
| 1 | 44 |
| 1 | 43 |
| 1 | 42 |
| 1 | 41 |
| 1 | 40 |
| 1 | 39 |
| 1 | 38 |
| 1 | 37 |
| 1 | 36 |
| 1 | 35 |
| 1 | 34 |
| 1 | 33 |
| 1 | 32 |
| 1 | 31 |
| 1 | 30 |
| 1 | 29 |
| 1 | 28 |
| 1 | 27 |
| 1 | 26 |
| 1 | 25 |
| 1 | 24 |
| 1 | 23 |
| 1 | 22 |
| 1 | 21 |
| 1 | 20 |
| 1 | 19 |
| 1 | 18 |
| 1 | 17 |
| 1 | 16 |
| 1 | 15 |
| 1 | 14 |
| 1 | 13 |
| 1 | 12 |
| 1 | 11 |
| 1 | 10 |
| 1 | 9  |
| 1 | 8  |
| 1 | 7  |
| 1 | 6  |
| 1 | 5  |
| 1 | 4  |
| 1 | 3  |
| 1 | 2  |

.UJNB 12345678901234567890123456789012345678901234567890  
IBER OF UNIGATED, BURNING AND BURNED-OUT CELLS = 2400

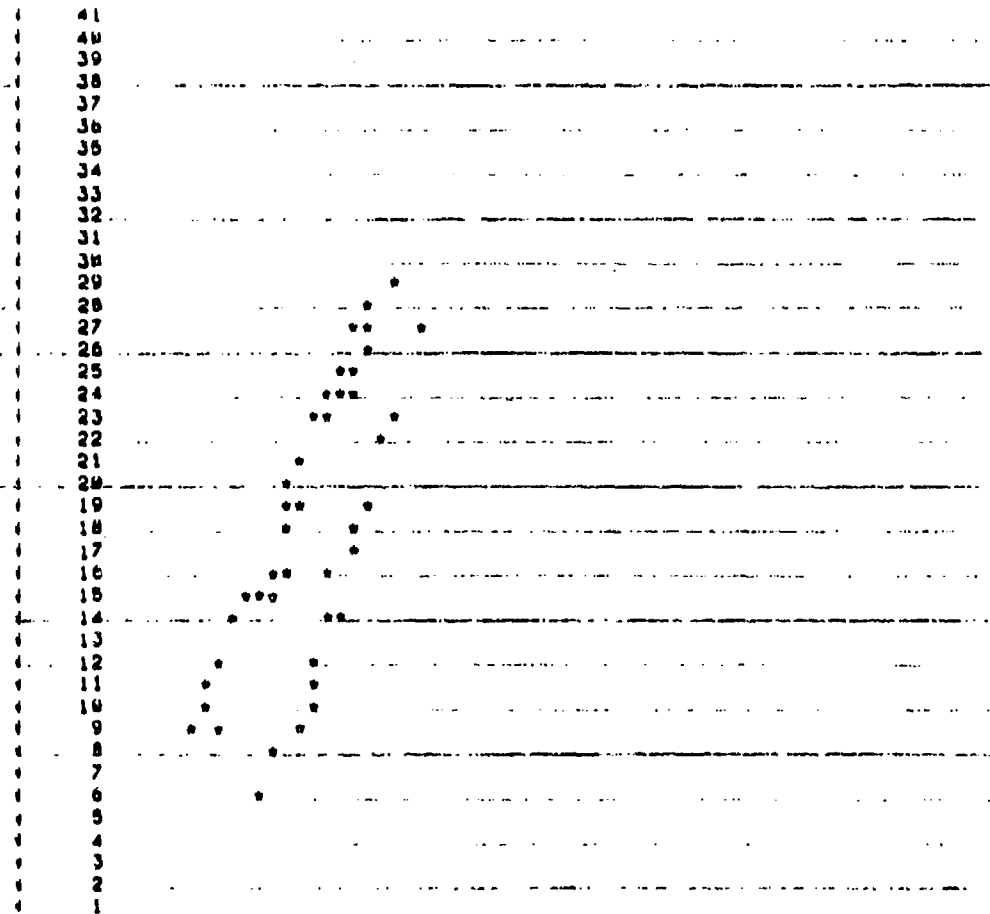
12

297

COLUMNS 12345678901234567890123456789012345678901234567890  
 NUMBER OF UNIGNITED, BURNING AND BURNED-OUT CELLS = 2488 12

IT SIMULATION TIME = 1758.00 SECONDS

IS 1 TO 80, COLUMNS 1 TO 80, ROWS 1 TO 40



COLUMNS 12345678901234567890123456789012345678901234567890  
 NUMBER OF UNIGNITED, BURNING AND BURNED-OUT CELLS = 2457 43

Figure 6-10(b). Cell state map for small area fire, ambient wind = 40 m/s.

49  
49  
48  
47  
46  
45  
44  
43  
42  
41  
40  
39  
38  
37  
36

UNMS 12345678901234567890123456789012345678901234567890  
NUMBER OF UNIGNITED, BURNING AND BURNED-OUT CELLS • 2532 168

299

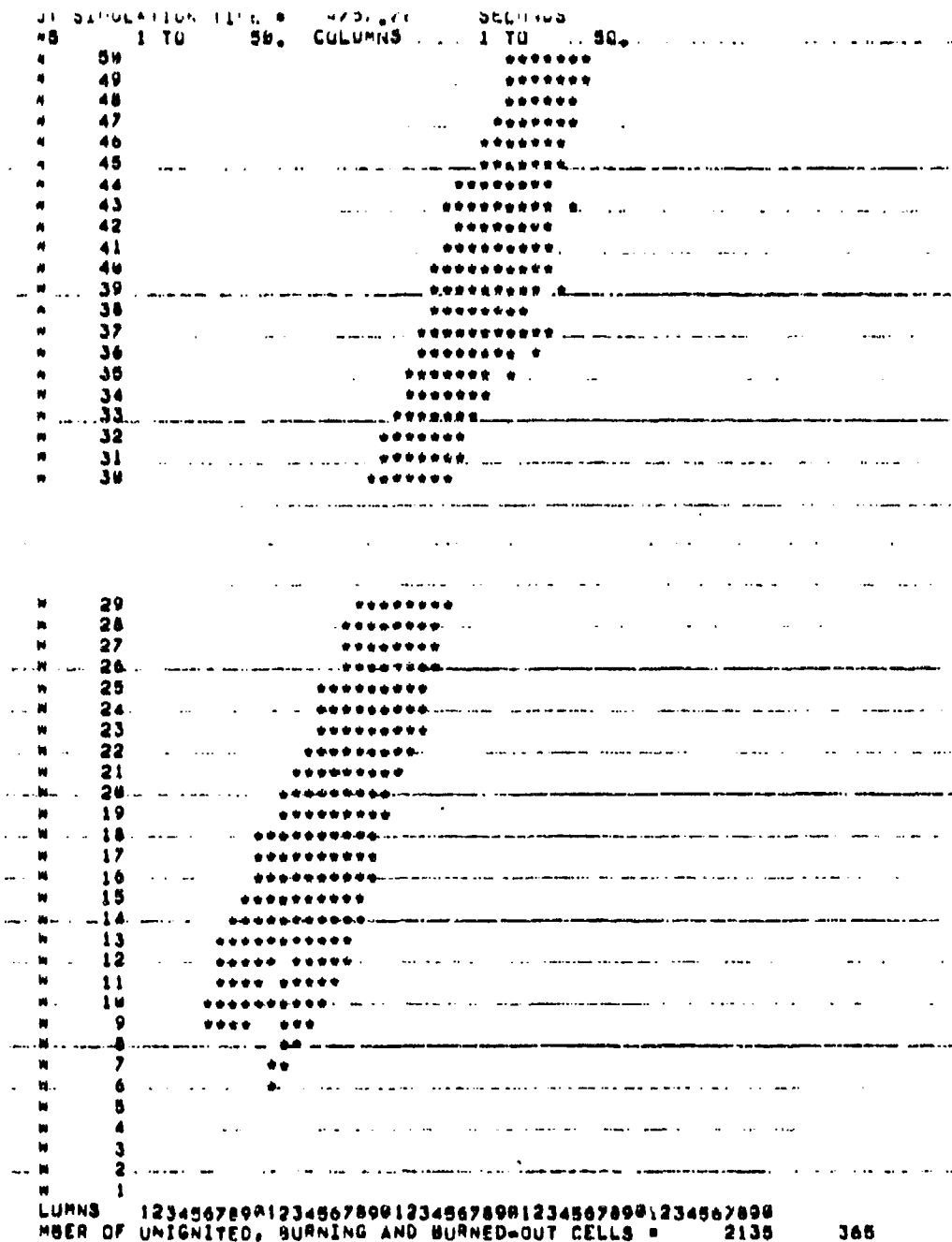


Figure 6-10(d). Cell state map for small area fire, ambient wind = 40 m/s.

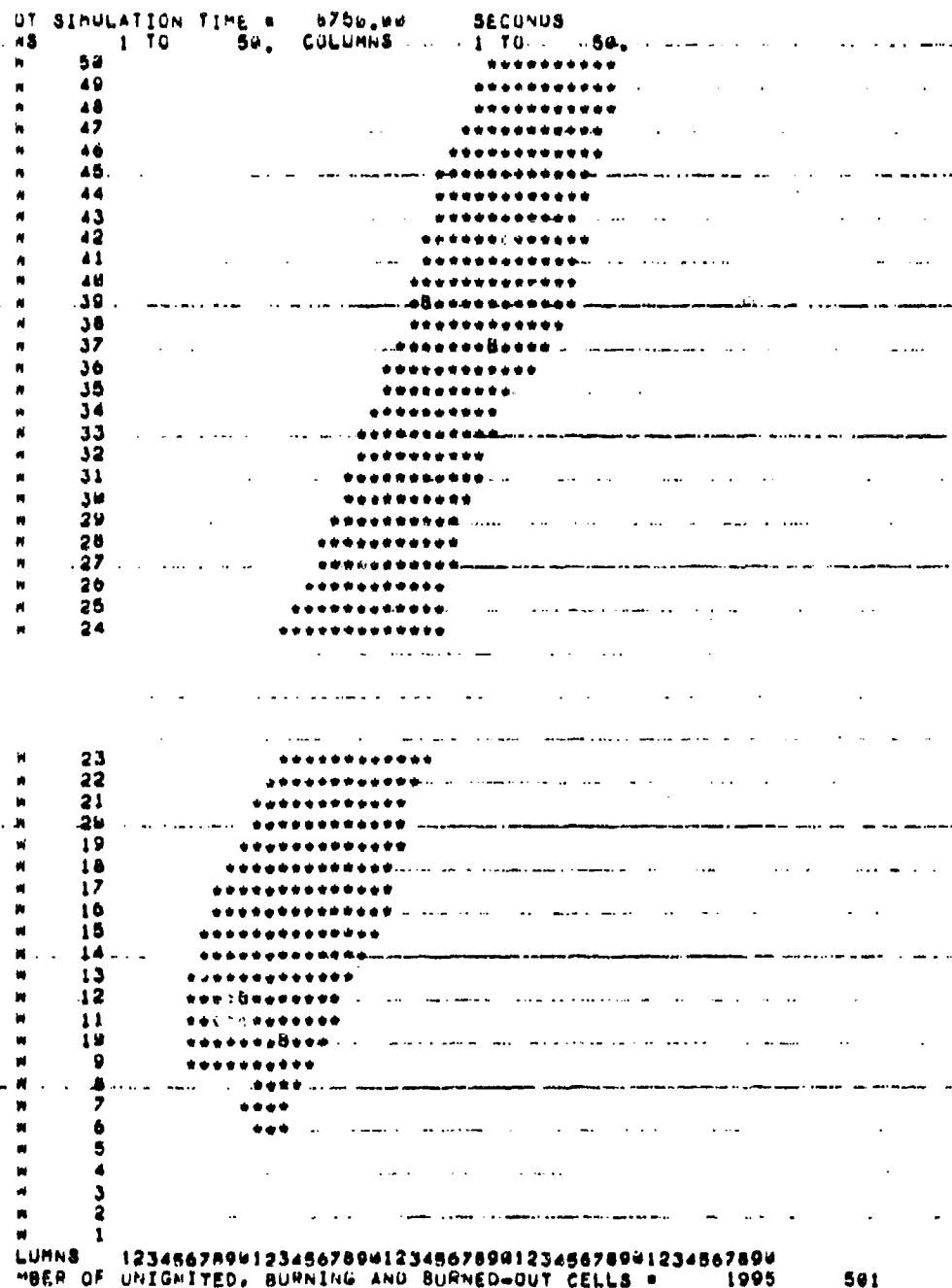


Figure 6-10(e). Cell state map for small area fire, ambient wind = 40 m/s.

DT SIMULATION TIME = 16754.0 SECONDS  
 WS 1 TO 50, COLUMNS 1 TO 50.

```

    50 *****
    49 *****
    48 *****
    47 *****
    46 *****B*****
    45 *****
    44 *****
    43 *****
    42 *****
    41 *****
    40 *****
    39 *****B*****
    38 *****
    37 *****B*****
    36 *****
    35 *****
    34 *****
    33 *****
    32 *****
    31 *****
    30 *****
    29 *****
    28 *****
    27 *****
    26 *****
    25 *****
    24 *****
    23 *****B*****
    22 *****
    21 *****B*****
    20 *****B*****
    19 *****
    18 *****

    17 *****
    16 *****
    15 *****
    14 *****B*****
    13 *****
    12 *****B*****
    11 *****B*****
    10 *****B*****
    9 *****B*****
    8 *****
    7 *****
    6 *****
    5
    4
    3
    2
    1
  
```

LUMNS 1234567890123456789012345678901234567890  
 MBER OF UNIGNITED, BURNING AND BURNED-OUT CELLS = 1772 767 21

Figure 6-10(f). Cell state map for small area fire, ambient wind  
 = 40 m/s.

OT SIMULATION TIME = 32750.0 SECONDS

MS 1 TO 50, COLUMNS 1 TO 50.

```

W 50 *****
W 49 *****
W 48 *****
W 47 *****
W 46 *****
W 45 *****
W 44 *****
W 43 *****
W 42 *****
W 41 *****
W 40 *****
W 39 *****
W 38 *****
W 37 *****
W 36 *****
W 35 *****
W 34 *****
W 33 *****
W 32 *****
W 31 *****
W 30 *****
W 29 *****
W 28 *****
W 27 *****
W 26 *****
W 25 *****
W 24 *****
W 23 *****
W 22 *****
W 21 *****
W 20 *****
W 19 *****
W 18 *****
W 17 *****
W 16 *****
W 15 *****
W 14 *****
W 13 *****
W 12 *****

```

```

W 11 *****
W 10 *****
W 9 *****
W 8 *****
W 7 *****
W 6 *****
W 5 *****
W 4 *****
W 3 *****
W 2 *****
W 1 *****

```

COLUMNS 12345678901234567890123456789012345678901234567890

NUMBER OF UNIGNITED, BURNING AND BURNED-OUT CELLS = 1410 514 57

Figure 6-10(g). Cell state map for small area fire, ambient wind = 40 m/s.

MISSION RESEARCH CORPORATION  
URBAN FIRE MODEL  
PLOT SIMULATION TIME = 1000.00 SECONDS  
TIME 1 TO 10 SECONDS 1 TO 10  
CELL NOT CONTAINING FIRE  
\*\*\* ONLY EVERY OTHER CELL AND ARE DRAWN IS PLOTTED \*\*\*  
SHOT SCALE IS LOGARITHMIC (BASE 10) (0-1.00 0-1.010)



1357913579135791357913579

MISSION RESEARCH CORPORATION  
URBAN FIRE MODEL  
PLOT SIMULATION TIME = 1750.00 SECONDS  
TIME 1 TO 10 SECONDS 1 TO 10  
CELL NOT CONTAINING FIRE  
\*\*\* ONLY EVERY OTHER CELL AND ARE DRAWN IS PLOTTED \*\*\*  
SHOT SCALE IS LOGARITHMIC (BASE 10) (0-1.00 0-1.010)



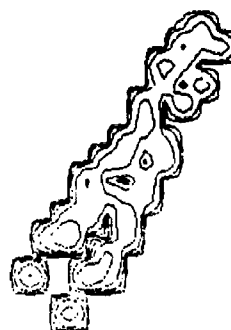
1357913579135791357913579

MISSION RESEARCH CORPORATION  
URBAN FIRE MODEL  
PLOT SIMULATION TIME = 1000.00 SECONDS  
TIME 1 TO 10 SECONDS 1 TO 10  
CELL NOT CONTAINING FIRE  
\*\*\* ONLY EVERY OTHER CELL AND ARE DRAWN IS PLOTTED \*\*\*  
SHOT SCALE IS LOGARITHMIC (BASE 10) (0-1.00 0-1.010)



1357913579135791357913579

MISSION RESEARCH CORPORATION  
URBAN FIRE MODEL  
PLOT SIMULATION TIME = 1750.00 SECONDS  
TIME 1 TO 10 SECONDS 1 TO 10  
CELL NOT CONTAINING FIRE  
\*\*\* ONLY EVERY OTHER CELL AND ARE DRAWN IS PLOTTED \*\*\*  
SHOT SCALE IS LOGARITHMIC (BASE 10) (0-1.00 0-1.010)

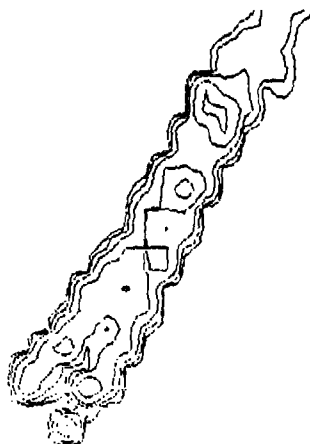


1357913579135791357913579

Figure 6-10(h). Heat production rate contour map for small area fire, ambient wind = 40 m/s.

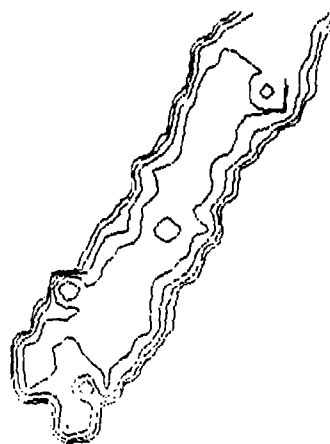


HERZOG RESEARCH CORPORATION  
URBAN FIRE MODEL  
FLUX SEPARATION TIME = 1700.00  
WIND 1 TO 10 10 10 10 10 10 10 10 10 10  
CELL SIZE CONTAINING 100  
\*\*\* ONLY EVERY OTHER CELL AND AND BOUNDARY IS PLOTTED \*\*\*  
GRID SCALE (3 LOGARITHMIC BYTES 10 (0-1.25 0-1.25))



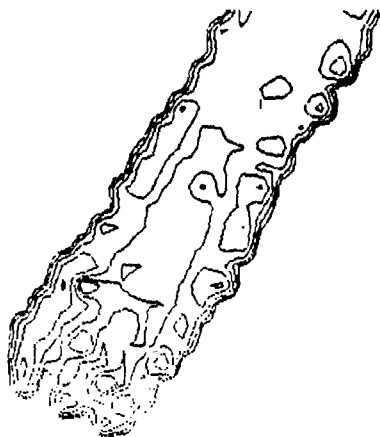
1357913579135791357913579

HERZOG RESEARCH CORPORATION  
URBAN FIRE MODEL  
FLUX SEPARATION TIME = 1700.00  
WIND 1 TO 10 10 10 10 10 10 10 10 10 10  
CELL SIZE CONTAINING 100  
\*\*\* ONLY EVERY OTHER CELL AND AND BOUNDARY IS PLOTTED \*\*\*  
GRID SCALE (3 LOGARITHMIC BYTES 10 (0-1.25 0-1.25))



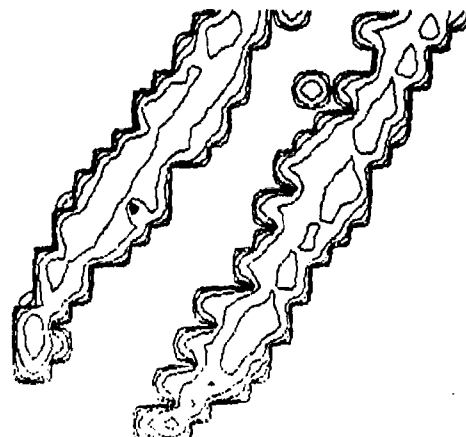
1357913579135791357913579

HERZOG RESEARCH CORPORATION  
URBAN FIRE MODEL  
FLUX SEPARATION TIME = 1700.00  
WIND 1 TO 10 10 10 10 10 10 10 10 10 10  
CELL SIZE CONTAINING 100  
\*\*\* ONLY EVERY OTHER CELL AND AND BOUNDARY IS PLOTTED \*\*\*  
GRID SCALE (3 LOGARITHMIC BYTES 10 (0-1.25 0-1.25))



1357913579135791357913579

HERZOG RESEARCH CORPORATION  
URBAN FIRE MODEL  
FLUX SEPARATION TIME = 1700.00  
WIND 1 TO 10 10 10 10 10 10 10 10 10 10  
CELL SIZE CONTAINING 100  
\*\*\* ONLY EVERY OTHER CELL AND AND BOUNDARY IS PLOTTED \*\*\*  
GRID SCALE (3 LOGARITHMIC BYTES 10 (0-1.25 0-1.25))



1357913579135791357913579

Figure 6-10(i). Heat production rate contour map for small area fire, ambient wind = 40 m/s.

# CHANGING NARRATIVE VOLUME

CONFIDENTIAL

COLEMAN, LUCAS, LUCAS, LUCAS, LUCAS

CONSTITUTIONAL COURT

306

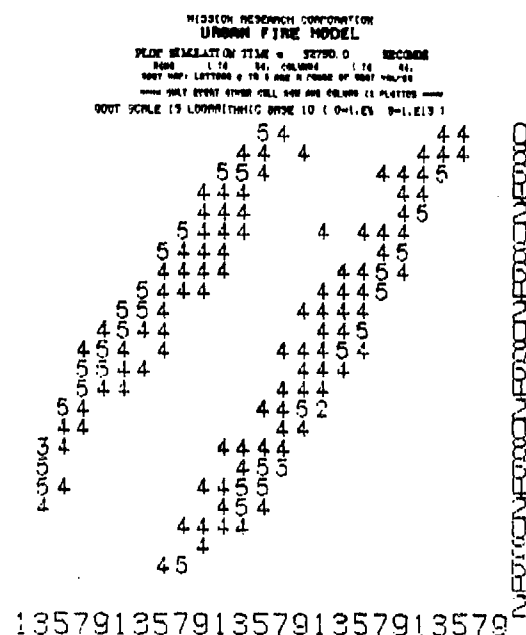
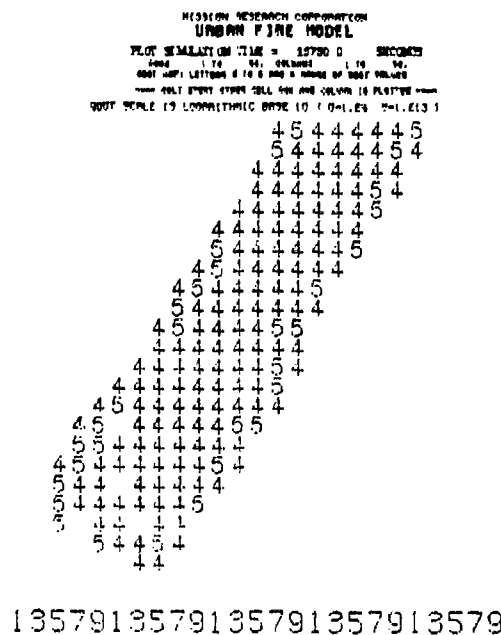
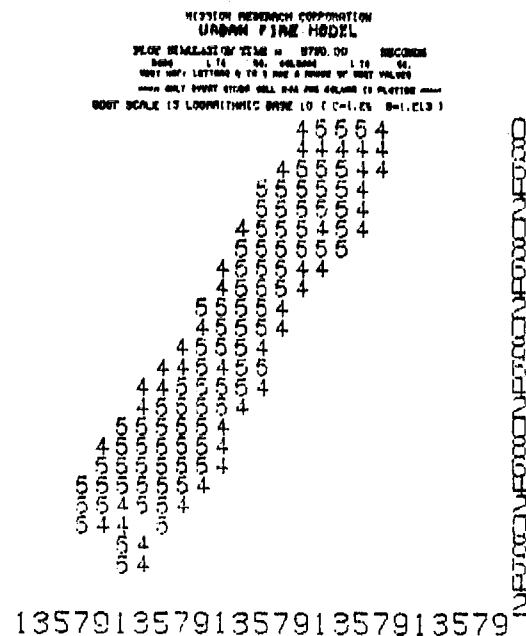
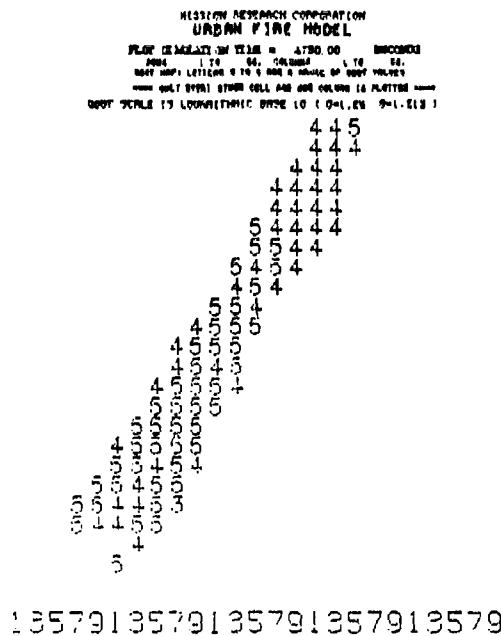


Figure 6-10(k). Cell heat production rate map for small area fire, ambient wind = 40 m/s.

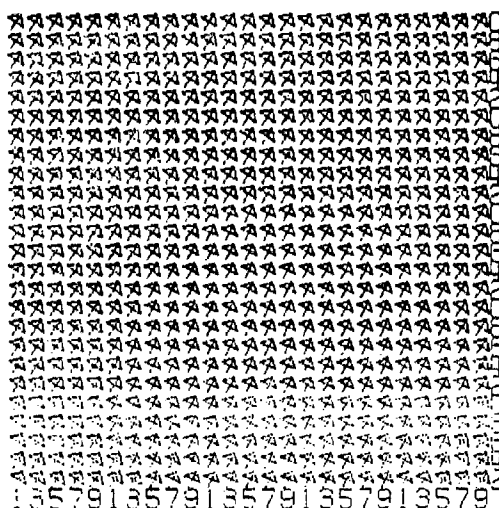
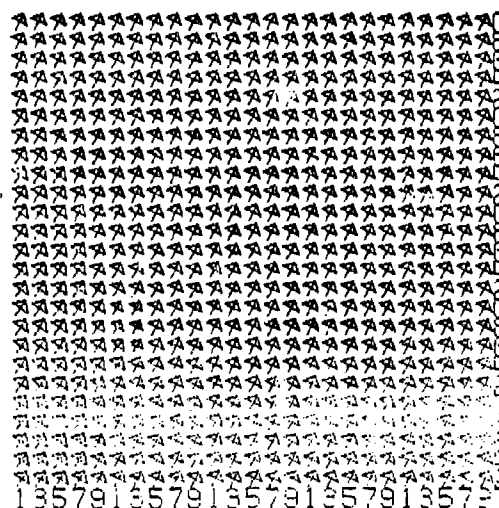
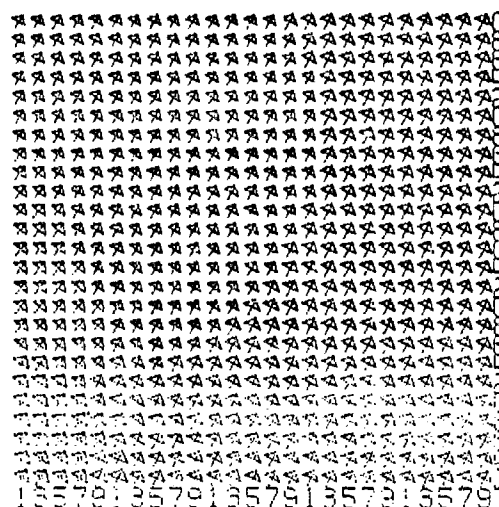
[illegible]

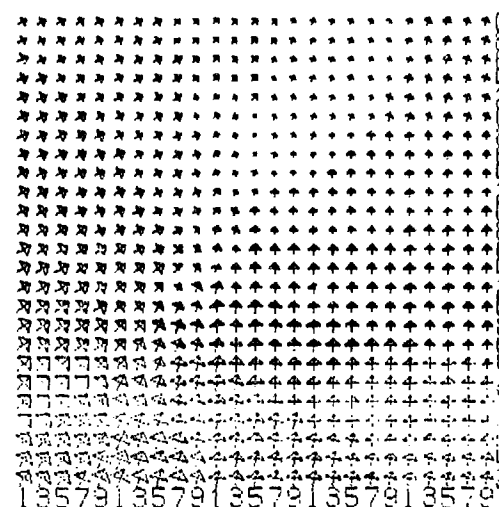
PLATE CHARACTERISTICS OF TUBE = 6X400P      MODULATION  
 GRID 1 TO 0V.      PLATE 1 TO 0V.  
 GMA. GMA. VOLTAGE SUP. 250V.      POINTS TO DIRECTOR OF REAR.  
 REAR.      SIDE 16.      POINTS TO THE REAR GMA.  
 REAR.      SIDE 16.      POINTS TO THE REAR GMA.  
 MAXIMUM WIND VELOCITY MEASUREMENT = 48.0 KNOTS



PLAN IN SALTATION FILE = 1980 DO RECORDS  
 DATE 1 14 04. 04.00000 1 14 04.  
 ALL RING VELOCITY INFO: NUMBER POINTS IN SPECTRUM OF RING.  
 ABOVE 1210 IS PHOTOGRAPHIC, 14 700 BLUE SPOTS  
 14 700: 14 700: OTHER DATA AND HAS COLUMN TO PLOTTER  
 RING RING VELOCITY MAGNITUDE = 94.7867



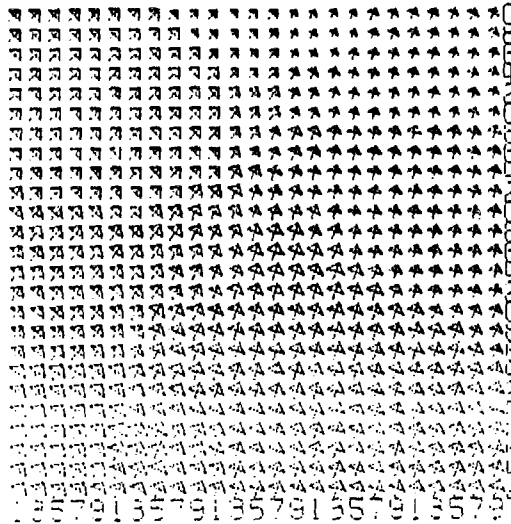
HEAT MEASUREMENT TIME = 1700.00      SMOKEOUT  
 1 TO 00. CALIBRATION      1 TO 00.  
 BALL WIND VELOCITY: 0000.0000 IN DIRECTION OF RISE.  
 NUMBER 110 IS POSITIVE, TO THE RISE 0000  
 BALL FLYING UPON BALL AND BALLS IN FLIGHT  
 MAXIMUM WIND VELOCITY MAGNITUDE = 00.872



308

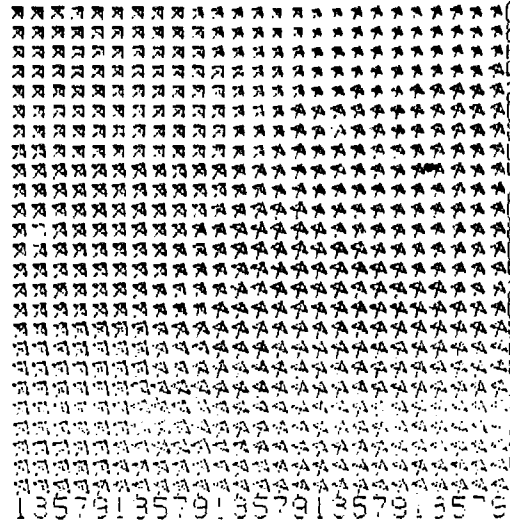
MISSION RESEARCH CORPORATION  
URBAN FIRE MODEL

PLATE RELEASE TIME = 4790.00 SECONDS  
FIRE 1 TO 50, RELEASE 1 TO 50  
WALL WIND VELOCITY MAP, WIND SPEED IN DIRECTION OF FIRE.  
WIND SPEED IS PROPORTIONAL TO THE WIND SPEED  
WIND SPEED FROM CELL 100 AND 1000 IS 10.0000  
MAXIMUM WIND VELOCITY MAGNITUDE = 50.3738



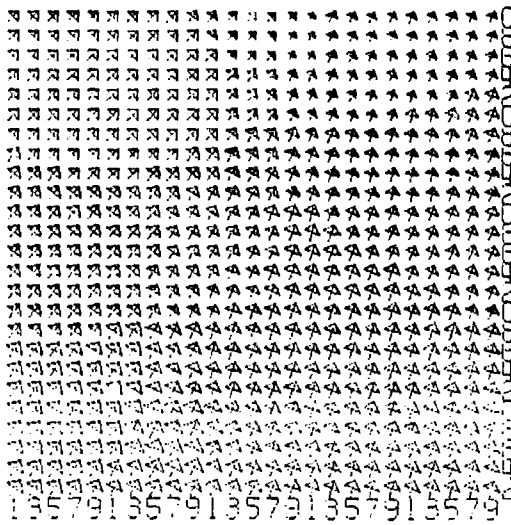
MISSION RESEARCH CORPORATION  
URBAN FIRE MODEL

PLATE RELEASE TIME = 5790.00 SECONDS  
FIRE 1 TO 50, RELEASE 1 TO 50  
WALL WIND VELOCITY MAP, WIND SPEED IN DIRECTION OF FIRE.  
WIND SPEED IS PROPORTIONAL TO THE WIND SPEED  
WIND SPEED FROM CELL 100 AND 1000 IS 10.0000  
MAXIMUM WIND VELOCITY MAGNITUDE = 51.8100



MISSION RESEARCH CORPORATION  
URBAN FIRE MODEL

PLATE RELEASE TIME = 10790.00 SECONDS  
FIRE 1 TO 50, RELEASE 1 TO 50  
WALL WIND VELOCITY MAP, WIND SPEED IN DIRECTION OF FIRE.  
WIND SPEED IS PROPORTIONAL TO THE WIND SPEED  
WIND SPEED FROM CELL 100 AND 1000 IS 10.0000  
MAXIMUM WIND VELOCITY MAGNITUDE = 51.9588



MISSION RESEARCH CORPORATION  
URBAN FIRE MODEL

PLATE RELEASE TIME = 13790.00 SECONDS  
FIRE 1 TO 50, RELEASE 1 TO 50  
WALL WIND VELOCITY MAP, WIND SPEED IN DIRECTION OF FIRE.  
WIND SPEED IS PROPORTIONAL TO THE WIND SPEED  
WIND SPEED FROM CELL 100 AND 1000 IS 10.0000  
MAXIMUM WIND VELOCITY MAGNITUDE = 50.1038

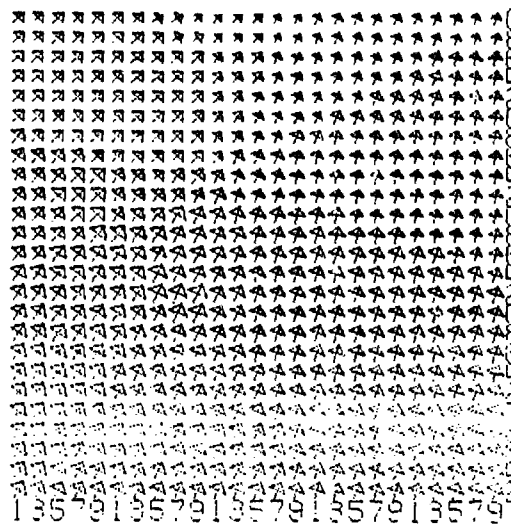


Figure 6-10(m). Wind velocity map for small area fire, ambient wind = 40 m/s.

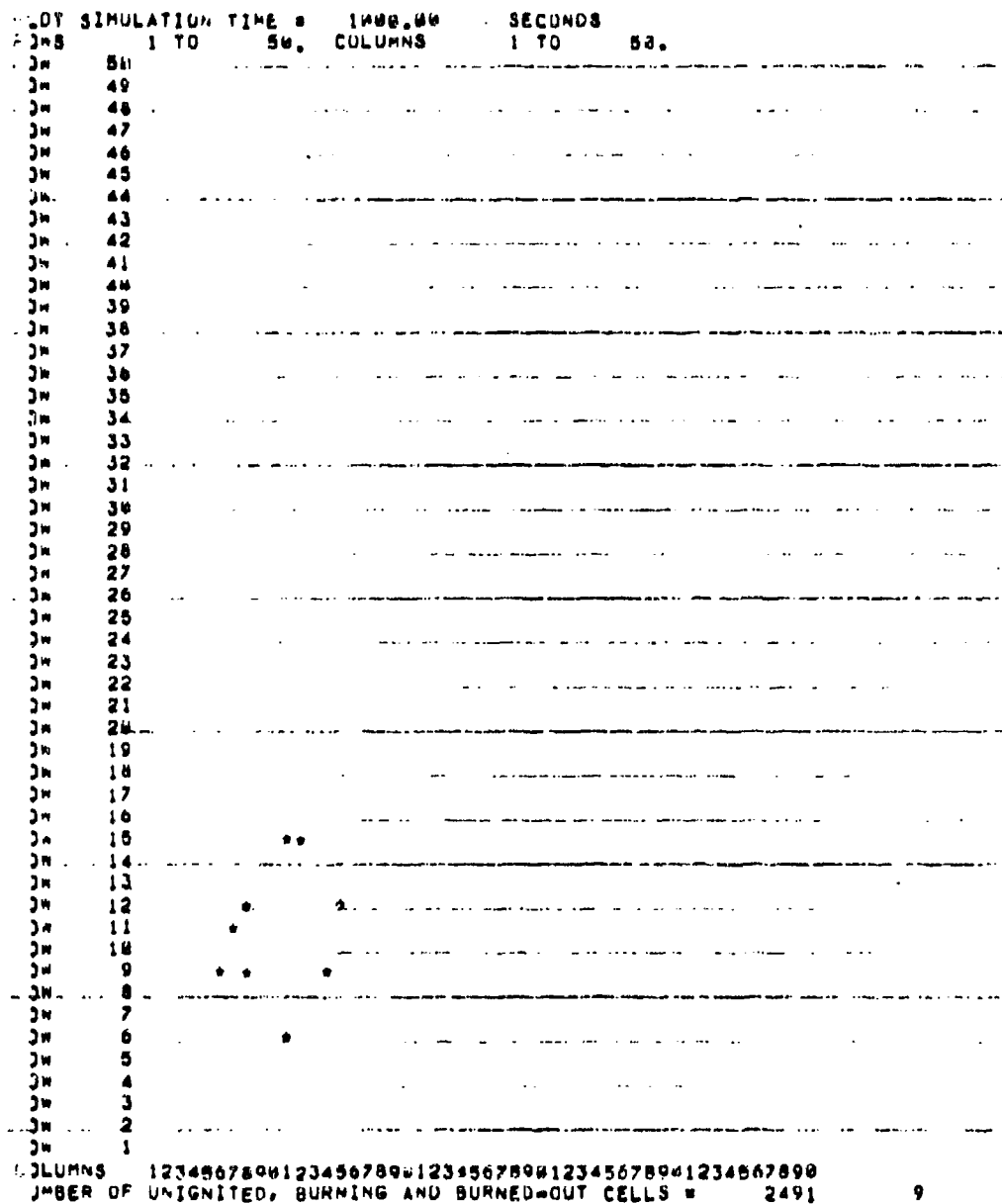


Figure 6-11. Cell state map for small area fire, ambient wind = 50 m/s.

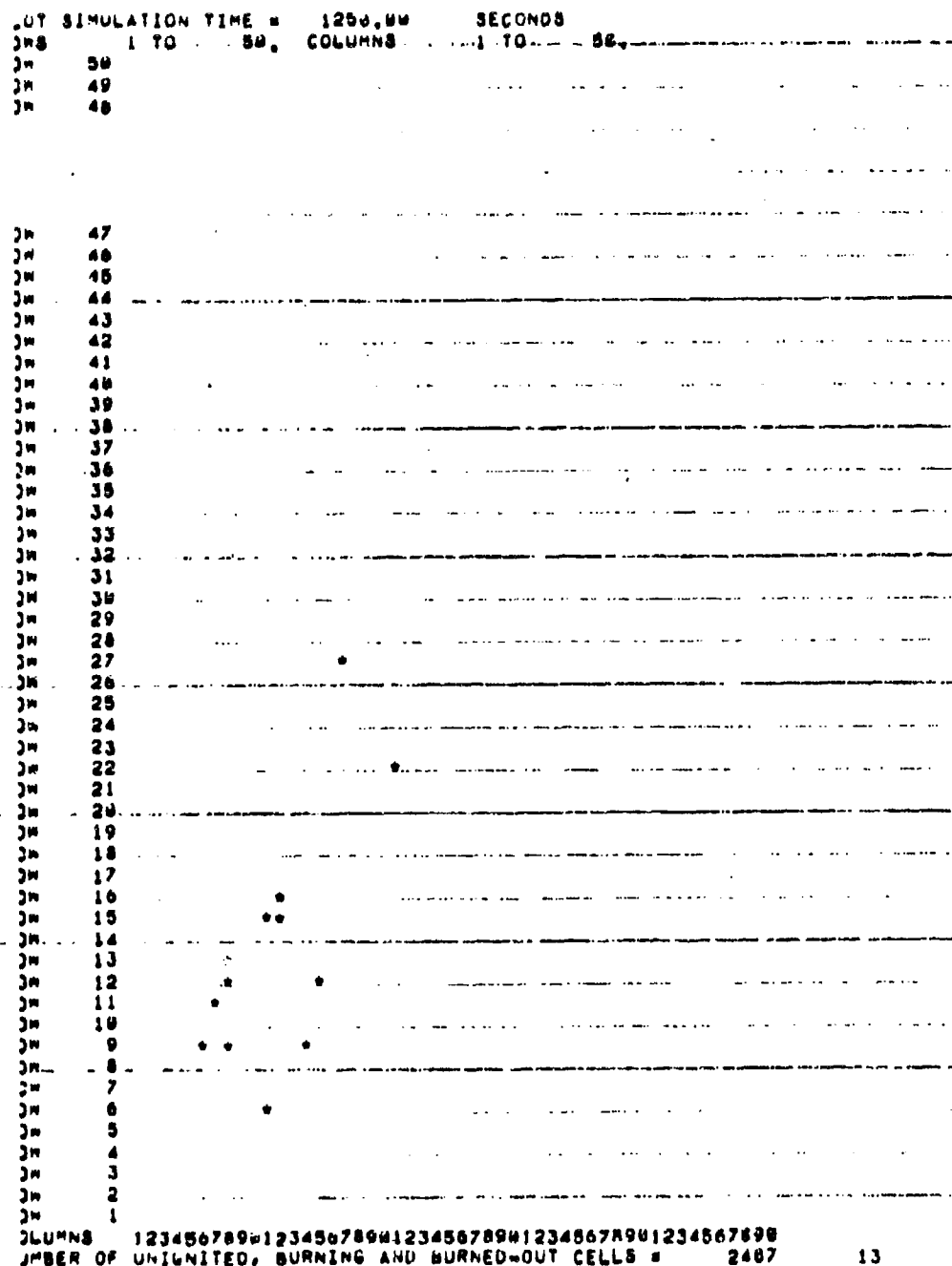


Figure 6-11(a). Cell state map for small area fire, ambient wind = 50 m/s.

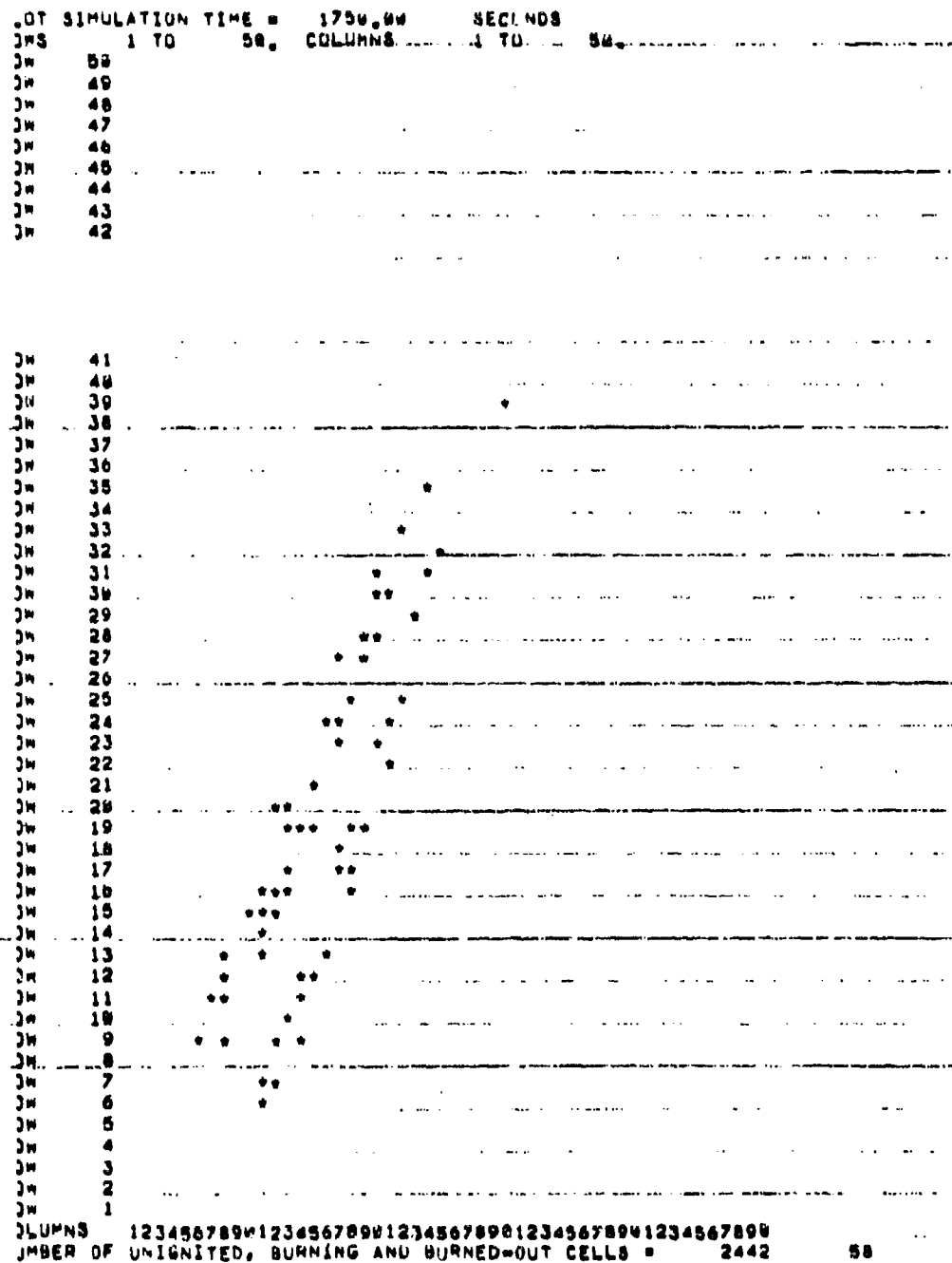


Figure 6-11(b). Cell state map for small area fire, ambient wind = 50 m/s.



```

JM 35 *****
JM 34 *****
JM 33 *****
JM 32 *****
JM 31 *****
JM 30 *****
JM 29 *****
JM 28 *****
JM 27 *****
JM 26 *****
JM 25 *****
JM 24 *****
JM 23 *****
JM 22 *****
JM 21 *****
JM 20 *****
JM 19 *****
JM 18 *****
JM 17 *****
JM 16 *****
JM 15 *****
JM 14 *****
JM 13 *****
JM 12 *****
JM 11 *****
JM 10 *****
JM 9 *****
JM 8 *****
JM 7 *****
JM 6 *****
JM 5 *****
JM 4 *****
JM 3 *****
JM 2 *****
JM 1 *****

```

COLUMNS 12345678901234567890123456789012345678901234567890  
 NUMBER OF UNIGNITED, BURNING AND BURNED-OUT CELLS • 2234 260

313

```

NOT SIMULATION TIME = 4750.00 SECONDS
JMS 1 TO 50. COLUMNS 1 TO 50.
JM 50 *****
JM 49 *****
JM 48 *****
JM 47 *****
JM 46 *****
JM 45 *****
JM 44 *****
JM 43 *****
JM 42 *****
JM 41 *****
JM 40 *****
JM 39 *****
JM 38 *****
JM 37 *****
JM 36 *****
JM 35 *****
JM 34 *****
JM 33 *****
JM 32 *****
JM 31 *****
JM 30 *****

JM 29 *****
JM 28 *****
JM 27 *****
JM 26 *****
JM 25 *****
JM 24 *****
JM 23 *****
JM 22 *****
JM 21 *****
JM 20 *****
JM 19 *****
JM 18 *****
JM 17 *****
JM 16 *****
JM 15 *****
JM 14 *****
JM 13 *****
JM 12 *****
JM 11 *****
JM 10 *****
JM 9 *****
JM 8 *****
JM 7 *****
JM 6 *****
JM 5 *****
JM 4 *****
JM 3 *****
JM 2 *****
JM 1 *****

COLUMN# 12345678901234567890123456789012345678901234567890
NUMBER OF UNIGNITED, BURNING AND BURNED-OUT CELLS = 2075 425

```

Figure 6-11(d). Cell state map for small area fire, ambient wind = 50 m/s.

```

      107 SIMULATION TIME = 8750.00 SECONDS
      108 1 TO 50, COLUMNS 1 TO 50,
      109 50
      110 49
      111 48
      112 47
      113 46
      114 45
      115 44
      116 43
      117 42
      118 41
      119 40
      120 39
      121 38
      122 37
      123 36
      124 35
      125 34
      126 33
      127 32
      128 31
      129 30
      130 29
      131 28
      132 27
      133 26
      134 25
      135 24

      136 23
      137 22
      138 21
      139 20
      140 19
      141 18
      142 17
      143 16
      144 15
      145 14
      146 13
      147 12
      148 11
      149 10
      150 9
      151 8
      152 7
      153 6
      154 5
      155 4
      156 3
      157 2
      158 1

      159 COLUMNS 12345678901234567890123456789012345678901234567890
      160 NUMBER OF UNIGNITED, BURNING AND BURNED-OUT CELLS = 1938 559 3

```

Figure 6-11(e). Cell state map for small area fire, ambient wind = 5 m/s.

```

OUT SIMULATION TIME = 1675.44 SECONDS
MS 1 TO 50, COLUMN# 1 TO 50
IN 50 *****
IN 49 *****
IN 48 *****
IN 47 *****
IN 46 *****
IN 45 *****
IN 44 *****
IN 43 *****
IN 42 *****
IN 41 *****
IN 40 *****
IN 39 *****
IN 38 *****
IN 37 *****
IN 36 *****
IN 35 *****
IN 34 *****
IN 33 *****
IN 32 *****
IN 31 *****
IN 30 *****
IN 29 *****
IN 28 *****
IN 27 *****
IN 26 *****
IN 25 *****
IN 24 *****
IN 23 *****
IN 22 *****
IN 21 *****
IN 20 *****
IN 19 *****
IN 18 *****

IN 17 *****
IN 16 *****
IN 15 *****
IN 14 *****
IN 13 *****
IN 12 *****
IN 11 *****
IN 10 *****
IN 9 *****
IN 8 *****
IN 7 *****
IN 6 *****
IN 5
IN 4
IN 3
IN 2
IN 1

COLUMNS 1234567890123456789012345678901234567890
NUMBER OF UNIGNITED, BURNING AND BURNED-OUT CELLS = 1703 646 15

```

Figure 6-11(f). Cell state map for small area fire, ambient wind = 50 m/s.

```

NOT SIMULATION TIME = 32/51.0 SECONDS
INS 1 TO 50, COLUMNS 1 TO 50,
)N 50 *****B*****
)N 49 *****B*****
)N 48 *****B*****
)N 47 *****B*****
)N 46 *****B*****
)N 45 *****B*****
)N 44 *****B*****
)N 43 *****B*****
)N 42 *****B*****
)N 41 *****B*****
)N 40 *****B*****
)N 39 *****B*****
)N 38 *****B*****
)N 37 *****B*****
)N 36 *****B*****
)N 35 *****B*****
)N 34 *****B*****
)N 33 *****B*****
)N 32 *****B*****
)N 31 *****B*****
)N 30 *****B*****
)N 29 *****B*****
)N 28 *****B*****
)N 27 *****B*****
)N 26 *****B*****
)N 25 *****B*****
)N 24 *****B*****
)N 23 *****B*****
)N 22 *****B*****
)N 21 *****B*****
)N 20 *****B*****
)N 19 *****B*****
)N 18 *****B*****
)N 17 *****B*****
)N 16 *****B*****
)N 15 *****B*****
)N 14 *****B*****
)N 13 *****B*****
)N 12 *****B*****

)N 11 *****B*****
)N 10 *****B*****
)N 9 *****B*****
)N 8 *****B*****
)N 7 *****B*****
)N 6 *****B*****
)N 5 *****B*****
)N 4 *****B*****
)N 3 *****B*****
)N 2 *****B*****
)N 1 *****B*****

)LUMS 12345678901234567890123456789012345678901234567890
)MUR OF UNIGNITED, BURNING AND BURNED-OUT CELLS = 1329 529 64

```

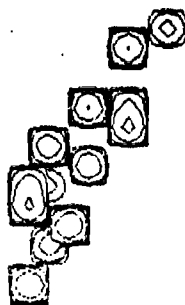
Figure 6-11(g). Cell state map for small area fire, ambient wind = 50 m/s.

MISSION RESEARCH CORPORATION  
UNBURN FINE MODEL  
PLOT SIMULATION TIME = 1000.00 SECONDS  
X AXIS 1 TO 50 Y AXIS 1 TO 50  
CELL SIZE 10000000  
\*\*\* ONLY EVERY OTHER CELL AND COLUMN IS PLOTTED \*\*\*  
WIND SCALE (S LOGARITHMIC BASE 10) (0-1.25 0-1.25)



1357913579135791357913579

MISSION RESEARCH CORPORATION  
UNBURN FINE MODEL  
PLOT SIMULATION TIME = 1750.00 SECONDS  
X AXIS 1 TO 50 Y AXIS 1 TO 50  
CELL SIZE 10000000  
\*\*\* ONLY EVERY OTHER CELL AND COLUMN IS PLOTTED \*\*\*  
WIND SCALE (S LOGARITHMIC BASE 10) (0-1.25 0-1.25)



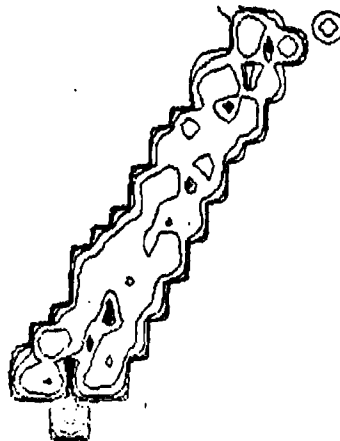
1357913579135791357913579

MISSION RESEARCH CORPORATION  
UNBURN FINE MODEL  
PLOT SIMULATION TIME = 1750.00 SECONDS  
X AXIS 1 TO 50 Y AXIS 1 TO 50  
CELL SIZE 10000000  
\*\*\* ONLY EVERY OTHER CELL AND COLUMN IS PLOTTED \*\*\*  
WIND SCALE (S LOGARITHMIC BASE 10) (0-1.25 0-1.25)



1357913579135791357913579

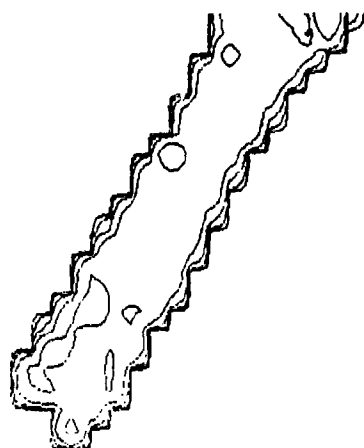
MISSION RESEARCH CORPORATION  
UNBURN FINE MODEL  
PLOT SIMULATION TIME = 1750.00 SECONDS  
X AXIS 1 TO 50 Y AXIS 1 TO 50  
CELL SIZE 10000000  
\*\*\* ONLY EVERY OTHER CELL AND COLUMN IS PLOTTED \*\*\*  
WIND SCALE (S LOGARITHMIC BASE 10) (0-1.25 0-1.25)



1357913579135791357913579

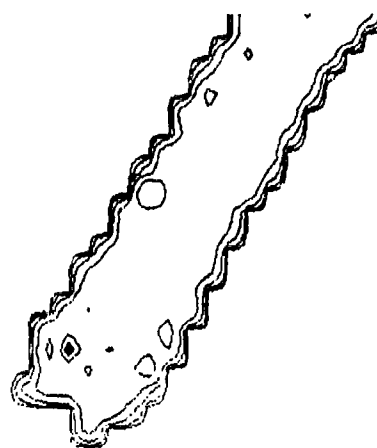
Figure 6-11(h). Heat production rate contour map for small area fire, ambient wind = 50 m/s.

MISSION RESEARCH CORPORATION  
URBAN FIRE MODEL  
PLAY RELEASE ON TIME = 4700.00 SECONDS  
RMS 1 TO 10 10 10 10 10 10  
WILL NOT COVER UP  
\*\*\* ONLY EVERY OTHER CELL SURF AND BELONG TO PLAYER \*\*\*  
BEST SCALE IS LOGARITHMIC (0-1.0E 0-1.0E 0-1.0E)



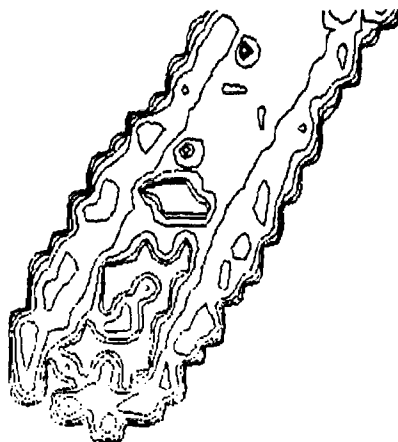
1357913579135791357913579

MISSION RESEARCH CORPORATION  
URBAN FIRE MODEL  
PLAY RELEASE ON TIME = 5700.00 SECONDS  
RMS 1 TO 10 10 10 10 10 10  
WILL NOT COVER UP  
\*\*\* ONLY EVERY OTHER CELL SURF AND BELONG TO PLAYER \*\*\*  
BEST SCALE IS LOGARITHMIC (0-1.0E 0-1.0E 0-1.0E)



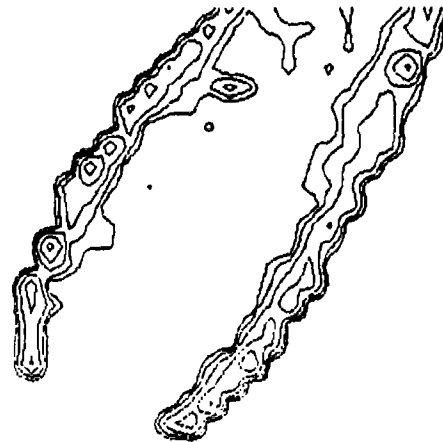
1357913579135791357913579

MISSION RESEARCH CORPORATION  
URBAN FIRE MODEL  
PLAY RELEASE ON TIME = 6700.00 SECONDS  
RMS 1 TO 10 10 10 10 10 10  
WILL NOT COVER UP  
\*\*\* ONLY EVERY OTHER CELL SURF AND BELONG TO PLAYER \*\*\*  
BEST SCALE IS LOGARITHMIC (0-1.0E 0-1.0E 0-1.0E)



1357913579135791357913579

MISSION RESEARCH CORPORATION  
URBAN FIRE MODEL  
PLAY RELEASE ON TIME = 7700.00 SECONDS  
RMS 1 TO 10 10 10 10 10 10  
WILL NOT COVER UP  
\*\*\* ONLY EVERY OTHER CELL SURF AND BELONG TO PLAYER \*\*\*  
BEST SCALE IS LOGARITHMIC (0-1.0E 0-1.0E 0-1.0E)



1357913579135791357913579

Figure 6-11(i). Heat production rate contour map for small area fire, ambient wind = 50 m/s.

1357913579135791357913579

1357913579135791357913579

1357913579135791357913579

1357913579135791357913579

320



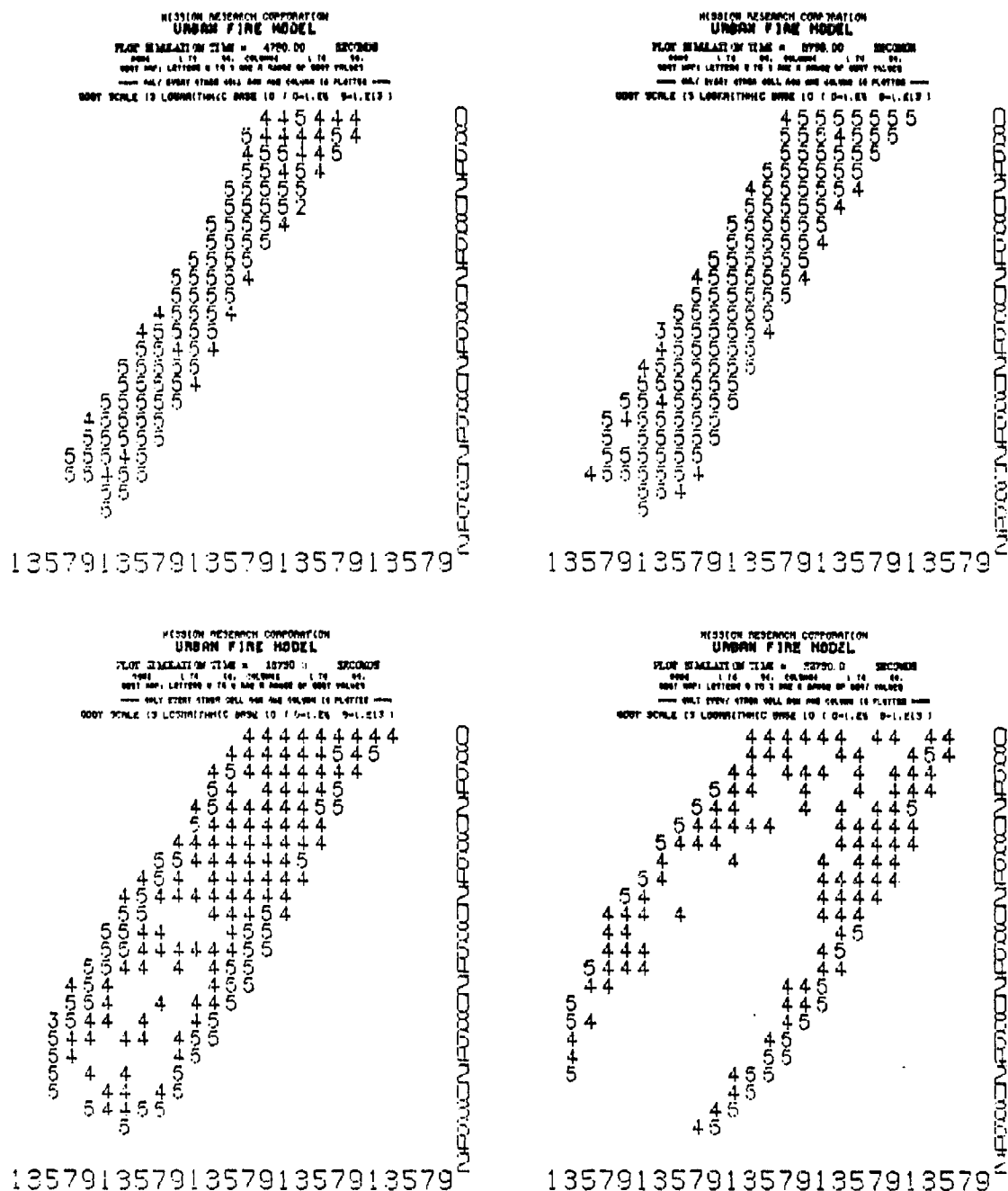
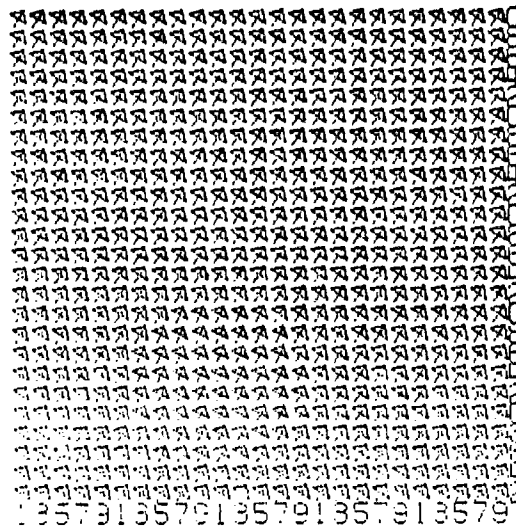


Figure 6-11(k). Cell heat production rate map for small area fire, ambient wind = 50 m/s.

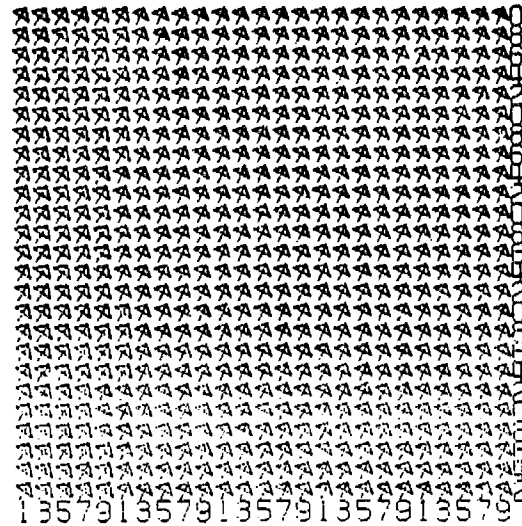
MISSION RESEARCH CORPORATION  
UPDOWN FIRE MODEL

PLATE RELOCATION TIME = 1000.00 SECONDS  
WIND VELOCITY MAP, WIND DIRECTION IN DEGREES OF TRUE.  
WIND SPEED IN METERS PER SECOND, TO THE RIGHT OF TRUE.  
WIND VELOCITY MAP, WIND DIRECTION IN DEGREES OF TRUE.  
WIND SPEED IN METERS PER SECOND, TO THE RIGHT OF TRUE.  
MAXIMUM WIND VELOCITY MAGNITUDE = 51.0000



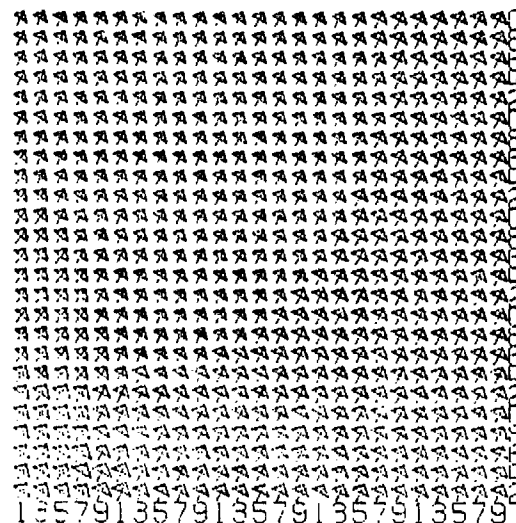
MISSION RESEARCH CORPORATION  
UPDOWN FIRE MODEL

PLATE RELOCATION TIME = 1000.00 SECONDS  
WIND VELOCITY MAP, WIND DIRECTION IN DEGREES OF TRUE.  
WIND SPEED IN METERS PER SECOND, TO THE RIGHT OF TRUE.  
WIND VELOCITY MAP, WIND DIRECTION IN DEGREES OF TRUE.  
WIND SPEED IN METERS PER SECOND, TO THE RIGHT OF TRUE.  
MAXIMUM WIND VELOCITY MAGNITUDE = 63.0071



MISSION RESEARCH CORPORATION  
UPDOWN FIRE MODEL

PLATE RELOCATION TIME = 1700.00 SECONDS  
WIND VELOCITY MAP, WIND DIRECTION IN DEGREES OF TRUE.  
WIND SPEED IN METERS PER SECOND, TO THE RIGHT OF TRUE.  
WIND VELOCITY MAP, WIND DIRECTION IN DEGREES OF TRUE.  
WIND SPEED IN METERS PER SECOND, TO THE RIGHT OF TRUE.  
MAXIMUM WIND VELOCITY MAGNITUDE = 56.1878



MISSION RESEARCH CORPORATION  
UPDOWN FIRE MODEL

PLATE RELOCATION TIME = 1700.00 SECONDS  
WIND VELOCITY MAP, WIND DIRECTION IN DEGREES OF TRUE.  
WIND SPEED IN METERS PER SECOND, TO THE RIGHT OF TRUE.  
WIND VELOCITY MAP, WIND DIRECTION IN DEGREES OF TRUE.  
WIND SPEED IN METERS PER SECOND, TO THE RIGHT OF TRUE.  
MAXIMUM WIND VELOCITY MAGNITUDE = 72.0578

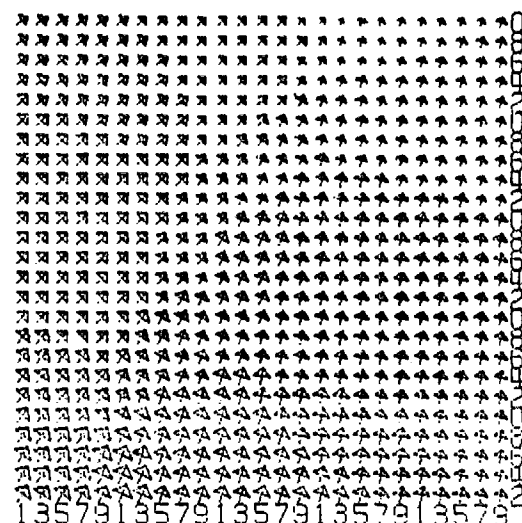
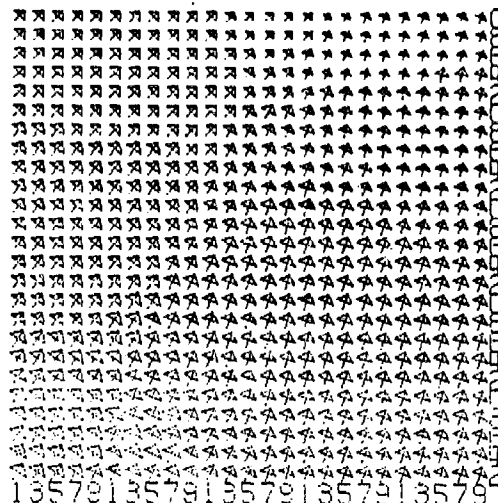


Figure 6-11(1). Wind velocity map for small area fire, ambient wind = 50 m/s.

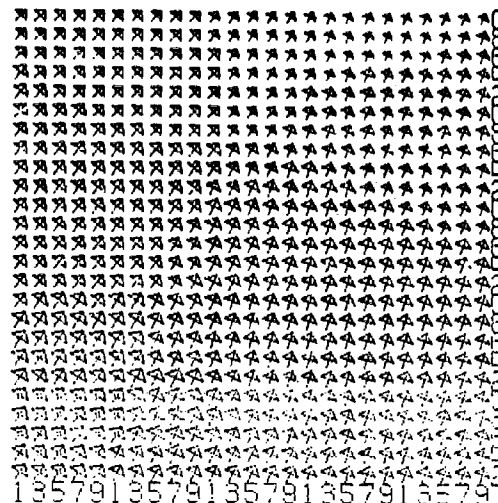
MISSION RESEARCH CORPORATION  
URBAN FIRE MODEL

PLATE RELEASED ON TIME = 4700.00 SCENARIO  
FROM 1 TO 91, 91, 91, 91, 91, 91  
CELL FIRE VELOCITY MAP, SHOWS POINTS IN DIRECTION OF WIND.  
WIND VELOCITY IS PROPORTIONAL TO THE SIZE OF THE  
CELL. ONLY THOSE CELLS WITH WIND VELOCITY IN PLATE  
MAXIMUM WIND VELOCITY MAGNITUDE = 84.879



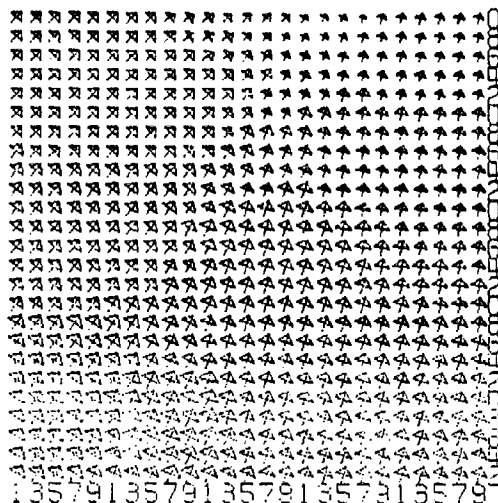
MISSION RESEARCH CORPORATION  
URBAN FIRE MODEL

PLATE RELEASED ON TIME = 5100.00 SCENARIO  
FROM 1 TO 91, 91, 91, 91, 91, 91  
CELL FIRE VELOCITY MAP, SHOWS POINTS IN DIRECTION OF WIND.  
WIND VELOCITY IS PROPORTIONAL TO THE SIZE OF THE  
CELL. ONLY THOSE CELLS WITH WIND VELOCITY IN PLATE  
MAXIMUM WIND VELOCITY MAGNITUDE = 85.8304



MISSION RESEARCH CORPORATION  
URBAN FIRE MODEL

PLATE RELEASED ON TIME = 5500.00 SCENARIO  
FROM 1 TO 91, 91, 91, 91, 91, 91  
CELL FIRE VELOCITY MAP, SHOWS POINTS IN DIRECTION OF WIND.  
WIND VELOCITY IS PROPORTIONAL TO THE SIZE OF THE  
CELL. ONLY THOSE CELLS WITH WIND VELOCITY IN PLATE  
MAXIMUM WIND VELOCITY MAGNITUDE = 87.0462



MISSION RESEARCH CORPORATION  
URBAN FIRE MODEL

PLATE RELEASED ON TIME = 5900.00 SCENARIO  
FROM 1 TO 91, 91, 91, 91, 91, 91  
CELL FIRE VELOCITY MAP, SHOWS POINTS IN DIRECTION OF WIND.  
WIND VELOCITY IS PROPORTIONAL TO THE SIZE OF THE  
CELL. ONLY THOSE CELLS WITH WIND VELOCITY IN PLATE  
MAXIMUM WIND VELOCITY MAGNITUDE = 88.0012

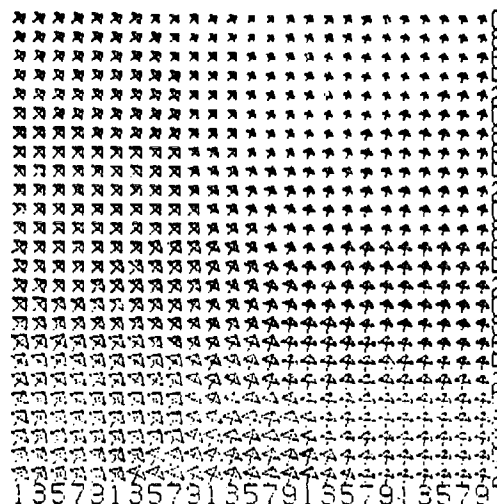


Figure 6-11(m). Wind velocity map for small area fire, ambient wind = 50 m/s.

## REFERENCES

1. Martin, Stanley B., The Role of Fire in Nuclear Warfare, DNA 2692F, URS Research Company, San Mateo, CA, August 1974.
2. Small, R.D., and H.L. Brode, Physics of Large Urban Fires, PSR Report 1010, Pacific Sierra Research Corporation, 1980.
3. Alger, R.S., and S.B. Martin, Blast/Fire Interactions, Asilomar Conference, March 1979, SRI International, September 1979.
4. Alger, R.S., and S.B. Martin, Blast/Fire Interactions, Asilomar Conference, May 1980, SRI International, February 1981.
5. Weisbecker, L.W., and H. Lee, Evaluation of Systems of Fire Development, Stanford Research Institute, August 1970.
6. Rodden, Robert M., F.I. John, and R. Laurino, Exploratory Analysis of Fire Storms, Stanford Research Institute, May 1965.
7. Lonnmassen, T.E., R.K. Miller, R.G. Kirkpatrick, and J.A. Keller, A 'Firestorm' Existence and Buildup Hypothesis, Dikewood Corporation, September 1968.
8. Baldwin, R., and M.A. North, The Firestorm--Its Size and Importance, Fire Research Note 645, Fire Research Station, Joint Fire Research Organization, United Kingdom, February 1967.
9. Countryman, Clive M., Project Flambeau, Final Report, Volume 1, Pacific SW Forest and Range Experiment Station, Berkeley, CA, Office of Civil Defense.
10. Countryman, Clive M., Mass Fires and Fire Behavior, U.S. Department of Agriculture, U.S. Forest Service Research Paper PSW-19, 1964.
11. Gaskin, A.S. (ed), Operation Euroka, Supplementary Papers, Department of Supply, Australian Defence Scientific Service, Defence Standards Laboratories (DSL), Maribyrnong, Victoria, Australia, July 1971.  
  
See also:  
Operation Euroka, An Australian Mass Fire Experiment, DSL Report 386, Commonwealth of Australia, September 1970.
12. Neilsen, Hugo J., Fire Storm Analysis, ITT Research Institute, January 1970.

13. Nielsen, H.J. and L.N. Tao, "The Fire Plume Above a Large Free-Burning Fire," Tenth Symposium (International) on Combustion, Combustion Institute, p. 965, 1965.
14. Gostintsev, Yu.A. and L.A. Sukhanov, "Convective Column Above a Linear Fire in Homogeneous Isothermal Atmosphere," Combustion, Explosion, and Shock Waves, 13, p. 570, 1977.
15. Gostintsev, Yu.A., and L.A. Sukhanov, "Interaction of Convective Columns Above Linear Sources of Heat," Combustion, Explosion, and Shock Waves, 14, p. 60, 1978.
16. Gostintsev, Yu.A. and L.A. Sukhanov, "Convective Column Above a Linear Fire in a Polytropic Atmosphere," Combustion, Explosion, and Shock Waves, 14, p. 271, 1978.
17. Gostintsev, Yu.A. and L.A. Sukhanov, "Interaction Between a Convective Column and a Wind Above a Linear Fire in a Polytropic Atmosphere," Combustion, Explosion, and Shock Waves, 14, p. 452, 1978.
18. Rothmal, Richard C., A Mathematical Model for Predicting Fire Spread in Wildland Fuels, U.S. Department of Agriculture, U.S. Forest Service, Research Paper INT-115, January 1972.
19. Sanderlin, J.C., and J.M. Sunderson, Wildland Fire Modeling for Planning Support, Volume III--A Prototype Segmented Perimeter Wildland Fire Propagation Model, MRC-R-470, Mission Research Corporation, August 1976.
20. Faus, W.R., "Analysis of Fire Spread in Light Forest Fuels," J. Agr. Res., Vol. 72, No. 3, pp 93-121, 1946.
21. Tarifa, C.S., and A.M. Tanalko, "Flame Propagation Along the Interface Between a Gas and a Reacting Medium," Eleventh International Symposium on Combustion, Berkeley, CA, 1967.
22. Frandsen, W.H., "Fire Spread Through Porous Fuels from the Conservation of Energy," Combustion and Flame, Vol. 16, pp 9-16, 1971.
23. Sanderlin, J.C., and J.M. Sunderson, Wildland Fire Modeling for Planning Support. Volume IV--Rate of Spread Model Assessment, MRC-R-470, Mission Research Corporation, August 1976.
24. McCaffrey, B.J., Meeting of Eastern Section of the Combustion Institute, November 1978.

25. Cox, G., and R. Chitty, "A Study of the Deterministic Properties of Unbounded Fire Plumes," Combustion and Flame, 39, pp. 191-209, 1980.
26. Scorer, R.S., Environmental Aerodynamics, Ellis Horwood Ltd. (John Wiley & Sons), New York, p. 276, 1978.
27. Morton, B.R., G. Taylor, and J.S. Turner, "Turbulent Gravitational Convection from Maintained and Instantaneous Sources," Proc. Roy. Soc., A24, pp 1-23, 1956.
28. Tarifa, Carlos S., P. Perez del Notario, and F. Garcia Moreno, "On the Flight Paths and Lifetimes of Burning Particles of Wood," Tenth Symposium (International) on Combustion, Combustion Institute, Pittsburgh, PA, 1965.

## DISTRIBUTION LIST

### DEPARTMENT OF DEFENSE

Defense Intelligence Agency  
ATTN: DB-4C2, C. Wiehle

Field Command  
Defense Nuclear Agency  
ATTN: FCTT, G. Ganong  
ATTN: FCTT, W. Summa

Defense Nuclear Agency  
ATTN: SPTD  
4 cy ATTN: TITL

Defense Technical Information Center  
12 cy ATTN: DD

### OTHER GOVERNMENT AGENCIES

Department of Commerce  
National Bureau of Standards  
ATTN: R. Levine

Director, FFASR  
U.S. Forest Service  
ATTN: C. Chandler

Federal Emergency Management Agency  
Office of Research  
ATTN: D. Bensen  
ATTN: J. Kerr

Office of Emergency Services  
ATTN: W. Tonguet

### DEPARTMENT OF ENERGY CONTRACTORS

Lawrence Livermore National Lab  
ATTN: B. Bowman

Los Alamos National Laboratory  
ATTN: J. Chapiak  
ATTN: Dr. D. Cagliostro

### DEPARTMENT OF DEFENSE CONTRACTORS

California Research & Technology, Inc  
ATTN: M. Rosenblatt

Center for Planning & Rsch, Inc  
ATTN: R. Laurino  
ATTN: J. Rempel

Charles Scawthorn  
ATTN: C. Scawthorn

Harvard University  
ATTN: Prof. G. Carrier

Institute for Defense Analyses  
ATTN: L. Schmidt

Kaman Tempo  
ATTN: DASIAC

### DEPARTMENT OF DEFENSE CONTRACTORS (Continued)

Management Science Associates  
ATTN: K. Kaplan

Mission Research Corp  
4 cy ATTN: J. Sanderlin  
4 cy ATTN: J. Ball  
4 cy ATTN: G. Johanson  
5 cy ATTN: Document Control

Modeling System, Inc  
ATTN: G. Berlin

University of Notre Dame  
ATTN: A. Murty Kanury

Pacific-Sierra Research Corp  
ATTN: R. Small  
ATTN: H. Brode, Chairman SAGE

R & D Associates  
ATTN: J. Carpenter  
ATTN: R. Port  
ATTN: D. Holliday  
ATTN: P. Haas

Research Triangle Institute  
ATTN: Sec Control Ofc for R. Frank

Science Applications, Inc  
ATTN: M. Drake  
ATTN: M. McKay  
ATTN: D. Groce

Science Applications, Inc  
ATTN: J. Cockayne

Scientific Services, Inc  
ATTN: C. Wilton

SRI International  
ATTN: R. McKee  
ATTN: T. Goodale  
ATTN: S. Martin  
ATTN: J. Backovsky

TRW Electronics & Defense Sector  
ATTN: F. Fendell

### FOREIGN GOVERNMENTS

Fire Research Establishment  
ATTN: Dr. P. Thomas

The Swedish Fire Research Board  
ATTN: V. Sjölin

**BLANK PAGE**